Appendix A
Complex Variable Theory

TO ACCOMPANY

AUTOMATIC CONTROL SYSTEMS
EIGHTH EDITION

BY

BENJAMIN C. KUO

FARID GOLNARAGHI

Complex-Variable Theory

▶ A-1 COMPLEX-VARIABLE CONCEPT

A-1-1 Complex Variable

A complex variable s has two components: a real component σ and an imaginary component ω. Graphically, the real component of s is represented by a σ axis in the horizontal direction, and the imaginary component is measured along the vertical $j\omega$ axis, in the complex s-plane. Figure A-1 illustrates the complex s-plane, in which any arbitrary point $s = s_1$ is defined by the coordinates $\sigma = \sigma_1$, and $\omega = \omega_1$, or simply $s_1 = \sigma_1 + j\omega_1$.

A-1-2 Functions of a Complex Variable

The function $G(s)$ is said to be a function of the complex variable s if for every value of s, there is one or more corresponding values of $G(s)$. Since s is defined to have real and imaginary parts, the function $G(s)$ is also represented by its real and imaginary parts; that is,

$$G(s) = \mathrm{Re}\,G(s) + j\,\mathrm{Im}\,G(s) \tag{A-1}$$

where $\mathrm{Re}\,G(s)$ denotes the real part of $G(s)$, and $\mathrm{Im}\,G(s)$ represents the imaginary part of $G(s)$. The function $G(s)$ is also represented by the complex $G(s)$-plane, with $\mathrm{Re}\,G(s)$ as the real axis and $\mathrm{Im}\,G(s)$ as the imaginary axis. If for every value of s there is only one corresponding value of $G(s)$ in the $G(s)$-plane, $G(s)$ is said to be a **single-valued function**, and the mapping from points in the s-plane onto points in the $G(s)$-plane is described
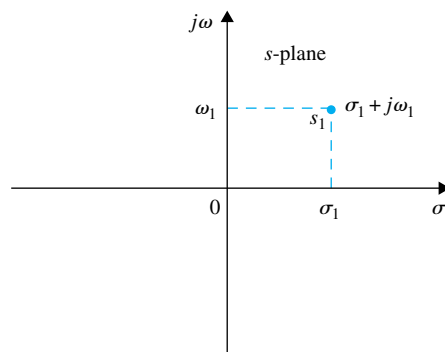
Figure A-1   The complex s-plane.
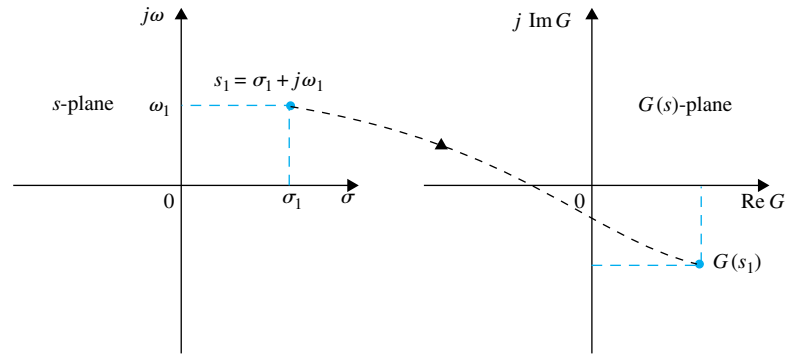
Figure A-2 Single-valued mapping from the s-plane to the G(s)-plane.

as **single-valued** (Fig. A-2). If the mapping from the $G(s)$-plane to the s-plane is also single-valued, the mapping is called **one-to-one**. However, there are many functions for which the mapping from the function plane to the complex-variable plane is not single-valued. For instance, given the function

$$G(s) = \frac{1}{s(s + 1)} \tag{A-2}$$

it is apparent that for each value of s, there is only one unique corresponding value for $G(s)$. However, the inverse mapping is not true; for instance, the point $G(s) = \infty$ is mapped onto two points, $s = 0$ and $s = -1$, in the s-plane.

A-1-3 Analytic Function

*A function $G(s)$ of the complex variable s is called an **analytic function** in a region of the s-plane if the function and all its derivatives exist in the region.* For instance, the function given in Eq. (A-2) is analytic at every point in the s-plane except at the point $s = 0$ and $s = -1$. At these two points, the value of the function is infinite. As another example, the function $G(s) = s + 2$ is analytic at every point in the finite s-plane.

A-1-4 Singularities and Poles of a Function

The **singularities** of a function are the points in the s-plane at which the function or its derivatives does not exist. A **pole** is the most common type of singularity and plays a very important role in the studies of classical control theory.

The definition of a pole can be stated as: *If a function $G(s)$ analytic and single-valued in the neighborhood of s_i, it is said to have a pole of order r at $s = s_i$ if the limit*

$$\lim_{s \to s_i}\left[(s - s_i)^r G(s)\right]$$

has a finite, nonzero value. In other words, the denominator of $G(s)$ must include the factor $(s - s_i)^r$, so when $s = s_i$, the function becomes infinite. If $r = 1$, the pole at $s = s_i$ is called a **simple pole**. As an example, the function

$$G(s) = \frac{10(s + 2)}{s(s + 1)(s + 3)^2} \tag{A-3}$$

has a pole of order 2 at $s = -3$ and simple poles at $s = 0$ and $s = -1$. It can also be said that the function $G(s)$ is analytic in the s-plane except at these poles.

A-1-5   Zeros of a Function

The definition of a **zero** of a function can be stated as: *If the function G(s) is analytic at s = s_i, it is said to have a zero of order r at s = s_i if the limit*

$$\lim_{s \to s_i}\left[(s - s_i)^{-r} G(s) \right]$$

• The total numbers of poles and zeros of a rational function is the same, counting the ones at infinity

has a finite, nonzero value. Or, simply, G(s) has a zero of order r at s = s_i if 1/G(s) has an rth-order pole at s = s_i. For example, the function in Eq. (2-3) has a simple zero at s = −2.

If the function under consideration is a rational function of s, that is, a quotient of two polynomials of s, the total number of poles equals the total number of zeros, counting the multiple-order poles and zeros, and taking into account of the poles and zeros at infinity. The function in Eq. (A-3) has four finite poles at s = 0, −1, −3, and −3; there is one finite zero at s = −2, but there are three zeros at infinity, since

$$\lim_{s \to \infty} G(s) = \lim_{s \to \infty} \frac{10}{s^3} = 0 \tag{A-4}$$

Therefore, the function has a total of four poles and four zeros in the entire s-plane, including infinity.

► REFERENCES

F. B. Hildebrand, *Methods of Applied Mathematics,* 2nd ed., Prentice Hall, Englewood Cliffs, NJ. 1965.

Appendix B
Differential and Difference Equations

Differential and Difference Equations

B-1-1 Linear Ordinary Differential Equations

A wide range of systems in engineering are modeled mathematically by differential equations. These equations generally involve derivatives and integrals of the dependent variables with respect to the independent variable. For instance, a series electric *RLC* (resistance-inductance-capacitance) network can be represented by the differential equation

$$Ri(t) + L\frac{di(t)}{dt} + \frac{1}{C}\int i(t)dt = e(t) \tag{B-1}$$

where R is the resistance; L, the inductance; C, the capacitance; $i(t)$, the current in the network; and $e(t)$, the applied voltage. In this case, $e(t)$ is the forcing function; t, the independent variable; and $i(t)$, the dependent variable or unknown that is to be determined by solving the differential equation.

Equation (B-1) is referred to as a second-order differential equation, and we refer to the system as a **second-order system**. Strictly speaking, Eq. (B-1) should be referred to as an integrodifferential equation, since an integral is involved.

In general, the differential equation of an nth-order system is written

$$\frac{d^n y(t)}{dt^n} + a_{n-1}\frac{d^{n-1}y(t)}{dt^{n-1}} + \cdots + a_1\frac{dy(t)}{dt} + a_0 y(t) = f(t) \tag{B-2}$$

which is also known as a **linear ordinary differential equation** if the coefficients a_0, a_1, … , a_{n-1} are not functions of $y(t)$.

In this text, since we treat only systems that contain lumped parameters, the differential equations encountered are all of the ordinary type. For systems with distributed parameters, such as in heat-transfer systems, partial differential equations are used.

B-1-2 Nonlinear Differential Equations

Many physical systems are nonlinear and must be described by nonlinear differential equations. For instance, the differential equation that describes the motion of the pendulum shown in Fig. B-1 is

$$ML\frac{d^2\theta(t)}{dt^2} + Mg \sin \theta(t) = 0 \tag{B-3}$$

B-1
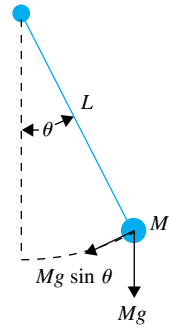
Figure B-1   Simple pendulum.

Since $\theta(t)$ appears as a sine function, Eq. (B-3) is nonlinear, and the system is called a **nonlinear system**.

B-1-3   First-Order Differential Equations: State Equations

In general, an nth-order differential equation can be decomposed into n first-order differential equations. Because, in principle, first-order differential equations are simpler to solve than higher-order ones, first-order differential equations are used in the analytical studies of control systems.

For the differential equation in Eq. (B-1), if we let

$$x_1(t) = \int i(t)dt \tag{B-4}$$

and

$$x_2(t) = \frac{dx_1(t)}{dt} = i(t) \tag{B-5}$$

then Eq. (B-1) is decomposed into the following two first-order differential equations:

$$\frac{dx_1(t)}{dt} = x_2(t) \tag{B-6}$$

$$\frac{dx_2(t)}{dt} = -\frac{1}{LC}x_1(t) - \frac{R}{L}x_2(t) + \frac{1}{L}e(t) \tag{B-7}$$

In a similar manner, for Eq. (B-2), let us define

$$x_1(t) = y(t)$$
$$x_2(t) = \frac{dy(t)}{dt}$$
$$x_n(t) = \frac{d^{n-1}y(t)}{dt^{n-1}} \tag{B-8}$$

then the nth-order differential equation is decomposed into n first-order differential equations:

$$\frac{dx_1(t)}{dt} = x_2(t)$$

$$\frac{dx_2(t)}{dt} = x_3(t)$$

$$\vdots$$

$$\frac{dx_n(t)}{dt} = -a_0x_1(t) - a_1x_2(t) - \cdots - a_{n-2}x_{n-1}(t) - a_{n-1}x_n(t) + f(t) \tag{B-9}$$

Notice that the last equation is obtained by equating the highest-ordered derivative term in Eq. (B-2) to the rest of the terms. In control systems theory, the set of first-order differential equations in Eq. (B-9) is called the **state equations**, and $x_1, x_2, \ldots, x_n$ are called the **state variables**.

Definition of State Variables

The **state** of a system refers to the **past**, **present**, and **future** conditions of the system. From a mathematical perspective, it is convenient to define a set of **state variables** and **state equations** to model dynamic systems. As it turns out, the variables $x_1(t), x_2(t), \ldots, x_n(t)$ defined in Eq. (B-8) are the state variables of the nth-order system described by Eq. (B-2), and the n first-order differential equations are the state equations. In general, there are some basic rules regarding the definition of a state variable and what constitutes a state equation. The state variables must satisfy the following conditions:

1. At any initial time $t = t_0$, the state variables $x_1(t_0), x_2(t_0), \ldots, x_n(t_0)$ define the **initial states** of the system.

2. Once the inputs of the system for $t \geq t_0$ and the initial states just defined are specified, the state variables should completely define the future behavior of the system.

*The state variables of a system are defined as a **minimal set** of variables, $x_1(t), x_2(t), \ldots, x_n(t)$, such that knowledge of these variables at any time t_0 and information on the input excitation subsequently applied are sufficient to determine the state of the system at any time $t > t_0$.*

The Output Equation

One should not confuse the state variables with the outputs of a system. An output of a system is a variable that can be **measured**, but a state variable does not always satisfy this requirement. For instance, in an electric motor, such state variables as the winding current, rotor velocity, and displacement can be measured physically, and these variables all qualify as output variables. On the other hand, magnetic flux can also be regarded as a state variable in an electric motor, since it represents the past, present, and future states of the motor, but it cannot be measured directly during operation and therefore does not ordinarily qualify as an output variable. In general, an output variable can be expressed as an algebraic combination of the state variables. For the system described by Eq. (B-2), if $y(t)$ is designated as the output, then the output equation is simply $y(t) = x_1(t)$.

Difference Equations

Because digital controllers are frequently used in control systems, it is necessary to establish equations that relate digital and discrete-time signals. Just as differential equations are used to represent systems with analog signals, difference equations are used for systems with discrete of digital data. Difference equations are also used to approximate differential equations, since the former are more easily programmed on a digital computer and are easier to solve.

A linear nth-order difference equation with constant coefficients can be written as

$$y(k + n) + a_{n-1}y(k + n - 1) + \cdots + a_1y(k + 1) + a_0y(k) = f(k) \quad \text{(B-10)}$$

where $y(i)$, $i = k, k + 1, \ldots, k + n$ denotes the discrete dependent variable y at the ith instant if the independent variable is time. In general, the independent variable can be any real quantity.

Similar to the case of the analog systems, it is convenient to use a set of first-order difference equations, or state equations, to represent a high-order difference equation. For the difference equation in Eq. (B-10), if we let

$$
\begin{aligned}
x_1(k) &= y(k) \\
x_2(k) &= x_1(k + 1) = y(k + 1) \\
&\vdots \\
x_{n-1}(k) &= x_{n-2}(k + 1) = y(k + n - 2) \\
x_n(k) &= x_{n-1}(k + 1) = y(k + n - 1)
\end{aligned}
\tag{B-11}
$$

then by equating the highest-order term to the rest, the equation is written as

$$
x_n(k + 1) = -a_0 x_1(k) - a_1 x_2(k) - \cdots - a_{n-1} x_n(k) + f(k)
\tag{B-12}
$$

The first $n - 1$ state equations are taken directly from the last $n - 1$ equations in Eq. (B-11), and the last one is given by Eq. (B-12). The n state equations are written in vector-matrix form:

$$
\mathbf{x}(k + 1) = \mathbf{A}\mathbf{x}(k) + \mathbf{B}u(k)
\tag{B-13}
$$

where

$$
\mathbf{x}(k) = \begin{bmatrix} x_1(k) \\ x_2(k) \\ \vdots \\ x_n(k) \end{bmatrix}
\tag{B-14}
$$

is the $n \times 1$ state vector, and

$$
\mathbf{A} = \begin{bmatrix}
0 & 1 & 0 & \cdots & 0 \\
0 & 0 & 1 & \cdots & 0 \\
\vdots & \vdots & \vdots & \ddots & \vdots \\
0 & 0 & 0 & 0 & 1 \\
-a_0 & -a_1 & -a_2 & \cdots & -a_{n-1}
\end{bmatrix}
\quad
\mathbf{B} = \begin{bmatrix} 0 \\ 0 \\ \vdots \\ 0 \\ 1 \end{bmatrix}
\tag{B-15}
$$

and $u(k) = f(k)$.

► REFERENCES

1. C. R. Wylie, Jr., *Advanced Engineering Mathematics*, 2nd ed. McGraw-Hill, New York, 1960.
2. B. C. Kuo, *Linear Networks and Systems*, McGraw-Hill, New York, 1967.

Appendix C
Elementary Matrix Theory and Algebra

ISBN 0-471-13476-7

Elementary Matrix Theory and Algebra

▶ C-1 ELEMENTARY MATRIX THEORY

In the study of modern control theory, it is often desirable to use matrix notation to simplify complex mathematical expressions. The matrix notation usually makes the equations much easier to handle and manipulate.

As a motivation to the reason of using matrix notation, let us consider the following set of n simultaneous algebraic equations:

$$
\begin{aligned}
a_{11}x_1 + a_{12}x_2 + \cdots + a_{1n}x_n &= y_1 \\
a_{21}x_1 + a_{22}x_2 + \cdots + a_{2n}x_n &= y_2 \\
&\cdots\cdots\cdots\cdots\cdots\cdots\cdots\cdots \\
a_{n1}x_1 + a_{n2}x_2 + \cdots + a_{nn}x_n &= y_n
\end{aligned}
\tag{C-1}
$$

We may use the matrix equation

$$
\mathbf{Ax} = \mathbf{y}
\tag{C-2}
$$

as a simplified representation of Eq. (C-1). The symbols $\mathbf{A}$, $\mathbf{x}$, and $\mathbf{y}$ are defined as **matrices**, which contain the coefficients and variables of the original equations as their elements. In terms of matrix algebra, which will be discussed shortly, Eq. (C-2) can be stated as *the product of the matrices* $\mathbf{A}$ *and* $\mathbf{x}$ *is equal to the matrix* $\mathbf{y}$. The three matrices involved are defined as

$$
\mathbf{A} =
\begin{bmatrix}
a_{11} & a_{12} & \cdots & a_{1n} \\
a_{21} & a_{22} & \cdots & a_{2n} \\
\vdots & \vdots & \ddots & \vdots \\
a_{n1} & a_{n2} & \cdots & a_{nn}
\end{bmatrix}
\tag{C-3}
$$

$$
\mathbf{x} =
\begin{bmatrix}
x_1 \\
x_2 \\
\vdots \\
x_n
\end{bmatrix}
\tag{C-4}
$$

$$
\mathbf{y} =
\begin{bmatrix}
y_1 \\
y_2 \\
\vdots \\
y_n
\end{bmatrix}
\tag{C-5}
$$

which are simply bracketed arrays of coefficients and variables. These examples of matrices prompted the following definition of a matrix.

C-1-1   Definition of a Matrix

• It is important to distinguish between a matrix and a determinant.

A matrix is a collection of elements arranged in a rectangular or square array. There are several ways of bracketing a matrix. In this text, the square brackets, such as those in Eqs. (C-3) through (C-5), are used to represent matrices. It is important to distinguish between a **matrix** and a **determinant**. The basic characteristics of these are listed as follows:

Matrix	**Determinant**
• An array of numbers or elements with n rows and m columns.	• An array of numbers or elements with n rows and n columns (always square).
• Does not have a value, although a square matrix ($n = m$) has a determinant.	• Has a value.

Some important definitions of matrices are given in the following paragraphs.

Matrix Elements: When a matrix is written

$$\mathbf{A} = \begin{bmatrix} a_{11} & a_{12} & a_{13} \\ a_{21} & a_{22} & a_{23} \\ a_{31} & a_{32} & a_{33} \end{bmatrix} \tag{C-6}$$

where a_{ij} is defined as the element in the ith **row** and the jth **column** of the matrix. As a rule, we always refer to the row first and the column last.

Order of a Matrix: *The order of a matrix refers to the total number of rows and columns of the matrix.* For example, the matrix in Eq. (C-6) has three rows and three columns and is called a 3×3 (three-by-three) matrix. A matrix with n rows and m columns is termed $n \times m$, or n by m.

Square Matrix: *A square matrix is one that has the same number of rows as columns.*

Column Matrix: *A column matrix is one that has one column and more than one row, that is, an $m \times 1$ matrix, $m > 1$.* Quite often, a column matrix is referred to as a **column vector** or simply an **m-vector** if there are m rows and one column. The matrix in Eq. (C-4) is a typical n-vector.

Row Matrix: *A row matrix is one that has one row and more than one column, that is, a $1 \times n$ matrix, where $n > 1$.* A row matrix can also be referred as a **row-vector**.

Diagonal Matrix: *A diagonal matrix is a square matrix with $a_{ij} = 0$ for all $i \neq j$.* Examples of a diagonal matrix are

$$\begin{bmatrix} a_{11} & 0 & 0 \\ 0 & a_{22} & 0 \\ 0 & 0 & a_{33} \end{bmatrix} \qquad \begin{bmatrix} 5 & 0 \\ 0 & 3 \end{bmatrix}$$

Unity Matrix (Identity Matrix):   *A unity matrix is a diagonal matrix with all the elements on the main diagonal ($i = j$) equal to 1.* A unity matrix is often designated by **I** or **U**. An example of a unity matrix is

$$\mathbf{I} = \begin{bmatrix} 1 & 0 & 0 \\ 0 & 1 & 0 \\ 0 & 0 & 1 \end{bmatrix} \tag{C-7}$$

Null Matrix: *A null matrix is one whose elements are all equal to zero.*

Symmetric Matrix: *A symmetric matrix is a square matrix that satisfies the condition* $a_{ij} = a_{ji}$ *for all i and j.* A symmetric matrix has the property that if its rows are interchanged with its columns, the same matrix is obtained. Two examples of the symmetric matrix are

$$\mathbf{A} = \begin{bmatrix} 6 & 5 & 1 \\ 5 & 0 & 10 \\ 1 & 10 & -1 \end{bmatrix} \qquad \mathbf{B} = \begin{bmatrix} 1 & -4 \\ -4 & 1 \end{bmatrix} \tag{C-8}$$

Determinant of a Matrix: *With each square matrix, a determinant having the same elements and order as the matrix may be defined. The determinant of a square matrix* **A** *is designated by*

$$\det \mathbf{A} = \Delta_{\mathbf{A}} = |\mathbf{A}| \tag{C-9}$$

For example, the determinant of the matrix in Eq. (C-6) is

$$|\mathbf{A}| = \begin{vmatrix} a_{11} & a_{12} & a_{13} \\ a_{21} & a_{22} & a_{23} \\ a_{31} & a_{32} & a_{33} \end{vmatrix} \tag{C-10}$$

Cofactor of a Determinant Element: *Given any nth-order determinant* $|\mathbf{A}|$, *the cofactor* A_{ij} *of any element* a_{ij} *is the determinant obtained by eliminating all elements of the ith row and jth column and then multiplied by* $(-1)^{i+j}$. For example, the cofactor of the element a_{11} of $|\mathbf{A}|$ in Eq. (C-10) is

$$A_{11} = (-1)^{1+1} \begin{vmatrix} a_{22} & a_{23} \\ a_{32} & a_{33} \end{vmatrix} = a_{22}a_{33} - a_{23}a_{32} \tag{C-11}$$

In general, the value of a determinant can be written in terms of the cofactors. Let **A** be an $n \times n$ matrix, then the determinant of **A** can be written in terms of the cofactor of any row or the cofactor of any column. That is,

$$\det \mathbf{A} = \sum_{j=1}^{n} a_{ij} A_{ij} \qquad (i = 1, \text{ or } 2, \dots, \text{ or } n) \tag{C-12}$$

or

$$\det \mathbf{A} = \sum_{i=1}^{n} a_{ij} A_{ij} \qquad (j = 1, \text{ or } 2, \dots, \text{ or } n) \tag{C-13}$$

▶ **EXAMPLE C-1** The value of the determinant in Eq. (C-10) is

$$\begin{aligned} \det \mathbf{A} = |\mathbf{A}| &= a_{11}A_{11} + a_{12}A_{12} + a_{13}A_{13} \\ &= a_{11}(a_{22}a_{33} - a_{23}a_{32}) - a_{12}(a_{21}a_{33} - a_{23}a_{31}) \\ &\quad + a_{13}(a_{21}a_{32} - a_{22}a_{31}) \end{aligned} \tag{C-14}$$

◀

Singular Matrix: *A square matrix is said to be singular if the value of its determinant is zero.* If a square matrix has a nonzero determinant, it is called a **nonsingular matrix**. When a matrix is singular, it usually means that not all the rows or not all the columns of the matrix are independent of each other. When the matrix is used to represent a set of algebraic equations, singularity of the matrix means that these equations are not independent of each other.

► **EXAMPLE C-2** Consider the following set of equations:

$$\begin{aligned} 2x_1 - 3x_2 + x_3 &= 0 \\ -x_1 + x_2 + x_3 &= 0 \\ x_1 - 2x_2 + 2x_3 &= 0 \end{aligned}$$
(C-15)

The third equation is equal to the sum of the first two. Thus, these three equations are not completely independent. In matrix form, these equations may be written as

$$\mathbf{Ax} = \mathbf{0}$$
(C-16)

where

$$\mathbf{A} = \begin{bmatrix} 2 & -3 & 1 \\ -1 & 1 & 1 \\ 1 & -2 & 2 \end{bmatrix} \qquad \mathbf{x} = \begin{bmatrix} x_1 \\ x_2 \\ x_3 \end{bmatrix}$$
(C-17)

and $\mathbf{0}$ is a 3×1 null matrix. The determinant of $\mathbf{A}$ is 0, and, thus, the matrix $\mathbf{A}$ is singular. In this case, the rows of $\mathbf{A}$ are dependent. ◄

Transpose of a Matrix: *The transpose of a matrix $\mathbf{A}$ is defined as the matrix that is obtained by interchanging the corresponding rows and columns in $\mathbf{A}$. Let $\mathbf{A}$ be an $n \times m$ matrix that is represented by*

$$\mathbf{A} = [a_{ij}]_{n,m}$$
(C-18)

The transpose of $\mathbf{A}$, denoted by $\mathbf{A}'$, is given by

$$\mathbf{A}' = \text{transpose of } \mathbf{A} = [a_{ij}]_{m,n}$$
(C-19)

Notice that the order of $\mathbf{A}$ is $n \times m$, but the order of $\mathbf{A}'$ is $m \times n$.

► **EXAMPLE C-3** Consider the 2×3 matrix

$$\mathbf{A} = \begin{bmatrix} 3 & 2 & 1 \\ 0 & -1 & 5 \end{bmatrix}$$
(C-20)

The transpose of $\mathbf{A}$ is obtained by interchanging the rows and the columns.

$$\mathbf{A}' = \begin{bmatrix} 3 & 0 \\ 2 & -1 \\ 1 & 5 \end{bmatrix}$$
(C-21)

◄

Some Properties of Matrix Transpose

1. $(\mathbf{A}')' = \mathbf{A}$ (C-22)
2. $(k\mathbf{A})' = k\mathbf{A}'$, where k is a scalar (C-23)
3. $(\mathbf{A} + \mathbf{B})' = \mathbf{A}' + \mathbf{B}'$ (C-24)
4. $(\mathbf{AB})' = \mathbf{B}'\mathbf{A}'$ (C-25)

Adjoint of a Matrix: *Let $\mathbf{A}$ be a square matrix of order n. The adjoint matrix of $\mathbf{A}$, denoted by* adj $\mathbf{A}$, *is defined as*

$$\text{adj } \mathbf{A} = [A_{ij} \text{ of det } \mathbf{A}]'_{n,n}$$
(C-26)

where A_{ij} denotes the cofactor of a_{ij}.

► **EXAMPLE C-4** Consider the 2×2 matrix

$$\mathbf{A} = \begin{bmatrix} a_{11} & a_{12} \\ a_{21} & a_{22} \end{bmatrix} \tag{C-27}$$

The cofactors are $A_{11} = a_{22}$, $A_{12} = -a_{21}$, $A_{21} = -a_{12}$, and $A_{22} = a_{11}$. Thus, the adjoint matrix of $\mathbf{A}$ is

$$\text{adj } \mathbf{A} = \begin{bmatrix} A_{11} & A_{12} \\ A_{21} & A_{22} \end{bmatrix}' = \begin{bmatrix} a_{22} & -a_{21} \\ -a_{12} & a_{11} \end{bmatrix}' = \begin{bmatrix} a_{22} & -a_{12} \\ -a_{21} & a_{11} \end{bmatrix} \tag{C-28}$$

◄

Trace of a Square Matrix: *Given an $n \times n$ matrix with elements a_{ij}, the* **trace of A**, *denoted as* tr(**A**), *is defined as the sum of the elements on the main diagonal of* **A**; *that is*

$$\text{tr}(\mathbf{A}) = \sum_{i=1}^{n} a_{ii} \tag{C-29}$$

The trace of a matrix has the following properties:

1. $\text{tr}(\mathbf{A}') = \text{tr}(\mathbf{A})$ (C-30)
2. For $n \times n$ square matrices **A** and **B**,
$$\text{tr}(\mathbf{A} + \mathbf{B}) = \text{tr}(\mathbf{A}) + \text{tr}(\mathbf{B}) \tag{C-31}$$

► C-2 MATRIX ALGEBRA

When carrying out matrix operations, it is necessary to define matrix algebra in the form of addition, subtraction, multiplication, and division.

C-2-1 Equality of Matrices

Two matrices **A** and **B** are said to be equal to each other if they satisfy the following conditions:

1. They are of the same order.
2. The corresponding elements are equal; that is,
$$a_{ij} = b_{ij} \qquad \text{for every } i \text{ and } j \tag{C-32}$$

► **EXAMPLE C-5**

$$\mathbf{A} = \begin{bmatrix} a_{11} & a_{12} \\ a_{21} & a_{22} \end{bmatrix} = \mathbf{B} = \begin{bmatrix} b_{11} & b_{12} \\ b_{21} & b_{22} \end{bmatrix} \tag{C-33}$$

implies that $a_{11} = b_{11}$, $a_{12} = b_{12}$, $a_{21} = b_{21}$, $a_{22} = b_{22}$. ◄

C-2-2 Addition and Subtraction of Matrices

Two matrices **A** and **B** can be added or subtracted to form $\mathbf{A} \pm \mathbf{B}$ if they are of the same order. That is

$$\mathbf{A} \pm \mathbf{B} = [a_{ij}]_{n,m} \pm [b_{ij}]_{n,m} = \mathbf{C} = [c_{ij}]_{n,m} \tag{C-34}$$

where

$$c_{ij} = a_{ij} \pm b_{ij} \qquad \text{for all } i \text{ and } j. \tag{C-35}$$

The order of the matrices is preserved after addition or subtraction.

▶ **EXAMPLE C-6** Consider the matrices

$$\mathbf{A} = \begin{bmatrix} 3 & 2 \\ -1 & 4 \\ 0 & -1 \end{bmatrix} \quad \mathbf{B} = \begin{bmatrix} 0 & 3 \\ -1 & 2 \\ 1 & 0 \end{bmatrix} \tag{C-36}$$

which are of the same order. Then the sum of **A** and **B** is

$$\mathbf{C} = \mathbf{A} + \mathbf{B} = \begin{bmatrix} 3+0 & 2+3 \\ -1-1 & 4+2 \\ 0+1 & -1+0 \end{bmatrix} = \begin{bmatrix} 3 & 5 \\ -2 & 6 \\ 1 & -1 \end{bmatrix} \tag{C-37}$$

◀

C-2-3 Associative Law of Matrix (Addition and Subtraction)

The associative law of scalar algebra still holds for matrix addition and subtraction. That is,

$$(\mathbf{A} + \mathbf{B}) + \mathbf{C} = \mathbf{A} + (\mathbf{B} + \mathbf{C}) \tag{C-38}$$

C-2-4 Commutative Law of Matrix (Addition and Subtraction)

The commutative law for matrix addition and subtraction states that the following matrix relationship is true:

$$\mathbf{A} + \mathbf{B} + \mathbf{C} = \mathbf{B} + \mathbf{C} + \mathbf{A} = \mathbf{A} + \mathbf{C} + \mathbf{B} \tag{C-39}$$

as well as other possible commutative combinations.

C-2-5 Matrix Multiplication

The matrices **A** and **B** may be multiplied together to form the product **AB** if they are **conformable**. This means that the number of columns of **A** must equal the number of rows of **B**. In other words, let

$$\mathbf{A} = [a_{ij}]_{n,p} \quad \mathbf{B} = [b_{ij}]_{q,m} \tag{C-40}$$

Then **A** and **B** are conformable to form the product

$$\mathbf{C} = \mathbf{AB} = [a_{ij}]_{n,p}[b_{ij}]_{q,m} = [c_{ij}]_{n,m} \tag{C-41}$$

if and only if $p = q$. The matrix **C** will have the same number of rows as **A** and the same number of columns as **B**.

It is important to note that **A** and **B** may be conformable to form **AB**, but they may not be conformable for the product **BA**, unless in Eq. (C-41), n also equals m. This points out an important fact that *the commutative law is not generally valid for matrix multiplication.* It is also noteworthy that even though **A** and **B** are conformable for both **AB** and **BA**, usually $\mathbf{AB} \neq \mathbf{BA}$. The following references are made with respect to matrix manipulation whenever they exist:

• Two matrices can be multiplied only if they are conformable.

$$\mathbf{AB} = \mathbf{A} \text{ postmultiplied by } \mathbf{B} \quad \text{or} \quad \mathbf{B} \text{ premultiplied by } \mathbf{A} \tag{C-42}$$

C-2-6 Rules of Matrix Multiplication

When the matrices **A** ($n \times p$) and **B** ($p \times m$) are conformable to form the matrix **C** = **AB**, the ijth element of **C**, c_{ij}, is given by

$$c_{ij} = \sum_{k=1}^{p} a_{ik}b_{kj} \tag{C-43}$$

for $i = 1, 2, \ldots, n$, and $j = 1, 2, \ldots, m$.

▶ **EXAMPLE C-7** Given the matrices

$$\mathbf{A} = [a_{ij}]_{2,3} \qquad \mathbf{B} = [b_{ij}]_{3,1} \tag{C-44}$$

The two matrices are conformable for the product **AB** but not for **BA**. Thus,

$$\mathbf{AB} = \begin{bmatrix} a_{11} & a_{12} & a_{13} \\ a_{21} & a_{22} & a_{23} \end{bmatrix} \begin{bmatrix} b_{11} \\ b_{21} \\ b_{31} \end{bmatrix} = \begin{bmatrix} a_{11}b_{11} + a_{12}b_{21} + a_{13}b_{31} \\ a_{21}b_{11} + a_{22}b_{21} + a_{23}b_{31} \end{bmatrix} \tag{C-45}$$

◀

▶ **EXAMPLE C-8** Given the matrices

$$\mathbf{A} = \begin{bmatrix} 3 & -1 \\ 0 & 1 \\ 2 & 0 \end{bmatrix} \qquad \mathbf{B} = \begin{bmatrix} 1 & 0 & -1 \\ 2 & 1 & 0 \end{bmatrix} \tag{C-46}$$

The two matrices are conformable for **AB** and **BA**.

$$\mathbf{AB} = \begin{bmatrix} 3 & -1 \\ 0 & 1 \\ 2 & 0 \end{bmatrix} \begin{bmatrix} 1 & 0 & -1 \\ 2 & 1 & 0 \end{bmatrix} = \begin{bmatrix} 1 & -1 & -3 \\ 2 & 1 & 0 \\ 2 & 0 & -2 \end{bmatrix} \tag{C-47}$$

$$\mathbf{BA} = \begin{bmatrix} 1 & 0 & -1 \\ 2 & 1 & 0 \end{bmatrix} \begin{bmatrix} 3 & -1 \\ 0 & 1 \\ 2 & 0 \end{bmatrix} = \begin{bmatrix} 1 & -1 \\ 6 & -1 \end{bmatrix} \tag{C-48}$$

Therefore, even though **AB** and **BA** both exist, they are not equal. In fact, in this case the products are not of the same order. ◀

Although the commutative law does not hold in general for matrix multiplication, the **associative** and **distributive** laws are valid. For the distributive law, we state that

$$\mathbf{A}(\mathbf{B} + \mathbf{C}) = \mathbf{AB} + \mathbf{AC} \tag{C-49}$$

if the products are conformable. For the associative law,

$$(\mathbf{AB})\mathbf{C} = \mathbf{A}(\mathbf{BC}) \tag{C-50}$$

if the product is conformable.

C-2-7   Multiplication by a Scalar *k*

Multiplying a matrix **A** *by any scalar k is equivalent to multiplying each element of* **A** *by k.*

C-2-8   Inverse of a Matrix (Matrix Division)

• Only square, nonsingular matrices have inverses.

In the algebra of scalar quantities, when we write $y = ax$, it implies that $x = y/a$ is also true. In matrix algebra, if $\mathbf{Ax} = \mathbf{y}$, the it *may be possible* to write

$$\mathbf{x} = \mathbf{A}^{-1}\mathbf{y} \tag{C-51}$$

where $\mathbf{A}^{-1}$ denotes the **matrix inverse** of **A**. The conditions that $\mathbf{A}^{-1}$ exists are

1. **A** is a square matrix.
2. **A** must be nonsingular.

3. If $\mathbf{A}^{-1}$ exists, it is given by

$$\mathbf{A}^{-1} = \frac{\text{adj } \mathbf{A}}{|\mathbf{A}|} \tag{C-52}$$

▶ **EXAMPLE C-9** Given the matrix

$$\mathbf{A} = \begin{bmatrix} a_{11} & a_{12} \\ a_{21} & a_{22} \end{bmatrix} \tag{C-53}$$

the inverse of $\mathbf{A}$ is given by

• The adjoint of a 2 by 2 matrix is obtained by interchanging the two main diagonal elements and changing the signs of the elements off the diagonal.

$$\mathbf{A}^{-1} = \frac{\text{adj } \mathbf{A}}{|\mathbf{A}|} = \frac{\begin{bmatrix} a_{22} & -a_{12} \\ -a_{21} & a_{11} \end{bmatrix}}{a_{11}a_{22} - a_{12}a_{21}} \tag{C-54}$$

where for $\mathbf{A}$ to be nonsingular, $|\mathbf{A}| \neq 0$, or $a_{11}a_{22} - a_{12}a_{21} \neq 0$.

Equation (C-54) shows that adj $\mathbf{A}$ of a 2×2 matrix is obtained by *interchanging the two elements on the main diagonal and changing the signs of the elements off the diagonal of $\mathbf{A}$.* ◀

▶ **EXAMPLE C-10** Given the matrix

$$\mathbf{A} = \begin{bmatrix} a_{11} & a_{12} & a_{13} \\ a_{21} & a_{22} & a_{23} \\ a_{31} & a_{32} & a_{33} \end{bmatrix} \tag{C-55}$$

To find the inverse of $\mathbf{A}$, the adjoint of $\mathbf{A}$ is

$$\text{adj } \mathbf{A} = \begin{bmatrix} a_{22}a_{33} - a_{23}a_{32} & (-a_{12}a_{33} - a_{13}a_{32}) & a_{12}a_{23} - a_{13}a_{22} \\ -(a_{21}a_{33} - a_{23}a_{31}) & a_{11}a_{33} - a_{13}a_{31} & -(a_{11}a_{23} - a_{21}a_{13}) \\ a_{21}a_{32} - a_{22}a_{31} & (-a_{11}a_{32} - a_{12}a_{31}) & a_{11}a_{22} - a_{12}a_{21} \end{bmatrix} \tag{C-56}$$

The determinant of $\mathbf{A}$ is

$$|\mathbf{A}| = a_{11}a_{22}a_{33} + a_{12}a_{23}a_{31} + a_{13}a_{32}a_{21} - a_{13}a_{22}a_{31} - a_{12}a_{21}a_{33} - a_{11}a_{23}a_{32} \tag{C-57}$$

◀

Some Properties of Matrix Inverse

1. $\mathbf{A}\mathbf{A}^{-1} = \mathbf{A}^{-1}\mathbf{A} = \mathbf{I}$ (C-58)

2. $(\mathbf{A}^{-1})^{-1} = \mathbf{A}$ (C-59)

3. In matrix algebra, in general, $\mathbf{AB} = \mathbf{AC}$ does not necessarily imply that $\mathbf{B} = \mathbf{C}$.

The reader can easily construct an example to illustrate this property. However, if $\mathbf{A}$ is a square, nonsingular matrix, we can premultiply both sides of $\mathbf{AB} = \mathbf{AC}$ by $\mathbf{A}^{-1}$. Then,

$$\mathbf{A}^{-1}\mathbf{AB} = \mathbf{A}^{-1}\mathbf{AC} \tag{C-60}$$

which leads to $\mathbf{B} = \mathbf{C}$.

4. If $\mathbf{A}$ and $\mathbf{B}$ are square matrices and are nonsingular, then

$$(\mathbf{AB})^{-1} = \mathbf{B}^{-1}\mathbf{A}^{-1} \tag{C-61}$$

C-2-9 Rank of a Matrix

The rank of a matrix $\mathbf{A}$ is the maximum number of linearly independent columns of $\mathbf{A}$; that is, it is the order of the largest nonsingular matrix contained in $\mathbf{A}$.

▶ **EXAMPLE C-11** Several examples on the rank of a matrix are as follows:

$$\begin{bmatrix} 0 & 1 \\ 0 & 0 \end{bmatrix} \quad \text{rank} = 1 \qquad \begin{bmatrix} 0 & 5 & 1 & 4 \\ 3 & 0 & 3 & 2 \end{bmatrix} \quad \text{rank} = 2$$

$$\begin{bmatrix} 3 & 9 & 2 \\ 1 & 3 & 0 \\ 2 & 6 & 1 \end{bmatrix} \quad \text{rank} = 2 \qquad \begin{bmatrix} 3 & 0 & 0 \\ 1 & 2 & 0 \\ 0 & 0 & 1 \end{bmatrix} \quad \text{rank} = 3$$

◀

The following properties are useful in the determination of the rank of a matrix. Given an $n \times m$ matrix **A**,

1. Rank of $\mathbf{A}' =$ Rank of **A**.
2. Rank of $\mathbf{A}'\mathbf{A} =$ Rank of **A**.
3. Rank of $\mathbf{AA}' =$ Rank of **A**.

Properties 2 and 3 are useful in the determination of rank; since $\mathbf{A}'\mathbf{A}$ and $\mathbf{AA}'$ are always square, the rank condition can be checked by evaluating the determinant of these matrices.

▶ C-3 COMPUTER-AIDED SOLUTIONS OF MATRICES

Many commercial software packages such as MATLAB, **Maple** and **MATHCAD** contain routines for matrix manipulations.

▶ REFERENCES

1. R. Bellman, *Introduction to Matrix Analysis*, McGraw-Hill, New York, 1960.
2. F. Ayres, Jr., *Theory and Problems of Matrices*, Shaum's Outline Series, McGraw-Hill, New York, 1962.

Appendix D
Laplace Transform Table

TO ACCOMPANY

AUTOMATIC CONTROL SYSTEMS
EIGHTH EDITION

BY

BENJAMIN C. KUO

FARID GOLNARAGHI

Laplace Transform Table

Laplace Transform $F(s)$	Time Function $f(t)$
1	Unit-impulse function $\delta(t)$
$\dfrac{1}{s}$	Unit-step function $u_s(t)$
$\dfrac{1}{s^2}$	Unit-ramp function t
$\dfrac{n!}{s^{n+1}}$	$t^n (n = \text{positive integer})$
$\dfrac{1}{s + \alpha}$	$e^{-\alpha t}$
$\dfrac{1}{(s + \alpha)^2}$	$te^{-\alpha t}$
$\dfrac{n!}{(s + \alpha)^{n+1}}$	$t^n e^{-\alpha t} (n = \text{positive integer})$
$\dfrac{1}{(s + \alpha)(s + \beta)}$	$\dfrac{1}{\beta - \alpha}(e^{-\alpha t} - e^{-\beta t})(\alpha \neq \beta)$
$\dfrac{s}{(s + \alpha)(s + \beta)}$	$\dfrac{1}{\beta - \alpha}(\beta e^{-\beta t} - \alpha e^{-\alpha t})(\alpha \neq \beta)$
$\dfrac{1}{s(s + \alpha)}$	$\dfrac{1}{\alpha}(1 - e^{-\alpha t})$
$\dfrac{1}{s(s + \alpha)^2}$	$\dfrac{1}{\alpha^2}(1 - e^{-\alpha t} - \alpha t e^{-\alpha t})$
$\dfrac{1}{s^2(s + \alpha)}$	$\dfrac{1}{\alpha^2}(\alpha t - 1 + e^{-\alpha t})$
$\dfrac{1}{s^2(s + \alpha)^2}$	$\dfrac{1}{\alpha^2}\left[t - \dfrac{2}{\alpha} + \left(t + \dfrac{2}{\alpha}\right)e^{-\alpha t}\right]$
$\dfrac{s}{(s + \alpha)^2}$	$(1 - \alpha t)e^{-\alpha t}$

(*continued*)

Laplace Transform $F(s)$	Time Function $f(t)$
$\dfrac{\omega_n}{s^2 + \omega_n^2}$	$\sin \omega_n t$
$\dfrac{s}{s^2 + \omega_n^2}$	$\cos \omega_n t$
$\dfrac{\omega_n^2}{s(s^2 + \omega_n^2)}$	$1 - \cos \omega_n t$
$\dfrac{\omega_n^2(s + \alpha)}{s^2 + \omega_n^2}$	$\omega_n \sqrt{\alpha^2 + \omega_n^2} \sin(\omega_n t + \theta)$ where $\theta = \tan^{-1}(\omega_n/\alpha)$
$\dfrac{\omega_n}{(s + \alpha)(s^2 + \omega_n^2)}$	$\dfrac{\omega_n}{\alpha^2 + \omega_n^2} e^{-\alpha t} + \dfrac{1}{\sqrt{\alpha^2 + \omega_n^2}} \sin(\omega_n t - \theta)$ where $\theta = \tan^{-1}(\omega_n/\alpha)$
$\dfrac{\omega_n^2}{s^2 + 2\zeta\omega_n s + \omega_n^2}$	$\dfrac{\omega_n}{\sqrt{1 - \zeta^2}} e^{-\zeta\omega_n t}\sin \omega_n \sqrt{1 - \zeta^2}\, t \qquad (\zeta < 1)$
$\dfrac{\omega_n^2}{s(s^2 + 2\zeta\omega_n s + \omega_n^2)}$	$1 - \dfrac{1}{\sqrt{1 - \zeta^2}} e^{-\zeta\omega_n t}\sin(\omega_n \sqrt{1 - \zeta^2}\, t + \theta)$ where $\theta = \cos^{-1}\zeta \qquad (\zeta < 1)$
$\dfrac{s\omega_n^2}{s^2 + 2\zeta\omega_n s + \omega_n^2}$	$\dfrac{-\omega_n^2}{\sqrt{1 - \zeta^2}} e^{-\zeta\omega_n t}\sin(\omega_n \sqrt{1 - \zeta^2}\, t - \theta)$ where $\theta = \cos^{-1}\zeta \qquad (\zeta < 1)$
$\dfrac{\omega_n^2(s + \alpha)}{s^2 + 2\zeta\omega_n s + \omega_n^2}$	$\omega_n \sqrt{\dfrac{\alpha^2 - 2\alpha\zeta\omega_n + \omega_n^2}{1 - \zeta^2}} e^{-\zeta\omega_n t}\sin(\omega_n \sqrt{1 - \zeta^2}\, t + \theta)$ where $\theta = \tan^{-1}\dfrac{\omega_n \sqrt{1 - \zeta^2}}{\alpha - \zeta\omega_n} \qquad (\zeta < 1)$
$\dfrac{\omega_n^2}{s^2(s^2 + 2\zeta\omega_n s + \omega_n^2)}$	$t - \dfrac{2\zeta}{\omega_n} + \dfrac{1}{\omega_n \sqrt{1 - \zeta^2}} e^{-\zeta\omega_n t}\sin(\omega_n \sqrt{1 - \zeta^2}\, t + \theta)$ where $\theta = \cos^{-1}(2\zeta^2 - 1) \qquad (\zeta < 1)$

Appendix E
Operational Amplifiers

TO ACCOMPANY

AUTOMATIC CONTROL SYSTEMS
EIGHTH EDITION

BY

BENJAMIN C. KUO

FARID GOLNARAGHI

Operational Amplifiers

▶ E-1 OPERATIONAL AMPLIFIERS

Operational amplifiers, or simply **op-amps**, offer a convenient way to build, implement, or realize continuous-data or s-domain transfer functions. In control systems, op-amps are often used to implement the controllers or compensators that evolve from the control-system design process, so in this appendix we illustrate common op-amp configurations. An in-depth presentation of op-amps is beyond the scope of this text. For those interested, many texts are available that are devoted to all aspects of op-amp circuit design and applications [References 1 and 2].

Our primary goal here is to show how to implement first-order transfer functions with op-amps, while keeping in mind that higher-order transfer functions are also important. In fact, simple high-order transfer functions can be implemented by connecting first-order op-amp configurations together. Only a representative sample of the multitude of op-amp configurations will be discussed.

Some of the practical issues associated with op-amps are demonstrated in simlab (see Chapter 11).

E-1-1   The Ideal Op-Amp

When good engineering practice is used, an op-amp circuit can be accurately analyzed by considering the op-amp to be ideal. The ideal op-amp circuit is shown in Fig. E-1, and has the following properties:

1. The voltage between the $+$ and $-$ terminals is zero, that is, $e^+ = e^-$. This property is commonly called the *virtual ground or virtual short.*

2. The currents into the $+$ and $-$ input terminals are zero. Thus, the input impedance is infinite.

3. The impedance seen looking into the output terminal is zero. Thus, the output is an ideal voltage source.

4. The input-output relationship is $e_o = A(e^+ - e^-)$ where the gain A approaches infinity.
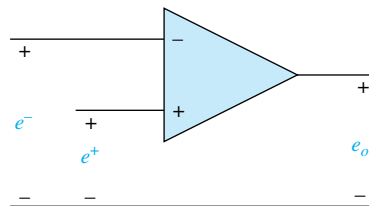
Figure E-1   Schematic diagram of an op-amp.

The input-output relationship for many op-amp configurations can be determined by using these principles. An op-amp cannot be used as shown in Fig. E-1. Rather, linear operation requires the addition of feedback of the output signal to the − input terminal.

E-1-2 Sums and Differences

As illustrated in the last chapter, one of the most fundamental elements in a block diagram or an SFG is the addition or subtraction of signals. When these signals are voltages, op-amps provide a simple way to add or subtract signals as shown in Fig. E-2,
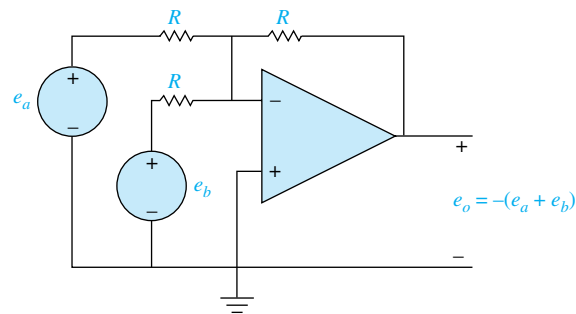
(a)
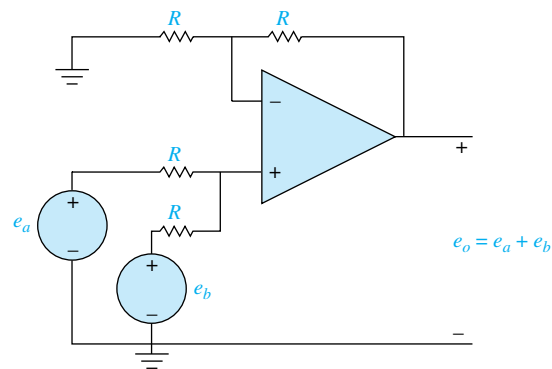
(b)
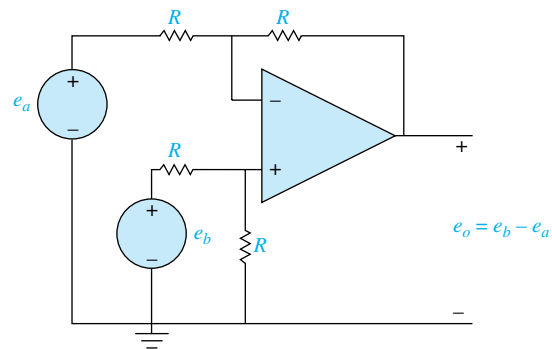
(c)

Figure E-2 Op-amps used to add and subtract signals.

where all the resistors have the same value. Using superposition and the ideal proper-ties given in the preceding section, the input-output relationship in Fig. E-2(a) is $v_o = -(v_a - v_b)$. Thus, the output is the negative sum of the input voltages. When a posi-tive sum is desired, the circuit shown in Fig. E-2(b) can be used. Here the output is given by $e_o = e_a + e_b$.

Modifying Fig. E-2(b) slightly gives the differencing circuit shown in Fig. E-2(c), which has an input-output relationship of $e_o = e_b - e_a$.

E-1-3   First-Order Op-Amp Configurations

In addition to adding and subtracting signals, op-amps can be used to implement transfer functions of continuous-data systems. While many alternatives are available, we will explore only those that use the inverting op-amp configuration shown in Fig. E-3. In the figure, $Z_1(s)$ and $Z_2(s)$ are impedances commonly composed of resistors and capacitors. Inductors are not commonly used because they tend to be bulkier and more expensive. Using ideal op-amp properties, the input-output relationship, or transfer function, of the circuit shown in Fig. E-3 can be written in a number of ways, such as

$$G(s) = \frac{E_o(s)}{E_i(s)} = -\frac{Z_2(s)}{Z_1(s)} = \frac{-1}{Z_1(s)Y_2(s)} \tag{E-1}$$

$$= -Z_2(s)Y_1(s) = -\frac{Y_1(s)}{Y_2(s)}$$

where $Y_1(s) = 1/Z_1(s)$ and $Y_2(s) = 1/Z(s)$ are the admittances associated with the circuit impedances. The different transfer function forms given in Eq. (E-1) apply conveniently to the different compositions of the circuit impedances.

Using the inverting op-amp configuration shown in Fig. E-3 and using resistors and capacitors as elements to compose $Z_1(s)$, and $Z_2(s)$, Table E-1 illustrates a number of common transfer function implementations. As shown in the Table E-1, it is possi-ble to implement poles and zeros along the negative real axis as well as at the origin in the s-plane. Because the inverting op-amp configuration was used, all the trans-fer functions have negative gains. The negative gain is usually not an issue, since it is simple to add a gain of -1 to the input and output signal to make the net gain positive.
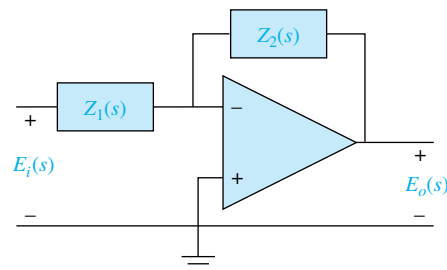
Figure E-3   Inverting op-amp configuration.

TABLE E-1 Inverting Op-Amp Transfer Functions

	Input Element	Feedback Element	Transfer Function	Comments
(a)	R_1 $Z_1 = R_1$	R_2 $Z_2 = R_2$	$-\dfrac{R_2}{R_1}$	Inverting gain. e.g., if $R_1 = R_2$, $e_o = -e_1$.
(b)	R_1 $Z_1 = R_1$	C_2 $Y_2 = sC_2$	$\left(\dfrac{-1}{R_1C_2}\right)\dfrac{1}{s}$	Pole at the origin. i.e., an integrator.
(c)	C_1 $Y_1 = sC_1$	R_2 $Z_2 = R_2$	$(-R_2C_1)s$	Zero at the origin. i.e., a differentiator.
(d)	R_1 $Z_1 = R_1$	R_2, C_2 $Y_2 = \dfrac{1}{R_2} + sC_2$	$-\dfrac{\dfrac{1}{R_1C_2}}{s + \dfrac{1}{R_2C_2}}$	Pole at $\dfrac{-1}{R_2C_2}$ with a dc gain of $-R_2/R_1$.
(e)	R_1 $Z_1 = R_1$	R_2, C_2 $Z_2 = R_2 + \dfrac{1}{sC_2}$	$\dfrac{-R_2}{R_1}\left(\dfrac{s + 1/R_2C_2}{s}\right)$	Pole at the origin and a zero at $-1/R_2C_2$, i.e., a PI Controller.
(f)	R_1, C_1 $Y_1 = \dfrac{1}{R_1} + sC_1$	R_2 $Z_2 = R_2$	$-R_2C_1\left(s + \dfrac{1}{R_1C_1}\right)$	Zero at $s = \dfrac{-1}{R_1C_1}$, i.e., a PD controller.
(g)	R_1, C_1 $Y_1 = \dfrac{1}{R_1} + sC_1$	R_2, C_2 $Y_2 = \dfrac{1}{R_2} + sC_2$	$\dfrac{\dfrac{-C_1}{C_2}\left(s + \dfrac{1}{R_1C_1}\right)}{s + \dfrac{1}{R_2C_2}}$	Pole at $s = \dfrac{-1}{R_2C_2}$ and a zero at $s = \dfrac{-1}{R_1C_1}$, i.e., a lead or lag controller.
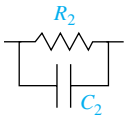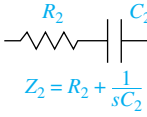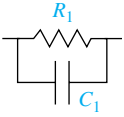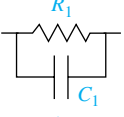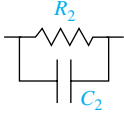
► **EXAMPLE E-1** As an example of op-amp realization of transfer functions, consider the transfer function

$$G(s) = K_p + \frac{K_I}{s} + K_D s \tag{E-2}$$

where K_P, K_D, and K_I are real constants. In Chapter 10 this transfer function will be called the **PID controller**, since the first term is a **P**roportional gain, the second an **I**ntegral term, and the third a **D**erivative term. Using Table E-1, the proportional gain can be implemented using line (a), the integral term can be implemented using line (b), and the derivative term can be implemented using line (c). By superposition, the output of $G(s)$ is the sum of the responses due to each term in $G(s)$. This sum can be implemented by adding an additional input resistance to the circuit shown in Fig. E-2(a). By making the sum negative, the negative gains of the proportional, integral, and derivative
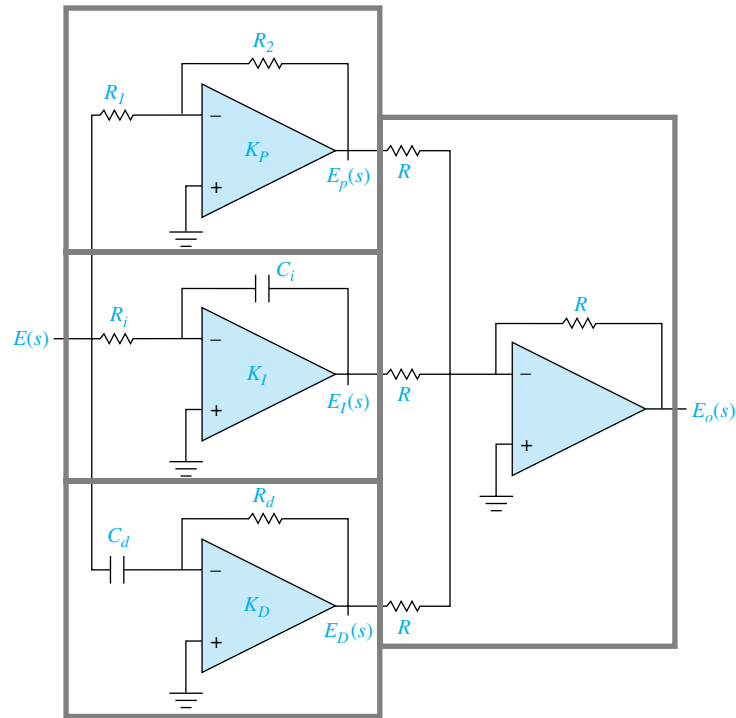
Figure E-4 Implementation of a PID controller.

term implementations are canceled, giving the desired result shown in Fig. E-4. The transfer functions of the components of the op-amp circuit in Fig. E-4 are

Proportional:
$$\frac{E_P(s)}{E(s)} = -\frac{R_2}{R_1} \tag{E-3}$$

Integral:
$$\frac{E_I(s)}{E(s)} = -\frac{1}{R_i C_i s} \tag{E-4}$$

Derivative:
$$\frac{E_D(s)}{E(s)} = -R_d C_d s \tag{E-5}$$

The output voltage is

$$E_o(s) = -[E_P(s) + E_I(s) + E_D(s)] \tag{E-6}$$

Thus, the transfer function of the PID op-amp circuit is

$$G(s) = \frac{E_o(s)}{E(s)} = \frac{R_2}{R_1} + \frac{1}{R_i C_i s} + R_d C_d s \tag{E-7}$$

By equating Eqs. (E-2) and (E-7), the design is completed by choosing the values of the resistors and the capacitors of the op-amp circuit so that the desired values of K_P, K_I, and K_D are matched. The design of the controller should be guided by the availability of standard capacitors and resistors.

It is important to note that Fig. E-4 is just one of many possible implementations of Eq. (E-2). For example, it is possible to implement the PID controller with just three op-amps. Also, it is common to add components to limit the high-frequency gain of the differentiator and to limit the integrator output magnitude, which is often referred to as *antiwindup* protection. One advantage of the implementation shown in Fig. E-4 is that each of the three constants K_P, K_I, and K_D can be adjusted or tuned individually by varying resistor values in their respective op-amp circuits.

Op-amps are also used in control systems for A/D and D/A converters, sampling devices, and realization of nonlinear elements for system compensation. ◀

▶ REFERENCES

1. E. J. Kennedy, *Operational Amplifier Circuits*, Holt, Rinehart and Winston, Fort Worth, TX, 1988.
2. J. V. Wait, L. P., Huelsman, and G. A. Korn, *Introduction to Operational Amplifier Theory and Applications*, Second Edition, McGraw-Hill, New York, 1992.

▶ PROBLEM

E-1. Find the transfer functions $E_o(s)/E(s)$ for the circuits shown in Fig. EP-1.
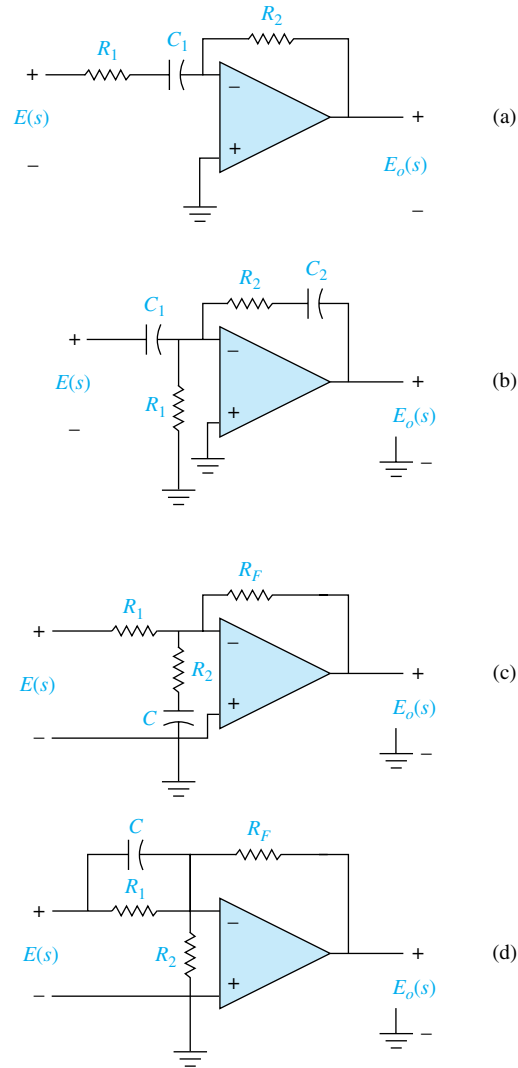
Figure EP-1

Appendix F
Properties and Construction of the Root Loci

Properties and Construction of the Root Loci

The following properties of the root loci are useful for constructing the root loci manually and for understanding the root loci. The properties are developed based on the relationship between the poles and zeros of $G(s)H(s)$ and the zeros of $1 + G(s)H(s)$, which are the roots of the characteristic equation.

▶ F-1 $K = 0$ and $K = \pm\infty$ Points

The $K = 0$ points on the root loci are at the poles of $G(s)H(s)$.
The $K = \pm\infty$ points on the root loci are at the zeros of $G(s)H(s)$.
The poles and zeros referred to here include those at infinity, if any.

The reason for this is seen from the condition of the root loci given by Eq. (8-12),

$$G_1(s)H_1(s) = -\frac{1}{K} \tag{F-1}$$

As the magnitude of K approaches zero, $G_1(s)H_1(s)$ approaches infinity, so s must approach the poles of $G_1(s)H_1(s)$ or $G(s)H(s)$. Similarly, as the magnitude of K approaches infinity, s must approach the poles of $G(s)H(s)$.

▶ **EXAMPLE F-1** Consider the equation

$$s(s + 2)(s + 3) + K(s + 1) = 0 \tag{F-2}$$

When $K = 0$, the three roots of the equation are at $s = 0$, -2, and -3. When the magnitude of K is infinite, the three roots of the equation are at $s = -1$, ∞ and ∞. It is useful to consider that infinity in the s-plane is a point concept. We can visualize that the finite s-plane is only a small portion of a sphere with an infinite radius. Then, infinity in the s-plane is a point on the opposite side of the sphere that we face.

Dividing both sides of Eq. (F-2) by the terms that do not contain K, we get

$$1 + G(s)H(s) = 1 + \frac{K(s + 1)}{s(s + 2)(s + 3)} = 0 \tag{F-3}$$

which gives

$$G(s)H(s) = \frac{K(s + 1)}{s(s + 2)(s + 3)} \tag{F-4}$$
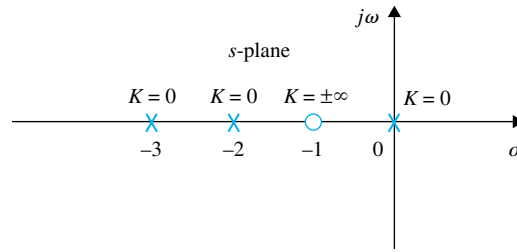
Figure F-1 Roots at which $K = 0$ on the root loci of $s(s + 2)(s + 3) + K(s + 1) = 0$.

Thus, the three roots of Eq. (F-2) when $K = 0$ are the same as the poles of the function $G(s)H(s)$. The three roots of Eq. (F-2) when $K = \pm\infty$ are at the three zeros of $G(s)H(s)$, including those at infinity. The three points on the root loci at which $K = 0$ and those at which $K = \pm\infty$ are shown in Fig. F-1. ◀

▶ F-2 NUMBER OF BRANCHES ON THE ROOT LOCI

A branch of the root loci is the locus of one root when K varies between $-\infty$ and ∞. The following property of the root loci results, since the number of branches of the root loci must equal the number of roots of the equation.

> **The number of branches of the root loci of $F(s) = P(s) + KQ(s) = 0$ is equal to the order of the polynomial.**

• It is important to keep track of the total number of branches of the root loci.

Keeping track of the individual branches and the total number of branches of the root locus diagram is important in making certain that the plot is done correctly. This is particularly true when the root locus plot is done by a computer, since unless each root locus branch is coded by a different color, it is up to the user to make the distinctions.

▶ **EXAMPLE F-2** The number of branches of the root loci of

$$s(s + 2)(s + 3) + K(s + 1) = 0 \tag{F-5}$$

is three, since the equation is of the third order. In other words, the equation has three roots, and thus there should be three root loci. ◀

▶ F-3 SYMMETRY OF THE ROOT LOCI

• It is important to pay attention to the symmetry of the root loci.

> *The root loci are symmetrical with respect to the real axis of the s-plane. In general, the root loci are symmetrical with respect to the axes of symmetry of the pole-zero configuration of $G(s)H(s)$.*

The reason behind this property is because for a polynomial with real coefficients the roots must be real or in complex-conjugate pairs. In general, if the poles and zeros of $G(s)H(s)$ is symmetrical to an axis in addition to the real axis in the s-plane, we can regard this axis of symmetry as if it were the real axis of a new complex plane obtained through a linear transformation.
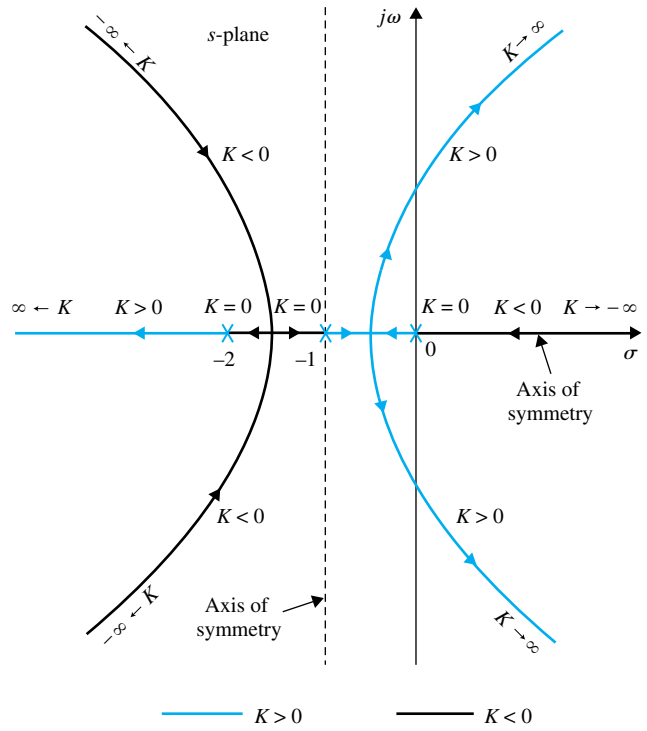
Figure F-2 Root loci of $s(s + 2)(s + 3) + K(s + 1) = 0$, showing the properties of symmetry.

▶ **EXAMPLE F-3** Consider the equation

$$s(s + 1)(s + 2) + K = 0 \tag{F-6}$$

Dividing both sides of the equation by the terms that do not contain K, we get

$$G(s)H(s) = \frac{K}{s(s + 1)(s + 2)} \tag{F-7}$$

The root loci of Eq. (F-6) are shown in Fig. F-2 for $K = -\infty$ to $K = \infty$. Since the pole-zero configuration of $G(s)H(s)$ is symmetrical with respect to the real axis as well as the $s = -1$ axis, the root locus plot is symmetrical to the two axes.

As a review of all the properties of the root loci presented thus far, we conduct the following exercise with regard to the root loci in Fig. F-2.

The points at which $K = 0$ are at the poles of $G(s)H(s)$, $s = 0$, -1, and -2. The function $G(s)H(s)$ has three zeros at $s = \infty$ at which $K = \pm\infty$. The reader should try to trace out the three separate branches of the root loci by starting from one of the $K = -\infty$ points, through the $K = 0$ point on same branch, and ending at $K = \infty$ at $s = \infty$. ◀

▶ **EXAMPLE F-4** When the pole-zero configuration of $G(s)H(s)$ is symmetrical with respect to a point in the s-plane, the root loci will also be symmetrical to that point. This is illustrated by the root locus plot of

$$s(s + 1)(s + 1 + j)(s + 1 - j) + K = 0 \qquad (F-8)$$

shown in Fig. F-3.
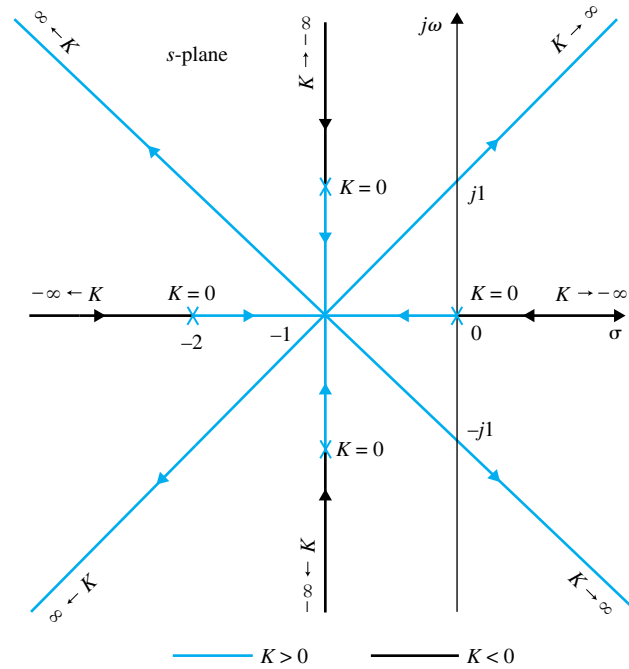
Figure F-3 Root loci of $s(s + 2)(s^2 + 2s + 2) + K = 0$, showing the properties of symmetry. ◀

▶ F-4 ANGLES OF ASYMPTOTES OF THE ROOT LOCI AND BEHAVIOR OF THE ROOT LOCI AT $|s| = \infty$

• Asymptotes of root loci refers to behavior of root loci at $s \to \infty$.

As shown by the root loci in Figs. F-2 and F-3, when n, the order of $P(s)$ is not equal to m, the order of $Q(s)$, $2|n - m|$ of the loci will approach infinity in the s-plane. The properties of the root loci near infinity in the s-plane are described by the **asymptotes** of the loci when $|s| \to \infty$. The angles of the asymptotes and their intersect with the real axis of the s-plane are described as follows.

For large values of s, the root loci for $K \geq 0$ (RL) are asymptotic to asymptotes with angles given by

$$\theta_i = \frac{(2i + 1)}{|n - m|} \times 180° \qquad n \neq m \qquad (F-9)$$

where $i = 0, 1, 2, \ldots , |n - m| - 1$; and n and m are the number of finite poles and zeros of $G(s)H(s)$, respectively.

For $K \leq 0$ (RL), the angles of the asymptotes are

$$\theta_i = \frac{2i}{|n - m|} \times 180° \qquad n \neq m \qquad \text{(F-10)}$$

where $i = 0, 1, 2, \ldots , |n - m| - 1$.

► F-5 INTERSECT OF THE ASYMPTOTES (CENTROID)

The intersection of the $2|n - m|$ asymptotes of the root loci lies on the real axis of the s-plane, at

$$\sigma_1 = \frac{\Sigma \text{ finite poles of } G(s)H(s) - \Sigma \text{ finite zeros of } G(s)H(s)}{n - m} \qquad \text{(F-11)}$$

where n is the number of finite poles and m is the number of finite zeros of $G(s)H(s)$, respectively. The intersection of the asymptotes σ_1 represents the center of gravity of the root loci, and is always a real number.

Since the poles and zeros of $G(s)H(s)$ are either real or in complex-conjugate pairs, the imaginary parts in the numerator of Eq. (8-35) always cancel each other out. Thus, in Eq. (F-11), the terms in the summations may be replaced by the real parts of the poles and zeros of $G(s)H(s)$, respectively. That is,

$$\sigma_1 = \frac{\Sigma \text{ real parts of poles of } G(s)H(s) - \Sigma \text{ real parts of zeros of } G(s)H(s)}{n - m} \qquad \text{(F-12)}$$

► **EXAMPLE F-5** Consider the transfer function

$$G(s)H(s) = \frac{K(s + 1)}{s(s + 4)(s^2 + 2s + 2)} \qquad \text{(F-13)}$$

which corresponds to the characteristic equation

$$s(s + 4)(s^2 + 2s + 2) + K(s + 1) = 0 \qquad \text{(F-14)}$$

The pole-zero configuration of $G(s)H(s)$ is shown in Fig. F-4. From the six properties of the root loci discussed so far, the following information concerning the root loci of Eq. (F-14) when K varies from $-\infty$ to ∞ is obtained:

1. $K = 0$: The points at which $K = 0$ on the root loci are at the poles of $G(s)H(s)$: $s = 0$, -4, $-1 +j$, and $-1 -j$.

2. $K = \pm\infty$: The points at which $K = \pm\infty$ on the root loci are at the zeros of $G(s)H(s)$: $s = -1, \infty, \infty,$ and ∞.

3. There are four root loci branches, since Eqs. (F-13) and (F-14) are of the fourth order.

4. The root loci are symmetrical to the real axis.
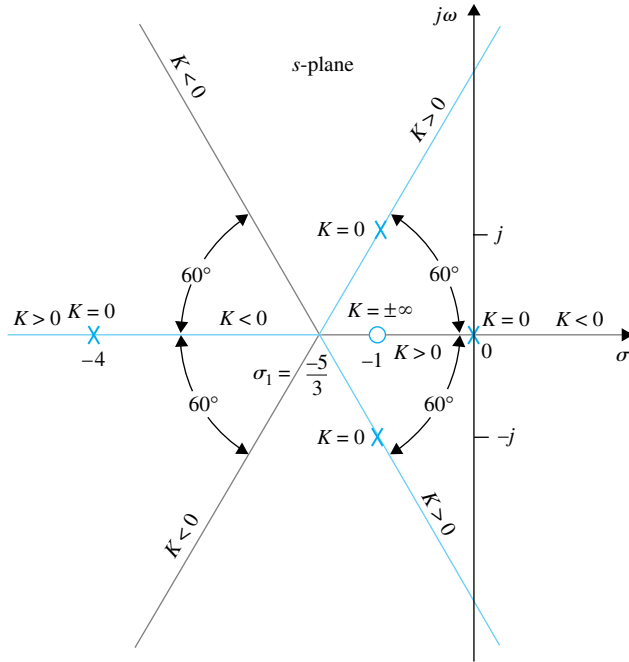
Figure F-4   Asymptotes of the root loci of
$s(s + 4)(s^2 + 2s + 2) + K(s + 1) = 0.$

5. Since the number of finite poles of $G(s)H(s)$ exceeds the number of finite zeros of $G(s)H(s)$ by three ($n - m = 4 - 1 = 3$), when $K = \pm\infty$, three root loci approach $s = \infty$.

The angles of the asymptotes of the RL ($K \geq 0$) are given by Eq. (F-9):

$$j = 0: \qquad \theta_0 = \frac{180°}{3} = 60°$$

$$j = 1: \qquad \theta_1 = \frac{540°}{3} = 180°$$

$$j = 2: \qquad \theta_2 = \frac{900°}{3} = 300°$$

The angles of the asymptotes of the root loci for $K \leq 0$ are given by Eq. (F-10), and are calculated to be 0°, 120°, and 240°.

6. The intersection of the asymptotes is given by Eq. (F-12):

$$\sigma_1 = \frac{(-4 - 1 - 1) - (-1)}{4 - 1} = -\frac{5}{3} \qquad\qquad \text{(F-15)}$$

The asymptotes of the root loci are shown in Fig. F-4.   ◀

► **EXAMPLE F-6** The asymptotes of the root loci of several equations are shown in Fig. F-5.

$$G(s)H(s) = \frac{K}{s(s + p_1)}$$

――― $K > 0$ ――― $K < 0$

$$G(s)H(s) = \frac{K}{s(s + p_1)(s + p_2)(s + p_3)}$$

――― $K > 0$ ――― $K < 0$

$$G(s)H(s) = \frac{K}{s^2(s + p_1)(s + p_2)(s + p_3)}$$

――― $K > 0$ ――― $K < 0$

$$G(s)H(s) = \frac{K(s + z_1)}{s^2(s + p_1)(s + p_2)(s + p_3)}$$

――― $K > 0$ ――― $K < 0$
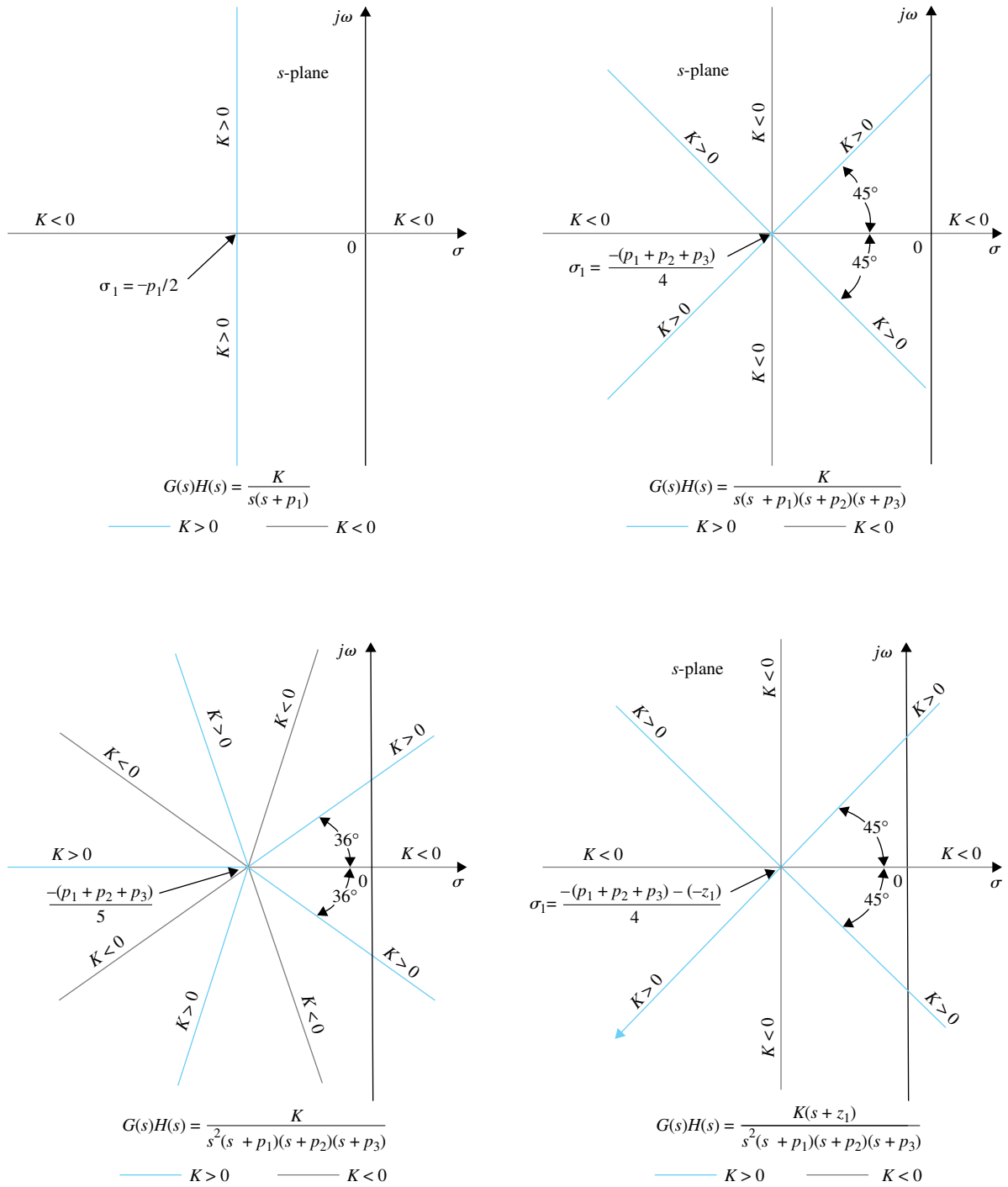
Figure F-5   Examples of the asymtotes of the root loci.   ◄

▶ F-6 ROOT LOCI ON THE REAL AXIS

• The entire real axis of the s-plane is occupied by root loci.

The entire real axis of the s-plane is occupied by the root loci **for** $-\infty \le K \le \infty$.

1. $K \ge 0$: *On a given section of the real axis, root loci are found in the section only if the total number of poles and zeros of G(s)H(s) to the right of the section is odd.*

2. $K \le 0$: *On a given section of the real axis, root loci are found in the section only if the total number of real poles and zeros of G(s)H(s) to the right of the section is even. Complex poles and zeros of G(s)H(s) do not affect the type of root loci found on the real axis.*

These properties are arrived at based on the following observations:

1. At any point s_1 on the real axis, the angles of the vectors drawn from the complex-conjugate poles and zeros of $G(s)H(s)$ add up to zero. Thus, only the real zeros and poles of $G(s)H(s)$ contribute to the angular relations in Eqs. (8-18) and (8-19).

2. Only the real poles and zeros of $G(s)H(s)$ that lie to the right of the point s_1 contribute to Eqs. (8-18) and (8-19), because real poles and zeros that lie to the left of the point contribute nothing.

3. Each real pole of $G(s)H(s)$ to the right of s_1 contributes -180 degrees, and each real zero of $G(s)H(s)$ to the right of s_1 contributes $+180$ degrees to Eqs. (8-18) and (8-19).

The last observation shows that for s_1 to be a point on the root locus, there must be an **odd** number of poles and zeros of $G(s)H(s)$ to the right of the point. For s_1 to be a point on the branch of the root loci for $K \le 0$, the total number of poles and zeros of $G(s)H(s)$ to the right of the point must be **even**. The following example illustrates the determination of the properties of the root loci on the real axis of the s-plane.

▶ **EXAMPLE F-7** The root loci on the real axis for two pole-zero configurations of $G(s)H(s)$ are shown in Fig. F-6. Notice that the entire real axis is occupied by the root loci for all values of K.
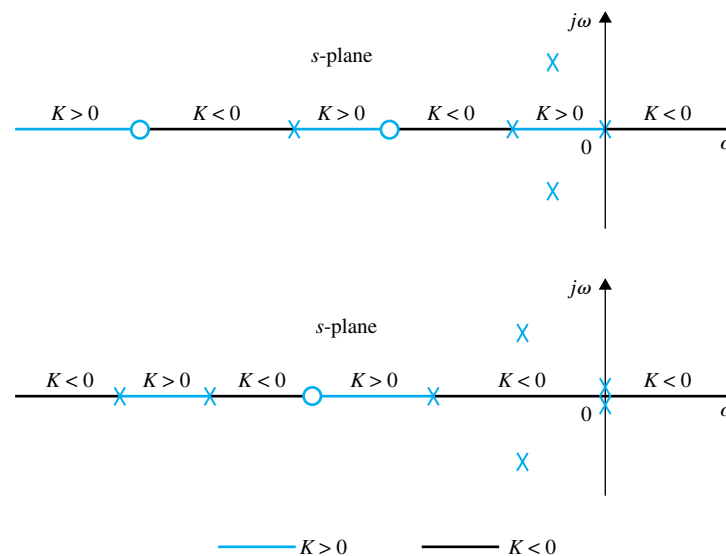
Figure F-6 Properties of root loci on the real axis.

▶ F-7 ANGLES OF DEPARTURE AND ANGLES
OF ARRIVAL OF THE ROOT LOCI

> *The angle of departure or arrival of a root locus at a pole or zero, respectively, of*
> *G(s)H(s) denotes the angle of the tangent to the locus near the point.*

The angles of departure and arrival are determined using Eq. (8-18) for root loci for
positive K and Eq. (8-19) for root loci for negative K. The details are illustrated by the
following example.

▶ **EXAMPLE F-8** For the root-locus diagram shown in Fig. F-7, the root locus near the pole $s = -1 + j$ may be more
accurately sketched by knowing the angle at which the root locus leaves the pole. As shown in Fig.
F-7, the angle of departure of the root locus at $s = -1 + j$ is represented by θ_2, measured with re-
spect to the real axis. Let us assign s_1 to be a point on the RL leaving the pole at $-1 + j$ and is
very close to the pole. Then, s_1 must satisfy Eq. (8-18). Thus,

$$\angle G(s_1)H(s_1) = -(\theta_1 + \theta_2 + \theta_3 + \theta_4) = (2i + 1)180° \qquad \text{(F-16)}$$

where i is any integer. Since s_1 is assumed to be very close to the pole at $-1 + j$, the angles of the
vectors drawn from the other three poles are approximated by considering that s_1 is at $-1 + j$. From
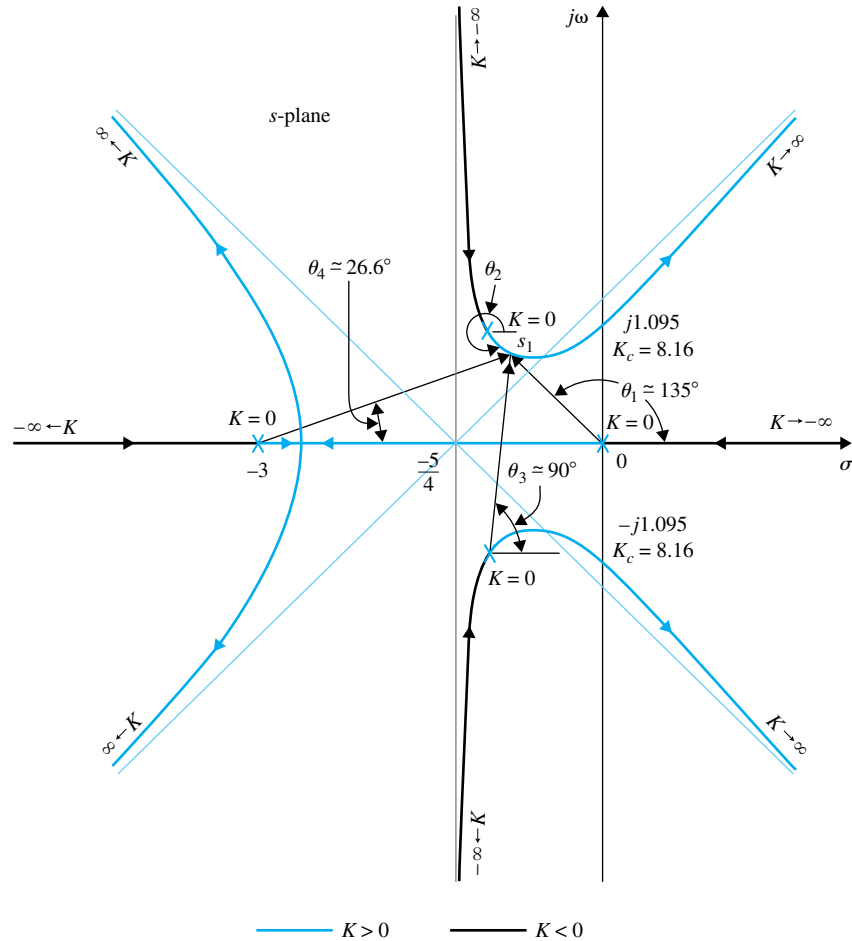
Figure F-7   Root loci of $s(s + 3)(s^2 + 2s + 2) + K = 0$ to illustrate the angles of
departure or arrival.
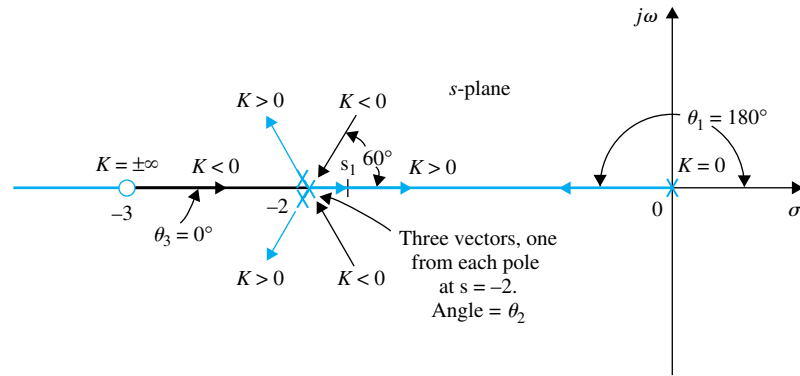
Figure F-8 Angles of departure and arrival at a third-order pole.

Fig. F-7, Eq. (F-16) is written

$$-(135° + \theta_2 + 90° + 26.6°) = (2i + 1)180° \qquad \text{(F-17)}$$

where θ_2 is the only unknown angle. In this case, we can set i to be -1, and the result for θ_2 is $-71.6°$.

When the angle of departure or arrival of a root locus for positive K at a simple pole or zero of $G(s)H(s)$ is determined, the angle of arrival or departure of the root locus for negative K at the same point differs from this angle by 180°, and Eq. (8-19) is now used. Figure F-7 shows that the angle of arrival of the root locus for negative K at $-1 + j$ is 108.4°, which is $180° - 71.6°$. Similarly, for the root-locus diagram in Fig. F-8, we can show that the root locus for negative K arrives at the pole $s = -3$ with an angle of 180°, and the root locus for positive K leaves the same pole at 0°. For the pole at $s = 0$, the angle of arrival of the negative-K root locus is 180°, whereas the angle of departure of the positive-K root locus is 180°. These angles are also determined from the knowledge of the type of root loci on sections of the real axis separated by the poles and zeros of $G(s)H(s)$. Since the total angles of the vectors drawn from complex-conjugate poles and zeros to any point on the real axis add up to be zero, the angles of arrival and departure of root loci on the real axis are not affected by the complex poles and zeros of $G(s)H(s)$. ◀

▶ **EXAMPLE F-9** In this example we examine the angles of departure and arrival of the root loci at a multiple-order pole or zero of $G(s)H(s)$. Consider that a $G(s)H(s)$ has a multiple-order (third-order) pole on the real axis, as shown in Fig. F-8. Only the real poles and zeros of $G(s)H(s)$ are shown, since the complex ones do not affect the type or the angles of arrival and departure of the root loci on the real axis. For the third-order pole at $s = -2$, there are three positive-K loci leaving and three negative-K loci arriving at the point. To find the angles of departure of the positive-K root loci, we assign a point s_1 on one of the loci near $s = -2$, and apply Eq. (8-18). The result is

$$-\theta_1 - 3\theta_2 + \theta_3 = (2i + 1)180° \qquad \text{(F-18)}$$

where θ_1 and θ_3 denote the angles of the vectors drawn from the pole at 0 and the zero at -3, respectively, to s_1. The angle θ_2 is multiplied by 3, since there are three poles at $s = -2$, so that there are three vectors drawn from -2 to s_1. Setting i to zero in Eq. (F-18), and since $\theta_1 = 180°$, $\theta_3 = 0°$ we have $\theta_2 = 0°$, which is the angle of departure of the positive-K root loci that lies between $s = 0$ and $s = -2$. For the angles of departure of the other two positive-K loci, we set $i = 1$ and $i = 2$ successively in Eq. (F-18), and we have $\theta_2 = 120°$ and $-120°$. Similarly, for the three negative-K root loci that arrive at $s = -2$, Eq. (8-19) is used, and the angles of arrivals are found to be 60°, 180°, and $-60°$. ◀

▶ F-8 INTERSECTION OF THE ROOT LOCI WITH THE IMAGINARY AXIS

• Routh-Hurwitz criterion may be used to find the intersection of the root loci on the imaginary axis.

The points where the root loci intersect the imaginary axis of the s-plane, and the corresponding values of K, may be determined by means of the Routh-Hurwitz criterion. For complex situations, when the root loci have multiple number of intersections on the imaginary axis, the intersects and the critical values of K can be determined with the help of the root-locus computer program. The Bode diagram method in Chapter 9, associated with the frequency response, can also be used for this purpose.

▶ **EXAMPLE F-10** The root loci shown in Fig. F-7 is for the equation

$$s(s + 3)(s^2 + 2s + 2) + K = 0 \qquad \text{(F-19)}$$

Figure F-7 shows that the root loci intersect the $j\omega$ axis at two points. Applying the Routh-Hurwitz criterion to Eq. (F-19), and by solving the auxiliary equation, we have the critical value of K for stability at $K = 8.16$, and the corresponding crossover points on the $j\omega$-axis are at $\pm j1.095$. ◀

▶ F-9 BREAKAWAY POINTS

F-9-1 (Saddle Points) on the Root Loci

Breakaway points on the root loci of an equation correspond to multiple-order roots of the equation.

Figure F-9(a) illustrates a case in which two branches of the root loci meet at the breakaway point on the real axis and then depart from the axis in opposite directions. In

(a)

(b)

(c)
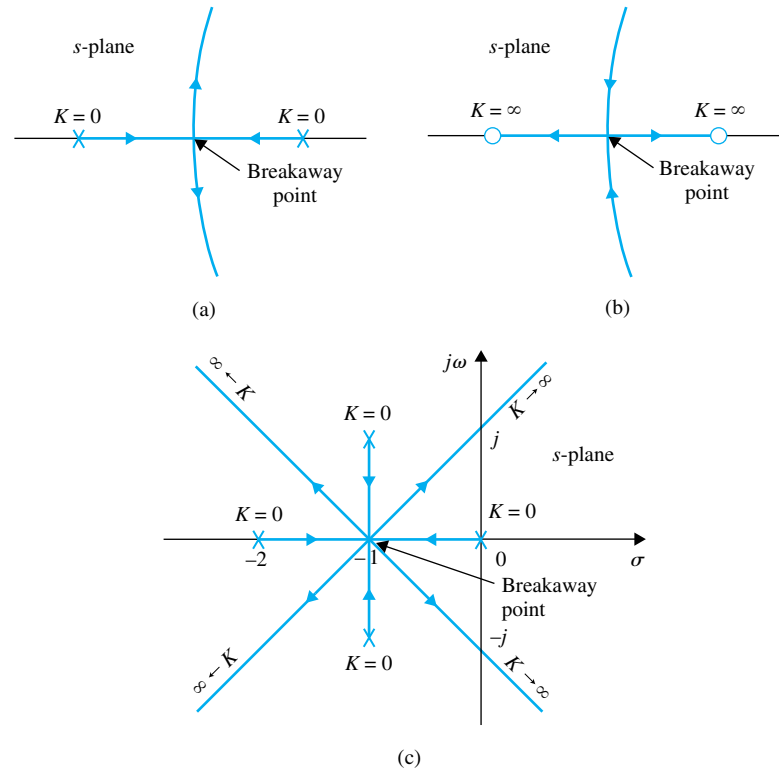
Figure F-9 Examples of breakaway points on the real axis in the s-plane.

this case, the breakaway point represents a double root of the equation when the value of K is assigned the value corresponding to the point. Figure F-9(b) shows another common situation when two complex-conjugate root loci approach the real axis, meet at the breakaway point, and then depart in opposite directions along the real axis. In general, a breakaway point may involve more than two root loci. Figure F-9(c) illustrates a situation when the breakaway point represents a fourth-order root.

• A root-locus plot may have more than one breakaway points.

A root-locus diagram can have, of course, more than one breakaway point. Moreover, the breakaway points need not always be on the real axis. Because of the conjugate symmetry of the root loci, the breakaway points not on the real axis must be in complex-conjugate pairs. Refer to Fig. F-12 for an example of root loci with complex breakaway points. The properties of the breakaway points of root loci are given as follows:

• Breakaway points may be complex conjugates in the s-plane.

The breakaway points on the root loci of $1 + KG_1(s)H_1(s) = 0$ ***must satisfy***

$$\frac{dG_1(s)H_1(s)}{ds} = 0 \tag{F-20}$$

It is important to point out that the condition for the breakaway point given in Eq. (F-20) is *necessary* but *not sufficient*. In other words, all breakaway points on the root loci for all values of K must satisfy Eq. (F-20), but not all solutions of Eq. (F-20) are breakaway points. To be a breakaway point, the solution of Eq. (F-20) must also satisfy the equation $1 + KG_1(s)H_1(s) = 0$, that is, must also be a point on the root loci for some real K. In general, the following conclusions may be made with regard to the solutions of Eq. (F-20):

1. All *real* solutions of Eq. (F-20) are breakaway points on the root loci for all values of K, since the entire real axis of the s-plane is occupied by the root loci.

2. The complex-conjugate solutions of Eq. (F-20) are breakaway points only if they satisfy the characteristic equation or are points on the root loci.

3. Since the condition of the root loci is

$$K = -\frac{1}{G_1(s)H_1(s)} \tag{F-21}$$

taking the derivative on both sides of the equation with respect to s, we have

$$\frac{dK}{ds} = \frac{dG_1(s)H_1(s)/ds}{[G_1(s)H_1(s)]^2} \tag{F-22}$$

Thus, the breakaway point condition can also be written as

$$\frac{dK}{ds} = 0 \tag{F-23}$$

where K is expressed as in Eq. (F-21).

F-9-2 The Angle of Arrival and Departure of Root Loci at the Breakaway Point

The angles at which the root loci arrive or depart from a breakaway point depend on the number of loci that are involved at the point. For example, the root loci shown in Figs. F-9(a) and F-9(b) all arrive and break away at 180° apart, whereas in Fig. F-9(c), the four root loci arrive and depart with angles 90° apart, whereas in Fig. F-9(c), the four root loci arrive and depart with angles 90° apart. In general,

n root loci ($-\infty \leq K \leq \infty$) ***arrive or depart a breakaway point at 180/n degrees apart.***

Many root-locus computer programs have features that will obtain the breakaway points, which a rather tedious task to do manually.

▶ **EXAMPLE F-11** Consider the second-order equation

$$s(s + 2) + K(s + 4) = 0 \tag{F-24}$$

Based on some of the properties of the root loci described thus far, the root loci of Eq. (F-24) are sketched as shown in Fig. F-10 for $-\infty < K < \infty$. It can be proven that the complex portion of the root loci is a circle. The two breakaway points are on the real axis, one between 0 and -2 and the other between -4 and $-\infty$. From Eq. (F-24), we have

$$G_1(s)H_1(s) = \frac{s + 4}{s(s + 2)} \tag{F-25}$$

Applying Eq. (F-20), the breakaway points on the root loci must satisfy

$$\frac{dG_1(s)H_1(s)}{ds} = \frac{s(s + 2) - 2(s + 1)(s + 4)}{s^2(s + 2)^2} = 0 \tag{F-26}$$

or

$$s^2 + 8s + 8 = 0 \tag{F-27}$$

Solving Eq. (F-27), we find the two breakaway points of the root loci at $s = -1.172$ and -6.828. Figure F-10 shows that the two breakaway points are all on the root loci for positive K.
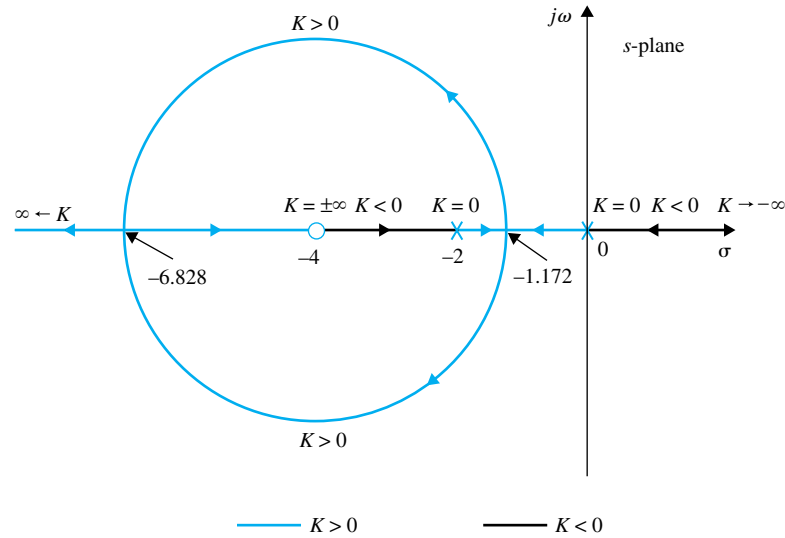
Figure F-10   Root loci of $s(s + 2) + K(s + 4) = 0$.

▶ **EXAMPLE F-12** Consider the equation

$$s^2 + 2s + 2 + K(s + 2) = 0 \tag{F-28}$$

The equivalent $G(s)H(s)$ is obtained by dividing both sides of Eq. (F-28) by the terms that do not contain K. We have

$$G(s)H(s) = \frac{K(s + 2)}{s^2 + 2s + 2} \tag{F-29}$$
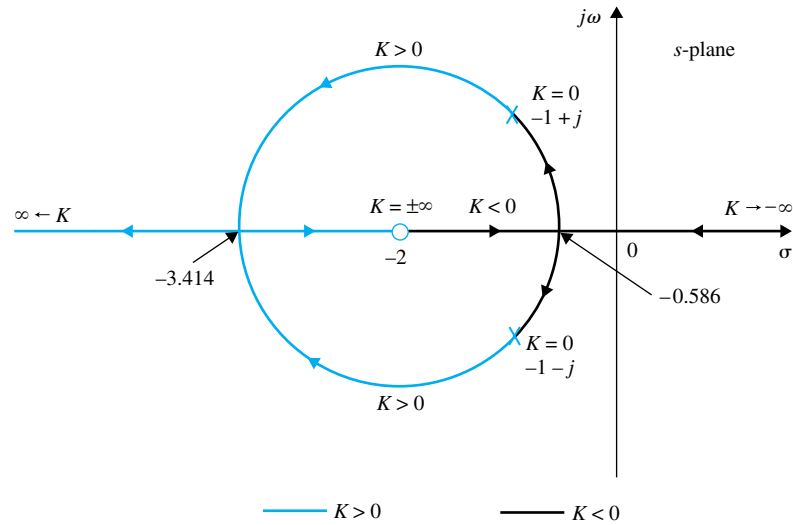
Figure F-11 Root loci of $s^2 + 2s + 2 + K(s + 2) = 0$.

Based on the poles and zeros of $G(s)H(s)$, the root loci of Eq. (F-29) are plotted as shown in Fig. F-11. The plot shows that there are two breakaway points, one for $K > 0$ and one for $K < 0$. These breakaway points are determined from

$$\frac{dG_1(s)H_1(s)}{ds} = \frac{d}{ds}\left(\frac{s + 2}{s^2 + 2s + 2}\right) = \frac{s^2 + 2s + 2 - 2(s + 1)(s + 2)}{(s^2 + 2s + 2)^2} = 0 \qquad \text{(F-30)}$$

or

$$s^2 + 4s + 2 = 0 \qquad \text{(F-31)}$$

The solution of this equation gives the breakaway point as $s = -0.586$ and $s = -3.414$. ◀

▶ **EXAMPLE F-13** Figure F-12 shows the root loci of the equation

$$s(s + 4)(s^2 + 4s + 20) + K = 0 \qquad \text{(F-32)}$$

Dividing both sides of the last equation by the terms that do not contain K, we have

$$1 + KG_1(s)H_1(s) = 1 + \frac{K}{s(s + 4)(s^2 + 4s + 20)} = 0 \qquad \text{(F-33)}$$

Since the poles of $G_1(s)H_1(s)$ are symmetrical about the axes $\sigma = -2$ and $\omega = 0$ in the s-plane, the root loci of the equation are also symmetrical with respect to these two axes. Taking the derivative of $G_1(s)H_1(s)$ with respect to s, we get

$$\frac{dG_1(s)H_1(s)}{ds} = -\frac{4s^3 + 24s^2 + 72s + 80}{[s(s + 4)(s^2 + 4s + 20)]^2} = 0 \qquad \text{(F-34)}$$

or

$$s^3 + 6s^2 + 18s + 20 = 0 \qquad \text{(F-35)}$$

The solutions of the last equation are $s = -2$, $-2 + j2.45$, and $-2 - j2.45$. In this case, Fig. F-12 shows that all the solutions of Eq. (F-35) are breakaway points on the root loci, and two of these points are complex.
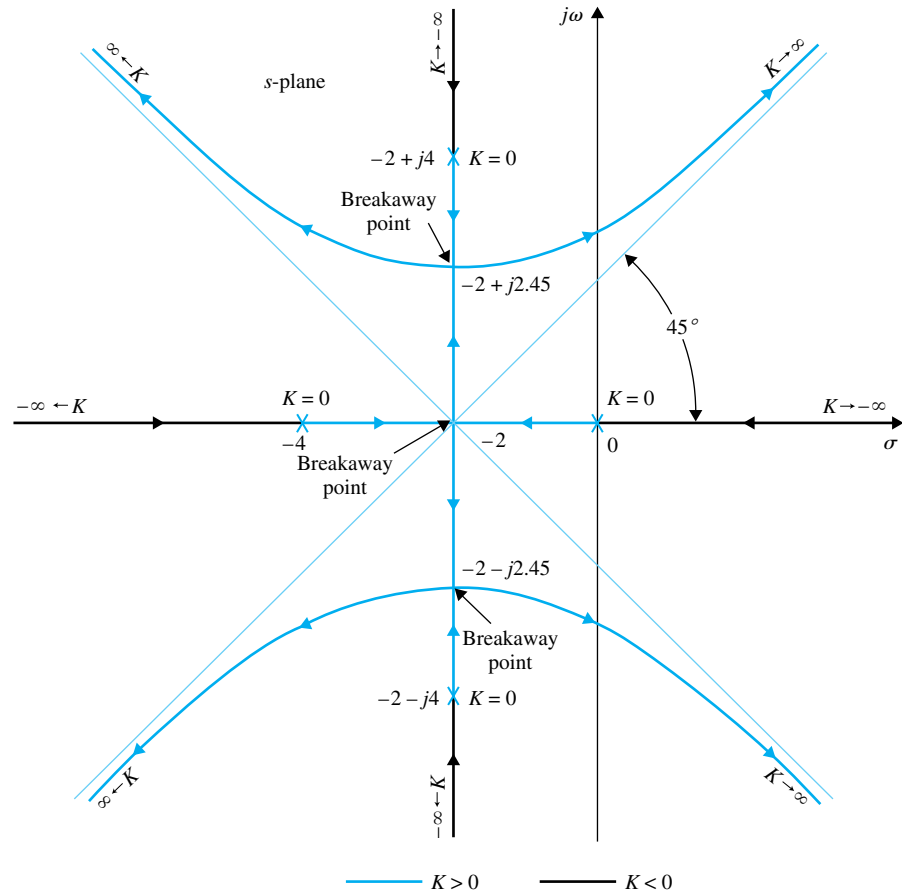
Figure F-12 Root loci of $s(s + 4)(s^2 + 4s + 20) + K = 0$. ◀

▶ **EXAMPLE F-14** In this example, we shall show that not all the solutions of Eq. (F-20) are breakaway points on the root loci. The root loci of the equation

$$s(s^2 + 2s + 2) + K = 0 \qquad \text{(F-36)}$$

are shown in Fig. F-13. The root loci show that neither the $K \geq 0$ loci nor the $K \leq 0$ loci has any breakaway point in this case. However, writing Eq. (F-36) as

$$1 + KG_1(s)H_1(s) = 1 + \frac{K}{s(s^2 + 2s + 2)} = 0 \qquad \text{(F-37)}$$

and applying Eq. (F-20), we have the equation for the breakaway points:

$$3s^2 + 4s + 2 = 0 \qquad \text{(F-38)}$$

The roots of Eq. (F-38) are $s = -0.667 + j0.471$ and $-0.667 - j0.471$. These two roots are **not** breakaway points on the root loci, since they do not satisfy Eq. (F-36) for any real value of K.
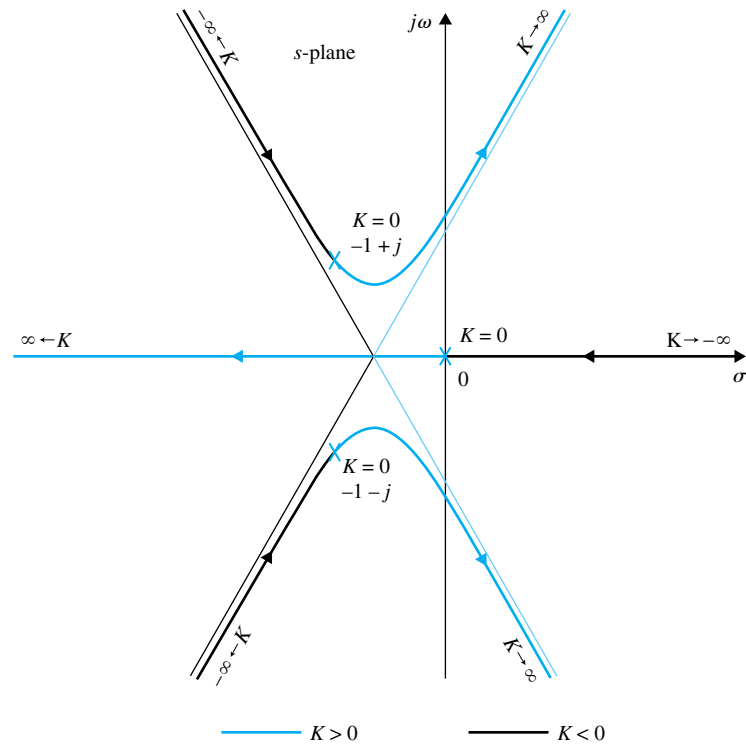
Figure F-13 Root loci of $s(s^2 + 2s + 2) + K = 0$.

▶ F-10 CALCULATION OF K ON THE ROOT LOCI

Once the root loci are constructed, the values of K at any point s_1 on the loci can be determined by use of the defining equation of Eq. (8-20). Graphically, the magnitude of K can be written as

$$|K| = \frac{\Pi \text{ lengths of vectors drawn from the poles of } G_1(s)H_1(s) \text{ to } s_1}{\Pi \text{ lengths of vectors drawn from the zeros of } G_1(s)H_1(s) \text{ to } s_1} \qquad \text{(F-39)}$$

▶ **EXAMPLE F-15** As an illustration on the determination of the value of K on the root loci, the root loci of the equation

$$s^2 + 2s + 2 + K(s + 2) = 0 \qquad \text{(F-40)}$$

are shown in Fig. F-14. The value of K at the point s_1 is given by

$$K = \frac{A \times B}{C} \qquad \text{(F-41)}$$

where A and B are the lengths of the vectors drawn from the poles of $G(s)H(s) = K(s + 2)/(s^2 + 2s + 2)$ to the point s_1, and C is the length of the vector drawn from the zero of $G(s)H(s)$ to s_1. In this case, s_1 is on the locus where K is positive. In general, the value of K at the point where the root loci intersect the imaginary axis can also be found by the method just described. Figure F-14 shows that the value of K at $s = 0$ is -1. The computer method and the Routh-Hurwitz criterion are other convenient alternatives of finding the critical value of K for stability.
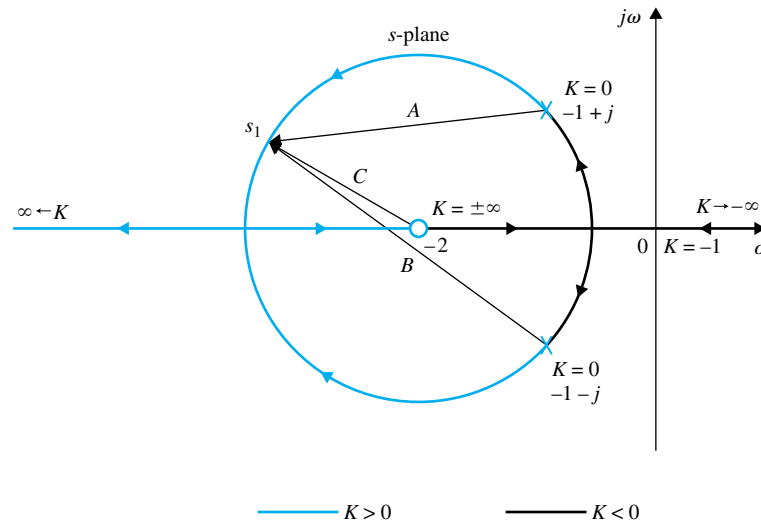
Figure F-14 Graphical method of finding the values of K on the real axis. ◀

In summary, except for extremely complex cases, the properties on the root loci presented here should be adequate for making a reasonably accurate sketch of the root-locus diagram short of plotting it point by point. The computer program can be used to solve for the exact root locations, the breakaway points, and some of the other specific details of the root loci, including the plotting of the final loci. However, one cannot rely on the computer solution completely, since the user still has to decide on the range and resolution of K so that the root-locus plot has a reasonable appearance. For quick reference, the important properties described are summarized in Table F-1.

TABLE F-1 Properties of the Root Loci of $F(s) = 1 + KG_1(s)H_1(s) = 0$

1. $K = 0$ points	The $K = 0$ points are at the poles of $G(s)H(s)$, including those at $s = \infty$.
2. $K = \pm\infty$ points	The $K = \pm\infty$ points are at the zeros of $G(s)H(s)$, including those at $s = \infty$.
3. Number of separate root loci	The total number of root loci is equal to the order of the equation $F(s) = 0$.
4. Symmetry of root loci	The root loci are symmetrical about the axes of symmetry of the pole-zero configuration of $G(s)H(s)$.
5. Asymptotes of root loci as $s \rightarrow \infty$	For large values of s, the root loci for $K > 0$ are asymptotic to asymptotes with angles given by

$$\theta_i = \frac{2i + 1}{|n - m|} \times 180°$$

For $K < 0$, the root loci are asymptotic to

$$\theta_i = \frac{2i}{|n - m|} \times 180°$$

where $i = 0, 1, 2, ..., |n - m| - 1$,
n = number of finite poles of $G(s)H(s)$, and
m = number of finite zeros of $G(s)H(s)$.

TABLE F-1 (*continued*)

6. Intersection of the asymptotes	(a) The intersection of the asymptotes lies only on the real axis in the *s*-plane. (b) The point of intersection of the asymptotes is given by

$$\sigma_1 = \frac{\Sigma \text{ real parts of poles of } G(s)H(s) - \Sigma \text{ real parts of zeros of } G(s)H(s)}{n - m}$$

7. Root loci on the real axis	Root loci for $K > 0$ are found in a section of the real axis only if the total number of real poles and zeros of $G(s)H(s)$ to the **right** of the section is **odd**. If the total number of real poles and zeros to the right of a given section is **even**, root loci for $K < 0$ are found.
8. Angles of departure	The angle of departure or arrival of the root loci from a pole or a zero of $G(s)H(s)$ can be determined by assuming a point s_1 that is very close to the pole, or zero, and applying the equation

$$\angle G(s_1)H(s_1) = \sum_{k=1}^{m} \angle (s_1 + z_k) - \sum_{j=1}^{n} \angle (s_1 + p_j)$$
$$= 2(i + 1)180° \qquad K > 0$$
$$= 2i \times 180° \qquad K < 0$$

where $i = 0, \pm1, \pm2, \ldots$.

9. Intersection of the root loci	The crossing points of the root loci on the imaginary axis and with the imaginary axis the corresponding values of K may be found by use of the Routh-Hurwitz criterion.
10. Breakaway points	The breakaway points on the root loci are determined by finding the roots of $dK/ds = 0$, or $dG(s)H(s)/ds = 0$. These are necessary conditions only.
11. Calculation of the values of K	The absolute value of K at any point s_1 on the root loci is on the root loci determined from the equation

$$|K| = \frac{1}{|G_1(s_1)H_1(s_1)|}$$

The following example illustrates the construction of a root locus diagram manually, step by step, using the root locus properties given in Table F-1.

▶ **EXAMPLE F-16** Consider the equation

$$s(s + 5)(s + 6)(s^2 + 2s + 2) + K(s + 3) = 0 \qquad \text{(F-42)}$$

Dividing both sides of the last equation by the terms that do not contain K, we have

$$G(s)H(s) = \frac{K(s + 3)}{s(s + 5)(s + 6)(s^2 + 2s + 2)} \qquad \text{(F-43)}$$

The following properties of the root loci are determined:

1. The $K = 0$ points are at the poles of $G(s)H(s)$: $s = -5, -6, -1 + j,$ and $-1 -j$.
2. The $K = \pm\infty$ points are at the zeros of $G(s)H(s)$: $s = -3, \infty, \infty, \infty$.
3. There are five separate branches on the root loci.
4. The root loci are symmetrical with respect to the real axis of the *s*-plane.

5. Since $G(s)H(s)$ has five poles and one finite zero, four RL and CRL should approach infinity along the asymptotes. The angles of the asymptotes of the RL are given by [Eq. (F-9)]

$$\theta_i = \frac{2i + 1}{|n - m|} 180° = \frac{2i + 1}{|5 - 1|} 180° \qquad 0 \le K < \infty \qquad \text{(F-44)}$$

for $i = 0, 1, 2, 3$. Thus, the four root loci that approach infinity as K approaches infinity should approach asymptotes with angles of 45°, −45°, 135°, and −135°, respectively. The angles of the asymptotes of the CRL at infinity are given by Eq. (F-10):

$$\theta_i = \frac{2i}{|n - m|} 180° = \frac{2i}{|5 - 1|} 180° \qquad -\infty < K \le 0 \qquad \text{(F-45)}$$

for $i = 0, 1, 2, 3$. Thus, as K approaches $-\infty$, four root loci for $K < 0$ should approach infinity along asymptotes with angles of 0°, 90°, 180°, and 270°.

6. The intersection of the asymptotes is given by [Eq. (F-12)]

$$\sigma_1 = \frac{\Sigma(-5 - 6 - 1 - 1) - (-3)}{4} = -2.5 \qquad \text{(F-46)}$$

The results from these six steps are illustrated in Fig. F-15. It should be pointed out that in general the properties of the asymptotes do not indicate on which side of the asymptotes
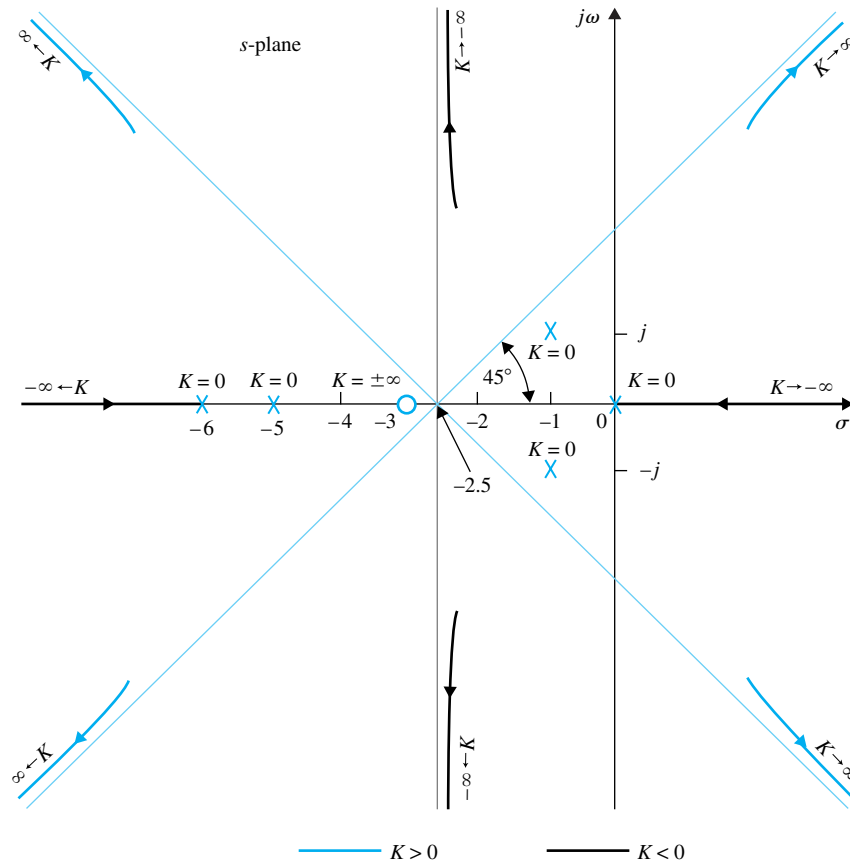
Figure F-15 Preliminary calculation of the root loci of
$s(s + 5)(s + 6)(s^2 + 2s + 2) + K(s + 3) = 0$.
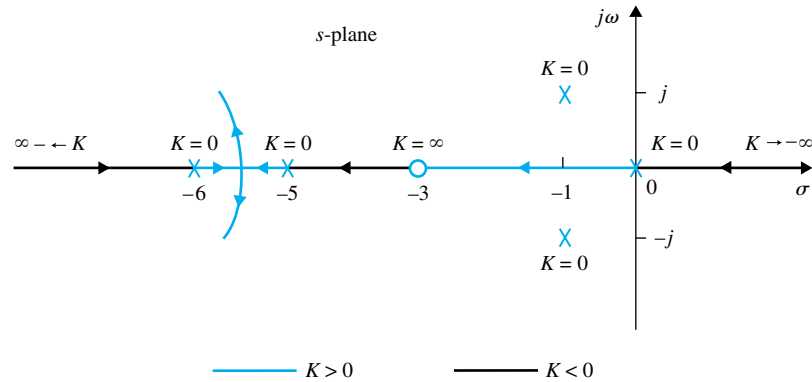
Figure F-16 Root loci of $s(s + 5)(s + 6)(s^2 + 2s + 2) + K(s + 3) = 0$ on the real axis.

the root loci lie. The asymptotes indicate nothing more than the behavior of the root loci as $s \to \infty$. In fact, the root locus can even cross an asymptote in the finite s domain. The segments of the root loci shown in Fig. F-15 can be accurately plotted only if additional information is obtained.

7. Root loci on the real axis: There are $K \geq 0$ root loci on the real axis between $s = 0$ and -3, and $s = -5$ and -6. There are $K \leq 0$ root loci on the remaining portions of the real axis, that is, between $s = -3$ and -5, and $s = -6$ and $-\infty$, as shown in Fig. F-16.

8. Angles of departure: The angle of departure θ of the root loci leaving the pole at $-1 + j$ is determined using Eq. (8-18). If s_1 is a point on the root loci leaving the pole at $-1 + j$, and s_1 is very close to the pole, as shown in Fig F-17, Eq. (8-18) gives

$$\angle(s_1 + 3) - \angle s_1 - \angle(s_1 + 1 + j) - \angle(s_1 + 5) - \angle(s_1 + 1 - j) \qquad \text{(F-47)}$$
$$= (2i + 1)180°$$

or

$$26.6° - 135° - 90° - 14° - 11.4° - \theta \cong (2i + 1)180° \qquad \text{(F-48)}$$

for $i = 0, \pm 1, \pm 2, \ldots$ Therefore, selecting $i = 2$,

$$\theta \cong -43.8° \qquad \text{(F-49)}$$
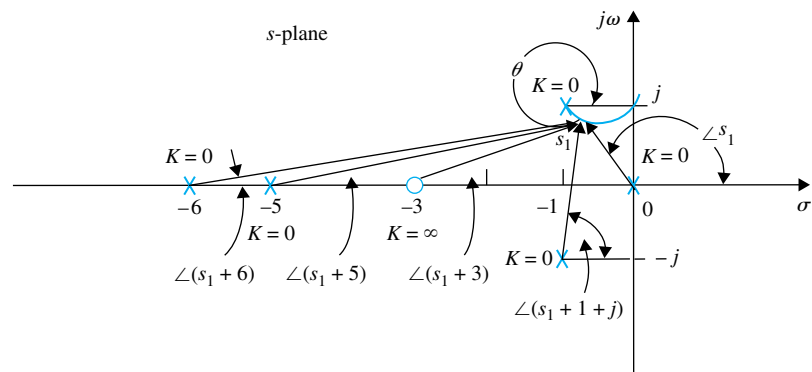
Figure F-17 Computation of angle of departure of the root loci of $s(s + 5)(s + 6)(s^2 + 2s + 2) + K(s + 3) = 0$.

Similarly, Eq. (8-19) is used to determine the angle of arrival θ' of the $K \leq 0$ root loci arriving at the pole $-1 + j$. It is easy to see that θ' differs from θ by 180°; thus,

$$\theta' = 180° - 43.8° = 136.2° \qquad (F\text{-}50)$$

9. The intersection of the root loci on the imaginary axis is determined using Routh's tabulation.

Equation (F-42) is written

$$s^5 + 13s^4 + 54s^3 + 82s^2 + (60 + K)s + 3K = 0 \qquad (F\text{-}51)$$

Routh's tabulation is

s^5	1	54	$60 + K$
s^4	13	82	$3K$
s^3	47.7	$0.769K$	0
s^2	$65.6 - 0.212K$	$3K$	0
s^1	$\dfrac{3940 - 105K - 0.163K^2}{65.6 - 0.212K}$	0	0
s^0	$3K$	0	0

For Eq. (F-51) to have no roots on the imaginary axis or in the right-half of the s-plane, the elements in the first column of Routh's tabulation must all be of the same sign. Thus, the following inequalities must be satisfied:

$$65.6 - 0.212K > 0 \qquad \text{or} \qquad K < 309 \qquad (F\text{-}52)$$
$$3940 - 105K - 0.163K^2 > 0 \qquad \text{or} \qquad K < 35 \qquad (F\text{-}53)$$
$$K > 0 \qquad (F\text{-}54)$$

Thus, all the roots of Eq. (F-51) will stay in the left-half s-plane if K lies between 0 and 35, which means that the root loci of Eq. (F-51) cross the imaginary axis when $K = 35$ and $K = 0$. The coordinates at the crossover points on the imaginary axis that correspond to $K = 35$ are determined from the auxiliary equation:

$$A(s) = (65.6 - 0.212K)s^2 + 3K = 0 \qquad (F\text{-}55)$$

which is obtained by using the coefficients from the row just above the row of zeros in the s^1 row that would have happened when K is set to 35. Substituting $K = 35$ in Eq. (F 55), we get

$$58.2s^2 + 105 = 0 \qquad (F\text{-}56)$$

The roots of Eq. (F-56) are $s = j1.34$ and $-j1.34$, which are the points at which the root loci cross the $j\omega$-axis.

10. Breakaway points: Based on the information gathered from the preceding nine steps, a trial sketch of the root loci indicates that there can be only one breakaway point on the entire root loci, and the point should lie between the two poles of $G(s)H(s)$ at $s = -5$ and -6. To find the breakaway point, we take the derivative on both sides of Eq. (F-43) with respect to s and set it to zero; the resulting equation is

$$s^5 + 13.5s^4 + 66s^3 + 142s^2 + 123s + 45 = 0 \qquad (F\text{-}57)$$

Since there is only one breakaway expected, only one root of the last equation is the correct solution of the breakaway point. The five roots of Eq. (F-57) are:

$$s = 3.33 + j1.204 \qquad s = 3.33 - j1.204$$
$$s = -0.656 + j0.468 \qquad s = -0.656 - j0.468$$
$$s = -5.53$$
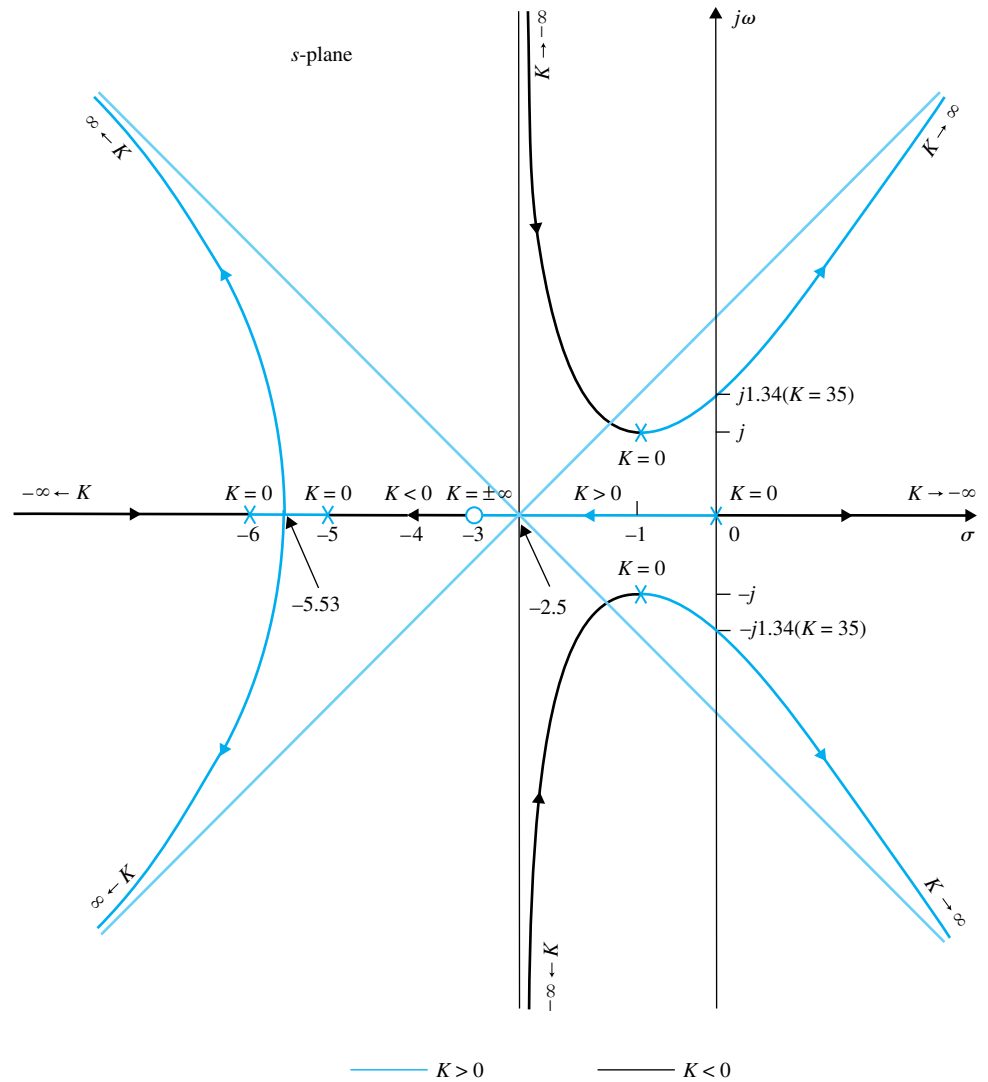
Figure F-18 Root loci of $s(s + 5)(s + 6)(s^2 + 2s + 2) + K(s + 3) = 0$.

Clearly, the breakaway point is at -5.53. The other four solutions do not satisfy Eq. (F-51) and are not breakaway points. Based on the information obtained in the last 10 steps, the root loci of Eq. (F-51) are sketched as shown in Fig. F-18 ◄

Appendix G
Frequency-Domain Plots

TO ACCOMPANY

AUTOMATIC CONTROL SYSTEMS
EIGHTH EDITION

BY

BENJAMIN C. KUO

FARID GOLNARAGHI

JOHN WILEY & SONS, INC.

Frequency-Domain Plots

Let $G(s)$ be the forward-path transfer function of a linear control system with unity feedback. The frequency-domain analysis of the closed-loop system can be conducted from the frequency-domain plots of $G(s)$ with s replaced by $j\omega$.

The function $G(j\omega)$ is generally a complex function of the frequency ω, and can be written as

$$G(j\omega) = |G(j\omega)|\angle G(j\omega) \qquad \text{(G-1)}$$

where $|G(j\omega)|$ denotes the magnitude of $G(j\omega)$, and $\angle G(j\omega)$ is the phase of $G(j\omega)$.

The following frequency-domain plots of $G(j\omega)$ versus ω are often used in the analysis and design of linear control systems in the frequency domain.

1. *Polar plot.* A plot of the magnitude versus phase in the polar coordinates as ω is varied from zero to infinity.
2. *Bode plot.* A plot of the magnitude in decibels versus ω (or $\log_{10}\omega$) in semilog (or rectangular) coordinates.
3. *Magnitude-phase plot.* A plot of the magnitude (in decibels) versus the phase on rectangular coordinates, with ω as a variable parameter on the curve.

▶ G-1 COMPUTER-AIDED CONSTRUCTION OF THE FREQUENCY-DOMAIN PLOTS

The data for plotting of the frequency-domain plots are usually quite time consuming to generate if the computation is to be carried out manually, especially if the function is of high order. In practice, a digital computer should be used to do the computation as well as plotting of the graph. Many software packages that are available commercially can be used for the construction of the frequency-domain plots. The **ACSYS** computer program can be used for this purpose.

From an analytical standpoint, the analyst and designer should be familiar with the properties of the frequency-domain plots so that proper interpretations can be made on these plots made by the computer.

▶ G-2 POLAR PLOTS

The polar plot of a function of the complex variable s, $G(s)$, is a plot of the magnitude of $G(j\omega)$ versus the phase of $G(j\omega)$ on polar coordinates as ω is varied from zero to infinity. From a mathematical viewpoint, the process can be regarded as the mapping of the positive half of the imaginary axis of the s-plane onto the $G(j\omega)$-plane. A simple example
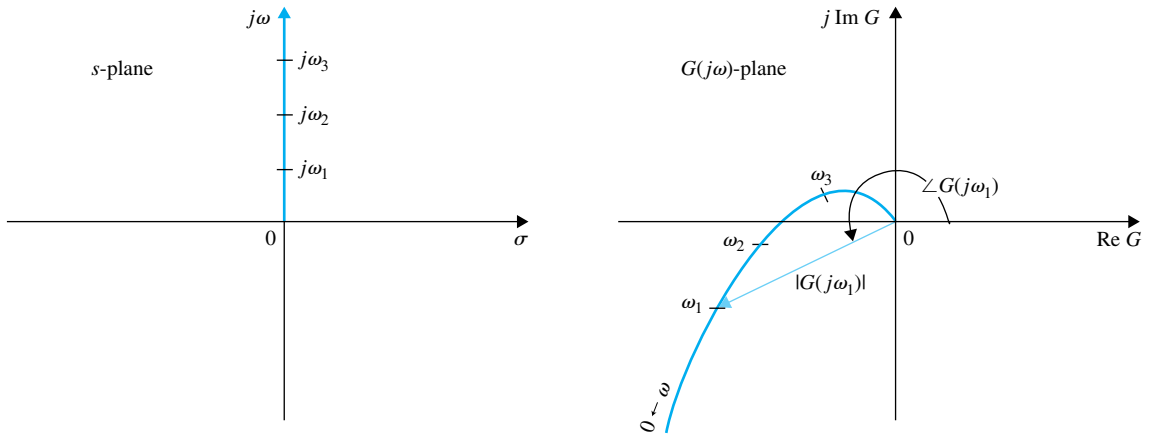
Figure G-1 Polar plot shown as a mapping of the positive half of the $j\omega$-axis in the s-plane onto the $G(j\omega)$-plane.

of this mapping is shown in Fig. G-1. For any frequency $\omega = \omega_1$, the magnitude and phase of $G(j\omega_1)$ are represented by a vector in the $G(j\omega)$-plane. In measuring the phase, counterclockwise is referred to as positive, and clockwise is negative.

▶ **EXAMPLE G-1** To illustrate the construction of the polar plot of a function $G(s)$, consider the function

$$G(s) = \frac{1}{1 + Ts} \tag{G-2}$$

where T is a positive constant. Setting $s = j\omega$, we have

$$G(j\omega) = \frac{1}{1 + j\omega T} \tag{G-3}$$

In terms of magnitude and phase, Eq. (G-3) is written

$$G(j\omega) = \frac{1}{\sqrt{1 + \omega^2 T^2}} \angle -\tan^{-1} \omega T \tag{G-4}$$

When ω is zero, the magnitude of $G(j\omega)$ is unity, and the phase of $G(j\omega)$ is at 0°. Thus, at $\omega = 0$, $G(j\omega)$ is represented by a vector of unit length directed in the 0° direction. As ω increases,
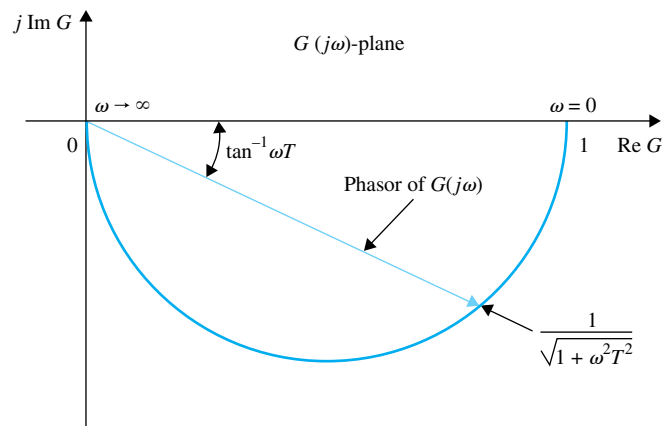
Figure G-2 Polar plot of $G(j\omega) = \dfrac{1}{(1 + j\omega T)}$.

the magnitude of $G(j\omega)$ decreases, and the phase becomes more negative. As ω increases, the length of the vector in the polar coordinates decreases, and the vector rotates in the clockwise (negative) direction. When ω approaches infinity, the magnitude of $G(j\omega)$ becomes zero, and the phase reaches $-90°$. This is presented by a vector with an infinitesimally small length directed along the $-90°$-axis in the $G(j\omega)$-plane. By substituting other finite values of ω into Eq. (G-4), the exact plot of $G(j\omega)$ turns out to be a semicircle, as shown in Fig. G-2. ◀

▶ **EXAMPLE G-2**   As a second illustrative example, consider the function

$$G(j\omega) = \frac{1 + j\omega T_2}{1 + j\omega T_1} \tag{G-5}$$

where T_1 and T_2 are positive real constants. Equation (G-5) is written

$$G(j\omega) = \sqrt{\frac{1 + \omega^2 T_2^2}{1 + \omega^2 T_1^2}} \angle (\tan^{-1} \omega T_2 - \tan^{-1} \omega T_1) \tag{G-6}$$

The polar plot of $G(j\omega)$, in this case, depends on the relative magnitudes of T_1 and T_2. If T_2 is greater than T_1, the magnitude of $G(j\omega)$ is always greater than unity as ω is varied from zero to infinity, and the phase of $G(j\omega)$ is always positive. If T_2 is less than T_1, the magnitude of $G(j\omega)$ is always less than unity, and the phase is always negative. The polar plots of $G(j\omega)$ of Eq. (G-6) that correspond to these two conditions are shown in Fig. G-3.
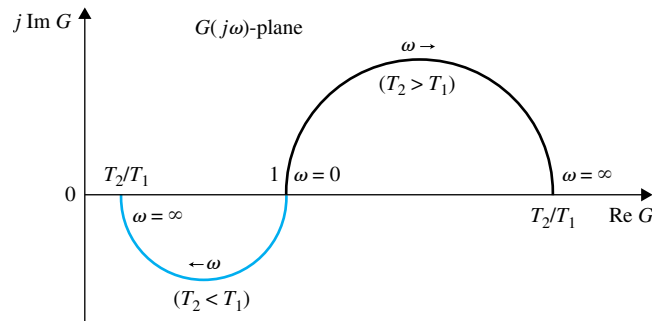
Figure G-3   Polar plots of $G(j\omega) = \dfrac{(1 + j\omega T_2)}{(1 + j\omega T_1)}$. ◀

In many control-system applications, such as the Nyquist stability criterion, an exact plot of the frequency response is not essential. Often, a rough sketch of the polar plot of the transfer function $G(j\omega)H(j\omega)$ is adequate for stability analysis in the frequency domain. The general shape of the polar plot of a function $G(j\omega)$ can be determined from the following information.

1.   The behavior of the magnitude and phase of $G(j\omega)$ at $\omega = 0$ and $\omega = \infty$

2.   The intersections of the polar plot with the real and imaginary axes, and the values of ω at these intersections

▶ **EXAMPLE G-3**   In frequency-domain analyses of control systems, often we have to determine the basic properties of a polar plot. Consider the following transfer function:

$$G(s) = \frac{10}{s(s + 1)} \tag{G-7}$$

By substituting $s = j\omega$ in Eq. (G-7), the magnitude and phase of $G(j\omega)$ at $\omega = 0$ and $\omega = \infty$ are computed as follows:

$$\lim_{\omega \to 0} |G(j\omega)| = \lim_{\omega \to 0} \frac{10}{\omega} = \infty \tag{G-8}$$

$$\lim_{\omega \to 0} \angle G(j\omega) = \lim_{\omega \to 0} \angle 10/j\omega = -90° \tag{G-9}$$

$$\lim_{\omega \to \infty} |G(j\omega)| = \lim_{\omega \to \infty} \frac{10}{\omega^2} = 0 \tag{G-10}$$

$$\lim_{\omega \to \infty} \angle G(j\omega) = \lim_{\omega \to \infty} \angle 10/(j\omega^2) = -180° \tag{G-11}$$

Thus, the properties of the polar plot of $G(j\omega)$ at $\omega = 0$ and $\omega = \infty$ are ascertained. Next, we determine the intersections, if any, of the polar plot with the two axes of the $G(j\omega)$-plane. If the polar plot of $G(j\omega)$ intersects the real axis, at the point of intersection, the imaginary part of $G(j\omega)$ is zero; that is,

$$\text{Im}[G(j\omega)] = 0 \tag{G-12}$$

To express $G(j\omega)$ as the sum of its real and imaginary parts, we must rationalize $G(j\omega)$ by multiplying its numerator and denominator by the complex conjugate of its denominator. Therefore, $G(j\omega)$ is written

$$G(j\omega) = \frac{10(-j\omega)(-j\omega + 1)}{j\omega(j\omega + 1)(-j\omega)(-j\omega + 1)} = \frac{-10\omega^2}{\omega^4 + \omega^2} - j\frac{10\omega}{\omega^4 + \omega^2} \tag{G-13}$$
$$= \text{Re}[G(j\omega)] + j\,\text{Im}[G(j\omega)]$$

When we set $\text{Im}[G(j\omega)]$ to zero, we get $\omega = \infty$, meaning that the $G(j\omega)$ plot intersects only with the real axis of the $G(j\omega)$-plane at the origin.

Similarly, the intersection of $G(j\omega)$ with the imaginary axis is found by setting $\text{Re}[G(j\omega)]$ of Eq. (G-13) to zero. The only real solution for ω is also $\omega = \infty$, which corresponds to the origin of the $G(j\omega)$-plane. The conclusion is that the polar plot of $G(j\omega)$ *does not* intersect any one of the axes at any finite nonzero frequency. Under certain conditions, we are interested in the properties of the $G(j\omega)$ at infinity, which corresponds to $\omega = 0$ in this case. From Eq. (G-13), we see that $\text{Im}[G(j\omega)] = \infty$ and $\text{Re}[G(j\omega)] = -10$ at $\omega = 0$. Based on this information, as well as knowledge of the angles of $G(j\omega)$ at $\omega = 0$ and $\omega = \infty$, the polar plot of $G(j\omega)$ is easily sketched without actual plotting, as shown in Fig. G-4.
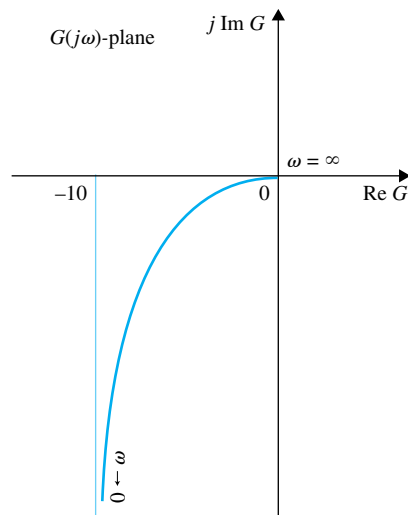
Figure G-4 Polar plot of $G(s) = \dfrac{10}{s(s + 1)}$.

▶ **EXAMPLE G-4**   Given the transfer function

$$G(s) = \frac{10}{s(s + 1)(s + 2)} \tag{G-14}$$

we want to make a rough sketch of the polar plot of $G(j\omega)$. The following calculations are made for the properties of the magnitude and phase of $G(j\omega)$ at $\omega = 0$ and $\omega = \infty$:

$$\lim_{\omega \to 0} |G(j\omega)| = \lim_{\omega \to 0} \frac{5}{\omega} = \infty \tag{G-15}$$

$$\lim_{\omega \to 0} \angle G(j\omega) = \lim_{\omega \to 0} \angle 5/j\omega = -90° \tag{G-16}$$

$$\lim_{\omega \to \infty} |G(j\omega)| = \lim_{\omega \to \infty} \frac{10}{\omega^3} = 0 \tag{G-17}$$

$$\lim_{\omega \to \infty} \angle G(j\omega) = \lim_{\omega \to \infty} \angle 10/(j\omega)^3 = -270° \tag{G-18}$$

To find the intersections of the $G(j\omega)$ plot on the real and imaginary axes of the $G(j\omega)$-plane, we rationalize $G(j\omega)$ to give

$$G(j\omega) = \frac{10(-j\omega)(-j\omega + 1)(-j\omega + 2)}{j\omega(j\omega + 1)(j\omega + 2)(-j\omega)(-j\omega + 1)(-j\omega + 2)} \tag{G-19}$$

After simplification, the last equation is written

$$G(j\omega) = \text{Re}[G(j\omega)] + j\text{Im}[G(j\omega)] = \frac{-30}{9\omega^2 + (2 - \omega^2)^2} - \frac{j10(2 - \omega^2)}{9\omega^3 + \omega(2 - \omega^2)^2} \tag{G-20}$$

Setting $\text{Re}[G(j\omega)]$ to zero, we have $\omega = \infty$, and $G(j\infty) = 0$, which means that the $G(j\omega)$ plot intersects the imaginary axis only at the origin. Setting $\text{Im}[G(j\omega)]$ to zero, we have $\omega = \pm\sqrt{2}$ rad/sec. This gives the point of intersection on the real axis at

$$G(\pm j\sqrt{2}) = -5/3 \tag{G-21}$$

The result, $\omega = -\sqrt{2}$ rad/sec, has no physical meaning, because the frequency is negative; it simply represents a mapping point on the negative $j\omega$-axis of the s-plane. In general, if $G(s)$ is a rational function of s (a quotient of two polynomials of s), the polar plot of $G(j\omega)$ for negative values of ω is the mirror image of that for positive ω, with the mirror placed on the real axis of the $G(j\omega)$-plane. From Eq. (G-20), we also see that $\text{Re}[G(j0)] = \infty$ and $\text{Im}[G(j0)] = \infty$. With this information, it is now possible to make a sketch of the polar plot for the transfer function in Eq. (G-14), as shown in Fig. G-5.
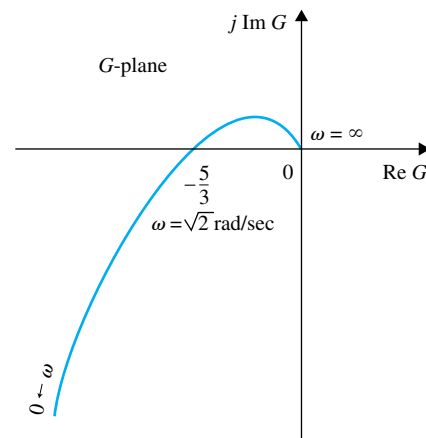
Figure G-5   Polar plot of $G(s) = \dfrac{10}{s(s + 1)(s + 2)}$.

Although the method of obtaining the rough sketch of the polar plot of a transfer function as described is quite straightforward, in general, for complicated transfer functions that may have multiple crossings on the real and imaginary axes of the transfer-function plane, the algebraic manipulation may again be quite involved. Furthermore, the polar plot is basically a tool for analysis; it is somewhat awkward for design purposes. We shall show in the next section that approximate information on the polar plot can always be obtained from the Bode plot, which can be sketched without any calculations. Thus, for more complicated transfer functions, sketches of the polar plots can be obtained with the help of the Bode plots, unless a digital computer is used.

▶ G-3 BODE PLOT (CORNER PLOT OR ASYMPTOTIC PLOT)

• A Bode plot is also known as a corner plot or an asymptotic plot.

The Bode plot of the function $G(j\omega)$ is composed of two plots, one with the amplitude of $G(j\omega)$ in decibels (dB) versus $\log_{10} \omega$ or ω, and the other with the phase of $G(j\omega)$ in degrees as a function of $\log_{10}\omega$ or ω. A Bode plot is also known as a **corner plot** or an **asymptotic plot** of $G(j\omega)$. These names stem from the fact that the Bode plot can be constructed by using straight-line approximations that are asymptotic to the actual plot.

In simple terms, the Bode plot has the following features:

1. Since the magnitude of $G(j\omega)$ in the Bode plot is expressed in dB, product and division factors in $G(j\omega)$ became additions and subtractions, respectively. The phase relations are also added and subtracted from each other algebraically.

2. The magnitude plot of the Bode plot of $G(j\omega)$ can be approximated by straight-line segments, which allow the simple sketching of the plot without detailed computation.

Since the straight-line approximation of the Bode plot is relatively easy to construct, the data necessary for the other frequency-domain plots, such as the polar plot and the magnitude-versus-phase plot, can be easily generated from the Bode plot.

Consider the function:

$$G(s) = \frac{K(s + z_1)(s + z_2)\cdots(s + z_m)}{s^j(s + p_1)(s + p_2)\cdots(s + p_n)}e^{-T_d s} \tag{G-22}$$

where K and T_d are real constants, and the zs and the ps may be real or complex (in conjugate pairs) numbers. In Chapter 8, Eq. (G-22) is the preferred form for root-locus construction, since the poles and zeros of $G(s)$ are easily identified. For constructing the Bode plot manually, $G(s)$ is preferably written in the following form:

$$G(s) = \frac{K_1(1 + T_1 s)(1 + T_2 s)\cdots(1 + T_m s)}{s^j(1 + T_a s)(1 + T_b s)\cdots(1 + T_n s)}e^{-T_d s} \tag{G-23}$$

where K_1 is a real constant, the Ts may be real or complex (in conjugate pairs) numbers, and T_d is the real time delay. If the Bode plot is to be constructed with a computer program, then either forms of Eq. (G-22) or Eq. (G-23) can be used.

Since practically all the terms in Eq. (G-23) are of the same form, then without loss of generality, we can use the following transfer function to illustrate the construction of the Bode diagram.

$$G(s) = \frac{K(1 + T_1 s)(1 + T_2 s)}{s(1 + T_a s)(1 + 2\zeta s/\omega_n + s^2/\omega_n^2)}e^{-T_d s} \tag{G-24}$$

where K, T_d, T_1, T_2, T_a, ζ, and ω_n are real constants. It is assumed that the second-order polynomial in the denominator has complex-conjugate zeros.

The magnitude of $G(j\omega)$ in dB is obtained by multiplying the logarithm (base 10) of $|G(j\omega)|$ by 20; we have

$$|G(j\omega)|_{dB} = 20\log_{10}|G(j\omega)| = 20\log_{10}|K| + 20\log_{10}|1 + j\omega T_1| + 20\log_{10}|1 + j\omega T_2|$$
$$\text{(G-25)}$$
$$- 20\log_{10}|j\omega| - 20\log_{10}|1 + j\omega T_a| - 20\log_{10}|1 + j2\zeta\omega - \omega^2/\omega_n^2|$$

The phase of $G(j\omega)$ is

$$\angle G(j\omega) = \angle K + \angle(1 + j\omega T_1) + \angle(1 + j\omega T_2) - \angle j\omega - \angle(1 + j\omega T_a)$$
$$- \angle(1 + 2\zeta\omega/\omega_n - \omega^2/\omega_n^2) - \omega T_d \quad \text{rad} \qquad \text{(G-26)}$$

In general, the function $G(j\omega)$ may be of higher order than that of Eq. (G-24) and have many more factored terms. However, Eqs. (G-25) and (G-26) indicate that additional terms in $G(j\omega)$ would simply produce more similar terms in the magnitude and phase expressions, so the basic method of construction of the Bode plot would be the same. We have also indicated that, in general, $G(j\omega)$ can contain just five simple types of factors:

1. Constant factor: K
2. Poles or zeros at the origin of order p: $(j\omega)^{\pm p}$
3. Poles or zeros at $s = -1/T$ of order q: $(1 + j\omega T)^{\pm q}$
4. Complex poles and zeros of order r: $(1 + j2\zeta\omega/\omega_n - \omega^2/\omega_n^2)^{\pm r}$
5. Pure time delay $e^{-j\omega T_d}$, where T_d, p, q, and r are positive integers.

Equations (G-25) and (G-26) verify one of the unique characteristics of the Bode plot in that each of the five types of factors listed can be considered as a separate plot; the individual plots are then added or subtracted accordingly to yield the total magnitude in dB and the phase plot of $G(j\omega)$. The curves can be plotted on semilog graph paper or linear rectangular-coordinate graph paper, depending on whether ω or $\log_{10}\omega$ is used as the abscissa.

We shall now investigate sketching the Bode plot of different types of factors.

G-3-1 Real Constant *K*

Since

$$K_{dB} = 20\log_{10} K = \text{constant} \qquad \text{(G-27)}$$

and

$$\angle K = \begin{cases} 0° & K > 0 \\ 180° & K < 0 \end{cases} \qquad \text{(G-28)}$$

the Bode plot of the real constant K is shown in Fig. G-6 in semilog coordinates.

G-3-2 Poles and Zeros at the Origin, $(j\omega)^{\pm p}$

The magnitude of $(j\omega)^{\pm p}$ in dB is given by

$$20\log_{10}|(j\omega)^{\pm p}| = \pm 20p\log_{10}\omega \quad \text{dB} \qquad \text{(G-29)}$$

for $\omega \geq 0$. The last expression for a given p represents a straight line in either semilog or rectangular coordinates. The slopes of these lines are determined by taking the derivative of Eq. (G-29) with respect to $\log_{10}\omega$; that is,

$$\frac{d}{d\log_{10}\omega}(\pm 20p\log_{10}\omega) = \pm 20p \quad \text{dB/decade} \qquad \text{(G-30)}$$
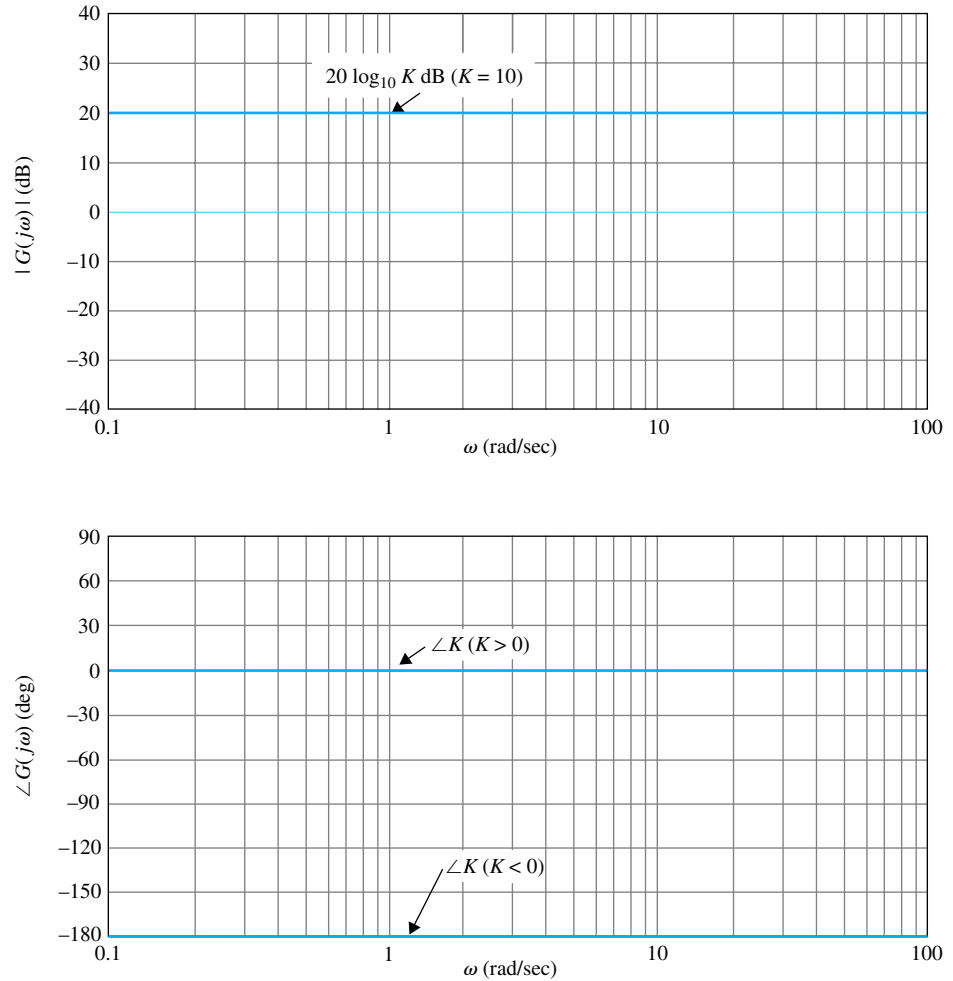
Figure G-6 Bode plot of constant K.

These lines pass through the 0-dB axis at $\omega = 1$. Thus, a unit change in $\log_{10}\omega$ corresponds to a change of $\pm 20p$ dB in magnitude. Furthermore, a unit change in $\log_{10}\omega$ in the rectangular coordinates is equivalent to one **decade** of variation in ω, that is, from 1 to 10, 10 to 100, and so on, in the semilog coordinates. Thus, the slopes of the straight lines described by Eq. (G-29) are said to be $\pm 20p$ dB/decade of frequency.

Instead of decades, sometimes **octaves** are used to represent the separation of two frequencies. The frequencies ω_1 and ω_2 are separated by one octave if $\omega_2/\omega_1 = 2$. The number of decades between any two frequencies ω_1 and ω_2 is given by

$$\text{number of decades} = \frac{\log_{10}(\omega_2/\omega_1)}{\log_{10} 10} = \log_{10}\left(\frac{\omega_2}{\omega_1}\right) \tag{G-31}$$

Similarly, the number of octaves between ω_2 and ω_1 is

$$\text{number of octaves} = \frac{\log_{10}(\omega_2/\omega_1)}{\log_{10} 2} = \frac{1}{0.301}\log_{10}\left(\frac{\omega_2}{\omega_1}\right) \tag{G-32}$$

Thus, the relation between octaves and decades is

$$\text{number of octaves} = 1/0.301 \text{ decades} = 3.32 \text{ decades} \qquad \text{(G-33)}$$

Substituting Eq. (G-33) into Eq. (G-30), we have

$$\pm 20p \text{ dB/decade} = \pm 20p \times 0.301 \cong 6p \quad \text{dB/octave} \qquad \text{(G-34)}$$

For the function $G(s) = 1/s$, which has a simple pole at $s = 0$, the magnitude of $G(j\omega)$ is a straight line with a slope of -20 dB/decade, and passes through the 0-dB axis at $\omega = 1$ rad/sec.

The phase of $(j\omega)^{\pm p}$ is written

$$\angle(j\omega)^{\pm p} = \pm p \times 90° \qquad \text{(G-35)}$$

The magnitude and phase curves of the function $(j\omega)^{\pm p}$ are shown in Fig. G-7 for several values of P.
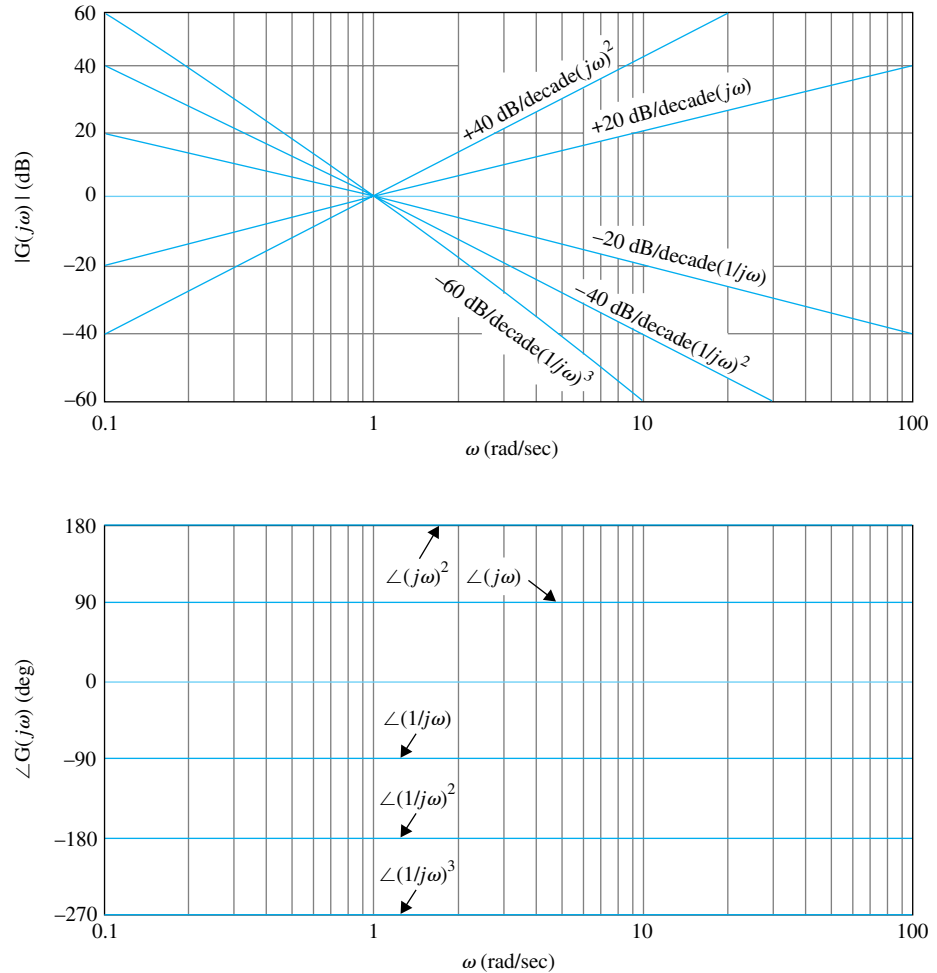
Figure G-7 Bode plots of $(j\omega)^p$.

G-3-3 Simple Zero, $1 + j\omega T$

Consider the function

$$G(j\omega) = 1 + j\omega T \tag{G-36}$$

where T is a positive real constant. The magnitude of $G(j\omega)$ in dB is

$$|G(j\omega)|_{dB} = 20\log_{10}|G(j\omega)| = 20\log_{10}\sqrt{1 + \omega^2T^2} \tag{G-37}$$

To obtain asymptotic approximations of $|G(j\omega)|_{dB}$, we consider both very large and very small values of ω. At very low frequencies, $\omega T \ll 1$, Eq. (G-37) is approximated by

$$|G(j\omega)|_{dB} \cong 20\log_{10} 1 = 0 \quad dB \tag{G-38}$$

since ω^2T^2 is neglected when compared with 1.

At very high frequencies, $\omega T \gg 1$, we can approximate $1 = \omega^2T^2$ by ω^2T^2; then Eq. (G-37) becomes

$$|G(j\omega)|_{dB} \cong 20\log_{10}\sqrt{\omega^2T^2} = 20\log_{10} \omega T \tag{G-39}$$

Equation (G-38) represents a straight line with a slope of 20 dB/decade of frequency. The intersect of these two lines is found by equating Eq. (G-38) to Eq. (G-39), which gives

$$\omega = 1/T \tag{G-40}$$

This frequency is also the intersect of high-frequency approximate plot and the low-frequency approximate plot, which is the 0-dB axis. The frequency given in Eq. (G-40) is also known as the **corner frequency** of the Bode plot of Eq. (G-36), since the asymptotic plot forms the shape of a corner at this frequency, as shown in Fig. G-8. The actual $|G(j\omega)|_{dB}$ plot of Eq. (G-36) is a smooth curve, and deviates only slightly from the straight-line approximation. The actual values and the straight-line approximation of $|1 + j\omega T|_{dB}$ as functions of ωT are tabulated in Table G-1. The error between the actual magnitude curve and the straight-line asymptotes is symmetrical with respect to the corner frequency $\omega = 1/T$. It is useful to remember that the error is 3 dB at the corner frequency, and 1 dB at 1 octave above ($\omega = 2/T$) and 1 octave below ($\omega = 1/2T$) the corner frequency. At 1 decade above and below the corner frequency, the error is dropped to approximately 0.3 dB. Based on these facts, the procedure of making of sketch of $|1 + j\omega T|_{dB}$ is as follows:

1. Locate the corner frequency $\omega = 1/T$ on the frequency axis.
2. Draw the 20-dB/decade (or 6-dB/octave) line and the horizontal line at 0 dB, with the two lines intersecting at $\omega = 1/T$.
3. If necessary, the actual magnitude curve is obtained by adding the errors to the asymptotic plot at the strategic frequencies. Usually, a smooth curve can be sketched simply by locating the 3-dB point at the corner frequency and the 1-dB points at 1 octave above and below the corner frequency.

The phase of $G(j\omega) = 1 + j\omega T$ is

$$\angle G(j\omega) = \tan^{-1} \omega T \tag{G-41}$$

Similar to the magnitude curve, a straight-line approximation can be made for the phase curve. Since the phase of $G(j\omega)$ varies from $0°$ to $90°$, we can draw a line from $0°$ at 1 decade below the corner frequency to $90°$ at 1 decade above the corner frequency. As shown in Fig. G-8, the maximum deviation between the straight-line approximation and the actual curve is less than $6°$. Table G-1 gives the values of $\angle(1 + j\omega T)$ versus ωT.
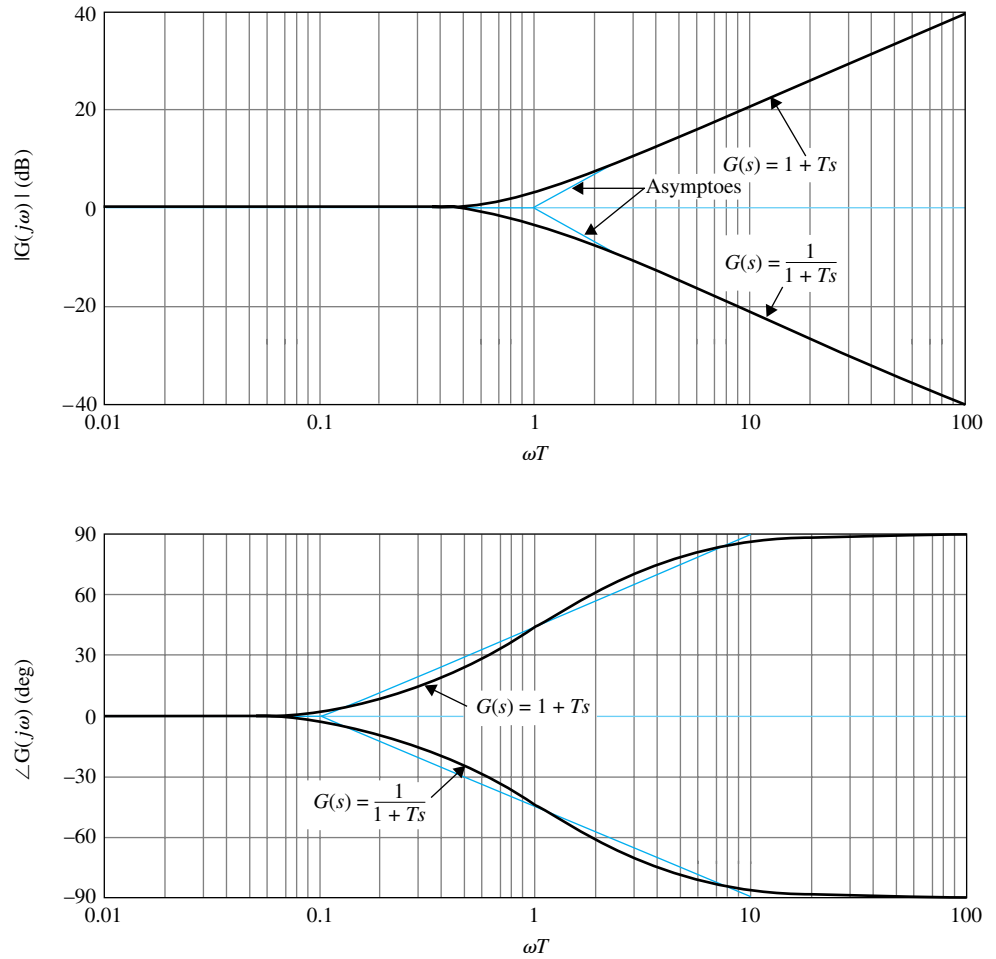
Figure G-8 Bode plots of $G(s) = 1 + Ts$ and $G(s) = \dfrac{1}{(1 + Ts)}$.

TABLE G-1

ωT	$\log_{10}\omega T$	$\|1 + j\omega T\|$	$\|1 + j\omega T\|_{dB}$	Straight-Line Approximation $\|1 + j\omega T\|_{dB}$	Error (dB)	$\angle(1 + j\omega T)$ (deg)
0.01	−2	1.0	0.000043	0	0.00043	0.5
0.10	−1	1.04	0.043	0	0.043	5.7
0.50	−0.3	1.12	1	0	1	26.6
0.76	−0.12	1.26	2	0	2	37.4
1.00	0	1.41	3	0	3	45.0
1.31	0.117	1.65	4.3	2.3	2	52.7
2.00	0.3	2.23	7.0	6.0	1	63.4
10.00	1.0	10.4	20.043	20.0	0.043	84.3
100.00	2.0	100.005	40.00043	40.0	0.00043	89.4

G-3-4 Simple Pole, $1/(1 + j\omega T)$

For the function

$$G(j\omega) = \frac{1}{1 + j\omega T} \tag{G-42}$$

the magnitude, $|G(j\omega)|$ in dB, is given by the negative of the right side of Eq. (G-37), and the phase $\angle G(j\omega)$ is the negative of the angle in Eq. (G-41). Therefore, it is simple to extend all the analysis for the case of the simple zero to the Bode plot of Eq. (G-42). The asymptotic approximations of $|G(j\omega)|_{dB}$ at low and high frequencies are

$$\omega T \ll 1 \quad |G(j\omega)|_{dB} \cong 0 \text{ dB} \tag{G-43}$$
$$\omega T \gg 1 \quad |G(j\omega)|_{dB} \cong -20\log_{10} \omega T \tag{G-44}$$

Thus, the corner frequency of the Bode plot of Eq. (G-42) is still at $\omega = 1/T$, except that at high frequencies the slope of the straight-line approximation is -20 dB/decade. The phase of $G(j\omega)$ is 0 degrees at $\omega = 0$, and $-90°$ when $\omega = \infty$. The magnitude in dB and phase of the Bode plot of Eq. (G-42) are shown in Fig. G-8. The data in Table G-1 are still useful for the simple-pole case if appropriate sign changes are made to the numbers. For instance, the numbers in the $|1 + j\omega T|_{dB}$, the straight-line approximation of $|1 + j\omega T|_{dB}$, the error (db), and the $\angle(1 + j\omega T)$ columns should all be negative. At the corner frequency, the error between the straight-line approximation and the actual magnitude curve is -3 dB.

G-3-5 Quadratic Poles and Zeros

Now consider the second-order transfer function

$$G(s) = \frac{\omega_n^2}{s^2 + 2\zeta\omega_n s + \omega_n^2} = \frac{1}{1 + (2\zeta/\omega_n)s + (1/\omega_n^2)s^2} \tag{G-45}$$

We are interested only in the case when $\zeta \leq 1$, since otherwise $G(s)$ would have two unequal real poles, and the Bode plot can be obtained by considering $G(s)$ as the product of two transfer functions with simple poles.

By letting $s = j\omega$, Eq. (G-45) becomes

$$G(j\omega) = \frac{1}{[1 - (\omega/\omega_n)^2] + j2\zeta(\omega/\omega_n)} \tag{G-46}$$

The magnitude of $G(j\omega)$ in dB is

$$20\log_{10}|G(j\omega)| = -20\log_{10}\sqrt{[1 - (\omega/\omega_n)^2]^2 + 4\zeta^2(\omega/\omega_n)^2} \tag{G-47}$$

At very low frequencies, $\omega/\omega_n \ll 1$; Eq. (G-47) can be approximated as

$$|G(j\omega)|_{dB} = 20\log_{10}|G(j\omega)| \cong -20\log_{10} 1 = 0 \quad \text{dB} \tag{G-48}$$

Thus, the low-frequency asymptote of the magnitude plot of Eq. (G-45) is a straight line that lies on the 0-dB axis. At very high frequencies, $\omega/\omega_n \gg 1$; the magnitude in dB of $G(j\omega)$ in Eq. (G-45) becomes

$$|G(j\omega)|_{dB} \cong -20\log_{10}\sqrt{(\omega/\omega_n)^4} = -40\log_{10}(\omega/\omega_n) \quad \text{dB} \tag{G-49}$$

This equation represents a straight line with a slope of -40 dB/decade in the Bode-plot coordinates. The intersection of the two asymptotes is found by equating Eq. (G-48) to Eq. (G-49), yielding the corner frequency at $\omega = \omega_n$. The actual magnitude cuve of $G(j\omega)$ in this case may differ strikingly from the asymptotic curve. The reason for this is that the amplitude and phase curves of the second-order $G(j\omega)$ depend not only on the
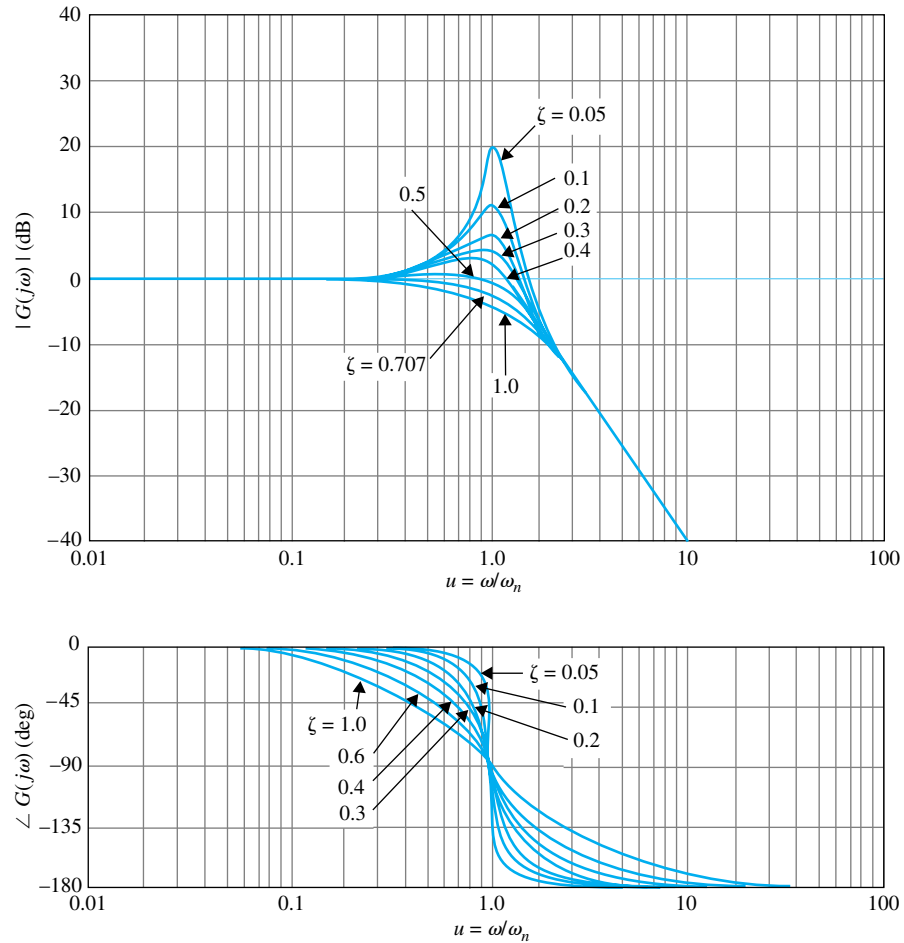
Figure G-9 Bode plot of $G(s) = \dfrac{1}{1 + 2\zeta(s/\omega_n) + (s/\omega_n)^2}$.

corner frequency ω_n, but also on the damping ratio ζ, which does not enter the asymptotic curve. The actual and the asymptotic curves of $|G(j\omega)|_{dB}$ are shown in Fig. G-9 for several values of ζ. The errors between the two sets of curves are shown in Fig. G-10 for the same set of values of ζ. The standard procedure of constructing the second-order $|G(j\omega)|_{dB}$ is to first locate the corner frequency ω_n, and -40-dB/decade line to the right of ω_n. The actual curve is obtained by making corrections to the asymptotes by using either the data from the error curves of Fig. G-10 or the curves in Fig. G-9 for the corresponding ζ.

The phase of $G(j\omega)$ is given by

$$\angle G(j\omega) = -\tan^{-1}\left\{\frac{2\zeta\omega}{\omega_n}\left[1 - \left(\frac{\omega}{\omega_n}\right)^2\right]\right\} \tag{G-50}$$

and is plotted as shown in Fig. G-9 for various values of ζ.

The analysis of the Bode plot of the second-order transfer function of Eq. (G-45) can be applied to the second-order transfer function with two complex zeros. For

$$G(s) = 1 + \frac{2\zeta}{\omega_n}s + \frac{1}{\omega_n^2}s^2 \tag{G-51}$$
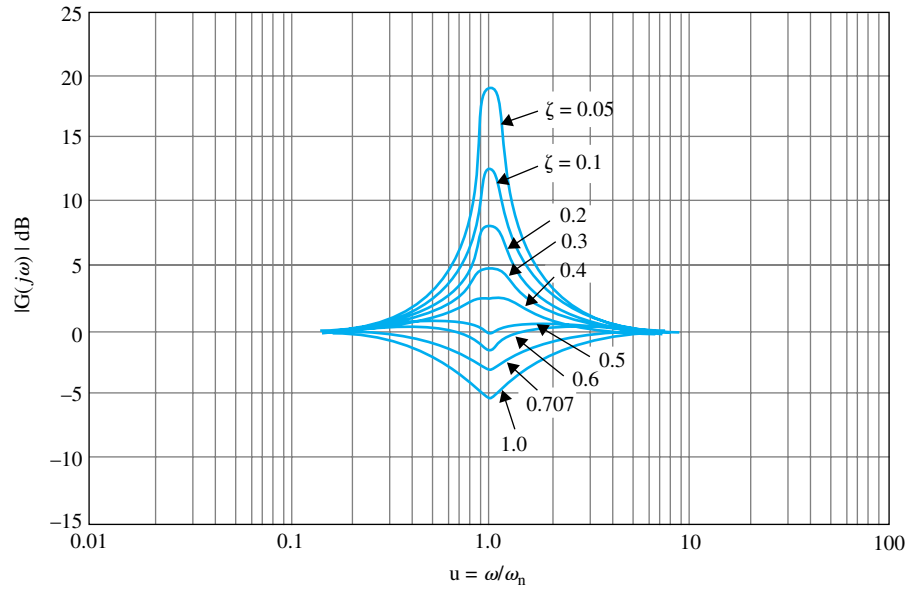
Figure G-10 Errors in magnitude curves of Bode plots of $G(s) = \dfrac{1}{1 + 2\zeta(s/\omega_n) + (s/\omega_n)^2}$.

the magnitude and phase curves are obtained by inverting those in Fig. G-9. The errors between the actual and the asymptotic curves in Fig. G-10 are also inverted.

G-3-6 Pure Time Delay, $e^{-j\omega T_d}$

• The magnitude of the pure time delay term is unity for all w.

The magnitude of the pure time delay term is equal to unity for all values of ω. The phase of the pure time delay term is

$$\angle e^{-j\omega T_d} = -\omega T_d \tag{G-52}$$

which decreases linearly as a function of ω. Thus, for the transfer function

$$G(j\omega) = G_1(j\omega)e^{-j\omega T_d} \tag{G-53}$$

the magnitude plot $|G(j\omega)|_{dB}$ is identical to that of $|G_1(j\omega)|_{dB}$. The phase plot $\angle G(j\omega)$ is obtained by subtracting ωT_d radians from the phase curve of $G_1(j\omega)$ at various ω.

► **EXAMPLE G-5** As an illustrative example on the manual contruction of Bode plot, consider the function

$$G(s) = \frac{10(s + 10)}{s(s + 2)(s + 5)} \tag{G-54}$$

The first step is to express $G(s)$ in the form of of Eq. (G-23) and set $s = j\omega$ (keeping in mind that for computer plotting, this step is unnecessary); we have

$$G(j\omega) = \frac{10(1 + j0.1\omega)}{j\omega(1 + j0.5\omega)(1 + j0.2\omega)} \tag{G-55}$$

Equation (G-54) shows that $G(j\omega)$ has corner frequencies at $\omega = 2$, 5, and 10 rad/sec. The pole at $s = 0$ gives a magnitude curve that is a straight line with slope of -20 dB/decade, passing through the $\omega = 1$ rad/sec point on the 0-dB axis. The complete Bode plot of the magnitude and phase of
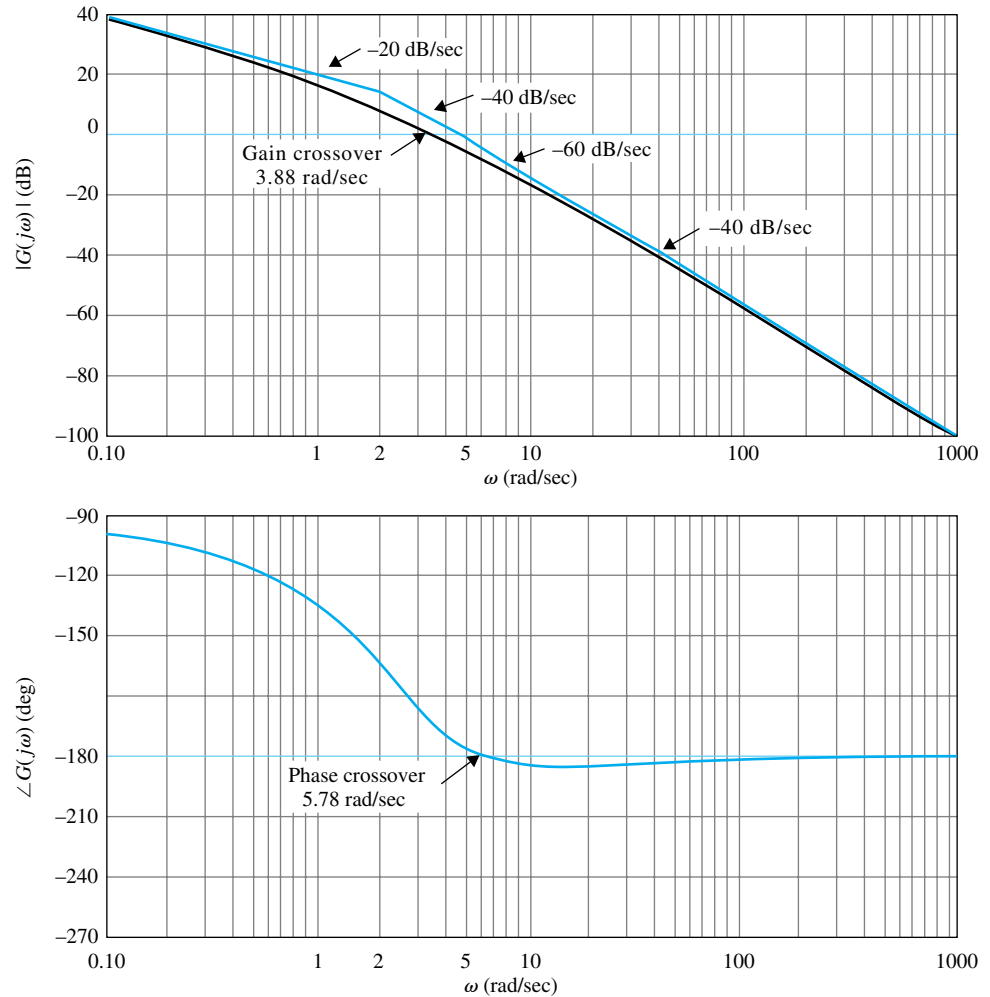
Figure G-11   Bode plot of $G(s) = \dfrac{10(s + 10)}{s(s + 2)(s + 5)}$.

$G(j\omega)$ is obtained by adding the component curves together, point by point, as shown in Fig. G-11. The actual curves can be obtained by a computer program and are shown in Fig. G-11.   ◄

► G-4 MAGNITUDE-PHASE PLOT

The magnitude-phase plot of $G(j\omega)$ is a plot of the magnitude of $G(j\omega)$ in dB versus its phase in degrees, with ω as a parameter on the curve. One of the most important applications of this type of plot is that when $G(j\omega)$ is the forward-path transfer function of a unity-feedback control system, the plot can be superposed on the Nichols chart (see Chapter 9) to give information on the relative stability and frequency response of the system. When the gain factor K of the transfer function varies, the plot is simply raised or lowered vertically according to the value of K in dB. However, in the construction of the plot, the property of adding the curves of the individual components of the transfer function in the Bode plot does not carry over to this case. Thus, it is best to make the magnitude-phase plot by computer or transfer the data from the Bode plot.

▶ **EXAMPLE G-6** As an illustrative example, the polar plot and the magnitude-phase plot of Eq. (G-54) are shown in Fig. G-12 and G-13, respectively. The Bode plot of the function is already shown in Fig. G-11. The relationships among these three plots are easily identified by comparing the curves in Figs. G-11, G-12, and G-13.
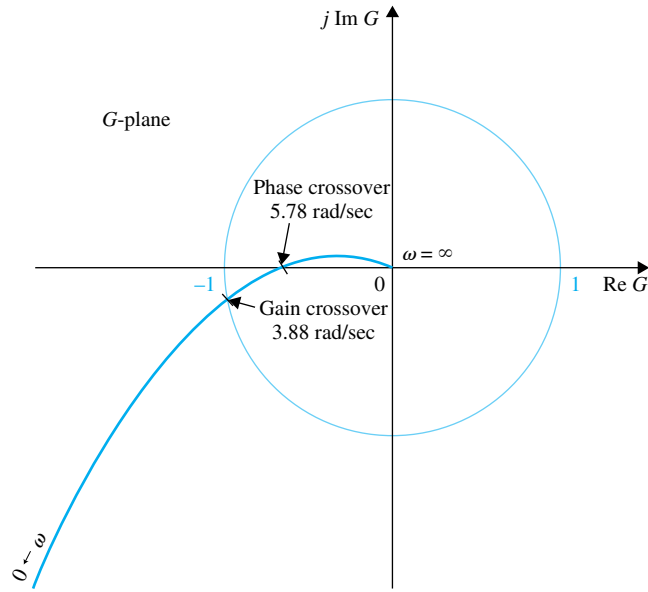
Figure G-12 Polar plot of
$$G(s) = \frac{10(s + 10)}{s(s + 2)(s + 5)}.$$
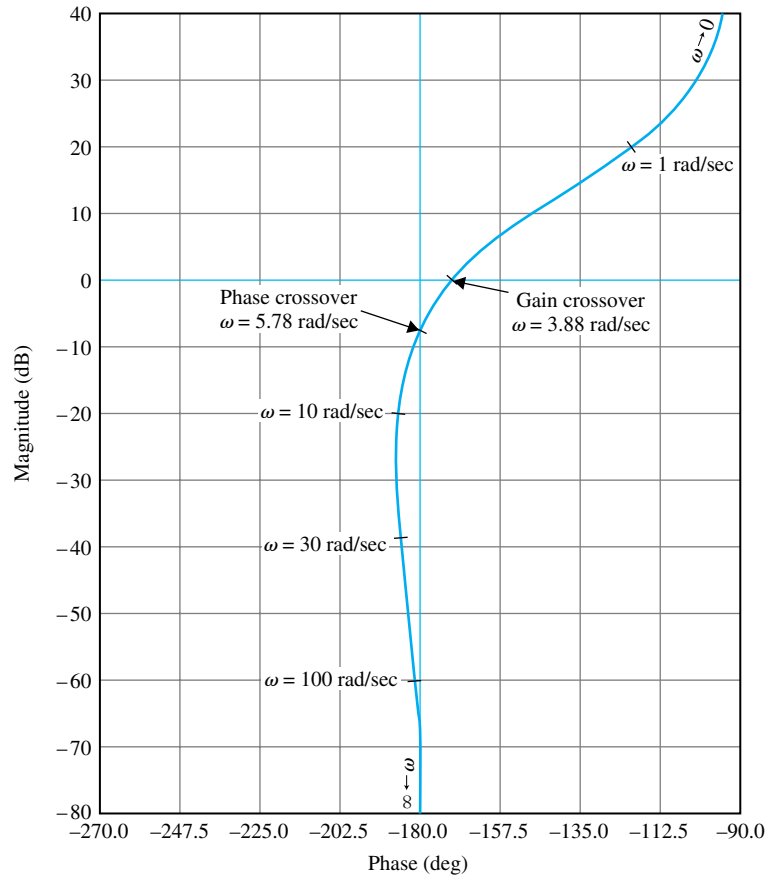
Figure G-13 Magnitude-phase plot of
$$G(s) = \frac{10(s + 10)}{s(s + 2)(s + 5)}.$$

▶ G-5 GAIN- AND PHASE-CROSSOVER POINTS

Gain- and phase-crossover points on the frequency-domain plots are important for analysis and design of control systems. These are defined as follows.

Gain-Crossover Point: The gain-crossover point on the frequency-domain plot of $G(j\omega)$ is the point at which $|G(j\omega)| = 1$ or $|G(j\omega)|_{dB} = 0$ dB. The frequency at the gain-crossover point is called the **gain-crossover frequency ω_g**.

Phase-Crossover Point: The phase-crossover point on the frequency-domain plot of $G(j\omega)$ is the point at which $\angle G(j\omega) = 180°$. The frequency at the phase-crossover point is called the **phase-crossover frequency ω_p**.

The gain and phase crossovers are interpreted with respect to three types of plots:

Polar Plot: The gain-crossover point (or points) is where $|G(j\omega)| = 1$. The phase-crossover point (or points) is where $\angle G(j\omega) = 180°$ (see Fig. G-12).

Bode Plot: The gain-crossover point (or points) is where the magnitude curve $|G(j\omega)|_{dB}$ crosses the 0-dB axis. The phase-crossover point (or points) is where the phase curve crosses the 180° axis (see Fig. G-11).

Magnitude-Phase Plot: The gain-crossover point (or points) is where the $G(j\omega)$ curve crosses the 0-dB axis. The phase-crossover point (or points) is where the $G(j\omega)$ curve crosses the 180° axis (see Fig. G-13).

▶ G-6 MINIMUM-PHASE AND NONMINIMUM-PHASE FUNCTIONS

A majority of the process transfer functions encountered in linear control systems do not have poles or zeros in the right-half s-plane. This class of transfer functions is called the **minimum-phase transfer functions**. When a transfer function has either a pole or a zero in the right-half s-plane, it is called a **nonminimum-phase transfer function**.

• The magnitude and phase characteristics of a minimum-phase function are uniquely related.

Minimum-phase transfer functions have an important property in that their magnitude and phase characteristics are uniquely related. In other words, given a minimum-phase function $G(s)$, knowing its magnitude characteristics $|G(j\omega)|$ completely defines the phase characteristics, $\angle G(j\omega)$. Conversely, given $\angle G(j\omega)$, $|G(j\omega)|$ is completely defined.

Nonminimum-phase transfer functions do not have the unique magnitude-phase relationships. For instance, given the function

$$G(j\omega) = \frac{1}{1 - j\omega T} \tag{G-56}$$

the magnitude of $G(j\omega)$ is the same whether T is positive (nonminimum phase) or negative (minimum phase). However, the phase of $G(j\omega)$ is different for positive and negative T.

Additional properties of the minimum-phase transfer functions are as follows:

1. For a minimum-phase transfer function $G(s)$ with m zeros and n poles, excluding the poles at $s = 0$, if any, when $s = j\omega$ and as ω varies from ∞ to 0, the total phase variation of $G(j\omega)$ is $(n - m)\pi/2$.

2. The value of a minimum-phase transfer function cannot become zero or infinity at any finite nonzero frequency.

3. A nonminimum-phase transfer function will always have a more positive phase shift as ω is varied from ∞ to 0.

▶ **EXAMPLE G-7** As an illustrative example of the properties of the nonminimum-phase transfer function, consider that the zero of the transfer function of Eq. (G-54) is in the right-half s-plane; that is,

$$G(s) = \frac{10(s - 10)}{s(s + 2)(s + 5)} \qquad (G\text{-}57)$$

The magnitude plot of the Bode diagram of $G(j\omega)$ is identical to that of the minimum-phase trans-fer function in Eq. (G-54), as shown in Fig. G-11. The phase curve of the Bode plot of $G(j\omega)$ of Eq. (G-57) is shown in Fig. G-14(a), and the polar plot is shown in Fig. G-14(b). Notice that the nonminimum-phase function has a net phase shift of 270° (from −180° to +90°) as ω varies from ∞ to 0, whereas the minimum-phase transfer function if Eq. (G-54) has a net phase change of only 90° (from −180° to −90°) over the same frequency range.

• Do not use the Bode plot and the gain-phase plot of a nonminimum-phase transfer function for stability studies.

Care should be taken when using the Bode diagram for the analysis and design of systems with nonminimum-phase transfer functions. For stability studies, the polar plot, when used along with the Nyquist criterion discussed in Chapter 9, is more convenient for nonminimum-phase systems. Bode diagrams of nonminimum-phase forward-path transfer functions *should not* be used for sta-bility analysis of closed-loop control systems. The same is true for the magnitude-phase plot.
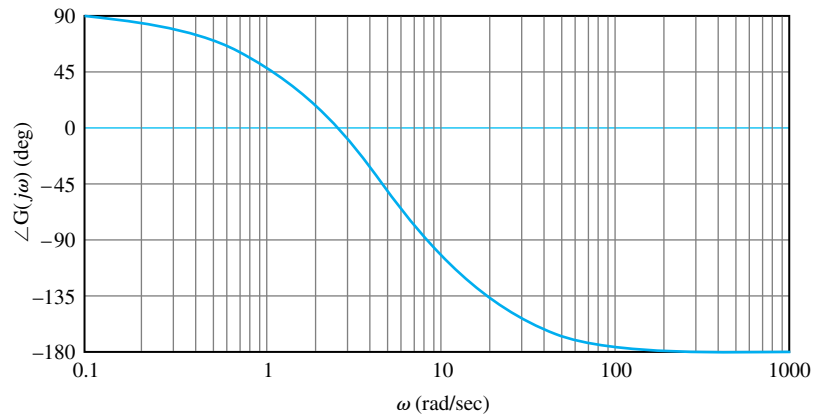
(a)
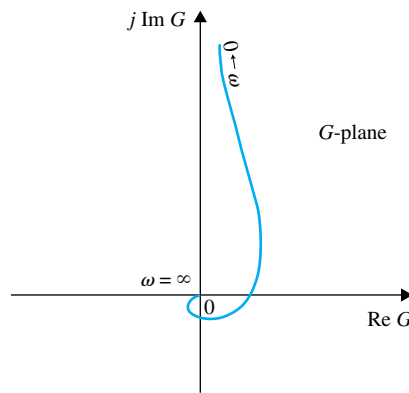
(b)

Figure G-14   (a) Phase curve of the Bode plot. (b) Polar plot. $G(s) = \dfrac{10(s - 10)}{s(s + 2)(s + 5)}$.   ◀

Appendix H
General Nyquist Criterion

General Nyquist Criterion

▶ H-1 FORMULATION OF NYQUIST CRITERION

The original Nyquist criterion presented in Chapter 9 is cumbersome to apply when the loop transfer function is of the nonminimum-phase type; that is, $L(s)$ has either poles and/or zeros in the right-half s-plane. We shall show that if the loop transfer function is of the nonminimum-phase type, then plotting the Nyquist plot of $L(s)$ only for $s = j\omega$ to $s = j0$ and not enclosing the $(-1, j0)$ point in the $L(s)$-plane is only a necessary but not sufficient condition for closed-loop stability. For a system with a nonminimum-phase loop transfer function $L(s)$, the original Nyquist criterion requires that the $L(s)$ plot that corresponds to the entire Nyquist path in Fig. 9-20 be made. If the loop transfer function $L(s)$ has poles or zeros on the $j\omega$-axis, then the Nyquist path of Fig. 9-20 must have small indentations around them on the $j\omega$-axis. This adds even more complexity to the construction of the $L(s)$ plot. Our MATLAB Toolbox (**ACSYS**) or other computer software can all be used to construct the plots of only functions that correspond to the positive $j\omega$-axis of the s-plane. The rest of the Nyquist plot that corresponds to the small indentations and the large semicircle on the Nyquist path have to be plotted manually. With modern computer facilities and software, the analyst should not be burdened with the chores of manual plotting. Therefore, we are introducing *a simplified Nyquist criterion that can be applied by using only the positive $j\omega$-axis of the Nyquist path and then observing its behavior with reference to the $(-1, j0)$ point.*

Yeung [1] introduced a general and yet simplified version of the Nyquist criterion that allows the determination of stability of closed-loop systems of minimum- as well as nonminimum-phase loop transfer functions by using only the positive part of the $j\omega$-axis of the Nyquist path. However, if the system is of the minimum-phase type, the test of whether the $(-1, j0)$ point is enclosed is still simpler to apply. We shall show that for nonminimum-phase systems, if the $(-1, j0)$ point is enclosed, the system is still unstable. However, if the $(-1, j0)$ point is not enclosed, then an additional angle condition is all that must be satisfied by the Nyquist plot of $L(s)$ for the system to be stable.

Let us consider the two Nyquist paths shown in Figs. H-1(a) and H-1(b). Apparently, the Nyquist path Γ_{s1}, in Fig. H-1(a) is the original one shown in Fig. 9-20, whereas the path Γ_{s2}, in Fig. H-1(b) encircles not only the entire right-half s-plane, but also all the poles and zeros of $L(s)$ on the $j\omega$-axis, if there are any. Let us define the following quantities.

Z = number of zeros of $1 + L(s)$ that are in the right-half s-plane.

P = number of poles of $L(s)$, or of $1 + L(s)$, that are in the right-half s-plane.

P_ω = number of poles of $L(s)$, or of $1 + L(s)$, that are on the $j\omega$-axis, including the origin.

N_1 = number of times the $(-1, j0)$ point of the $L(s)$-plane that is encircled by the Nyquist plot of $L(s)$ corresponding to Γ_{s1}.
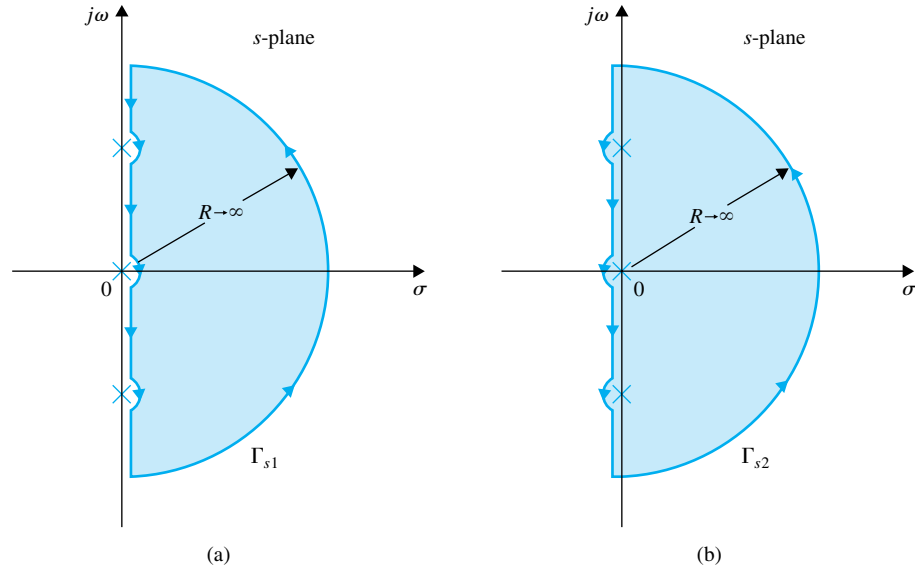
Figure H-1 (a) Nyquist path, (b) An alternative Nyquist path, (Source: K. S. Yeung, "A Reformulation of Nyquist's Criterion," *IEEE Trans. Educ.*, Vol. E-28, pp. 58–60, February 1985.)

N_2 = number of times the $(-1, j0)$ point of the $L(s)$-plane that is encircled by the Nyquist plot of $L(s)$ corresponding to Γ_{s2}.

Then, with reference to the two Nyquist paths in Fig. H-1, and according to the Nyquist criterion,

$$N_1 = Z - P \tag{H-1}$$

and

$$N_2 = Z - P - P_\omega \tag{H-2}$$

Let Φ_1 and Φ_2 represent the net angles traversed by the Nyquist plot of $L(s)$ with respect to the $(-1, j0)$ point, corresponding to Γ_{s1} and Γ_{s2}, respectively. Then,

$$\Phi_1 = N_1 \times 360° = (Z - P)360° \tag{H-3}$$
$$\Phi_2 = N_2 \times 360° = (Z - P - P_\omega)360° \tag{H-4}$$

Let us consider that each of the Nyquist paths Γ_{s1} and Γ_{s2} is composed of three portions:

1. The portion from $s = -j\infty$ to $+j\infty$ along the semicircle with infinite radius
2. The portion along the $j\omega$-axis, excluding all the small indentations
3. All the small indentations on the $j\omega$-axis

Since the Nyquist paths in Fig. H-1 are symmetrical about the real axis in the s-plane, the angles traversed by the Nyquist plots are identical for positive and negative values of ω. Thus, Φ_1 and Φ_2 are written

$$\Phi_1 = 2\Phi_{11} + \Phi_{12} + \Phi_{13} \tag{H-5}$$
$$\Phi_2 = 2\Phi_{11} - \Phi_{12} + \Phi_{13} \tag{H-6}$$

where Φ_{11} = angle traversed by the Nyquist plot of $L(s)$ with respect to the $(-1, j0)$ point, corresponding to the positive $j\omega$-axis or the $-j\omega$-axis of the s-plane, excluding the small indentations.

Φ_{12} = angle traversed by the Nyquist plot of $L(s)$ with respect to the $(-1, j0)$ point, corresponding to the small indentations on the $j\omega$-axis of Γ_{s1}. Since on Γ_{s2} the directions of the small indentations are opposite to that of Γ_{s1}, the sign of Φ_{12} in Eq. (H-5) is negative.

Φ_{13} = angle traversed by the Nyquist plot of $L(s)$ with respect to the $(-1, j0)$ point, corresponding to the semicircle with infinite radius on the Nyquist paths.

For a transfer function $L(s)$ that does not have more zeros than poles, the Nyquist plot of $L(s)$ that corresponds to the infinite semicircle must either be a point on the real axis or a trajectory around the origin of the $L(s)$-plane. Thus, the angle Φ_{13} traversed by the phasor drawn from the $(-1, j0)$ point to the Nyquist plot along the semicircle with infinite radius is always zero.

Now adding Eq. (H-5) to Eq. (H-6) and using Eqs. (H-3) and (H-4), we get

$$\Phi_1 + \Phi_2 = 4\Phi_{11}$$
$$= (2Z - 2P - P_\omega)360° \qquad \text{(H-7)}$$

Solving for Φ_{11}, we get

$$\Phi_{11} = (Z - P - 0.5P_\omega)180° \qquad \text{(H-8)}$$

The equation states:

The total angle traversed by the phasor drawn from the $(-1, j0)$ point to the $L(s)$ Nyquist plot that corresponds to the portion on the positive $j\omega$-axis of the s-plan, excluding the small indentations, if any, equals

The number of zeros of $1 + L(s)$ in the right-half s-plane
$-$ the number of poles of $L(s)$ in the right-half s-plane   (H-9)
-0.5(the number of poles of $L(s)$ on the $j\omega$-axis)180°

• In general, Nyquist criterion can be carried out by drawing the Nyquist plot of $L(j\omega)$ that corresponds to $\omega = \infty$ to $\omega = 0$.

Thus, *the Nyquist stability criterion can be carried out by constructing only the Nyquist plot that corresponds to the $s = j\infty$ to $s = 0$ portion on the Nyquist path.* Furthermore, if the closed-loop system is unstable, by knowing the values of Φ_{11}, P_ω, and P, Eq. (H-8) gives the number of roots of the characteristic equation that are in the right-half s-plane.

For the closed-loop system to be stable, Z must equal zero. Thus, the Nyquist criterion for stability of the closed-loop system is

$$\Phi_{11} = -(0.5P_\omega + P)180° \qquad \text{(H-10)}$$

Since P_ω and P cannot be negative, the last equation indicates that

• The angle Φ_{11} is an **angle variation**, so that $\Phi_{11} = -270°$ is not the same as $\Phi_{11} = 90°$.

if the phase traversed by the Nyquist plot of $L(j\omega)$ as ω varies from ∞ to 0, Φ_{11}, is positive with respect to the $(-1, j0)$ point, the closed-loop system is unstable.

However, if Φ_{11} is negative, it still has to satisfy Eq. (H-9) for the system to be stable. With reference to the Nyquist plot of $L(j\omega)$ and the $(-1, j0)$ point, we see that when the angle variation Φ_{11} is positive, it corresponds to the $(-1, j0)$ point being enclosed. Thus, the condition that the Nyquist plot of $L(j\omega)$ not enclosing the $(-1, j0)$ point is a necessary condition for closed-loop stability for nonminimum-phase systems. However, if the $(-1, j0)$ point is not enclosed by the Nyquist plot of $L(j\omega)$, for the non-minimum-phase system to be closed-loop stable, the angle variation Φ_{11} still has to satisfy Eq. (H-9).

H-1-1 System with Minimum-Phase Loop Transfer Functions

If $L(s)$ is of the minimum-phase type, then $P = 0$ and P_ω denotes the number of poles of $L(s)$ that are at the origin. Eq. (H-8) becomes

$$\Phi_{11} = (Z - 0.5P_\omega)180° \qquad \text{(H-11)}$$

For closed-loop stability, $Z = 0$; Eq. (H-11) becomes

$$\Phi_{11} = -P_\omega \times 90° \qquad \text{(H-12)}$$

Since P_ω denotes the number of poles of $L(s)$ that are at the origin, it is easy to see that if the $(-1, j0)$ point is not enclosed by the Nyquist plot of $L(s)$, Φ_{11} will always be given by Eq. (H-12). Thus, when $L(s)$ is of the minimum-phase type, the condition that the $(-1, j0)$ point not be enclosed by the Nyquist plot is a necessary and sufficient condition for closed-loop stability.

H-1-2 Systems with Improper Loop Transfer Functions

Equation (H-8) is derived based on the condition that $\Phi_{13} = 0$, which is true only if $L(s)$ is strictly proper; that is, it has more poles than zeros. For improper transfer functions, we can again use the method discussed in Section 9-6 by plotting the Nyquist plot of $1/L(s)$.

▶ H-2 ILLUSTRATIVE EXAMPLES—GENERAL NYQUIST CRITERION MINIMUM AND NONMINIMUM TRANSFER FUNCTIONS

In the following example we shall show that the Nyquist plot of a nonminimum-phase transfer function does not enclose the $(-1, j0)$ point, and yet the system is unstable.

▶ **EXAMPLE H-1** Consider that the loop transfer function of a control system is given by

$$L(s) = \frac{s^2 - s + 1}{s(s^2 - 6s + 5)} \qquad \text{(H-13)}$$
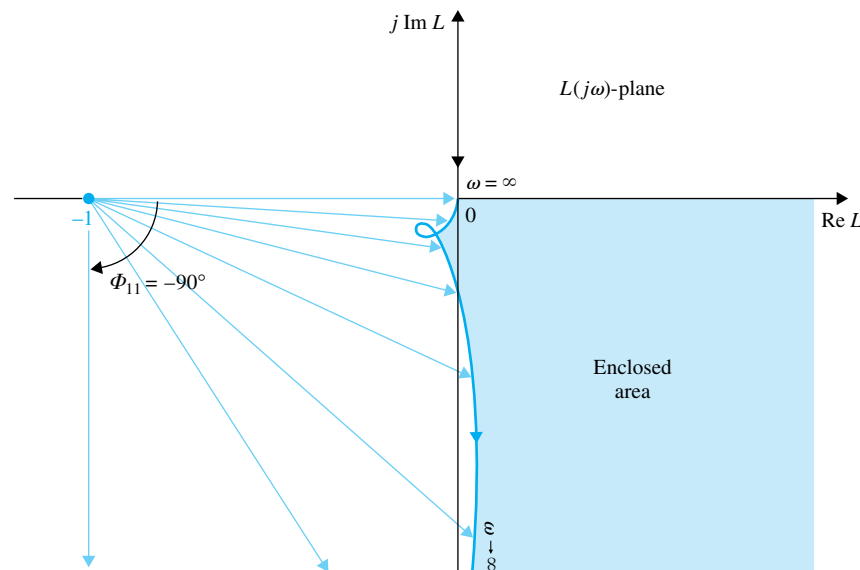
Figure H-2 Nyquist plot of $L(s) = \dfrac{s^2 - s + 1}{s(s^2 - 6s + 5)}$.

Since $L(s)$ has one pole at the origin, and two poles in the right-half s-plane, $P_\omega = 1$ and $P = 2$. From Eq. (H-9), the closed-loop system is stable if the following condition is satisfied:

$$\Phi_{11} = -(0.5P_\omega + P)180° = -450° \tag{H-14}$$

The Nyquist plot of $L(j\omega)$ for $\omega = \infty$ to $\omega = 0$ is plotted as shown in Fig. H-2. Apparently, in this case, the $(-1, j0)$ point is not enclosed by the Nyquist plot. However, since Φ_{11} is $-90°$, and not $-450°$, the system is unstable. Substituting $\Phi_{11} = 90°$ into Eq. (9-82) and solving for Z, we have $Z = 2$, which means that there are two closed-loop poles in the right-half s-plane. ◀

▶ **EXAMPLE H-2** Consider the system described in Example 9-1. the loop transfer function of the system, $L(s)$, is given in Eq. (9-59), and is repeated below.

$$L(j\omega) = \frac{K}{s(s + 2)(s + 10)} \tag{H-15}$$

The Nyquist plot of $L(j\omega)$ is shown in Fig. 9-25. It is shown in Example 9-1 that for closed-loop stability, the $(-1, j0)$ point in the $L(j\omega)$-plane must be to the left of the intersect of the Nyquist plot with the real axis.

Now we shall apply the generalized Nyquist criterion to the system. Since $L(s)$ is of the minimum-phase type, $P = 0$, and it has one pole at the origin, thus, $P_\omega = 1$. Substituting these quantities into Eq. (H-11), we have

$$\Phi_{11} = (Z - 0.5)180° \tag{H-16}$$

For closed-loop stability, Z must equal zero; thus the last equation gives $\Phi_{11} = -90°$. This means that the phasor drawn from the $(-1, j0)$ to the Nyquist plot, from $\omega = \infty$ to $\omega = 0$, must equal $-90°$, or $90°$ in the CW direction. Figure H-3(a) shows that if the $(-1, j0)$ point is to the left of the intersect of $L(j\omega)$ with the real axis, Φ_{11} is indeed $-90°$. On the other hand, if the $(-1, j0)$ point is to the right of the intersect as shown in Fig. H-3(b) when the value of K is greater than 240, then, Φ_{11} is $+270°$, or (more easily observed when the critical point is enclosed), the system would be unstable. Substituting, $\Phi_{11} = 270°$ into Eq. (H-16), we get $Z = 2$, which means that the characteristic equation has two roots in the right-half s-plane. Thus, for systems with minimum-phase loop transfer functions, the Nyquist criterion with the "enclosure" test is easier to observe, but when the system is unstable, it does not tell how many characteristic equation roots are in the right-half plane; the general Nyquist criterion does.
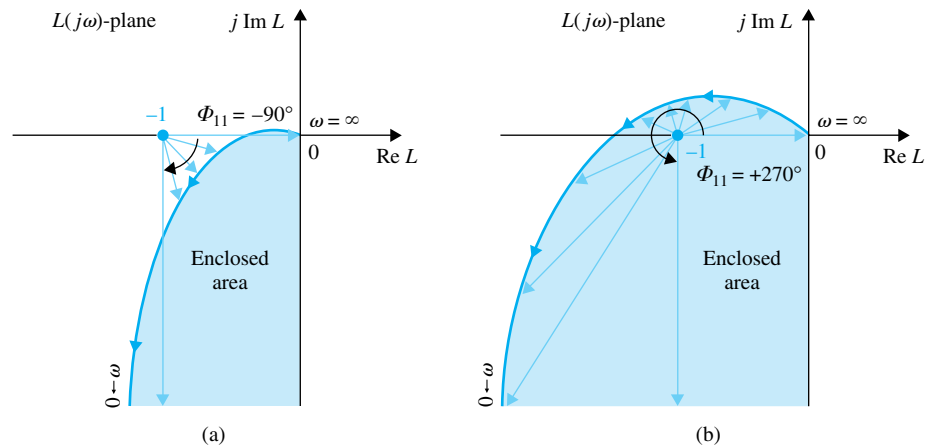
Figure H-3   Nyquist plot of $L(s) = \dfrac{K}{s(s + 2)(s + 10)}$.   (a) $K < 240$. (b) $K > 240$. ◀

► **EXAMPLE H-3** Consider that a control system has the loop transfer function

$$L(s) = \frac{K(s-1)}{s(s+1)} \tag{H-17}$$

We observed from the last equation that $P_\omega = 1$, and $P = 0$. The function $L(s)$ is of the nonminimum-phase type, since it has a zero at $s = 1$. Thus, the Nyquist criterion on enclosure cannot be used adequately in this case. From Eq. (H-8), the requirement for closed-loop stability is

$$\Phi_{11} = -(0.5P_\omega + P)180° = -90° \tag{H-18}$$

Thus, the stability criterion requires that the phasor drawn from the $(-1, j0)$ point to the Nyquist plot of $L(j\omega)$ should traverse $-90°$ as ω varies from ∞ to 0.

To sketch the Nyquist plot of $L(s)$ that corresponds to the positive portion of the $j\omega$-axis of the s-plane, we set $s = j\omega$ in Eq. (H-17). We get

$$L(j\omega) = \frac{K(j\omega - 1)}{j\omega(j\omega + 1)} = \frac{K(j\omega - 1)}{-\omega^2 + j\omega} \tag{H-19}$$

When $\omega = \infty$,

$$L(j\infty) = \left.\frac{K}{j\omega}\right|_{\omega=\infty} = 0\angle -90° \tag{H-20}$$

When $\omega = 0$,

$$L(j0) = \left.\frac{K}{j\omega}\right|_{\omega=0} = \infty\angle 90° \tag{H-21}$$

To find the intersect of the $L(j\omega)$ plot on the real axis, we rationalize the function by multiplying the numerator and the denominator of Eq. (H-19) by $-\omega^2 - j\omega$. We have

$$L(j\omega) = \frac{K(j\omega - 1)(-\omega^2 - j\omega)}{\omega^4 + \omega^2} = \frac{K[2\omega + j(1 - \omega^2)]}{\omega(\omega^2 + 1)} \tag{H-22}$$

Setting the imaginary part of $L(j\omega)$ to zero and solving for ω^2, we have

$$\omega^2 = \pm 1 \text{ rad/sec} \tag{H-23}$$

For $\omega = 1$,

$$L(j1) = K \tag{H-24}$$

NYQUIST PLOT FOR $K > 0$. Based on the preceding information, the Nyquist plot of $L(j\omega)$ that corresponds to the positive portion of the $j\omega$-axis is sketched as shown in Fig. H-4 for $K > 0$. Figure H-4 shows that as ω varies from ∞ to 0 along the Nyquist plot, the net angle Φ_{11} traversed by the phasor drawn from the $(-1, j0)$ point to the Nyquist plot is $+90°$. Thus, the system is unstable because Φ_{11} is positive. We can also readily see that $(-1, j0)$ is enclosed by the Nyquist plot, and so the same conclusion on closed-loop stability can be drawn.

From Eq. (H-7),

$$\Phi_{11} = (Z - 0.5P_\omega - P)180° = (Z - 0.5)180° = 90° \tag{H-25}$$

Thus, $Z = 1$, which means that the characteristic equation of the closed-loop system has one root in the right-half s-plane. The characteristic equation of the system is

$$s^2 + (1 + K)s - K = 0 \tag{H-26}$$

We can easily verify that stability requires

$$0 > K > -1 \tag{H-27}$$

NYQUIST PLOT FOR $K < 0$. Figure H-5(a) shows the Nyquist plot of $L(j\omega)$ when K lies between 0 and -1. Notice that the plot is obtained by *rotating* the $L(j\omega)$ plot of Fig. H-4 by $180°$
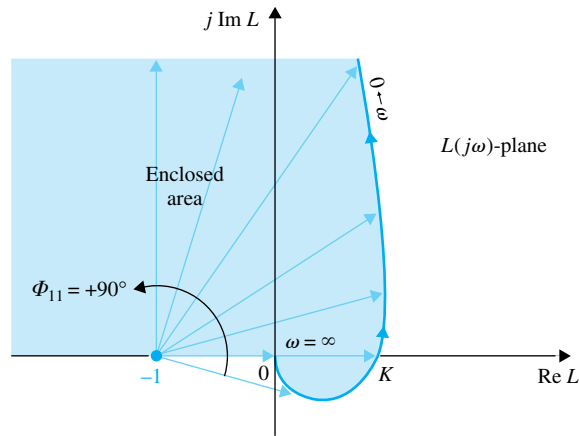
Figure H-4 Nyquist plot of the system in Example H-3.

$$L(s) = \frac{K(s-1)}{s(s+1)}.$$

about the origin. As ω is varied from ∞ to 0, the angle Φ_{11} in Fig. H-5(a) has a net rotation of $-90°$, which agrees with the stability requirement in Eq. (H-18), and the closed-loop system is stable. It should be reminded that since $L(j\omega)$ is of the minimum-phase type, the fact that the Nyquist plot of $L(j\omega)$ of Fig. H-5(a) does not enclose the $(-1, j0)$ is *not* the reason that the system is stable.

Figure H-5(b) shows the Nyquist plot when $K < -1$. Now we see that the $(-1, j0)$ point is enclosed, so system is unstable. Checking the value of Φ_{11}, we have $\Phi_{11} = 270°$, which differs from the required $-90°$. Using Eq. (H-8),

$$\Phi_{11} = (Z - 0.5P_\omega - P)180° = (Z - 0.5)180° = 270° \qquad \text{(H-28)}$$

Thus, $Z = 2$, which means that the characteristic equation has two roots in the right-half s-plane.

In general, when K changes sign, it is not necessary to redraw the Nyquist plot as shown in Fig. H-5. Equation (9-40) can be written as

$$1 + L(s) = 1 + KL_1(s) = 0 \qquad \text{(H-29)}$$

(a)

(b)
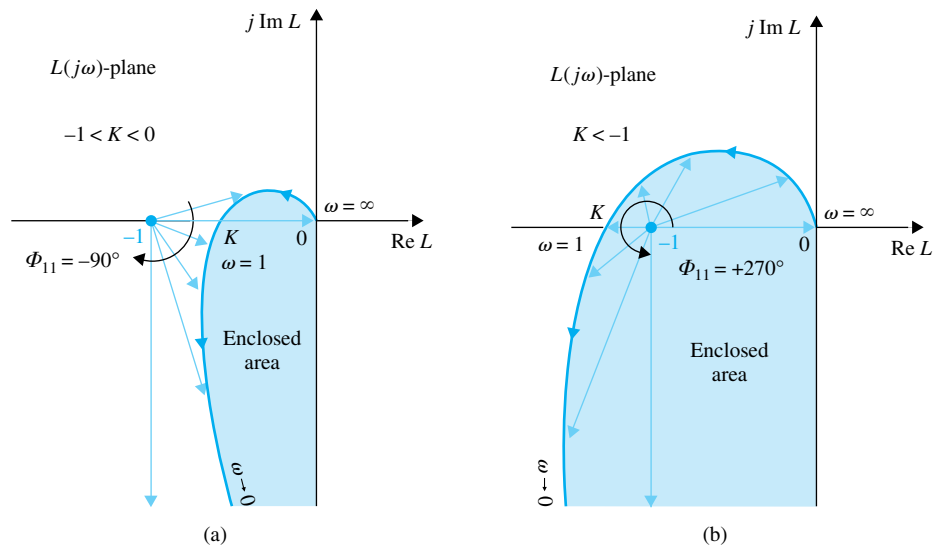
Figure H-5 Nyquist plots of the system in Example H-3. $L(s) = \dfrac{K(s-1)}{s(s+1)}$.

(a) $-1 < K < 0$.   (b) $K < -1$.
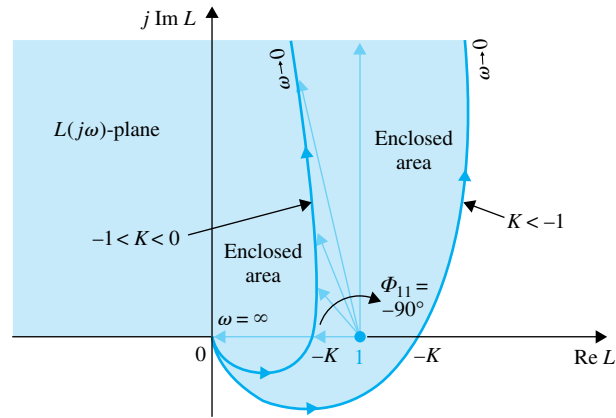
Figure H-6 Nyquist plot of $L(s) = \dfrac{K(s-1)}{s(s+1)}$ with $K < 0$. The $(+1, j0)$ point is the critical point.

where K is positive. For negative K, the last equation can be written as

$$1 - KL_1(s) = 0 \tag{H-30}$$

or

$$KL_1(s) = 1 \tag{H-31}$$

where K is now positive. Thus, Eq. (H-31) shows that when K is negative, we can still use the $L(j\omega)$ plot for positive K, but designate the $(+1, j0)$ point as the critical point for stability analysis.

Figure H-6 shows the Nyquist plot of Eq. (H-17) for $K > 0$. When K is negative, the $(+1, j0)$ point is regarded as the critical point. As shown in Fig. H-6, for $-1 < K < 0$, Φ_{11} is $-90°$, which is the required value, and the system is stable. When $K < -1$, the $(+1, j0)$ point is enclosed by the Nyquist plot, and the system is unstable. These results agree with those obtained from Fig. H-5 when the Nyquist plots for $K < 0$ were actually constructed.

It is of interest to compare the Nyquist stability analysis with the root-locus analysis. Figure H-7 shows the root loci of the characteristic equation of the system with the loop transfer function
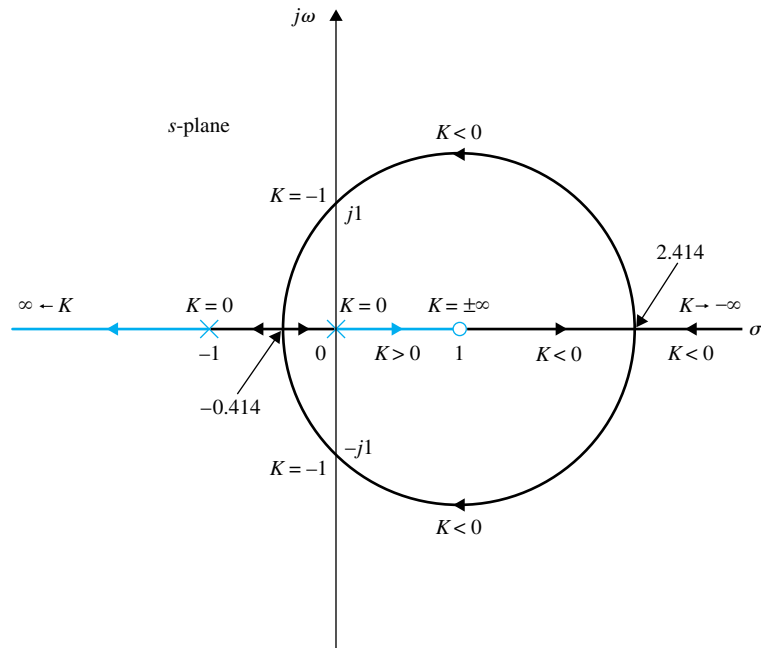
Figure H-7 Complete root loci of system in Example H-3.

given in Eq. (H-17). The stability condition of the system as a function of K is clearly indicated by the root-locus diagram. The RL between 0 and $+1$ on the real axis indicates that the system is unstable for $0 < K < \infty$. The RL indicates that for negative values of K, the system is unstable for $-\infty < K < -1$, and the system is stable only for the range of $-1 < K < 0$. The root loci cross the $j\omega$-axis at $\omega = \pm 1$ rad/sec, which are the values of ω at which the Nyquist plot of $L(j\omega)$ intersects the negative real axis. ◀

▶ **EXAMPLE H-4** Consider the control system shown in Fig. H-8. It is desired to determine the range of K for which the system is stable. The loop transfer function of the system is

$$L(s) = \frac{Y(s)}{E(s)} = \frac{10K(s + 2)}{s^3 + 3s^2 + 10} \tag{H-32}$$

The poles of $L(s)$ are found to be at $s = -3.72$, $0.361 + j1.6$, and $0.361 - j1.6$. Or, we can use the Routh-Hurwitz criterion to verify that $L(s)$ has two poles in the right-half s-plane. Thus, $P = 2$, and $P_\omega = 0$. The transfer function $L(s)$ is of the nonminimum-phase type. From Eq. (H-9), the requirement for the closed-loop system to be stable is

$$\Phi_{11} = -(0.5P_\omega + P)180° = -360° \tag{H-33}$$

Setting $s = j\omega$, Eq. (H-32) becomes

$$L(j\omega) = \frac{10K(j\omega + 2)}{(10 - 3\omega^2) - j\omega^3} \tag{H-34}$$

At $\omega = \infty$,

$$L(j\infty) = 0\angle 180° \tag{H-35}$$

At $\omega = 0$,

$$L(j0) = 2K \tag{H-36}$$

To find the intersect on the real axis of the $L(j\omega)$-plane, we rationalize $L(j\omega)$ as

$$L(j\omega) = \frac{10K\{2(10 - 3\omega^2) - \omega^4 + j[\omega(10 - 3\omega^2) + 2\omega^2]\}}{(10 - 3\omega^2)^2 + \omega^6} \tag{H-37}$$

Setting the imaginary part of $L(j\omega)$ to zero, we have

$$\omega(10 - 3\omega^2) + 2\omega^3 = 0 \tag{H-38}$$

The solutions of the last equation are $\omega = 0$ and $\omega = \pm\sqrt{10} = 3.16$ rad/sec, which are the frequencies at which the $L(j\omega)$ plot intersects the real axis of the $L(j\omega)$-plane. When $\omega = 0$, we already have $L(j0) = 2K$ in Eq. (H-36). When $\omega = 3.16$ rad/sec,

$$L(j3.16) = -K \tag{H-39}$$
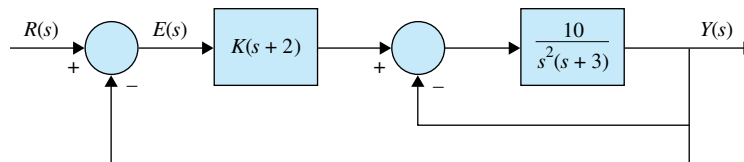
Figure H-8 Block diagram of the control system in Example H-4.
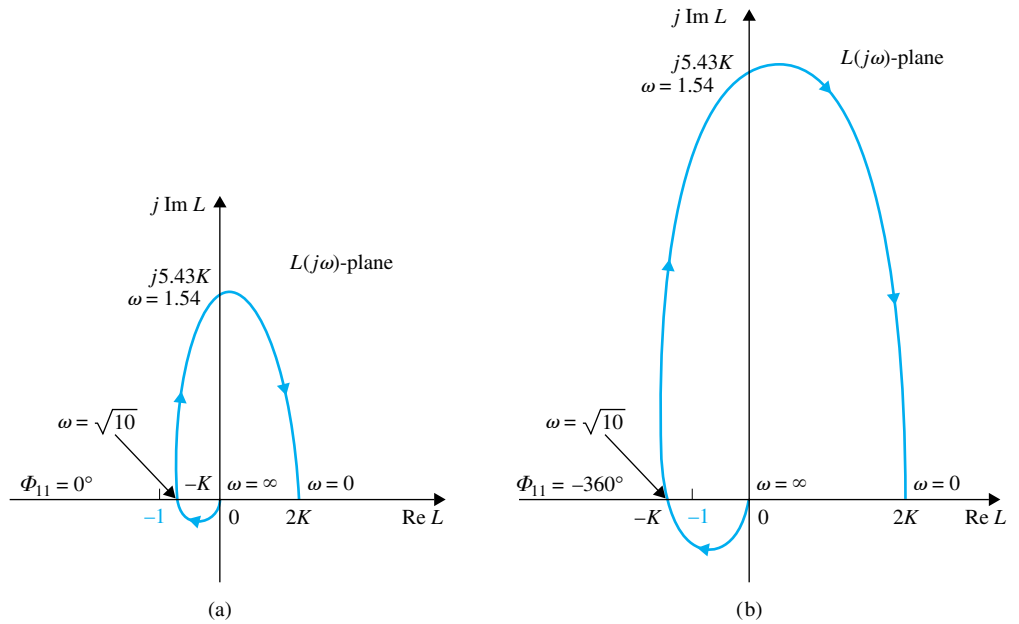
Figure H-9 Nyquist plots of the system in Example H-4. (a) $1 > K > 0$. (b) $K > 1$.

Figure H-9(a) shows the Nqyuist plot of $L(j\omega)$ for $0 < K < 1$. Since the $(-1, j0)$ point is enclosed by the Nyquist plot, the closed-loop system is unstable. We can also show that the angle traversed by Φ_{11} is $0°$, not $-360°$, as required in Eq. (H-33). Figure H-9(b) shows the Nyquist plot of $L(j\omega)$ when K is greater than unity. In this case, the angle Φ_{11} rotates a total of $-360°$, thus, the system is stable.
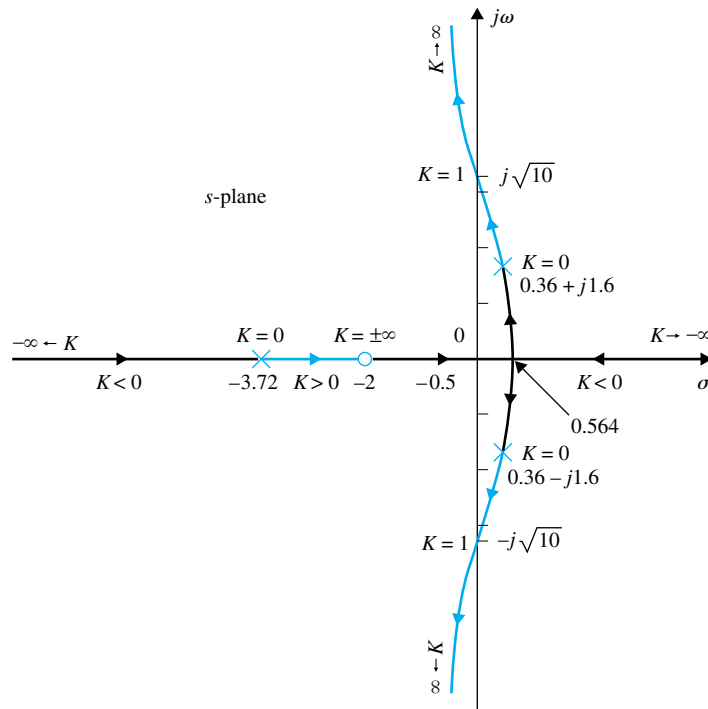
Figure H-10 Complete root loci of the system in Example H-4.

When K is negative, we can use the plots in Fig. H-9, and regard the $(+1, j0)$ point as the critical point. The following stability conditions are observed:

$2K < -1$:   The $(+1, j0)$ point lies between 0 and $2K$, and is not enclosed by $L(j\omega)$, but $\Phi_{11} = -180°$; the system is unstable. For stability, Φ_{11} must equal $-360°$.

$-1 < 2K < 0$:   The $(+1, j0)$ point is to the right of the point $2K$, and is enclosed by the Nyquist plot; the system is unstable. In this case, $\Phi_{11} = 0°$.

The conclusion is that the system is stable for $K > 1$. The root loci of the system are shown in Fig. H-10. Clearly, when K is negative, one branch of the RL will always stay in the right-half plane, and the system is unstable. The system is stable only for $K > 1$, and the root loci cross the $j\omega$-axis at $\omega = \pm 3.16$ rad/sec, which corresponds to the frequency at which the $L(j\omega)$ plot intersects the negative real axis. The value of K at the crossing point on the $j\omega$-axis is 1. ◀

▶ **EXAMPLE H-5** Consider a control system with the loop transfer function

$$L(s) = \frac{K}{(s + 2)(s^2 + 4)} \qquad (H-40)$$

which has a pair of imaginary poles at $s = j2$ and $-j2$. Thus, $P_\omega = 2$, and $P = 0$. To apply the Nyquist criterion in the original form, we would have to define the Nyquist path with small indentations around these poles.

Instead of constructing the entire Nyquist plot, the portion that corresponds to $s = j\infty$ to $j0$ is plotted as shown in Fig. H-11. The data for this Nyquist plot are easily obtained using any of the frequency-domain program mentioned earlier.
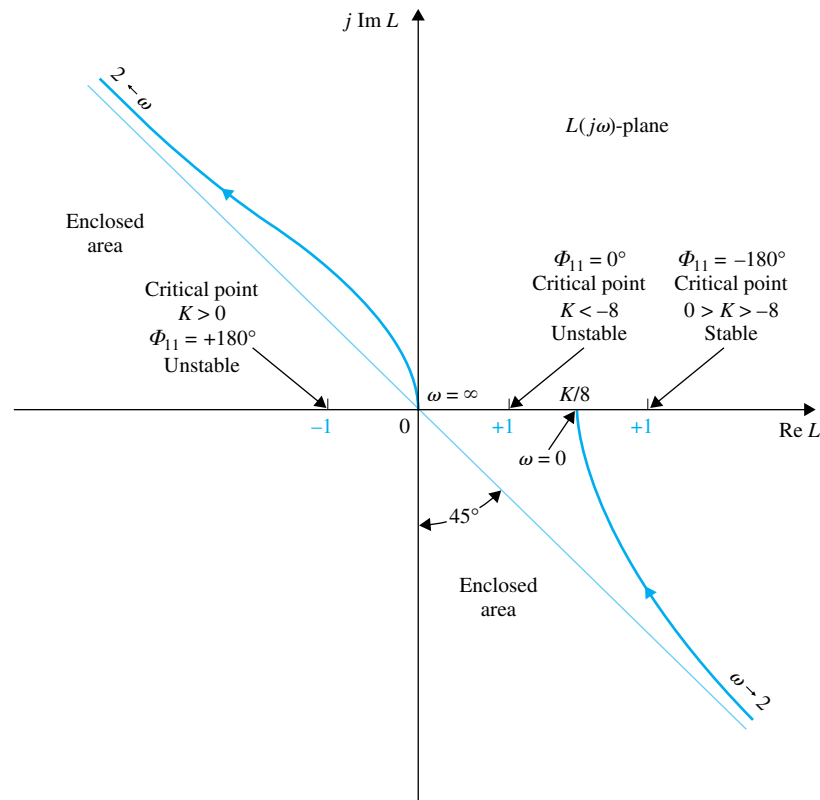
Figure H-11   Nyquist plot of the control system in Example H-5.

From Eq. (H-9), the value of Φ_{11} required for stability is

$$\Phi_{11} = -(0.5P_\omega + P)180° = -180° \qquad \text{(H-41)}$$

As seen from Fig. H-11, the magnitude of $L(j\omega)$ goes to infinity when $\omega = 2$ rad/sec. When K is positive, the critical point $(-1, j0)$ is not enclosed by the Nyquist plot, and the system is unstable. For the angle check, when ω varies from ∞ to 2, the angle Φ_{11} is $+135°$, and for the portion of $\omega = 2$ to 0, Φ_{11} is $+45°$. Thus, the total Φ_{11} is $+180°$, not $-180°$. The system is unstable for all positive values of K.

When K is negative, the critical point in Fig. H-11 is at $(+1, j0)$. Figure H-11 shows that if the $(+1, j0)$ point lies between 0 and $K/8$, it is enclosed by the Nyquist path, and the system is unstable. Thus, the system is unstable for $K < -8$. When the $(+1, j0)$ point is to the right of the $K/8$ point, Φ_{11} from $\omega = \infty$ to $\omega = 2$ is $-45°$, and from $\omega = 2$ to $\omega = 0$ is $-135°$. Thus the total Φ_{11} as ω varies from ∞ to 0 is $-180°$, which agrees with the value required in Eq. (H-41). The system is stable for $0 > K > -8$. The summary of the Nyquist criterion application to this system is as follows.

Range of K	Φ_{11} (deg) for $\omega = 2$ to 0	Φ_{11} (deg) for $\omega = 2$ to ∞	Total Φ_{11} (deg)	Critical Point	Stability Condition
$K > 0$	$+135$	$+45$	$+180$	-1 point enclosed	Unstable
$K < -8$	-45	$+45$	0	$+1$ point enclosed	Unstable
$-8 < K < 0$	-45	-135	-180		Stable

The complete root loci of the characteristic equation of the system are constructed in Fig. H-12 using the pole-zero configuration of Eq. (H-40). The stability condition of $-8 < K < 0$ is easily viewed from the root loci.
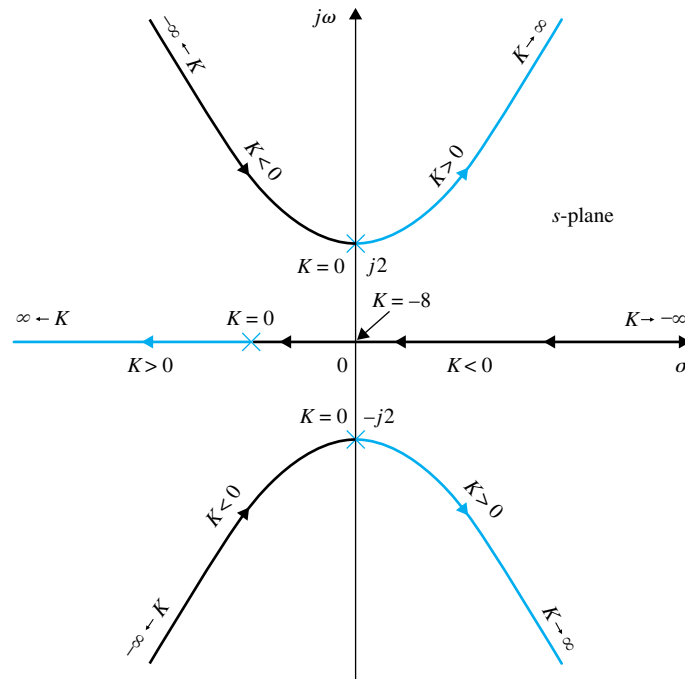
Figure H-12 Complete root loci of the system in Example H-5. ◀

▶ H-3 STABILITY ANALYSIS OF MULTILOOP SYSTEMS

The Nyquist stability analyses conducted in the preceding sections are all directed toward the loop transfer function $L(s)$. It does not matter whether the system is with single loop or multiple loops, since once the loop transfer function is obtained, stability analysis can be conducted using either the Routh-Hurwitz criterion, root loci, or the Nyquist criterion.

For multiloop feedback systems, it may be advantageous to analyze the stability of the system by working from the inner loop toward the outer loop, one at a time. This way, more insight may be gained on the stability of the individual loops of the system. The following example will illustrate this approach.

▶ **EXAMPLE H-6** Figure H-13 shows the block diagram of a system that controls the gun turret of a tank. During servicing of the turret control system, the mechanic accidentally opened the outer loop of the system. With the power turned on, the gun turret went out of control, and finally flew apart. The purpose of this example is to show that it is inadequate to investigate just the stability of the overall system. In general, for a multiloop control system, one should conduct a systematic stability analysis of all the inner loops of the system. It is admissible to have unstable inner loops, as long as the overall system is stable. However, if such a situation exists, it is important to forewarn or take precautionary measures to prevent opening the loops during operation.

The loop transfer function of the inner loop is

$$G(s) = \frac{6}{s(s + 1)(s + 2)} \tag{H-42}$$

Figure H-14 shows the Nyquist plot of $G(s)$. Since the plot intersects the real axis at the -1 point at $\omega = 1.414$ rad/sec, the inner loop is marginally stable. Therefore, if the outer loop of the system is opened, the system will oscillate continuously with a frequency of 1.414 rad/sec. The loop transfer function of the overall system is

$$L(s) = \frac{G_c(s)G(s)}{1 + G(s)} = \frac{100(s + 0.1)}{(s + 10)(s^3 + 3s^2 + 2s + 6)} \tag{H-43}$$
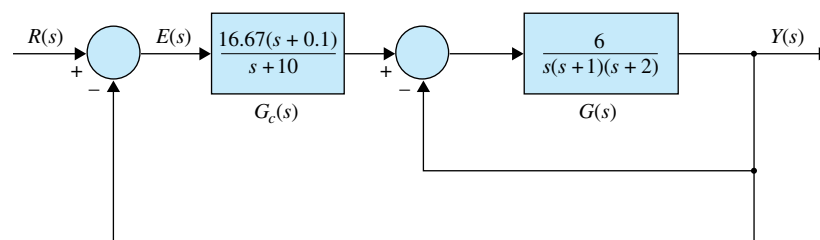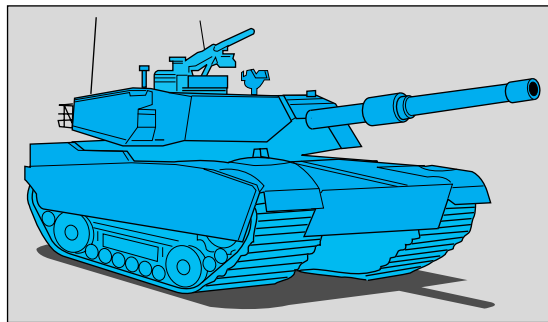
Figure H-13 Multiloop feedback control system for tank turret control.
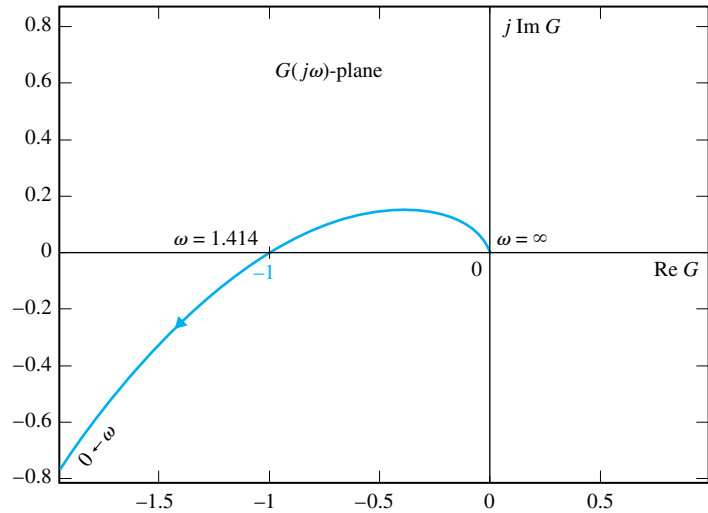
Figure H-14 Nyquist plot of $G(s) = \dfrac{6}{s(s + 1)(s + 2)}$.

Since $L(s)$ has two poles on the $j\omega$-axis and the rest are in the left-half s-plane, $P_\omega = 2$ and $P = 0$. The function is also of the nonminimum-phase type, so we must use Eq. (H-9) for the stability test of the overall system. Thus,

$$\Phi_{11} = -(0.5P_\omega + P)180° = -180° \tag{H-44}$$

The Nyquist plot of $L(s)$ is plotted as shown in Fig. H-15. The angle Φ_{11} for $\omega = \infty$ to $\omega = 1.414$ rad/sec is $-90°$, and from $\omega = 1.414$ rad/sec to $\omega = 0$ is $-90°$. Thus, the total value of Φ_{11} for $\omega = \infty$ to $\omega = 0$ is $-180°$, and the overall system is stable.

In general, when more than two loops are involved, the proper way is to start with the stability of the innermost loop by opening all the outer loops, and then add one loop at a time, until the outermost loop is closed.
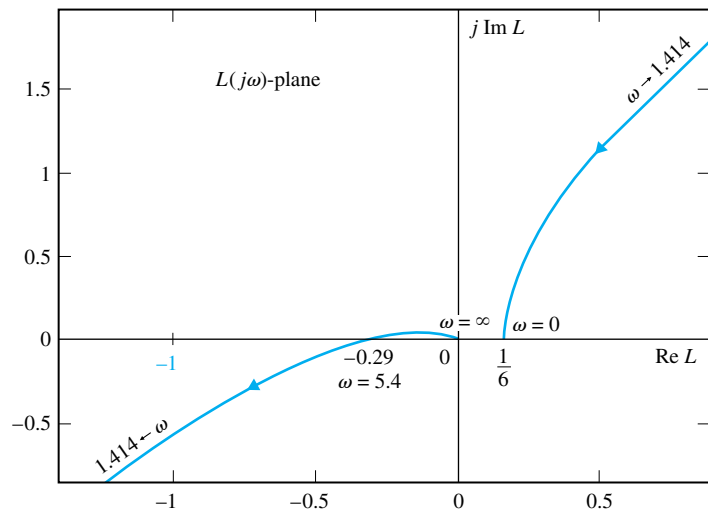
Figure H-15 Nyquist plot of $L(s) = \dfrac{100(s + 0.1)}{(s + 10)(s^3 + 3s^2 + 2s + 6)}$.

▶ **REFERENCE**

1. K. S. Yeung, "A Reformulation of Nyquist's Criterion," *IEEE Trans. Educ.*, Vol. E-28, pp. 58–60, February 1985.

▶ **PROBLEMS**

• Stability analysis with Nyquist criterion.

H-1. The loop transfer functions $L(s)$ of single-feedback-loop systems are given in the following equations. Sketch the Nyquist plot of $L(j\omega)$ for $\omega = 0$ to ∞. Determine the stability of the closed-loop system. If the system is unstable, find the number of poles of the closed-loop transfer function that are in the right-half s-plane. Solve for the intersect of $L(j\omega)$ on the negative real axis of the $L(j\omega)$-plane analytically. You may construct the Nyquist plot of $L(j\omega)$ using any computer program.

(a) $L(s) = \dfrac{5(s-2)}{s(s+1)(s-1)}$

(b) $L(s) = \dfrac{50}{s(s+5)(s-1)}$

(c) $L(s) = \dfrac{3(s+2)}{s(s^3+3s+1)}$

(d) $L(s) = \dfrac{100}{s(s+1)(s^2+2)}$

(e) $L(s) = \dfrac{s^2-5s+2}{s(s^3+2s^2+2s+10)}$

(f) $L(s) = \dfrac{-0.1(s^2-1)(s+2)}{s(s^2+s+1)}$

H-2. The loop transfer functions of single-feedback-loop control systems are given in the following equations. Apply the Nyquist criterion and determine the values of K for the system to be stable. Sketch the Nyquist plot of $L(j\omega)$ with $K = 1$ for $\omega = 0$ to $\omega = \infty$. You may use a computer program to plot the Nyquist plots.

(a) $L(s) = \dfrac{K(s-2)}{s(s^2-1)}$

(b) $L(s) = \dfrac{K}{s(s+10)(s-2)}$

(c) $L(s) = \dfrac{K(s+1)}{s(s^3+3s+1)}$

(d) $L(s) = \dfrac{K(s^2-5s+2)}{s(s^3+2s^2+2s+10)}$

(e) $L(s) = \dfrac{K(s^2-1)(s+2)}{s(s^2+s+1)}$

(f) $L(s) = \dfrac{K(s^2-5s+1)}{s(s+1)(s^2+4)}$

H-3. Figure HP-3 shows the Nyquist plots of the loop transfer function $L(j\omega)$ for $\omega = 0$ to $\omega = \infty$ for single-feedback-loop control systems. The number of poles of $L(j\omega)$ that are on the $j\omega$-axis, P_{ω}, and in the right-half s-plane, P, are indicated for each case. Determine the stability of the closed-loop system by applying the Nyquist criterion. For the unstable systems, give the number of zeros of $1 + L(s)$ that are in the right-half s-plane.

H-4. It was mentioned in the text that when the function $L(j\omega)$ has more zeros than poles, it is necessary to plot the Nyquist plot of $1/L(j\omega)$ to apply the simplified Nyquist criterion. Determine the stability of the systems described by the function $1/L(j\omega)$ shown in Fig. HP-4. For each case, the values of P_{ω} and P for the function $1/L(j\omega)$ are given, where P_{ω} refers to the number of poles of $1/L(j\omega)$ that are on the $j\omega$-axis, and P refers to the number of poles of $1 + 1/L(j\omega)$ that are in the right-half s-plane.

H-5. Figure HP-5 shows the Nyquist plots of loop transfer function $L(j\omega)$ for $\omega = 0$ to $\omega = \infty$ for single-feedback-loop control systems. The gain K appears as a multiplying factor in $L(s)$. The number of poles of $L(j\omega)$ that are on the $j\omega$-axis and in the right-half s-plane are indicated in each case. Determine the range(s) of K for closed-loop system stability.

• Application of Nyquist and Routh-Hurwitz criteria.

H-6. The characteristic equations of linear control systems are given below. Apply the Nyquist criterion to determine the values of K for system stability. Check the answers by means of the Routh-Hurwitz criterion.

(a) $s^3 + 4Ks^2 + (K+5)s + 10 = 0$

(b) $s^3 + K(s^3 + 2s^2 + 1) = 0$

(c) $s(s+1)(s^2+4) + K(s^2+1) = 0$

(d) $s^3 + 2s^2 + 20s + 10K = 0$

(e) $s(s^3+3s+3) + K(s+2) = 0$

Figure HP-3

(a) j Im L, L-plane, $\omega \to 0$, $\omega \to \infty$, -1, 0, Re L, $P_\omega = 3$, $P = 0$

(b) j Im L, L-plane, $0 \leftarrow \omega$, -1, $\omega \to \infty$, 0, Re L, $P_\omega = 2$, $P = 0$

(c) j Im L, L-plane, $\omega = 0$, $\omega \to \infty$, -1, Re L, $P_\omega = 0$, $P = 2$

(d) j Im L, L-plane, $\omega = 0$, -1, 0, $\omega \to \infty$, Re L, $P_\omega = 0$, $P = 0$

(e) j Im L, L-plane, $\omega \to \infty$, $\omega \to 2$, $18°$, 1, -1, 0, $\omega = 0$, Re L, $2 \leftarrow \omega$, $P_\omega = 2$, $P = 0$

(f) j Im L, L-plane, $\omega \to \infty$, -1, 0, Re L, $0 \leftarrow \omega$, $P_\omega = 1$, $P = 0$

Figure HP-4

(a) j Im $\frac{1}{L}$, $\frac{1}{L}$-plane, $\omega \to 0$, $\omega \to \infty$, -1, 0, Re $\frac{1}{L}$, $P_\omega = 3$, $P = 0$

(b) j Im $\frac{1}{L}$, $\frac{1}{L}$-plane, $\omega \to \infty$, -1, 0, Re $\frac{1}{L}$, $P_\omega = 2$, $P = 0$

(a)

(b)

(c)

(d)
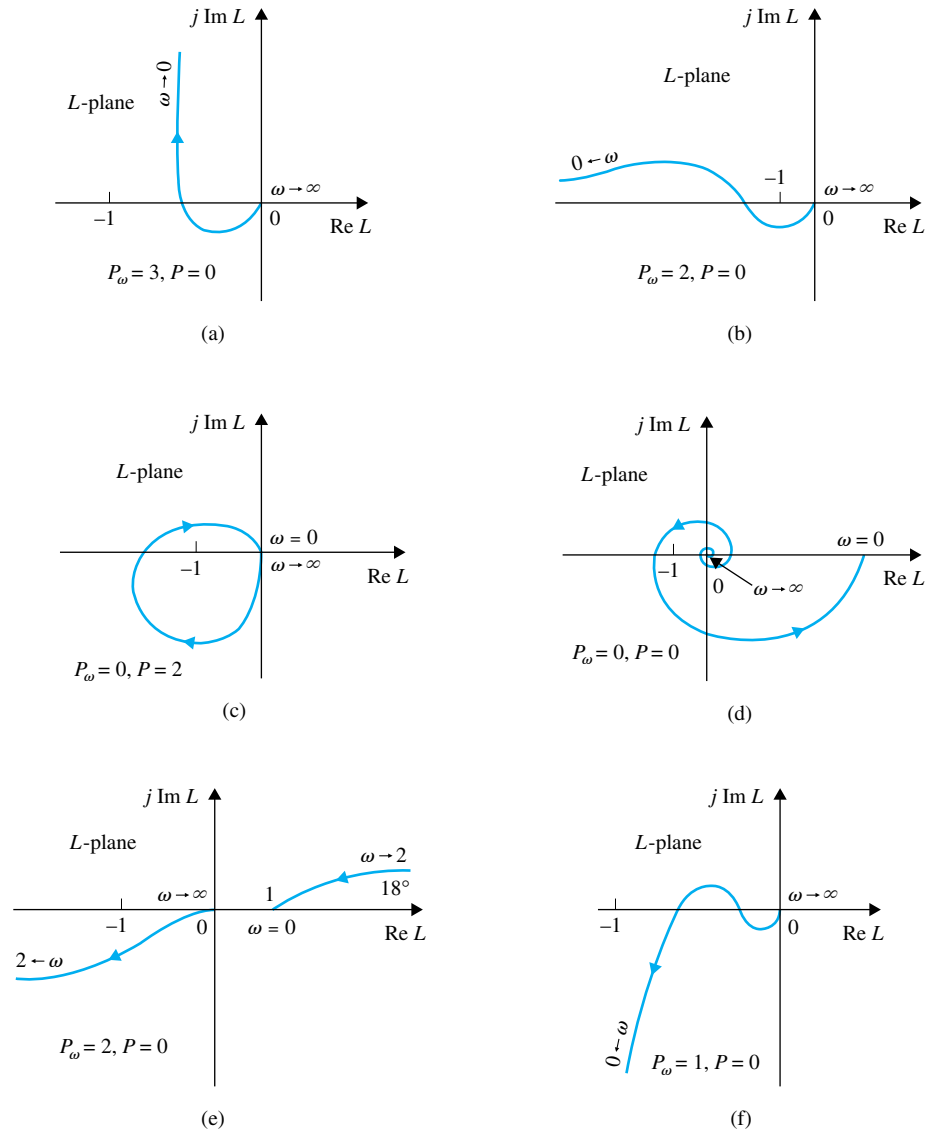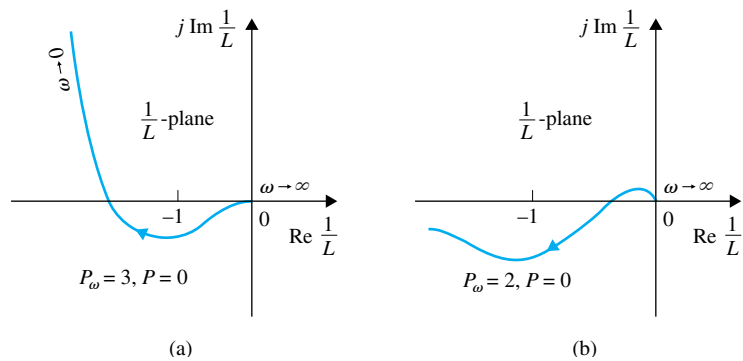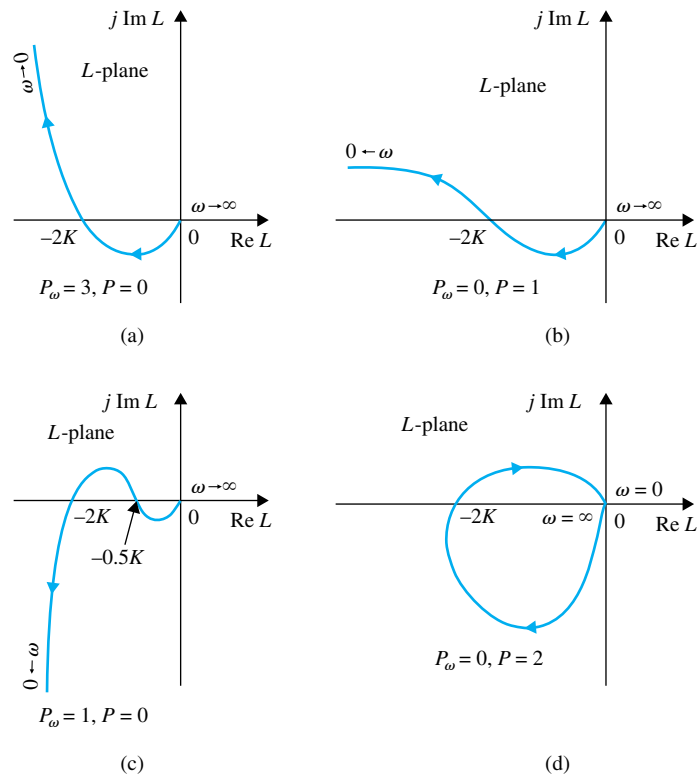
Figure HP-5

Appendix I
Discrete-Data Control Systems

TO ACCOMPANY

AUTOMATIC CONTROL SYSTEMS
EIGHTH EDITION

BY

BENJAMIN C. KUO

FARID GOLNARAGHI

Discrete-Data Control Systems

► I-1 INTRODUCTION

In recent years discrete-data and digital control systems have become more important in industry, mainly because of advances made in microprocessors and microcomputers. In addition, there are distinct advantages working with digital versus analog signals.

The block diagram of a typical digital control system is shown in Fig. I-1. The system is characterized by digitally coded signals at various parts of the system. However, the output device of the system is usually an analog component, such as a dc motor, driven by analog signals. Therefore, a digital control system often requires the use of digital-to-analog (D/A) and analog-to-digital (A/D) converters.

► I-2 THE z-TRANSFORM

Just as linear continuous-data systems are described by differential equations, linear digital control systems are described by difference equations (see Appendix B). We have seen that Laplace transform is a powerful method of solving linear time-invariant differential equations. Similarly, z-transform is an operational method of solving linear time-invariant difference equations.

I-2-1 Definition of the z-Transform

Consider the sequence $y(k)$, $k = 0, 1, 2, \ldots$, where $y(k)$ could represent a sequence of numbers or events. The z-transform of $y(k)$ is defined as

$$Y(z) = z\text{-transform of } y(k) = \mathcal{Z}[y(k)]$$

$$= \sum_{k=0}^{\infty} y(k)z^{-k} \tag{I-1}$$

where z is a complex variable with real and imaginary parts. The significance of this definition will become clear later. One important property of the z-transform is that it can
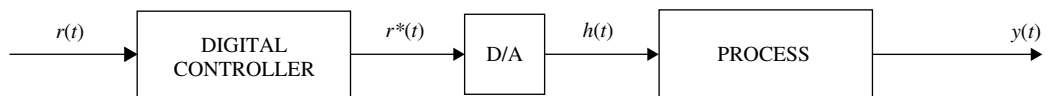
Figure I-1 Block diagram of a typical digital control system.

convert a sequence of numbers in the real domain into an expression in the complex z-domain. The following examples illustrate the derivation of the z-transforms of two simple functions.

► **EXAMPLE I-1** Consider the sequence

$$y(k) = e^{-\alpha k} \qquad k = 0, 1, 2, \ldots \tag{I-2}$$

where α is a real constant. Applying Eq. (I-1), the z-transform of $y(k)$ is written

$$Y(z) = \sum_{k=0}^{\infty} e^{-\alpha k} z^{-k} = 1 + e^{-\alpha} z^{-1} + e^{-2\alpha} z^{-2} + \cdots \tag{I-3}$$

which converges for $|e^{-\alpha} z^{-1}| < 1$.

Multiplying both sides of the last equation by $e^{-\alpha} z^{-1}$, subtracting the resulting equation from Eq. (I-3), and solving for $Y(z)$, the latter is expressed in closed form as

$$Y(z) = \frac{1}{1 - e^{-\alpha} z^{-1}} = \frac{z}{z - e^{-\alpha}} \tag{I-4}$$

for $|e^{-\alpha} z^{-1}| < 1$. ◄

► **EXAMPLE I-2** In Example I-1, if $\alpha = 0$, we have

$$y(k) = 1 \qquad k = 0, 1, 2, \ldots \tag{I-5}$$

which represents a sequence of ones. Then, the z-transform of $y(k)$ is

$$Y(z) = 1 + z^{-1} + z^{-2} + \cdots = \frac{z}{z - 1} \tag{I-6}$$

which converges for $|z| > 1$. ◄

I-2-2   Relationship between the Laplace Transform and the *z*-Transform

While the mathematicians like to talk about sequences, engineers feel more at home dealing with signals. It may be useful to represent the sequence $y(kT)$, $k = 0, 1, 2, \ldots$ as a train of impulses separated by the time interval T. The latter is defined as the **sampling period**. The impulse at the kth time instant, $\delta(t - kT)$, carries the value of $y(kT)$. This situation occurs quite often in digital and sampled-data control systems in which a signal $y(t)$ is digitized or sampled every T seconds to form a time sequence that represents the signal at the sampling instants. Thus, we can relate the sequence $y(kT)$ with a signal that can be expressed as

$$y*(t) = \sum_{k=0}^{\infty} y(kT)\delta(t - kT) \tag{I-7}$$

Taking the Laplace transform on both sides of Eq. (I-7), we have

$$Y*(s) = \mathcal{L}[y*(t)] = \sum_{k=0}^{\infty} y(kT)e^{-kTs} \tag{I-8}$$

Comparing Eq. (I-8) with Eq. (I-1), we see that the z-transform may be related to the Laplace transform through

$$z = e^{Ts} \tag{I-9}$$

In fact, the z-transform as defined in Eq. (I-1) may be regarded as a special case with $T = 1$. The definition of the z-transform in Eq. (I-9) allows us to treat sampled systems and perform digital simulation of continuous-data systems. Thus, we can summarize the definition of the z-transform as

$$Y(z) = \mathcal{Z}[y(kT)] = \mathcal{Z}[y^*(t)] = \mathcal{Z}[Y^*(s)] \tag{I-10}$$

Or, we can write

$$Y(z) = \mathcal{Z}[y(t)] = \mathcal{Z}[Y(s)] \tag{I-11}$$

with the understanding that the function $y(t)$ is first sampled or discretized to get $y^*(t)$ before taking the z-transform.

▶ **EXAMPLE I-3** Consider the time function

$$y(t) = e^{-\alpha t} u_s(t) \tag{I-12}$$

The z-transform of $y(t)$ is obtained by performing the following steps:

1. Represent the values of $y(t)$ at the time instants $t = kT$, $k = 0, 1, 2, \ldots$, to form the function $y^*(t)$:

$$y^*(t) = \sum_{k=0}^{\infty} e^{-\alpha kT} \delta(t - kT) \tag{I-13}$$

2. Take the Laplace transform on both sides of Eq. (I-13):

$$Y^*(s) = \sum_{k=0}^{\infty} e^{-\alpha kT} e^{-kTs} = \sum_{k=0}^{\infty} e^{-(s+\alpha)kT} \tag{I-14}$$

3. Express $Y^*(s)$ in closed form and apply Eq. (I-9), giving the z-transform,

$$Y(z) = \frac{z}{z - e^{-\alpha T}} \tag{I-15}$$

In general, the z-transforms of more complex functions may be obtained with the help of some of the z-transform theorems that follow. For engineering purposes, a z-transform table such as that in Appendix J may be used to transform from $y(k)$ to $Y(z)$. ◀

I-2-3 Some Important Theorems of the *z*-Transform

Some of the commonly used theorems of the z-transform are stated in the following without proof. Just as in the case of the Laplace transform, these theorems are useful in many aspects of the z-transform analysis. For uniformity, the real sequence is expressed as $y(kT)$, and if a sampling period is not involved, T can be set to unity.

■ **Theorem 1.** *Addition and Subtraction*

If $y_1(kT)$ and $y_2(kT)$ have z-transforms $Y_1(z)$ and $Y_2(z)$, respectively, then
$$\mathcal{Z}[y_1(kT) \pm y_2(kT)] = Y_1(z) \pm Y_2(z) \tag{I-16}$$

■ **Theorem 2.** *Multiplication by a Constant*

$$\mathcal{Z}[\alpha y(kT)] = \alpha \mathcal{Z}[y(kT)] = \alpha Y(z) \tag{I-17}$$

where α is a constant.

■ **Theorem 3.** *Real Translation (Time Delay and Time Advance)*

$$\mathcal{Z}[y(kT - nT)] = z^{-n}Y(z) \tag{I-18}$$

and

$$\mathcal{Z}[y(kT + nT)] = z^n\left[Y(z) - \sum_{k=0}^{n-1} y(kT)z^{-k}\right] \tag{I-19}$$

where n is a positive integer.

Equation (I-18) represents the *z*-transform of a time sequence that is shifted to the right by *nT*, and Eq. (I-19) denotes that of a time sequence shifted to the left by *nT*. The reason that the right-hand side of Eq. (I-19) is not just $z^nY(z)$ is because the one-sided *z*-transform, similar to the Laplace transform, is defined only for $k \geq 0$. Thus, the second term on the right-hand side of Eq. (I-19) simply represents the sequence that is lost after it is shifted to the left of $k = 0$.

■ **Theorem 4.** *Complex Translation*

$$\mathcal{Z}[e^{\mp\alpha kT}y(kT)] = Y(ze^{\pm\alpha T}) \tag{I-20}$$

where α is a constant. Y(z) is the z-transform of y(kT).

■ **Theorem 5.** *Initial-Value Theorem*

$$\lim_{k\to 0} y(kT) = \lim_{z\to\infty} Y(z) \tag{I-21}$$

if the limit exists.

• The final-value theorem is valid only if $(1 - z^{-1})Y(z)$ does not have poles on or inside the unit circle |z| = 1.

■ **Theorem 6.** *Final-Value Theorem*

$$\lim_{k\to\infty} y(kT) = \lim_{z\to 1}(1 - z^{-1})Y(z) \tag{I-22}$$

if the function $(1 - z^{-1})Y(z)$ has no poles on or outside the unit circle $|z| = 1$ in the z-plane.

■ **Theorem 7.** *Real Convolution*

$$Y_1(z)Y_2(z) = \mathcal{Z}\left[\sum_{k=0}^{N} y_1(kT)y_2(NT - kT)\right] = \mathcal{Z}\left[\sum_{k=0}^{N} y_2(kT)y_1(NT - kT)\right]$$
$$= \mathcal{Z}[y_1(kT) * y_2(kT)] \tag{I-23}$$

where "*" denotes real convolution in the discrete-time domain.

Thus, we see that as in the Laplace transform, the *z*-transform of the product of two real functions $y_1(k)$ and $y_2(k)$ is **not** equal to the product of the *z*-transforms $Y_1(z)$ and $Y_2(z)$. One exception to this in the case of the *z*-transform is if one of the two functions is the delay e^{-NT_s}, where *N* is a positive integer, then

$$\mathcal{Z}[e^{-NT_s}Y(s)] = \mathcal{Z}[e^{-NT_s}]\mathcal{Z}[Y(s)] = z^{-N}Y(z) \tag{I-24}$$

Table I-1 summarizes the theorems on the *z*-transform just given. The following examples illustrate the usefulness of some of these theorems.

TABLE I-1   Theorems of *z*-Transforms

Addition and subtraction	$\mathcal{Z}[y_1(kT) \pm y_2(kT)] = Y_1(z) \pm Y_2(z)$
Multiplication by a constant	$\mathcal{Z}[\alpha y(kT)] = \alpha\mathcal{Z}[y(kT)] = \alpha Y(z)$
Real translation	$\mathcal{Z}[y(k-n)T] = z^{-n}Y(z)$ **(time delay)**
	$\mathcal{Z}[y(k+n)T] = z^n\left[Y(z) - \sum_{k=0}^{n-1} y(kT)z^{-k}\right]$ **(time advance)**
	where n = positive integer
Complex translation	$\mathcal{Z}[e^{\mp \alpha kT}y(kT)] = Y(ze^{\pm \alpha T})$
Initial-value theorem	$\lim_{k\to 0} y(kT) = \lim_{z\to\infty} Y(z)$
Final-value theorem	$\lim_{k\to\infty} y(kT) = \lim_{z\to 1}(1 - z^{-1})Y(z)$
	if $(1 - z^{-1})Y(z)$ has no poles on or inside $|z| = 1$.
	$Y_1(z)Y_2(z) = \mathcal{Z}\left[\sum_{k=0}^{n} y_1(kT)y_2(NT - kT)\right]$
Real convolution	$= \mathcal{Z}\left[\sum_{k=0}^{n} y_2(kT)y_1(NT - kT)\right]$
	$= \mathcal{Z}[y_1(kT) * y_2(kT)]$

▶ **EXAMPLE I-4** (*complex translation theorem*) To find the *z*-transform of $y(t) = te^{-\alpha t}$, let $f(t) = t$, $t \geq 0$; then

$$F(z) = \mathcal{Z}[tu_s(t)] = \mathcal{Z}(kT) = \frac{Tz}{(z-1)^2} \tag{I-25}$$

Using the complex translation theorem in Eq. (I-20), we obtain

$$Y(z) = \mathcal{Z}[te^{-\alpha t}u_s(t)] = F(ze^{\alpha T}) = \frac{Tze^{-\alpha T}}{(z - e^{-\alpha T})^2} \tag{I-26}$$

◀

▶ **EXAMPLE I-5** (*final-value theorem*) Given the function

$$Y(z) = \frac{0.792 z^2}{(z-1)(z^2 - 0.146z + 0.208)} \tag{I-27}$$

determine the value of $y(kT)$ as k approaches infinity.

Since the function $(1 - z^{-1})Y(z)$ does not have any pole on or outside the unit circle $|z| = 1$ in the *z*-plane, the final-value theorem in Eq. (I-22) can be applied. Thus,

$$\lim_{k\to\infty} y(kT) = \lim_{z\to 1} \frac{0.792z}{z^2 - 0.416z + 0.208} \tag{I-28}$$

◀

I-2-4   Inverse *z*-Transform

• The inverse *z*-transform of $Y(z)$ is $y(kT)$, not $y(t)$.

Just as in the Laplace transform, one of the major objectives of the *z*-transform is that algebraic manipulations can be made first in the *z*-domain, and then the final time response determined by the inverse *z*-transform. *In general, the inverse z-transform of a function Y(z) yields information on y(kT) only, not on y(t). In other words, the z-transform carries*

information only at the sampling instants. With this in mind, the inverse *z*-transform can be carried out by one of the following three methods:

1. Partial-fraction expansion
2. Power-series method
3. The inverse formula

Partial-Fraction Expansion Method

• If $Y(s)$ has at least one zero at $z = 0$, the partial-fraction expansion of $Y(z)/z$ should first be performed.

The *z*-transform function $Y(z)$ is expanded by partial-fraction expansion into a sum of simple recognizable terms, and the *z*-transform table is used to determine the corresponding $y(kT)$. In carrying out the partial-fraction expansion, there is a slight difference between the *z*-transform and the Laplace transform procedures. With reference to the *z*-transform table, we note that practically all the *z*-transform functions have the term *z* in the numerator. Therefore, we should expand $Y(z)$ into the form of

$$Y(z) = \frac{K_1 z}{z - e^{-\alpha T}} + \frac{K_2 z}{z - e^{-\beta T}} + \cdots \tag{I-29}$$

To do this, first expand $Y(z)/z$ into fractions and then multiply by *z* to obtain the final expression. The following example will illustrate this procedure.

▶ **EXAMPLE I-6** Given the *z*-transform function

$$Y(z) = \frac{(1 - e^{-\alpha T})z}{(z - 1)(z - e^{-\alpha T})} \tag{I-30}$$

find the inverse *z*-transform. Expanding $Y(z)/z$ by partial-fraction expansion, we have

$$\frac{Y(z)}{z} = \frac{1}{z - 1} - \frac{1}{z - e^{-\alpha T}} \tag{I-31}$$

The final expanded expression for $Y(z)$ is

$$Y(z) = \frac{z}{z - 1} - \frac{z}{z - e^{-\alpha T}} \tag{I-32}$$

From the *z*-transform table in Appendix J, the corresponding inverse *z*-transform of $Y(z)$ is found to be

$$y(kT) = 1 - e^{-\alpha kT} \quad k = 0, 1, 2, \ldots \tag{I-33}$$

◀

• If $Y(s)$ does not have any zeros at $z = 0$, then perform the partial-fraction expansion of $Y(z)$ directly.

It should be pointed out that if $Y(z)$ does not contain any factors of *z* in the numerator, this usually means that the time sequence has a delay, and the partial-fraction expansion of $Y(z)$ should be carried out without first dividing the function by *z*. The following example illustrates this situation.

▶ **EXAMPLE I-7** Consider the function

$$Y(z) = \frac{(1 - e^{-\alpha T})}{(z - 1)(z - e^{-\alpha T})} \tag{I-34}$$

which does not contain any powers of *z* as a factor in the numerator. In this case, the partial-fraction expansion of $Y(z)$ is carried out directly. We have

$$Y(z) = \frac{1}{z - 1} - \frac{1}{z - e^{-\alpha T}} \tag{I-35}$$

Although the z-transform table does not contain exact matches for the components in Eq. (I-35), we recognize that the inverse z-transform of the first term on the right-hand side can be written as

$$\mathcal{Z}^{-1}\left[\frac{1}{z-1}\right] = \mathcal{Z}^{-1}\left[z^{-1}\frac{z}{z-1}\right] = \sum_{k=1}^{\infty}z^{-1}$$

$$= u_k[(k-1)T] \qquad k = 1, 2, \ldots \qquad (\text{I-36})$$

Similarly, the second term on the right-hand side of Eq. (I-35) can be identified with a time delay of T seconds. Thus, the inverse z-transform of $Y(z)$ is written

$$y(kT) = (1 - e^{-\alpha(k-1)T})u[(k-1)T] \qquad k = 1, 2, \ldots \qquad (\text{I-37})$$

◀

I-2-5   Computer Solution of the Partial-Fraction Expansion of $Y(z)/z$

Whether the function to be expanded by partial fraction is in the form of $Y(z)/z$ or $Y(z)$, the computer programs designed for performing the partial-fraction of Laplace transform functions can still be applied.

Power-Series Method
The definition of the z-transform in Eq. (I-1) gives a straightforward method of carrying out the inverse z-transform. Based on Eq. (I-1) we can clearly see that in the sampled case the coefficient of z^{-k} in $Y(z)$ is simply $y(kT)$. Thus, if we expand $Y(z)$ into a power series in powers of z^{-k}, we can find the values of $y(kT)$ for $k = 0, 1, 2, \ldots$.

▶ **EXAMPLE I-8** Consider the function $Y(z)$ given in Eq. (I-30), which can be expanded into a power series of z^{-1} by dividing the numerator polynomial by the denominator polynomial by long division. The result is

$$Y(z) = (1 - e^{-\alpha T})z^{-1} + (1 - e^{-2\alpha T})z^{-2} + \cdots + (1 - e^{-k\alpha T})z^{-k} + \cdots \qquad (\text{I-38})$$

Thus, it is apparent that

$$y(kT) = 1 - e^{-\alpha kT} \qquad k = 0, 1, 2, \ldots \qquad (\text{I-39})$$

which is the same result as in Eq. (I-33). ◀

Inversion Formula
The time sequence $y(kT)$ can be determined from $Y(z)$ by use of the inversion formula:

$$y(kT) = \frac{1}{2\pi j}\oint_{\Gamma} Y(z)z^{k-1}dz \qquad (\text{I-40})$$

which is a contour integration along the path Γ, that is, a circle of radius $|z| = e^{cT}$ centered at the origin in the z-plane, and c is a value such that the poles of $Y(z)z^{k-1}$ are inside the circle. The inversion formula of the z-transform is similar to that of the inverse Laplace-transform integral given in Eq. (2-10). One way of evaluating the contour integration of Eq. (I-40) is to use the residue theorem of complex-variable theory (the details are not covered here).

I-2-6   Application of the z-Transform to the Solution of Linear Difference Equations

The z-transform can be used to solve linear difference equations. As a simple example, let us consider the first-order unforced difference equation

$$y(k+1) + y(k) = 0 \qquad (\text{I-41})$$

To solve this equation, we take the z-transform on both sides of the equation. By this, we mean that we multiply both sides of the equation by z^{-k} and take the sum from $k = 0$ to $k = \infty$. We have

$$\sum_{k=0}^{\infty} y(k+1)z^{-k} + \sum_{k=0}^{\infty} y(k)z^{-k} = 0 \tag{I-42}$$

By using the definition of $Y(z)$ and the real translation theorem of Eq. (I-19) for time advance, the last equation is written

$$z[Y(z) - y(0)] + Y(z) = 0 \tag{I-43}$$

Solving for $Y(z)$, we get

$$Y(z) = \frac{z}{z+1} y(0) \tag{I-44}$$

The inverse z-transform of the last equation can be obtained by expanding $Y(z)$ into a power series in z^{-1} by long division. We have

$$Y(z) = (1 - z^{-1} + z^{-2} - z^{-3} + \cdots)x(0) \tag{I-45}$$

Thus, $y(k)$ is written

$$y(k) = (-1)^k y(0) \qquad k = 0, 1, 2, \ldots \tag{I-46}$$

Equation (I-41) is recognized as a single state equation. The z-transform solution of high-order discrete-data systems described by state equations is treated in Section I-3.

The following example shows the z-transform solution of a second-order difference equation.

▶ **EXAMPLE I-9** Consider the second-order difference equation

$$y(k+2) + 0.5y(k+1) + 0.2y(k) = u(k) \tag{I-47}$$

where

$$u(k) = u(k) = 1 \qquad \text{for } k = 0, 1, 2, \ldots \tag{I-48}$$

The initial conditions of $y(k)$ are: $y(0) = 0$ and $y(1) = 0$.

Taking the z-transform on both sides of Eq. (I-47), we get

$$[z^2 Y(z) - z^2 y(0) - zy(1)] + 0.5[zY(z) - zy(0)] + 0.2Y(z) = U(z) \tag{I-49}$$

The z-transform of $u(k)$ is $U(z) = z/(z - 1)$. Substituting the initial conditions of $y(k)$ and the expression of $U(z)$ into Eq. (I-49) and solving for $Y(z)$, we have

$$Y(z) = \frac{z}{(z-1)(z^2 + 0.5z + 0.2)} \tag{I-50}$$

The partial-fraction expansion of $Y(z)/z$ is

$$\frac{Y(z)}{z} = \frac{0.588}{z-1} - \frac{1.036e^{j1.283}}{z + 0.25 + j0.37} - \frac{1.036e^{-j1.283}}{z + 0.25 - j0.37} \tag{I-51}$$

where the exponents in the numerator coefficients are in radians.

Taking the inverse z-transform of $Y(z)$, we get

$$\begin{aligned} y(k) &= 0.588 - 1.036(0.447)^k[e^{-j(2.165k - 1.283)} + e^{j(2.165k - 1.283)}] \\ &= 0.588 - 2.072(0.447)^k \cos(2.165k - 1.283) \qquad k \geq 0 \end{aligned} \tag{I-52}$$

◀
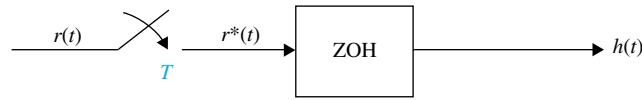
Figure I-2 Sample-and-hold (S/H) device.

► I-3 TRANSFER FUNCTIONS OF DISCRETE-DATA SYSTEMS

• The ideal sampler is not a physical entity. It is used only for the representation of discrete data.

Discrete-data control systems have the unique features that the signals in these systems either are in the form of pulse trains or are digitally coded, and the controlled processes often contain analog components. For instance, a dc motor, which is an analog device, can be controlled either by a controller that outputs analog signals or by a digital controller that outputs digital data. In the latter case, an interface such as a digital-to-analog (D/A) converter is necessary to couple the digital component to the analog devices. The input and output of the discrete-data system in Fig. I-1 can be represented by number sequences with the numbers separated by the sampling period T. For linear operation, the D/A converter can be represented by a **sample-and-hold (S/H)** device, which consists of a sampler and a data-hold device. The S/H that is most often used for the analysis of discrete-data systems consists of an **ideal sampler** and a **zero-order-hold (ZOH)** device. Thus, the system shown in Fig. I-1 can be functionally represented by the block diagram in Fig. I-2. Figure I-3 shows the typical operation of an ideal sampler and a ZOH. The continuous data $r(t)$ is sampled with a sampling period T by the ideal sampler. The output of the ideal sampler $r^*(t)$ is a train of impulses with the magnitudes of $r(t)$ at T carried by the strengths of the impulses. Note that the ideal sampler is not a physical entity. It is devised simply to represent the discrete-time signal mathematically. In Fig. I-3, the arrows at the sampling instants represent impulses. Since, by definition, an impulse has zero pulse width and infinite height, the lengths of the arrows simply represent the areas
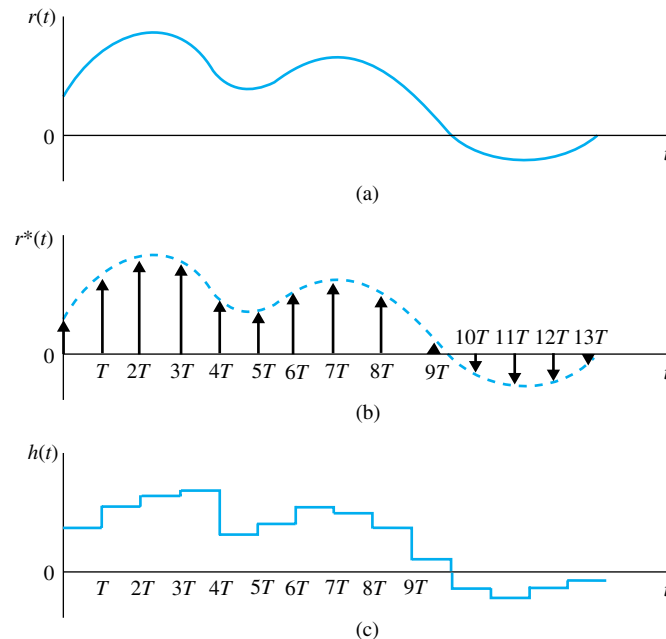
Figure I-3 (a) Input signal to an ideal sampler. (b) Output signal of an ideal sampler. (c) Output signal of a zero-order-hold (ZOH) device.
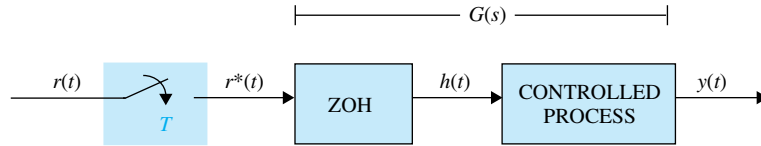
Figure I-4 Block diagram of a discrete-data system.

under the impulses and are the magnitudes of the input signal $r(t)$ at the sampling instants. The ZOH simply holds the magnitude of the signal carried by the incoming impulse at a given time instant, say, kT, for the entire sampling period t until the next impulse arrives at $t = (k + 1)T$. The output of the ZOH is a staircase approximation of the input to the ideal sampler, $r(t)$. As the sampling period T approaches zero, the output of the ZOH, $h(t)$ approaches $r(t)$, that is,

$$\lim_{T \to 0} h(t) = r(t) \tag{I-53}$$

However, since the output of the sampler, $r^*(t)$, is an impulse train, its limit as T approaches zero *does not* have any physical meaning. Based on the preceding discussions, a typical open-loop discrete-data system is modeled as shown in Fig. I-4.

There are several ways of deriving the transfer-function representation of the system in Fig. I-5. The following derivation is based on the Fourier-series representation of the signal $r^*(t)$. We begin by writing

$$r^*(t) = r(t)\delta_T(t) \tag{I-54}$$

where $\delta_T(t)$ is the unit-impulse train,

$$\delta_T(t) = \sum_{k=-\infty}^{\infty} \delta(t - kT) \tag{I-55}$$

Since $\delta_T(t)$ is a periodic function with period T, it can be expressed as a Fourier series:

$$\delta_T(t) = \sum_{n=-\infty}^{\infty} C_n e^{j2\pi nt/T} \tag{I-56}$$

where C_n is the Fourier coefficient, and is given by

$$C_n = \frac{1}{T}\int_0^T \delta_T(t)e^{-jn\omega_s t}dt \tag{I-57}$$

where $\omega_s = 2\pi/T$ is the **sampling frequency** in rad/sec.
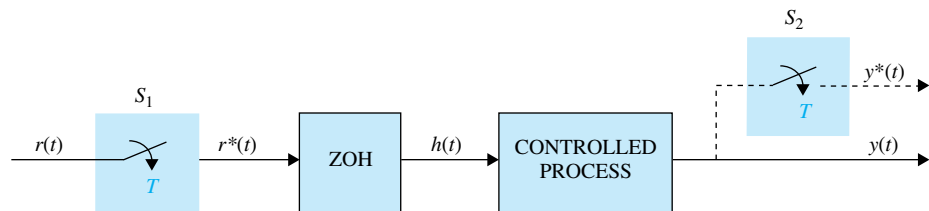
Figure I-5 Discrete-data system with a fictitious sampler.

Since the unit impulse is defined as a pulse with a width of δ and a height of $1/\delta$, and $\delta \to 0$, C_n is written

$$C_n = \lim_{\delta \to 0} \frac{1}{T\delta} \int_0^\delta e^{-jn\omega_s t} \, dt = \lim_{\delta \to 0} \frac{1 - e^{-jn\omega_s \delta}}{jn\omega_s T\delta} = \frac{1}{T} \tag{I-58}$$

Substituting Eq. (I-58) in Eq. (I-56), and then the latter in Eq. (I-54), we get

$$r^*(t) = \frac{1}{T} \sum_{n=-\infty}^{\infty} r(t)e^{jn\omega_s t} \tag{I-59}$$

Taking the Laplace transform on both sides of Eq. (I-59), and using the complex shifting property of Eq. (2-23), we get

$$R^*(s) = \frac{1}{T} \sum_{n=-\infty}^{\infty} R(s - jn\omega_s) = \frac{1}{T} \sum_{n=-\infty}^{\infty} R(s + jn\omega_s) \tag{I-60}$$

Equation (I-60) represents the Laplace transform of the sampled signal $r^*(t)$. It is an alternative expression to Eq. (I-8). From Eq. (I-8), $R^*(s)$ can be written as

$$R^*(s) = \sum_{k=0}^{\infty} r(kT)e^{-kTs} \tag{I-61}$$

Since the summing limits of $R^*(s)$ range from $-\infty$ to ∞, if s is replaced by $s + jm\omega_s$ in Eq. (I-60), where m is any integer, we have

$$R^*(s + jm\omega_s) = R^*(s) \tag{I-62}$$

Pulse-Transfer Function

Now we are ready to derive the transfer function of the discrete-data system shown in Fig. I-4. The Laplace transform of the system output $y(t)$ is written

$$Y(s) = G(s)R^*(s) \tag{I-63}$$

Although the output $y(t)$ is obtained from $Y(s)$ by taking the inverse Laplace transform on both sides of Eq. (I-63), this step is difficult to execute because $G(s)$ and $R^*(s)$ represent different types of signals. To overcome this problem, we apply a fictitious sampler at the output of the system, as shown in Fig. I-5. The fictitious sampler S_2 has the same sampling period T and is synchronized to the original sampler S_1. The sampled form of $y(t)$ is $y^*(t)$. Applying Eq. (I-60) to $y^*(t)$, and using Eq. (I-63), we have

$$Y^*(s) = \frac{1}{T} \sum_{n=-\infty}^{\infty} G(s + jn\omega_s)R^*(s + jn\omega_s) \tag{I-64}$$

In view of the relationship in Eq. (I-62), Eq. (64) is written

$$Y^*(s) = R^*(s)\frac{1}{T} \sum_{n=-\infty}^{\infty} G(s + jn\omega_s) = R^*(s)G^*(s) \tag{I-65}$$

where $G^*(s)$ is defined the same way as $R^*(s)$ in Eq. (I-60), and is called the **pulse-transfer function** of $G(s)$.

z-Transfer Function

Now that all the functions in Eq. (I-65) are in sampled form, where $R^*(s)$, $G^*(s)$, and $Y^*(s)$ all have the form of Eq. (I-61), we can take the z-transform on both sides of the

(a)

(b)
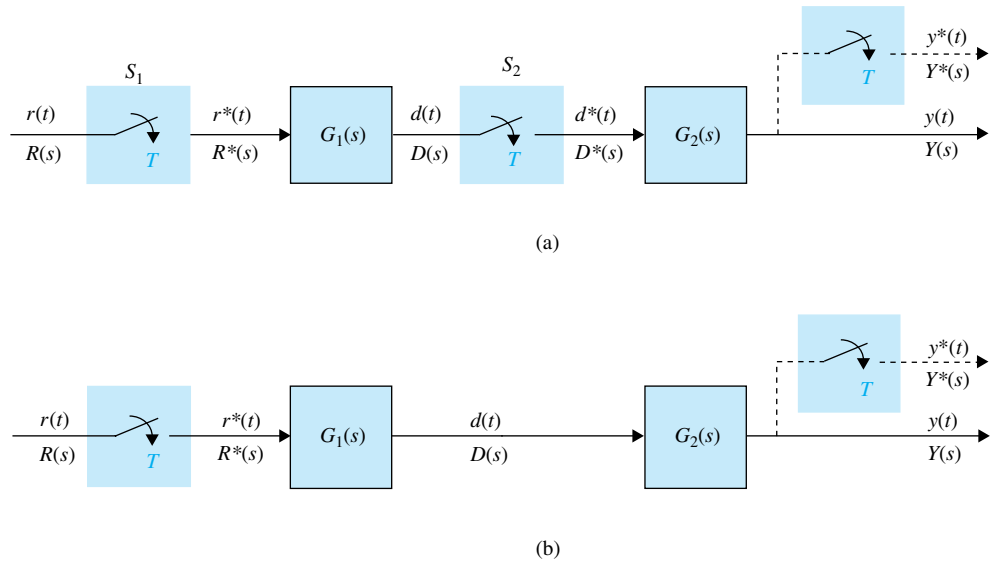
Figure I-6 (a) Discrete-data system with cascaded elements and a sampler separating the two elements. (b) Discrete-data system with cascaded elements and no sampler in between.

equation by substituting $z = e^{Ts}$. We have

$$Y(z) = G(z)R(z) \tag{I-66}$$

where $G(z)$ is defined as the **z-transfer function** of $G(s)$, and is given by

$$G(z) = \sum_{k=0}^{\infty} g(kT)z^{-k} \tag{I-67}$$

Thus, for the discrete-data system shown in Figs. I-5 and I-6, the z-transform of the output is equal to the z-transfer function of the process and the z-transform of the input.

I-3-1 Transfer Functions of Discrete-Data Systems with Cascade Elements

The transfer-function representation of discrete-data systems with elements connected in cascade is slightly more involved than that for continuous-data systems, because of the variation of having or not having samplers in between the elements. Figure I-6 shows two different discrete-data systems that contain two elements connected in cascade. In the system of Fig. I-6(a), the two elements are separated by the sampler S_2, which is synchronized to, and has the same period as, the sampler S_1. The two elements in the system of Fig. I-6(b) are connected directly together. It is important to distinguish these two cases when deriving the pulse-transfer function and the z-transfer function. For the system in Fig. I-6(a), the output of $G_1(s)$ is written

$$D(s) = G_1(s)R^*(s) \tag{I-68}$$

and the system output is

$$Y(s) = G_2(s)D^*(s) \tag{I-69}$$

Taking the pulse transform on both sides of Eq. (I-68), and using Eq. (I-62), we have

$$D^*(s) = G_1^*(s)R^*(s) \tag{I-70}$$

Now substituting Eq. (I-70) in Eq. (I-69) and taking the pulse transform, we get

$$Y^*(s) = G_1^*(s)G_2^*(s)R^*(s) \tag{I-71}$$

> • The z-transform of two systems separated by a sampler is equal to the product of the z-transforms of the two systems.

The corresponding z-transform expression of Eq. (I-71) is

$$Y(z) = G_1(z)G_2(z)R(z) \tag{I-72}$$

We conclude that *the z-transform of two systems separated by a sampler is equal to the product of the z-transforms of the two systems.*

The Laplace transform of the output of the system in Fig. I-6(b) is

$$Y(s) = G_1(s)G_2(s)R^*(s) \tag{I-73}$$

Taking the pulse transform on both sides of the last equation, we get

$$Y^*(s) = [G_1(s)G_2(s)]^*R^*(s) \tag{I-74}$$

where

$$[G_1(s)G_2(s)]^* = \frac{1}{T}\sum_{n=-\infty}^{\infty} G_1(s + jn\omega_s)G_2(s + jn\omega_s) \tag{I-75}$$

Notice that since $G_1(s)$ and $G_2(s)$ are not separated by a sampler, they have to be treated as one system when taking the pulse transform.

Taking the z-transform on both sides of Eq. (I-74) gives

$$Y(z) = \mathcal{Z}\{[G_1(s)G_2(s)]^*\}R(z) \tag{I-76}$$

Let

$$\mathcal{Z}\{[G_1(s)G_2(s)]^*\} = G_1G_2(z) \tag{I-77}$$

Then, Eq. (I-76) is written

$$Y(z) = G_1G_2(z)R(z) \tag{I-78}$$

I-3-2 Transfer Function of the Zero-Order-Hold

Based on the description of the ZOH given earlier, its impulse response is shown in Fig. I-7. The transfer function of the ZOH is written

$$G_h(s) = \mathcal{L}[g_h(t)] = \frac{1 - e^{-Ts}}{s} \tag{I-79}$$

Thus, if the ZOH is connected in cascade with a linear process using transfer function $G_p(s)$, as shown in Fig. I-5, the z-transform of the combination is written

$$G(z) = \mathcal{Z}[G_h(s)G_p(s)] = \mathcal{Z}\left(\frac{1 - e^{-Ts}}{s}G_p(s)\right) \tag{I-80}$$
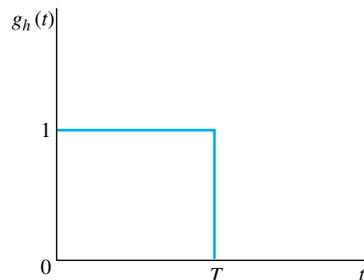
Figure I-7 Impulse response of the ZOH.

By using the time-delay property of z-transforms, Eq. (I-18), Eq. (I-80) is simplified to

$$G(z) = (1 - z^{-1})\mathcal{Z}\left(\frac{G_p(s)}{s}\right) \tag{I-81}$$

▶ **EXAMPLE I-10** Consider that for the system shown in Fig. I-5,

$$G_p(s) = \frac{1}{s(s + 0.5)} \tag{I-82}$$

The sampling period is 1 second. The z-transfer function of the system between the input and the output is determined using Eq. (I-81).

$$G(z) = (1 - z^{-1})\mathcal{Z}\left(\frac{1}{s^2(s + 0.5)}\right)$$

$$= (1 - z^{-1})\mathcal{Z}\left(\frac{2}{s^2} - \frac{4}{s} + \frac{4}{s + 0.5}\right) = \frac{0.426z + 0.361}{z^2 - 1.606z + 0.606} \tag{I-83}$$

◀

I-3-3   Transfer Functions of Closed-Loop Discrete-Data Systems

The transfer functions of closed-loop discrete-data systems are derived using the following procedures:

1. Regard the outputs of samplers as inputs to the system.
2. All other noninputs of the system are treated as outputs.
3. Write cause-and-effect equations between the inputs and the outputs of the system using the SFG gain formula.
4. Take the pulsed transform or the z-transform of the equations obtained in step 3, and manipulate these equations to get the pulse-transfer function or the z-transfer function.

Reference [1] describes the sampled signal flow graph that can be used to implement step 4 using the SFG gain formula.

The following examples illustrate the algebraic procedure of finding the transfer functions of closed-loop discrete-data systems.

▶ **EXAMPLE I-11** Consider the closed-loop discrete-data system shown in Fig. I-8. The output of the sampler is re-garded as an input to the system. Thus, the system has inputs $R(s)$ and $E^*(s)$. The signals $E(s)$ and $Y(s)$ are regarded as the outputs of the system.

Writing the cause-and-effect equations for $E(s)$ and $Y(s)$ using the gain formula, we get

$$E(s) = R(s) - G(s)H(s)E^*(s) \tag{I-84}$$
$$Y(s) = G(s)E^*(s) \tag{I-85}$$
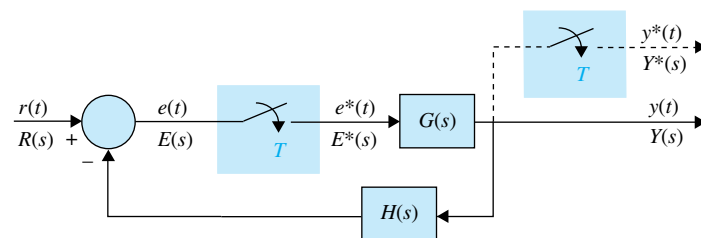
Figure I-8   Closed-loop discrete-data system.

Notice that the right-hand side of the last two equations contains only the inputs $R(s)$ and $E^*(s)$ and the transfer functions. Taking the pulse transform on both sides of Eq. (I-60) and solving for $E^*(s)$, we get

$$E^*(s) = \frac{R^*(s)}{1 + [G(s)H(s)]^*} \tag{I-86}$$

Substituting $E^*(s)$ from Eq. (I-86) into Eq. (I-85), we get

$$Y(s) = \frac{G(s)}{1 + [G(s)H(s)]^*} R^*(s) \tag{I-87}$$

Taking the pulse transform on both sides of Eq. (I-87), and using Eq. (I-62), we arrive at the pulse-transfer function of the closed-loop system,

$$\frac{Y^*(s)}{R^*(s)} = \frac{G^*(s)}{1 + [G(s)H(s)]^*} \tag{I-88}$$

Taking the z-transform on both sides of the last equation, we have

$$\frac{Y(z)}{R(z)} = \frac{G(z)}{1 + GH(z)} \tag{I-89}$$

◀

▶ **EXAMPLE I-12** We show in this example that although it is possible to define an input-output transfer function for the system in Fig. I-8, this may not be possible for all discrete-data systems. Let us consider the system shown in Fig. I-9, which has a sampler in the feedback path. In this case, the outputs of the sampler $Y^*(s)$ and $R(s)$ are the inputs of the system; $Y(s)$ and $E(s)$ are regarded as the outputs. Writing $E(s)$ and $Y(s)$ in terms of the inputs using the gain formula, we get

$$Y(s) = G(s)E(s) \tag{I-90}$$
$$E(s) = R(s) - H(s)Y^*(s) \tag{I-91}$$

Taking the pulse transform on both sides of the last two equations and after simple algebraic manipulations, the pulse transform of the output is written

$$Y^*(s) = \frac{[G(s)R(s)]^*}{1 + [G(s)H(s)]^*} \tag{I-92}$$

Note that the input $R(s)$ and the transfer function $G(s)$ are now combined as one function, $[G(s)R(s)]^*$, and we cannot define a transfer function in the form of $Y^*(s)/R^*(s)$. The z-transform of the output is written

$$Y(z) = \frac{GR(z)}{1 + GH(z)} \tag{I-93}$$
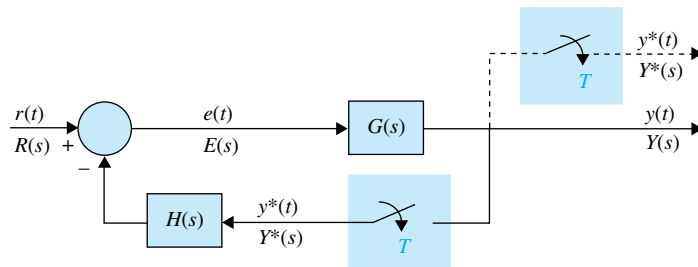
Figure I-9 Closed-loop discrete-data system.

◀

Although we have been able to arrive at the input-output transfer function and transfer relation of the systems in Figs. I-8 and I-9 by algebraic means without difficulty, for more complex system configurations, the algebraic method may become tedious. The signal-flow graph method may be extended to the analysis of discrete-data systems; the reader may refer to [1] for details.

▶ I-4 STATE EQUATIONS OF LINEAR DISCRETE-DATA SYSTEMS

Just as for continuous-data systems, the modern way of modeling a discrete-data system is by discrete state equations. As described earlier, when dealing with discrete-data systems, we often encounter two situations. The first one is that the system contains continuous-data components, but the signals at certain points of the system are discrete with respect to time because of sample-and-hold (S/H) operations. In this case, the components of the system are still described by differential equations, but because of the discrete-time data, the differential equations are discretized to yield a set of difference equations. The second situation involves systems that are completely discrete with respect to time, and the system dynamics should be difference equations from the outset.

I-4-1 Discrete State Equations

Let us consider the discrete-data control system with an S/H device, as shown in Fig. I-10. Typical signals that appear at various points in the system are shown in the figure. The output signal $y(t)$ ordinarily is a continuous-data signal. The output of the S/H, $h(t)$, is a sequence of steps. Therefore, we can write

$$h(t) = h(kT) = r(kT) \tag{I-94}$$

for $kT \leq t < (k + 1)T$, $k = 0, 1, 2, \ldots$.

Now we let the linear process G be described by the state equation and output equation:

$$\frac{d\mathbf{x}(t)}{dt} = \mathbf{A}\mathbf{x}(t) + \mathbf{B}h(t) \tag{I-95}$$

$$y(t) = \mathbf{C}\mathbf{x}(t) + \mathbf{D}h(t) \tag{I-96}$$

where $\mathbf{x}(t)$ is the $n \times n$ state vector, and $h(t)$ and $y(t)$ are the scalar input and output, respectively. The matrices $\mathbf{A}$, $\mathbf{B}$, $\mathbf{C}$, and $\mathbf{D}$ are coefficient matrices. By using Eq. (5-44), the state transition equation is

$$\mathbf{x}(t) = \boldsymbol{\phi}(t - t_0)\mathbf{x}(t_0) + \int_{t_0}^{t} \boldsymbol{\phi}(t - \tau)\mathbf{B}h(\tau)d\tau \tag{I-97}$$

for $t \geq t_0$. If we are interested only in the responses at the sampling instants, we let $t = (k + 1)T$ and $t_0 = kT$. Then Eq. (I-97) becomes

$$\mathbf{x}[(k + 1)T] = \boldsymbol{\phi}(T)\mathbf{x}(kT) + \int_{kT}^{(k+1)T} \boldsymbol{\phi}[(k + 1)T - \tau]\mathbf{B}h(\tau)d\tau \tag{I-98}$$

Since $h(t)$ is piecewise constant, as defined in Eq. (I-95), the input $h(\tau)$ in Eq. (I-98) can be taken outside of the integral sign. Equation (I-98) is written

$$\mathbf{x}[(k + 1)T] = \boldsymbol{\phi}(T)\mathbf{x}(kT) + \int_{kT}^{(k+1)T} \boldsymbol{\phi}[(k + 1)T - \tau]\mathbf{B}d\tau \, h(kT) \tag{I-99}$$

or

$$\mathbf{x}[(k + 1)T] = \boldsymbol{\phi}(T)\mathbf{x}(kT) + \boldsymbol{\theta}(T)h(kT) \tag{I-100}$$
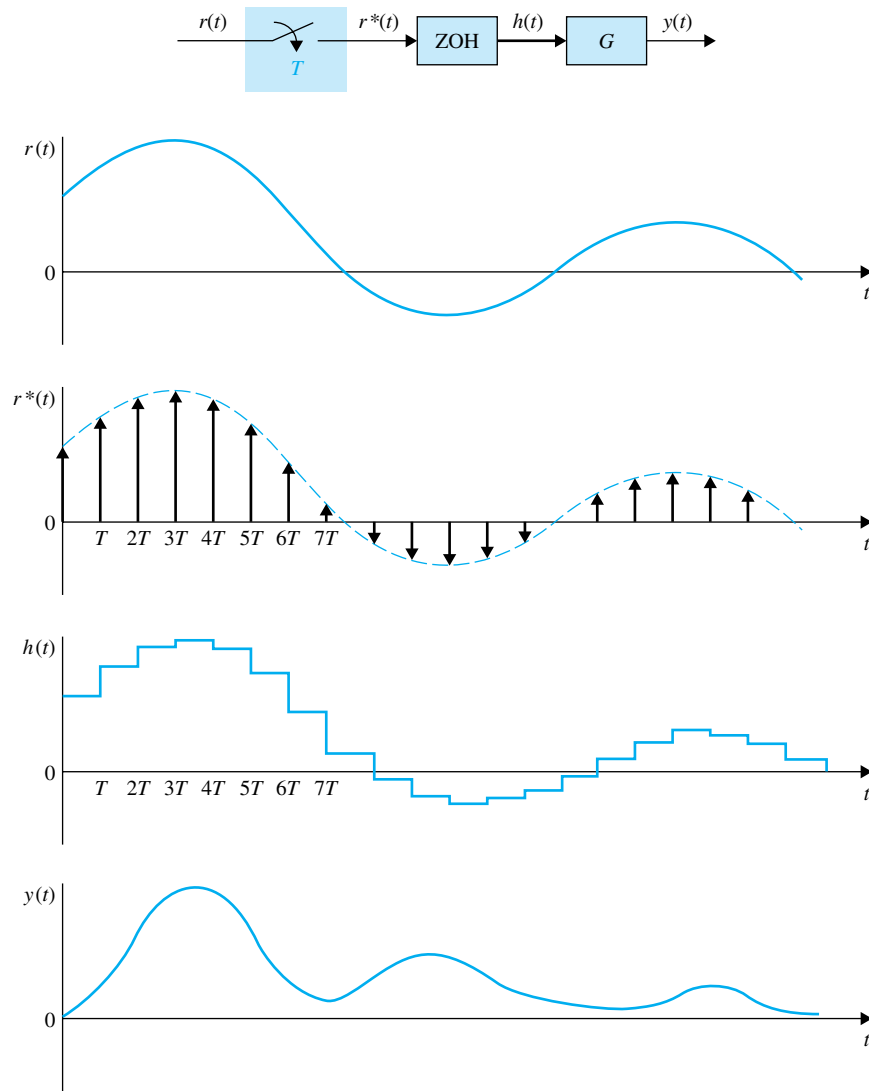
Figure I-10 Discrete-data system with sample-and-hold (S/H).

where

$$\theta(T) = \int_{kT}^{(k+1)T} \phi[(k+1)T - \tau]\mathbf{B}d\tau = \int_0^T \phi(T - \tau)\mathbf{B}d\tau \qquad (I\text{-}101)$$

Equation (I-100) is of the form of a set of linear first-order difference equations in vector-matrix form, and is referred to as the **vector-matrix discrete state equation**.

I-4-2   Solutions of the Discrete State Equations: Discrete State-Transition Equations

The discrete state equations represented by Eq. (I-100) can be solved by using a simple recursion procedure. By setting $k = 0, 1, 2, \ldots$ successively in Eq. (I-100), the following

equations result:

$$k = 0: \qquad \mathbf{x}(T) \; = \boldsymbol{\phi}(T)\mathbf{x}(0) + \boldsymbol{\theta}(T)h(0) \tag{I-102}$$

$$k = 1: \qquad \mathbf{x}(2T) = \boldsymbol{\phi}(2T) = \boldsymbol{\phi}(T)\mathbf{x}(T) + \boldsymbol{\theta}(T)h(T) \tag{I-103}$$

$$k = 2: \qquad \mathbf{x}(3T) = \boldsymbol{\phi}(3T) = \boldsymbol{\phi}(T)\mathbf{x}(2T) + \boldsymbol{\theta}(T)h(2T) \tag{I-104}$$

$$\vdots \qquad\qquad \vdots$$

$$k = n - 1: \qquad \mathbf{x}(nT) = \boldsymbol{\phi}(T)\mathbf{x}[(n-1)T] + \boldsymbol{\theta}(T)h[(n-1)T] \tag{I-105}$$

Substituting Eq. (I-102) into Eq. (I-103), then Eq. (I-103) into Eq. (I-104), and so on, we obtain the following solution for Eq. (I-100):

$$\mathbf{x}(nT) = \boldsymbol{\phi}^n(T)\mathbf{x}(0) + \sum_{i=0}^{n-1} \boldsymbol{\phi}^{n-i-1}(T)\boldsymbol{\theta}(T)h(iT) \tag{I-106}$$

where, from Eq. (5-36), $\boldsymbol{\phi}^n(T) = [\boldsymbol{\phi}(T)]^n = \boldsymbol{\phi}(nT)$.

Equation (I-106) is defined as the **discrete state-transition equation** of the discrete-data system. It is interesting to note that Eq. (I-106) is analogous to its continuous-data counterpart in Eq. (5-41). The state-transition equation of Eq. (I-97) describes the state of the system of Fig. I-10 for all values of t, whereas the discrete state-transition equation in Eq. (I-106) describes the states only at the sampling instants $t = nT$, $n = 0, 1, 2, \ldots$.

With nT considered as the initial time, where n is any positive integer, the state-transition equation is

$$\mathbf{x}[(n + N)T] = \boldsymbol{\phi}^N(T)\mathbf{x}(nT) + \sum_{i=0}^{N-1} \boldsymbol{\phi}^{N-i-1}(T)\boldsymbol{\theta}(T)h[(n+i)T] \tag{I-107}$$

where N is a positive integer.

The output of the system at the sampling instants is obtained by substituting $t = nT$ and Eq. (I-106) into Eq. (I-96), yielding

$$y(nT) = \mathbf{C}\mathbf{x}(nT) + \mathbf{D}h(nT)$$

$$= \mathbf{C}\boldsymbol{\phi}(nT)\mathbf{x}(0) + \mathbf{C}\sum_{i=0}^{n-1} \boldsymbol{\phi}[(n-i-1)T]\boldsymbol{\theta}(T)h(iT) + \mathbf{D}h(nT) \tag{I-108}$$

An important advantage of the state-variable method over the z-transform method is that it can be modified easily to describe the states and the output between sampling instants. In Eqs. (I-97), if we let $t = (n + \Delta)T$, where $0 < \Delta \le 1$ and $t_0 = nT$, we get

$$\mathbf{x}[(n + \Delta)T] = \boldsymbol{\phi}(\Delta T)\mathbf{x}(nT) + \int_{nT}^{(n+\Delta)T} \boldsymbol{\phi}[(n + \Delta)T - \tau]\mathbf{B}d\tau h(nT)$$

$$= \boldsymbol{\phi}(\Delta T)\mathbf{x}(nT) + \boldsymbol{\theta}(\Delta T)h(nT) \tag{I-109}$$

By varying the value of Δ between 0 and 1, the information on the state variables between the sampling instants is completely described by Eq. (I-109).

When a linear system has only discrete data through the system, its dynamics can be described by a set of discrete state equations:

$$\mathbf{x}[(k + 1)T] = \mathbf{A}\mathbf{x}(kT) + \mathbf{B}r(kT) \tag{I-110}$$

and output equations:

$$\mathbf{y}(kT) = \mathbf{C}\mathbf{x}(kT) + \mathbf{D}r(kT) \tag{I-111}$$

where $\mathbf{A}$, $\mathbf{B}$, $\mathbf{C}$, and $\mathbf{D}$ are coefficient matrices of the appropriate dimensions. Notice that Eq. (I-110) is basically of the same form as Eq. (I-100). The only difference in the two

situations is the starting point of system representation. In the case of Eq. (I-100), the starting point is the continuous-data state equations of Eq. (I-95); $\phi(T)$ and $\theta(T)$ are determined from the **A** and **B** matrices, and must satisfy the conditions and properties of the state transition matrix. In the case of Eq. (I-110), the equation itself represents an outright description of the discrete-data system, and there are no restrictions on the matrices **A** and **B**.

The solution of Eq. (I-110) follows directly from that of Eq. (I-100), and is

$$\mathbf{x}(nT) = \mathbf{A}^n\mathbf{x}(0) + \sum_{i=0}^{n-1}\mathbf{A}^{n-i-1}\mathbf{Br}(iT) \tag{I-112}$$

where

$$\mathbf{A}^n = \mathbf{AAAA}\cdots\mathbf{A}$$
$$|\leftarrow \ n \ \rightarrow| \tag{I-113}$$

I-4-3   *z*-Transform Solution of Discrete State Equations

In Section I-1-5, we illustrated the solution of a simple discrete state equation by the *z*-transform method. In this section, the discrete state equations in vector-matrix form of an *n*th-order system are solved by *z*-transformation. Consider the discrete state equations

$$\mathbf{x}[(k + 1)T] = \mathbf{Ax}(kT) + \mathbf{Br}(kT) \tag{I-114}$$

Taking the *z*-transform on both sides of the last equation, we get

$$z\mathbf{X}(z) - z\mathbf{x}(0) = \mathbf{AX}(z) + \mathbf{BR}(z) \tag{I-115}$$

Solving for **X**(*z*) from Eq. (I-115), we get

$$\mathbf{X}(z) = (z\mathbf{I} - \mathbf{A})^{-1}z\mathbf{x}(0) + (z\mathbf{I} - \mathbf{A})^{-1}\mathbf{BR}(z) \tag{I-116}$$

Taking the inverse *z*-transform on both sides of Eq. (I-116), we have

$$\mathbf{x}(nT) = \mathcal{Z}^{-1}[(z\mathbf{I} - \mathbf{A})^{-1}z]\mathbf{x}(0) + \mathcal{Z}^{-1}[(z\mathbf{I} - \mathbf{A})^{-1}\mathbf{BR}(z)] \tag{I-117}$$

In order to carry out the inverse *z*-transform operation of the last equation, we write the *z*-transform of $\mathbf{A}^n$ as

$$\mathcal{Z}(\mathbf{A}^n) = \sum_{n=0}^{\infty}\mathbf{A}^n z^{-n} = \mathbf{I} + \mathbf{A}z^{-1} + \mathbf{A}^2 z^{-2} + \cdots \tag{I-118}$$

Premultiplying both sides of Eq. (I-118) by $\mathbf{A}z^{-1}$ and subtracting the result from the last equation, we get

$$(\mathbf{I} - \mathbf{A}z^{-1})\mathcal{Z}(\mathbf{A}^n) = \mathbf{I} \tag{I-119}$$

Therefore, solving for $\mathcal{Z}(\mathbf{A}^n)$ from the last equation yields

$$\mathcal{Z}(\mathbf{A}^n) = (\mathbf{I} - \mathbf{A}z^{-1})^{-1} = (z\mathbf{I} - \mathbf{A})^{-1}z \tag{I-120}$$

or

$$\mathbf{A}^n = \mathcal{Z}^{-1}[(z\mathbf{I} - \mathbf{A})^{-1}z] \tag{I-121}$$

Equation (I-121) represents a way of finding $\mathbf{A}^n$ by using the *z*-transform method. Similarly, we can prove that

$$\mathcal{Z}^{-1}[(z\mathbf{I} - \mathbf{A})^{-1}\mathbf{BR}(z)] = \sum_{i=0}^{n-1}\mathbf{A}^{n-i-1}\mathbf{Br}(iT) \tag{I-122}$$

Now we substitute Eqs. (I-121) and (I-122) into Eq. (I-117), $\mathbf{x}(nT)$ becomes

$$\mathbf{x}(nT) = \mathbf{A}^n \mathbf{x}(0) + \sum_{i=0}^{n-1} \mathbf{A}^{n-i-1} \mathbf{Br}(iT) \tag{I-123}$$

which is identical to Eq. (I-112).

I-4-4 Transfer-Function Matrix and the Characteristic Equation

Once a discrete-data system is modeled by the dynamic equations of Eqs. (I-110) and (I-111), the transfer-function relation of the system can be expressed in terms of the coefficient matrices. By setting the initial state $\mathbf{x}(0)$ to zero, Eq. (I-116) becomes

$$\mathbf{X}(z) = (z\mathbf{I} - \mathbf{A})^{-1} \mathbf{BR}(z) \tag{I-124}$$

Substituting Eq. (I-124) into the z-transformed version of Eq. (I-111), we have

$$\mathbf{Y}(z) = [\mathbf{C}(z\mathbf{I} - \mathbf{A})^{-1}\mathbf{B} + \mathbf{D}]\mathbf{R}(z) = \mathbf{G}(z)\mathbf{R}(z) \tag{I-125}$$

where the transfer-function matrix of the system is defined as

$$\mathbf{G}(z) = \mathbf{C}(z\mathbf{I} - \mathbf{A})^{-1}\mathbf{B} + \mathbf{D} \tag{I-126}$$

or

$$\mathbf{G}(z) = \frac{\mathbf{C}[\mathrm{adj}(z\mathbf{I} - \mathbf{A})\mathbf{B} + |z\mathbf{I} - \mathbf{A}|\mathbf{D}]}{|z\mathbf{I} - \mathbf{A}|} \tag{I-127}$$

The characteristic equation of the system is defined as

$$|z\mathbf{I} - \mathbf{A}| = 0 \tag{I-128}$$

In general, a linear time-invariant discrete-data system with one input and one output can be described by the following difference equation with constant coefficients:

$$\begin{aligned}
y[(k+n)T] &+ a_{n-1}y[(k+n-1)T] + a_{n-2}y[(k+n-2)T] \\
&+ \cdots + a_1 y[((k+1))T] + a_0 y(kT) \\
&= b_m r[(k+m)T] + b_{m-1}r[(k+m-1)T] \\
&+ \cdots + b_1 r[((k+1))T] + b_0 r(kT) \qquad n \geq m
\end{aligned} \tag{I-129}$$

Taking the z-transform on both sides of Eq. (I-129) and setting zero initial conditions, the transfer function of the system is written

$$\frac{Y(z)}{R(s)} = \frac{b_m z^m + b_{m-1}z^{m-1} + \cdots + b_1 z + b_0}{z^n + a_{n-1}z^{n-1} + \cdots + a_1 z + a_0} \qquad n \geq m \tag{I-130}$$

The characteristic equation is obtained by equating the denominator polynomial of the transfer function to zero.

$$z^n + a_{n-1}z^{n-1} + \cdots + a_1 z + a_0 = 0 \tag{I-131}$$

▶ **EXAMPLE I-13** Consider that a discrete-data system is described by the difference equation

$$y(k+2) + 5y(k+1) + 3y(k) = r(k+1) + 2r(k) \tag{I-132}$$

The transfer function of the system is simply

$$\frac{Y(z)}{R(z)} = \frac{z+2}{z^2 + 5z + 3} \tag{I-133}$$

The characteristic equation is

$$z^2 + 5z + 3 = 0 \tag{I-134}$$

The state variables of the system may be defined as

$$x_1(k) = y(k) \tag{I-135}$$
$$x_2(k) = x_1(k + 1) - r(k) \tag{I-136}$$

Substituting the last two equations into Eq. (I-132) gives the two state equations as

$$x_1(k + 1) = x_2(k) + r(k) \tag{I-137}$$
$$x_2(k + 1) = -3x_1(k) - 5x_2(k) - 3r(k) \tag{I-138}$$

from which we have the matrices **A** and **B**:

$$\mathbf{A} = \begin{bmatrix} 0 & 1 \\ -3 & -5 \end{bmatrix} \qquad \mathbf{B} = \begin{bmatrix} 1 \\ -3 \end{bmatrix} \tag{I-139}$$

The same characteristic equation as in Eq. (I-134) is obtained by using $|z\mathbf{I} - \mathbf{A}| = 0$. ◀

I-4-5 State Diagrams of Discrete-Data Systems

When a discrete-data system is described by difference or discrete state equations, a **discrete state diagram** may be constructed for the system. Similar to the relations between the analog-computer block diagram and the state diagram for continuous-data systems, the elements of a discrete state diagram resemble the computing elements of a digital computer. Some of the operations of a digital computer are **multiplication by a constant**, **addition of several variables**, and **time delay** or **shifting**. The discrete state diagram can be used to determine the transfer functions as well as for digital implementation of the system. The mathematical description of these basic digital computations and their corresponding z-transform expressions are as follows:

1. *Multiplication by a constant*:

$$x_2(kT) = ax_1(kT) \tag{I-140}$$
$$X_2(z) = aX_1(z) \tag{I-141}$$

2. *Summing*:

$$x_2(kT) = x_1(kT) + x_3(kT) \tag{I-142}$$
$$X_2(z) = X_1(z) + X_3(z) \tag{I-143}$$

3. *Shifting or time delay*:

$$x_2(kT) = x_1[(k + 1)T] \tag{I-144}$$
$$X_2(z) = zX_1(z) - zx_1(0) \tag{I-145}$$

or

$$X_1(z) = z^{-1}X_2(z) + x_1(0) \tag{I-146}$$

The state diagram representation of these operations are illustrated in Fig. I-11. The initial time $t = 0$ in Eqs. (I-145) and (I-146) can be generalized to $t = t_0$. Then the equations represent the discrete-time state transition from $t \geq t_0$.

$$X_2(z) = aX_1(z)$$

$$X_2(z) = X_0(z) + X_1(z)$$

$$X_1(z) = z^{-1}X_2(z) + x_1(0)$$
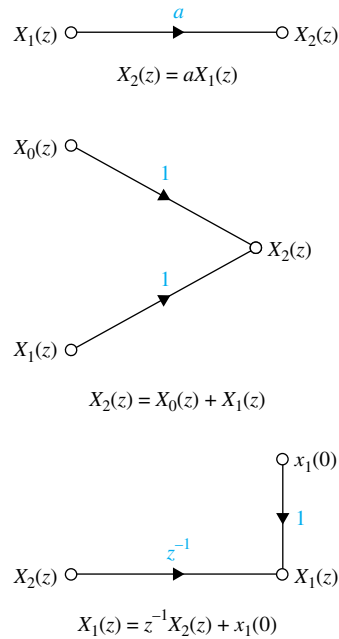
Figure I-11   Basic elements of a discrete state diagram.

▶ **EXAMPLE I-14**   Consider again the difference equation in Eq. (I-132), which is

$$y(k + 2) + 5y(k + 1) + 3y(k) = r(k + 1) + 2r(k) \qquad \text{(I-147)}$$

One way of constructing the discrete state diagram for the system is to use the state equations. In this case, the state equations are already defined in Eqs. (I-137) and (I-138). By using essentially the same principle as the state diagram for continuous-data systems, the state diagram for Eqs. (I-137) and (I-138) is shown in Fig. I-12. The time delay unit z^{-1} is used to relate $x_1(k + 1)$ to $x_2(k)$. *The state variables are defined as the outputs of the delay units in the state diagram.*

• The state variables are defined as the outputs of the delay units in the state diagram.

The state-transition equations of the system can be obtained directly from the state diagram using the SFG gain formula. By referring to $X_1(z)$ and $X_2(z)$ as the output nodes and $x_1(0)$, $x_2(0)$, and $R(z)$ as input nodes in Fig. I-12, the state-transition equations are written as

$$\begin{bmatrix} X_1(z) \\ X_2(z) \end{bmatrix} = \frac{1}{\Delta}\begin{bmatrix} 1 + 5z^{-1} & z^{-1} \\ -3z^{-1} & 1 \end{bmatrix}\begin{bmatrix} x_1(0) \\ x_2(0) \end{bmatrix} + \frac{1}{\Delta}\begin{bmatrix} z^{-1}(1 + 5z^{-1}) - 3z^{-2} \\ -3z^{-1} - 3z^{-2} \end{bmatrix}R(z) \qquad \text{(I-148)}$$
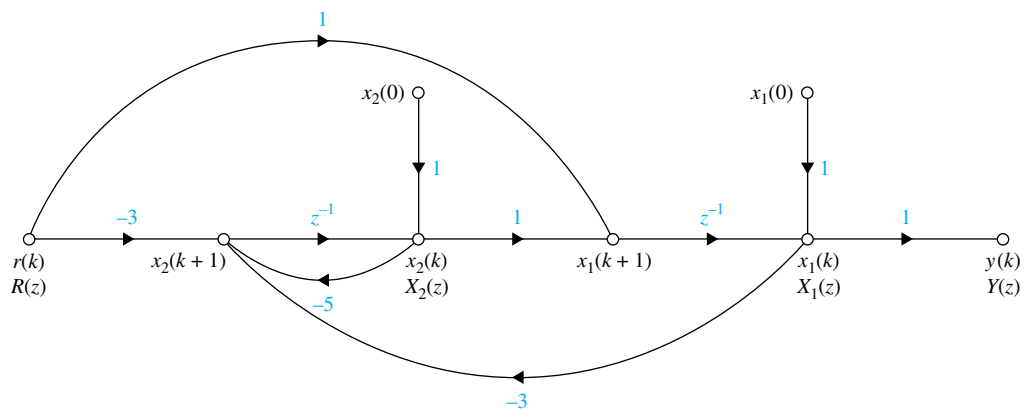
Figure I-12   Discrete state diagram of the system described by the difference equation of Eq. (I-132) or by the state equations of Eqs. (I-137) and (I-138).

(a) Direct decomposition

(b) Cascade decomposition
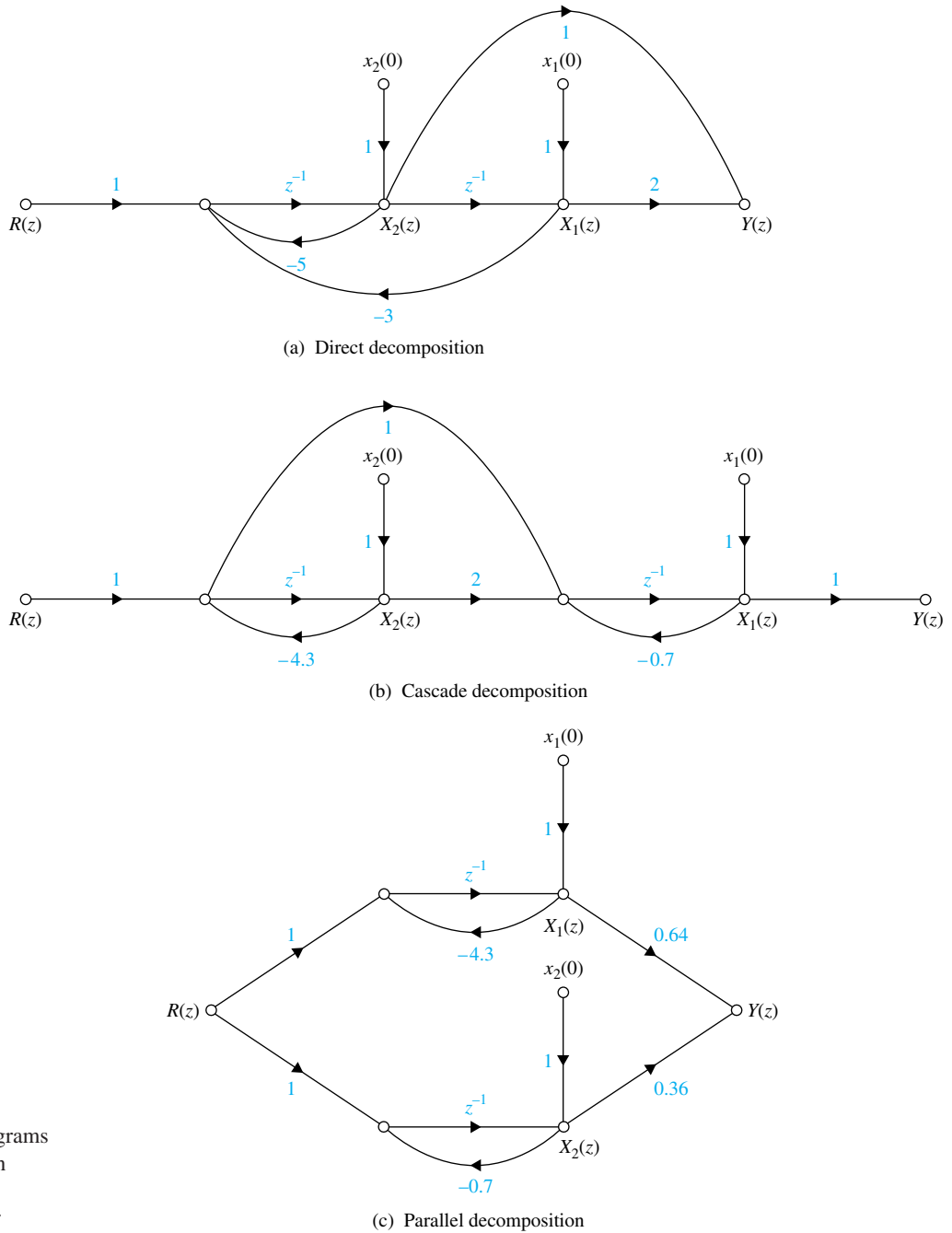
Figure I-13 State diagrams of the transfer function

$$\frac{Y(z)}{R(z)} = \frac{(z + 2)}{(z^2 + 5z + 3)}.$$

(c) Parallel decomposition

where

$$\Delta = 1 + 5z^{-1} + 3z^{-2} \qquad \text{(I-149)}$$

The same transfer function between $R(z)$ and $Y(z)$ as in Eq. (I-133) can be obtained directly from the state diagram in Fig. I-13 by applying the SFG gain formula between these two nodes.

As an alternative, the discrete state diagram can be drawn directly from the difference equation via the transfer function, using the decomposition schemes (Fig. I-13). The decomposition of a discrete-data transfer function follows basically the same procedure as that of an analog transfer function covered in Section 5-9, and so the details are not repeated here. ◀

$e(kT^+)$ ○ —— $\frac{1}{s}$ —— ○ $H(s)$
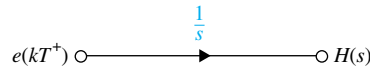
Figure I-14 State-diagram representation of the zero-order-hold (ZOH).

I-4-6 State Diagrams for Sampled-Data Systems

When a discrete-data system has continuous-data as well as discrete-data elements, with the two types of elements separated by sample-and-hold devices, a state diagram model for the sample-and-hold (zero-order-hold) must be established.

Consider that the input of the ZOH is denoted by $e^*(t)$, which is a train of impulses, and the output by $h(t)$. Since the ZOH simply holds the strength of the input impulse at the sampling instant until the next input comes, the signal $h(t)$ is a sequence of steps. The input-output relation in the Laplace domain is

$$H(s) = \frac{1 - e^{-Ts}}{s} E^*(s) \tag{I-150}$$

In the time domain, the relation is simply

$$h(t) = e(kT^+) \tag{I-151}$$

for $kT \le t < (k + 1)T$.

In the state-diagram notation, we need the relation between $H(s)$ and $e(kT^+)$. For this purpose, we take the Laplace transform on both sides of Eq. (I-151) to give

$$H(s) = \frac{e(kT^+)}{s} \tag{I-152}$$

for $kT \le t < (k + 1)T$. The state-diagram representation of the zero-order-hold is shown in Fig. I-14.

▶ **EXAMPLE I-15** As an illustrative example on how the state diagram of a sampled-data system is constructed, let us consider the system in Fig. I-15. We shall demonstrate the various ways of modeling the input-output relations of the system. First, the Laplace transform of the output of the system is written in terms of the input to the ZOH.

$$Y(s) = \frac{1 - e^{-Ts}}{s} \frac{1}{s + 1} E^*(s) \tag{I-153}$$

Taking the z-transform on both sides of Eq. (I-153), we get

$$Y(z) = \frac{1 - e^{-T}}{z - e^{-T}} E(z) \tag{I-154}$$

Figure I-16 shows the state diagram for Eq. (I-154). The discrete dynamic equations of the system are written directly from the state diagram.

$$x_1[(k + 1)T] = -e^{-T}x_1(kT) + (1 - e^{-T})e(kT^+) \tag{I-155}$$
$$y(kT) = x_1(kT) \tag{I-156}$$

$e(t)$ —— /⟍ —— $e^*(t)$ —— | ZOH | —— $h(t)$ —— | $G(s) = \dfrac{1}{s + 1}$ | —— $y(t)$

T
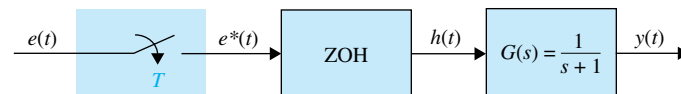
Figure I-15 Sampled-data system.
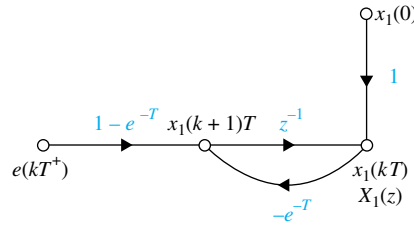
Figure I-16 Discrete state diagram of the system in Fig. I-15. ◀

▶ I-5 STABILITY OF DISCRETE-DATA SYSTEMS

The definitions of BIBO and zero-input stability can be readily extended to linear time-invariant SISO discrete-data control systems.

I-5-1 BIBO Stability

Let $u(kT)$, $y(kT)$, and $g(kT)$ be the input, output, and impulse sequence of a linear time-invariant SISO discrete-data system, respectively. With *zero initial conditions, the system is said to be BIBO stable, or simply stable, if its output sequence $y(kT)$ is bounded to a bounded input $u(kT)$*. As with the treatment in Section 6-1, we can show that for the system to be BIBO stable, the following condition must be met:

$$\sum_{k=0}^{\infty} |g(kT)| < \infty \tag{I-157}$$

I-5-2 Zero-Input Stability

For zero-input stability, the output sequence of the system must satisfy the following conditions:

1. $|y(kT)| \leq M < \infty$ (I-158)
2. $\lim_{k\to\infty} |y(kT)| = 0$ (I-159)

Thus, zero-input stability can also be referred to as **asymptotic stability**. We can show that *both the BIBO stability and the zero-input stability of discrete-data systems require that the roots of the characteristic equation lie inside the unit circle $|z| = 1$ in the z-plane.* This is not surprising, since the $j\omega$-axis of the s-plane is mapped onto the unit circle in the z-plane. The regions of stability and instability for discrete-data systems in the z-plane are shown in Fig. I-17. Let the characteristic equation roots of a linear discrete-data time-invariant SISO system be z_i, $i = 1, 2, \ldots, n$. The possible stability conditions of the system are summarized in Table I-2 with respect to the roots of the characteristic equation.

TABLE I-2 Stability Conditions of Linear Time-Invariant Discrete-Data SISO Systems

Stability condition	Root values
Asymptotically stable or simply stable	$|z_i| < 1$ for all i, $i = 1, 2, \ldots, n$ (all roots inside the unit circle)
Marginally stable or marginally unstable	$|z_i| = 1$ for any i for simple roots, and no $|z_i| > 1$ for $i = 1, 2, \ldots, n$ (at least one simple root, no multiple-order roots on the unit circle, and no roots outside the unit circle)
Unstable	$|z_i| > 1$ for any i, or $|z_i| = 1$ for any multiple-order root. $i = 1, 2, \ldots, n$ (at least one simple root outside the unit circle and at least one multiple-order root on the unit circle)
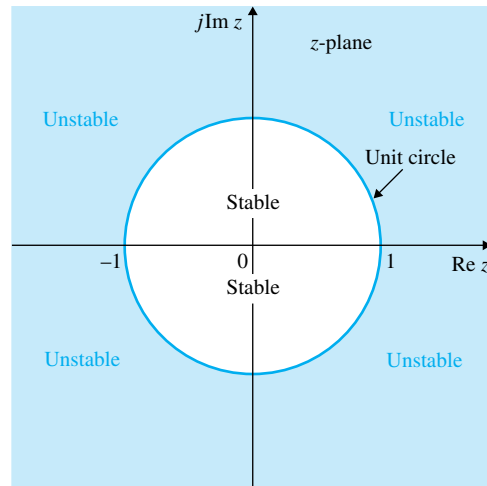
Figure I-17 Stable and unstable regions for discrete-data systems in the z-plane.

The following example illustrates the relationship between the closed-loop transfer-function poles, which are the characteristic equation roots, and the stability condition of the system.

▶ **EXAMPLE I-16**

$$M(z) = \frac{5z}{(z - 0.2)(z - 0.8)} \qquad \text{Stable system}$$

$$M(z) = \frac{5z}{(z + 1.2)(z - 0.8)} \qquad \text{Unstable system due to the pole at } z = -1.2$$

$$M(z) = \frac{5(z + 1)}{z(z - 1)(z - 0.8)} \qquad \text{Marginally stable due to } z = 1$$

$$M(z) = \frac{5(z + 1.2)}{z^2(z + 1)^2 (z + 0.1)} \qquad \text{Unstable due to second-order pole at } z = -1$$

◀

I-5-3 Stability Tests of Discrete-Data Systems

We pointed out in Section I-5 that the stability test of a linear discrete-data system is essentially a problem of investigating whether all the roots of the characteristic equation are inside the unit circle $|z| = 1$ in the z-plane. The Nyquist criterion, root-locus diagram, and Bode diagram, originally devised for continuous-data systems, can all be extended to the stability studies of discrete-data systems. One exception is the Routh-Hurwitz criterion, which in its original form is restricted to only the imaginary axis of the s-plane as the stability boundary, and thus can be applied only to continuous-data systems.

Bilinear Transformation Method [1]
We can still apply the Routh-Hurwitz criterion to discrete-data systems if we can find a transformation that transforms the unit circle in the z-plane onto the imaginary axis of another complex plane. We cannot use the z-transform relation $z = \exp(Ts)$ or $s = (\ln z)/T$,

since it would transform an algebraic equation in z into a nonalgebraic equation in s, and the Routh test still cannot be applied. However, there are many bilinear transformations of the form of

$$z = \frac{ar + b}{cr + d} \tag{I-160}$$

where a, b, c, d are real constants, *and* r is a complex variable, that will transform circles in the z-plane onto straight lines in the r-plane. One such transformation that transforms the interior of the unit circle of the z-plane onto the left half of the r-plane is

$$z = \frac{1 + r}{1 - r} \tag{I-161}$$

which is referred to as the **r-transformation**. Once the characteristic equation in z is transformed into the r domain using Eq. (I-161), the Routh-Hurwitz criterion can again be applied to the equation in r.

The r-transformation given in Eq. (I-161) is probably the simplest form that can be used for manual transformation of an equation $F(z)$ to an equation in r. Another transformation that is often used in discrete-data control-system design in the frequency domain is

$$z = \frac{(2/T) + w}{(2/T) - w} \tag{I-162}$$

or

$$w = \frac{2}{T}\frac{z - 1}{z + 1} \tag{I-163}$$

which is called the **w-transformation**. Note that the w-transformation becomes the r-transformation when $T = 2$. The advantage of the w-transformation over the r-transformation is that the imaginary axis of the w-plane resembles that of the s-plane. To show this, we substitute

$$z = e^{j\omega T} = \cos \omega T + j \sin \omega T \tag{I-164}$$

into Eq. (I-163), and we get

$$w = \frac{2}{T}\frac{\cos wT + j\sin \omega T - 1}{\cos \omega T + j\sin \omega T + 1} \tag{I-165}$$

Rationalizing the last equation, and simplifying, we get

$$w = j\omega_w = j\frac{2}{T}\tan\frac{\omega T}{2} \tag{I-166}$$

Thus, the unit circle in the z-plane is mapped onto the imaginary axis $w = j\omega_w$ in the w-plane. the relationship between ω_w and ω, the real frequency, is

$$\omega_w = \frac{2}{T}\tan\frac{\omega T}{2} = \frac{\omega_s}{\pi}\tan\frac{\pi\omega}{\omega_s} \tag{I-167}$$

where ω_s is the sampling frequency in rad/sec. The correlation between ω and ω_w is that they both go to 0 and ∞ at the same time. For Routh-Hurwitz criterion, of course, the w-transformation is more difficult to use, especially since the sampling period T appears in Eq. (I-163). However, if computer programs are available for the transformations, the difference is insignificant.

The following examples illustrate the application of the r-transformation to a characteristic equation in z so that the equation can be tested by Routh-Hurwitz criterion in the r-domain.

▶ **EXAMPLE I-17** Consider that the characteristic equation of a discrete-data control system is

$$z^3 + 5.94z^2 + 7.7z - 0.368 = 0 \tag{I-168}$$

Substituting Eq. (I-161) into the last equation and simplifying, we get

$$3.128r^3 - 11.74r^2 + 2.344r + 14.27 = 0 \tag{I-169}$$

Routh's tabulation of the last equation is

r^3	3.128	2.344
Sign change		
r^2	-11.74	14.27
Sign change		
r^1	6.146	0
r^0	14.27	

Since there are two sign changes in the first column of the tabulation, Eq. (I-169) has two roots in the right half of the r-plane. This corresponds to Eq. (I-168) having two roots outside the unit circle in the z-plane. This result can be checked by solving the two equations in z and r. For Eq. (I-168), the roots are: $z = -2.0$, $z = -3.984$, and $z = 0.0461$. The three corresponding roots in the r-plane are: $r = 3.0$, $r = 1.67$, and $r = -0.9117$, respectively. ◀

▶ **EXAMPLE I-18** Let us consider a design problem using the bilinear transformation and Routh-Hurwitz criterion. The characteristic equation of a linear discrete-data control system is given as

$$F(z) = z^3 + z^2 + z + K = 0 \tag{I-170}$$

where K is a real constant. The problem is to find the range of values of K so that the system is stable. We first transform $F(z)$ into an equation in r using the bilinear transformation of Eq. (I-161). The result is

$$(1 - K)r^3 + (1 + 3K)r^2 + 3(1 - K)r + 3 + K = 0 \tag{I-171}$$

Routh's tabulation of the last equation is

r^3	$1 - K$	$3(1 - K)$
r^2	$1 + 3K$	$3 + K$
r^1	$\dfrac{8K(1 - K)}{1 + 3K}$	0
r^0	$3 + K$	

For a stable system, the numbers in the first column of the tabulation must be of the same sign. We can show that these numbers cannot be all negative, since the conditions contradict each other. Next, for all the numbers to be positive, we have the following conditions:

$$1 - K > 0 \qquad 1 + 3K > 0 \qquad K > 0 \qquad 3 + K > 0$$

which lead to the condition for stability:

$$0 < K < 1 \tag{I-172}$$

◀

Direct Stability Tests

There are stability tests that can be applied directly to the characteristic equation in z with reference to the unit circle in the z-plane. One of the first methods that gives the necessary

and sufficient conditions for the characteristic equation roots to lie inside the unit circle is the Schur-Cohn criterion [2]. A simpler tabulation method was devised by Jury and Blanchard [3, 4] and is called **Jury's stability criterion** [6]. R. H. Raible [5] devised an alternate tabular form of Jury's stability test. Unfortunately, these analytical tests all become very tedious for equations higher than the second order, especially when the equation has unknown parameter(s) in it. Then, there is no reason to use any of these tests if all the coefficients of the equation are known, since we can always use a root-finding program on a computer. Weighing all the pros and cons, this author believes that when the characteristic equation has at least one unknown parameter, the bilinear transformation method is still the best manual method for determining stability of linear discrete-data systems. However, it is useful to introduce the necessary condition of stability that can be checked by inspection.

Consider that the characteristic equation of a linear time-invariant discrete-data system is

$$F(z) = a_n z^n + a_{n-1} z^{n-1} + \cdots + a_1 z + a_0 = 0 \tag{I-173}$$

where all the coefficients are real. Among all the conditions provided in Jury's test, the following *necessary* conditions must be satisfied for $F(z)$ to have no roots on or outside the unit circle.

$$
\begin{aligned}
&F(1) > 0 \\
&F(-1) > 0 \qquad \text{if } n = \text{even integer} \\
&F(-1) < 0 \qquad \text{if } n = \text{odd integer} \\
&|a_0| < a_n
\end{aligned}
\tag{I-174}
$$

If an equation of the form of Eq. (I-173) violates any one of these conditions, then not all of the roots are inside the unit circle, and the system would not be stable. Apparently, these necessary conditions can be checked easily by inspection.

► **EXAMPLE I-19**   Consider the equation

$$F(z) = z^3 + z^2 + 0.5z + 0.25 = 0 \tag{I-175}$$

Applying the conditions in Eq. (I-174), we have

$$
\begin{aligned}
&F(1) = 2.75 > 0 \qquad \text{and} \qquad F(-1) = -0.25 < 0 \qquad \text{for } n = 3, \text{ which is odd} \\
&|a_0| = 0.25 < a_3 = 1
\end{aligned}
$$

Thus, the conditions in Eq. (I-174) are all satisfied, but nothing can be said about the stability of the system. ◄

► **EXAMPLE I-20**   Consider the equation

$$F(z) = z^3 + z^2 + 0.5z + 1.25 = 0 \tag{I-176}$$

The conditions in Eq. (6-58) are

$$
\begin{aligned}
&F(-1) = 0.75 > 0 \qquad \text{for } n = 3, \text{ which is odd} \\
&|a_0| = 1.25, \text{ which is not less than } a_3, \text{ which equals 1.}
\end{aligned}
$$

Since for odd n $F(-1)$ must be negative, the equation in Eq. (I-176) has at least one root outside the unit circle. The condition on the absolute value of a_0 is also not met. ◄

Second-Order Systems
The conditions in Eq. (I-174) become *necessary and sufficient* when the system is of the second order. That is, the necessary and sufficient conditions for the second-order equation

$$F(z) = a_2 z^2 + a_1 z + a_0 = 0 \tag{I-177}$$

to have no roots on or outside the unit circle are

$$F(1) > 0$$
$$F(-1) > 0 \tag{I-178}$$
$$|a_0| < a_2$$

▶ **EXAMPLE I-21** Consider the equation

$$F(z) = z^2 + z + 0.25 = 0 \tag{I-179}$$

Applying the conditions in Eq. (I-178), we have

$$F(1) = 2.25 > 0 \qquad F(-1) = 0.25 > 0 \qquad \text{for } n = 2, \text{ which is even}$$
$$|a_0| = 0.25 < a_2 = 1$$

Thus, the conditions in Eq. (I-178) are all satisfied. The two roots in Eq. (I-179) are all inside the unit circle, and the system is stable. ◀

▶ I-6 TIME-DOMAIN PROPERTIES OF DISCRETE-DATA SYSTEMS

I-6-1 Time Response of Discrete-Data Control Systems

To carry out the design of discrete-data control systems in the time domain or the z-domain, we must first study the time- and z-domain properties of these systems. We learned from the previous sections that the output responses of most discrete-data control systems are functions of the continuous-time variable t. Thus, the time-domain specifications such as the maximum overshoot, rise time, damping ration, and so forth, can still be applied to discrete-data systems. The only difference is that in order to make use of the analytical tools such as z-transforms, the continuous data found in a discrete-data system are sampled so that the independent time variable is kT, where T is the sampling period in seconds. Also, instead of working in the s-plane, the transient performance of a discrete-data system is characterized by poles and zeros of the transfer function in the z-plane.

The objectives of the following sections are as follows:

1. To present methods of finding the discretized time responses of discrete-data control systems
2. To describe the important characteristics of the discretized time response $y(kT)$
3. To establish the significance of pole and zero locations in the z-plane
4. To provide comparison between time responses of continuous-data and discrete-data control systems

Let us refer to the block diagram of the discrete-data control system shown in Fig. I-18. The transfer function of the system is

$$\frac{Y(z)}{R(z)} = \frac{G(z)}{1 + GH(z)} \tag{I-180}$$

where $GH(z)$ denotes the z-transform of $G(s)H(s)$. Once the input $R(z)$ is given, the output sequence $y(kT)$ can be determined using one of the following two methods:

1. Take the inverse z-transform of $Y(z)$ using the z-transform table.
2. Expand $Y(z)$ into a power series of z^{-k}.
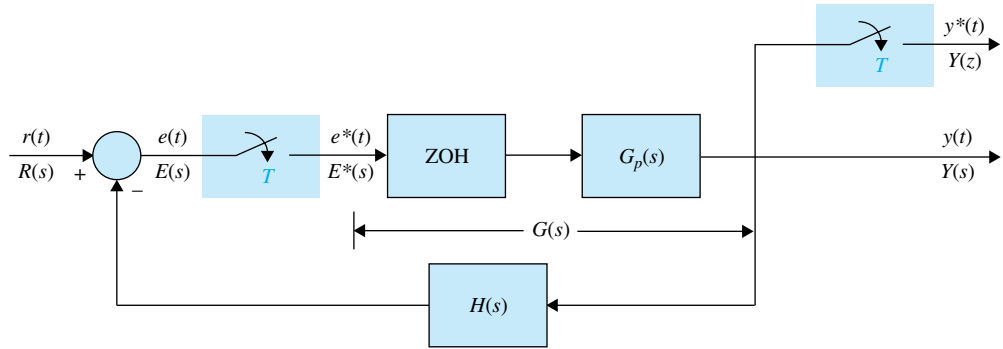
Figure I-18 Block diagram of a discrete-data control system.

The z-transform of the output is defined as

$$Y(z) = \sum_{k=0}^{\infty} y(kT)z^{-k} \qquad \text{(I-181)}$$

The discrete-time response $y(kT)$ can be determined by referring to the coefficient of z^{-k} for $k = 0, 1, 2, \ldots$. Remember that $y(kT)$, $k = 0, 1, 2, \ldots$ contains only the sampled information on $y(t)$ at the sampling instants. If the sampling period is large relative to the most significant time constant of the system, $y(kT)$ may not be an accurate representation of $y(t)$.

▶ **EXAMPLE I-22** Consider that the position-control system described in Section 7-7 has discrete data in the forward path, so that the system is now described by the block diagram of Fig. I-18. For $K = 14.5$, the transfer function of the controlled process is

$$G_p(s) = \frac{65,250}{s(s + 361.2)} \qquad \text{(I-182)}$$

The forward-path transfer function of the discrete-data system is

$$G_{h0}G_p(z) = \mathcal{Z}[G_{h0}G_p(s)] = (1 - z^{-1})\mathcal{Z}\left[\frac{G_p(s)}{s}\right] \qquad \text{(I-183)}$$

For a sampling period of $T = 0.001$ second, the z-transfer function in Eq. (I-183) is evaluated as

$$G_{h0}G_p(z) = \frac{0.029z + 0.0257}{z^2 - 1.697z + 0.697} \qquad \text{(I-184)}$$

The closed-loop transfer function of the system is

$$\frac{Y(z)}{R(z)} = \frac{G_{h0}G_p(z)}{1 + G_{h0}G_p(z)} = \frac{0.029z + 0.0257}{z^2 - 1.668z + 0.7226} \qquad \text{(I-185)}$$

where $R(z)$ and $Y(z)$ represent the z-transforms of the input and the output, respectively. For a unit-step input, $R(z) = z/(z - 1)$. The output transform $Y(z)$ becomes

$$Y(z) = \frac{z(0.029z + 0.0257)}{(z - 1)(z^2 - 1.668z + 0.7226)} \qquad \text{(I-186)}$$

The output sequence $y(kT)$ can be determined by dividing the numerator polynomial of $Y(z)$ by its denominator polynomial to yield a power series in z^{-1}. Figure I-20 shows the plot of $y(kT)$ (dots) versus kT, when $T = 0.001$ second. For comparison, the unit-step response of the continuous-data system in Section 7-6 with $K = 14.5$ is shown in the same figure. As seen in Fig. I-19, when the sampling period is small, the output responses of the discrete-data and the continuous-data systems are very similar. The maximum value of $y(kT)$ is 1.0731, or a 7.31 percent maximum overshoot, as against the 4.3 percent maximum overshoot for the continuous-data system.
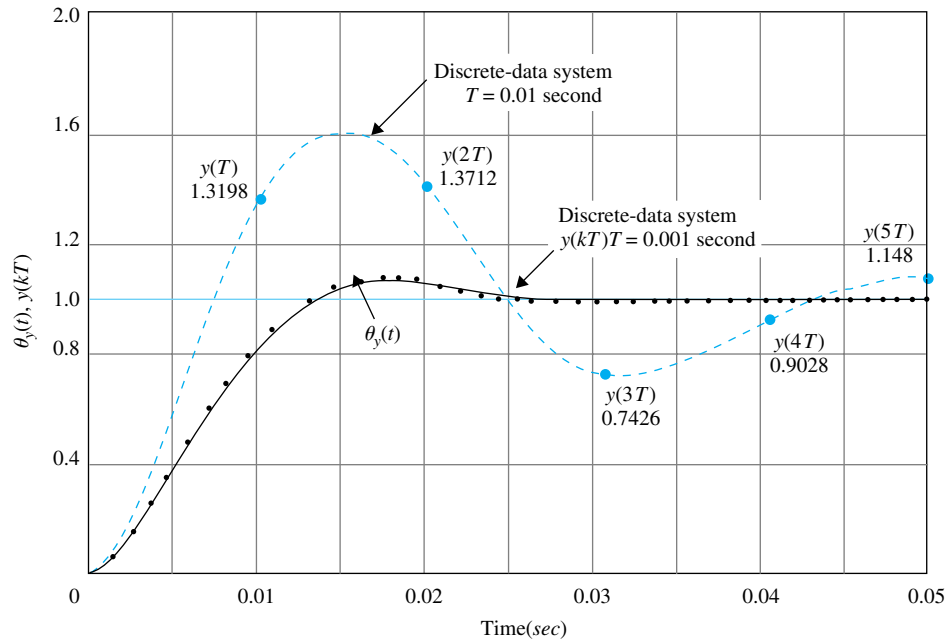
Figure I-19 Comparison of unit-step responses of discrete-data and continuous-data systems.

When the sampling period is increased to 0.01 second, the forward-path transfer function of the discrete-data system is

$$G_{h0}G_p(z) = \frac{1.3198z + 0.4379}{z^2 - 1.027z + 0.027} \tag{I-187}$$

and the closed-loop transfer function is

$$\frac{Y(z)}{R(z)} = \frac{1.3198z + 0.4379}{z^2 + 0.2929z + 0.4649} \tag{I-188}$$

• Two equal characteristic equation roots on the negative real axis in the z-plane do not correspond to critical damping.

The output sequence $y(kT)$ with $T = 0.01$ second is shown in Fig. I-19 with $k = 0, 1, 2, 3, 4,$ and 5. The true continuous-time output of the discrete-data system is shown as the dotted curve. Notice that the maximum value of $y(kT)$ is 1.3712, but the true maximum overshoot is considerably higher than that. Thus, the larger sampling period only makes the system less stable, but the sampled output no longer gives an accurate measure of the true output.

When the sampling period is increased to 0.01658 second, the characteristic equation of the discrete-data system is

$$z^2 + 1.4938z + 0.4939 = 0 \tag{I-189}$$

• When one or more characteristic equation roots lie on the negative axis in the z-plane, response will oscillate with positive and negative peaks.

which has roots at $z = -0.494$ and $z = -1.000$. The root at -1.000 causes the step response of the system to oscillate with a constant amplitude, and the system is marginally stable. Thus, for all sampling periods greater than 0.01658 second, the discrete-data system will be unstable. From Section 7-6, we learned that the second-order continuous-data system is always stable for finite positive values of K. For the discrete-data system, the sample-and-hold has the effect of making the system less stable, and if the value of T is too large, the second-order system can become unstable. Figure I-20 shows the trajectories of the two characteristic-equation roots of the discrete-data system as the sampling period T varies. Notice that when the sampling period is very small, the two characteristic-equation roots are very close to the $z = 1$ point and are complex. When $T = 0.01608$ second, the two roots become equal and real and are negative. Unlike the continuous-data system, the case of two identical roots on the *negative* real axis in the z-plane *does not* correspond to critical damping. For discrete-data systems, when one or more characteristic-equation roots lie on the negative real axis of the z-plane, the system response will oscillate with positive and negative peaks. Figure I-21 shows the oscillatory response of $y(kT)$ when $T = 0.01658$ second, which is the critical value for stability. Beyond this value of T, one root will move outside the unit circle, and the system will become unstable.
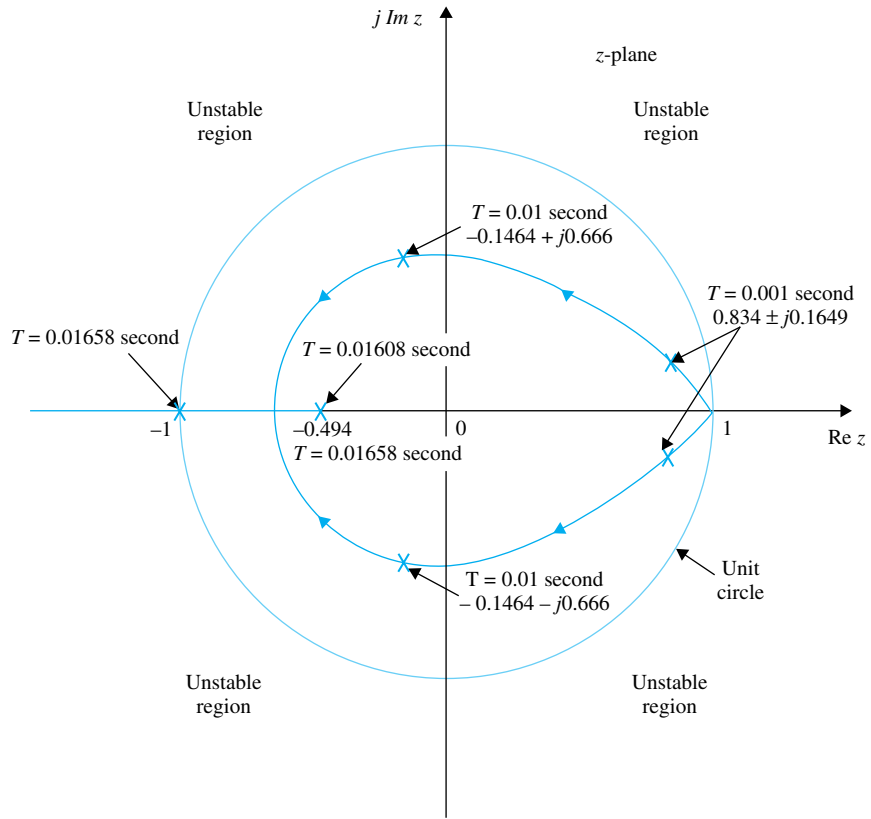
Figure I-20 Trajectories of roots of a second-order discrete-data control system as the sampling period T varies.
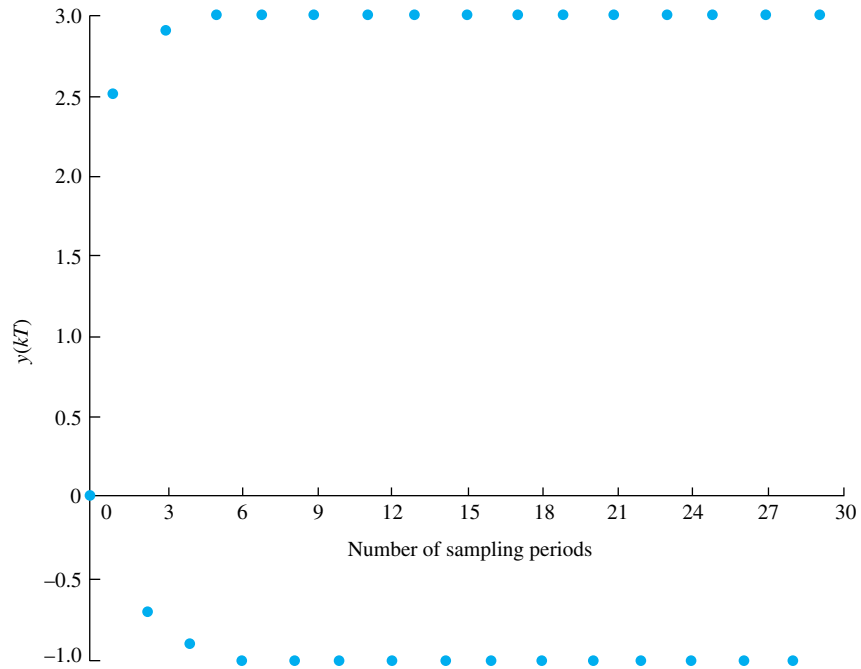
Figure I-21 Oscillatory response of a discrete-data system with a sampling period $T = 0.01658$ second.

I-6-2 Mapping between s-Plane and z-Plane Trajectories

For analysis and design purposes, it is important to study the relation between the location of the characteristic-equation roots in the z-plane and the time response of the discrete-data system. In Section I-2, the periodic property of the Laplace transform of the Laplace transform of the sampled signal $R^*(s)$ is established by Eq. (I-62); that is, $R^*(s + jm\omega_s) = R^*(s)$, where m is an integer. In other words, given any point s_1 in the s-plane, the function $R^*(s)$ has the same value at all periodic points $s = s_1 + jm\omega_s$. Thus, the s-plane is divided into an infinite number of periodic strips, as shown in Fig. I-22(a). The strip between

(a)

(b)
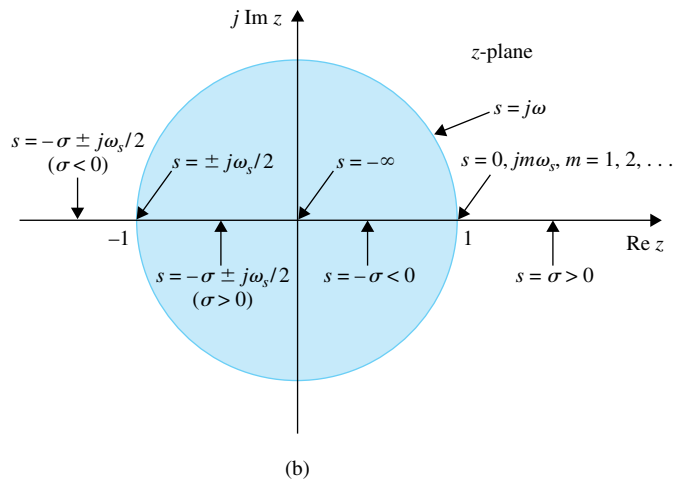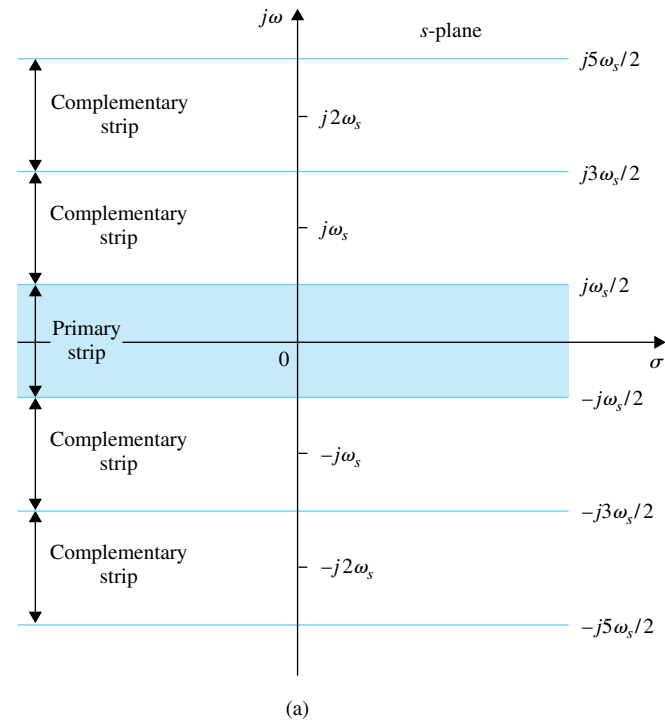
Figure I-22 Periodic strips in the s-plane and the corresponding points and lines between the s-plane and the z-plane.

$\omega = \omega_s/2$ is called the **primary strip**, and all others at higher frequencies are called the **complementary strips**. Figure I-22(b) shows the mapping of the periodic strips from the s-plane to the z-plane, and the details are explained as follows.

1. The $j\omega$-axis in the s-plane is mapped onto the unit circle $|z| = 1$ in the z-plane.
2. The boundaries of the period strips, $s = jm\omega_s/2$, $m = \pm1, \pm3, \pm5, \ldots$, are mapped onto the negative real axis of the z-plane. The portion inside the unit circle corresponds to $\sigma < 0$, and the portion outside the unit circle corresponds to $\sigma > 0$.
3. The center lines of the periodic strips, $s = jm\omega_s$, $m = 0, \pm2, \pm4, \ldots$, are mapped onto the positive real axis of the z-plane. The portion inside the unit circle corresponds to $\sigma < 0$, and the portion outside the unit circle corresponds to $\sigma > 0$.
4. Regions shown in the periodic strips in the left-half s-plane are mapped onto the interior of the unit circle in the z-plane.
5. The point $z = 1$ in the z-plane corresponds to the origin, $s = 0$, in the x-plane.
6. The origin, $z = 0$, in the z-plane corresponds to $s = -\infty$ in the s-plane.

In the time-domain analysis of continuous-data systems, we devise the damping factor α, the damping ratio ζ, and the natural undamped frequency ω_n to characterize the system dynamics. The same parameters can be defined for discrete-data systems with respect to the characteristic-equation roots in the z-plane. The loci of the constant-α, constant-ζ, constant-ω, and constant-ω_n in the z-plane are described in the following sections.

Constant-Damping Loci: For a constant-damping factor $\sigma = \alpha$ in the s-plane, the corresponding trajectory in the z-plane is described by

$$z = e^{\alpha T} \tag{I-190}$$

which is a circle centered at the origin with a radius of $e^{\alpha T}$, as shown in Fig. I-23.

Constant-Frequency Loci: The constant-frequency $\omega = \omega_1$ locus in the s-plane is a horizontal line parallel to the σ-axis. The corresponding z-plane locus is a straight line emanating from the origin at an angle of $\theta = \omega_1 T$ radians, measured from the real axis, as shown in Fig. I-24.
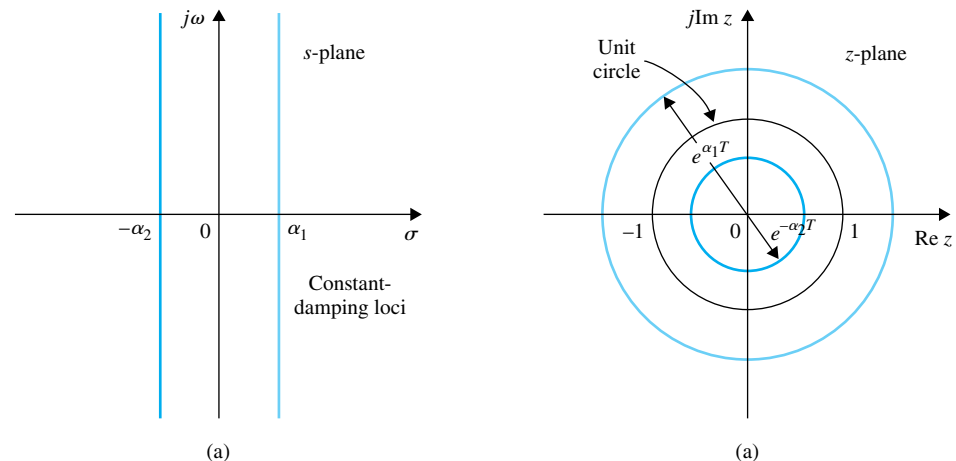
Figure I-23 Constant-damping loci in the s-plane and the z-plane.
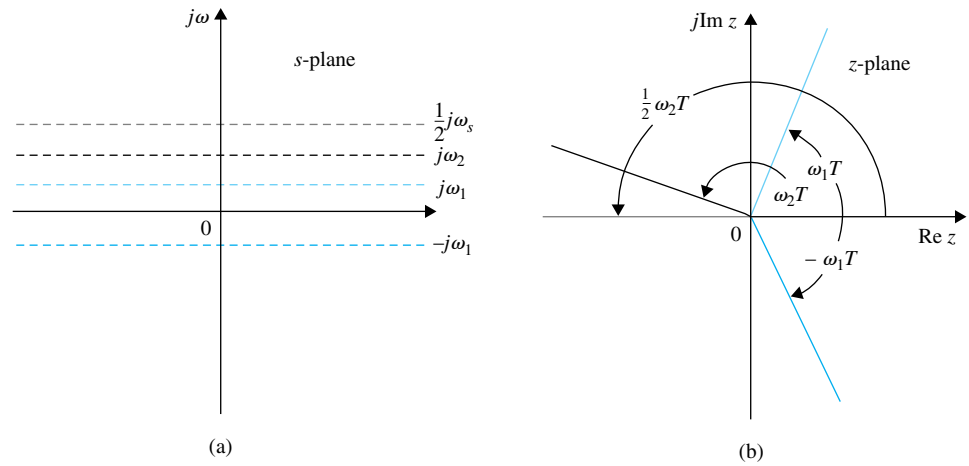
Figure I-24 Constant-frequency loci in the s-plane and the z-plane.

Constant Natural-Undamped Frequency Loci: The constant-ω_n loci in the s-plane are concentric circles with the center at the origin, and the radius is ω_n. The corresponding constant-ω_n loci in the z-plane are shown in Fig. I-25 for $\omega_n = \omega_s/16$ to $\omega_s/2$. Only the loci inside the unit circle are shown.

Constant-Damping Ratio Loci: For a constant-damping ratio ζ, the s-plane loci are described by

$$s = -\omega \tan \beta + j\omega \qquad (I-191)$$

The constant-ζ loci in the z-plane are described by

$$z = e^{Ts} = e^{-2\pi(\tan\beta)/\omega_s} \angle 2\pi\omega/\omega_s \qquad (I-192)$$
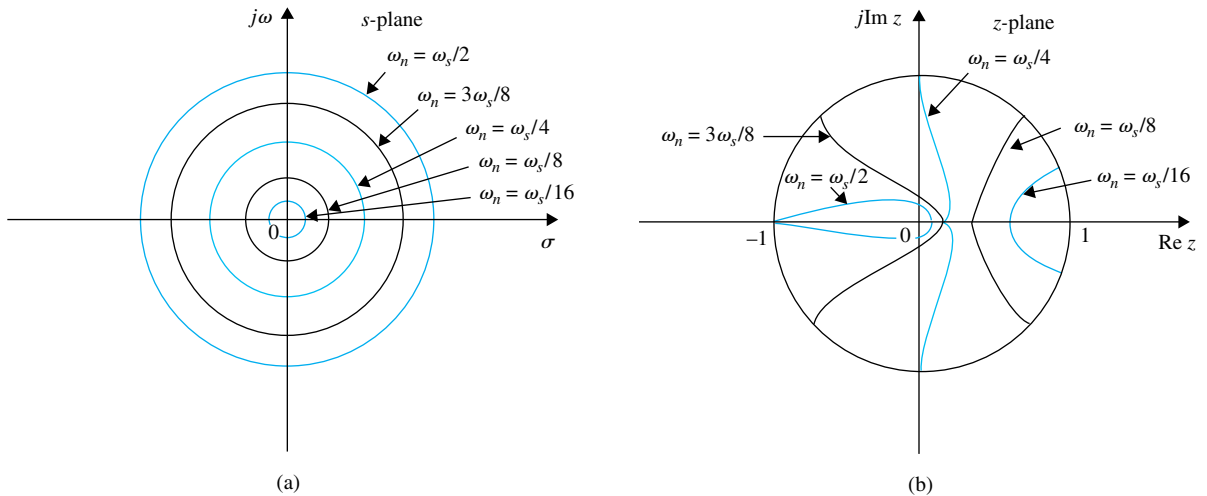
Figure I-25 Constant-natural-undamped frequency loci in the s-plane and the z-plane.
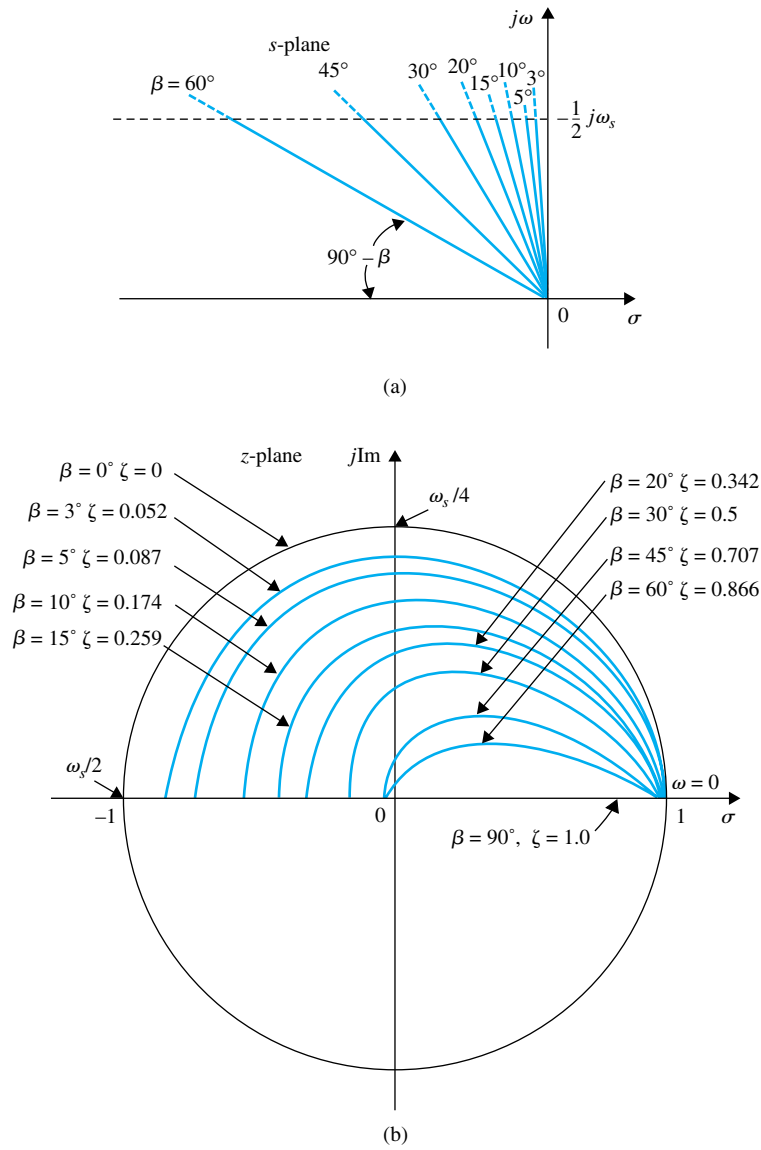
Figure I-26 Constant-damping-ratio loci in the *s*-plane and the *z*-plane.

where

$$\beta = \sin^{-1}\zeta = \text{constant} \tag{I-193}$$

For a given value of β, the constant-ζ locus in the *z*-plane, described by Eq. (I-193), is a logarithmic spiral for $0° < \beta < 90°$. Figure I-26 shows several typical constant-ζ loci in the top half of the *z*-plane.

I-6-3 Relation between Characteristic-Equation Roots and Transient Response

Based on the discussions given in the last section, we can establish the basic relation between the characteristic-equation roots and the transient response of a discrete-data system,
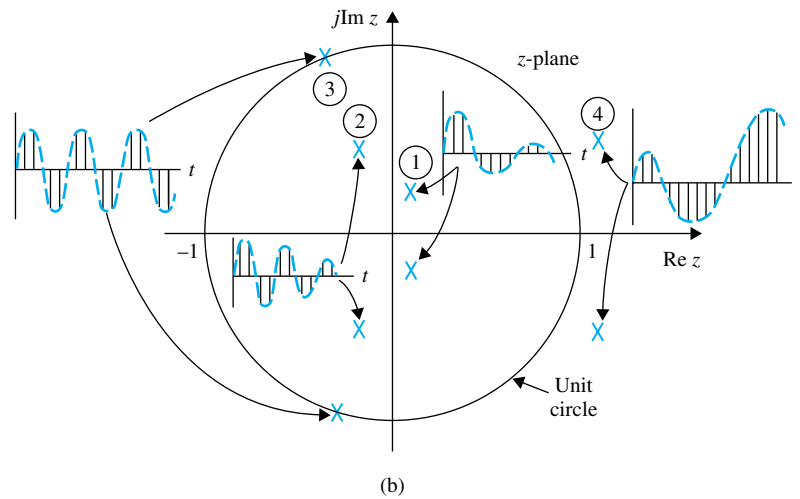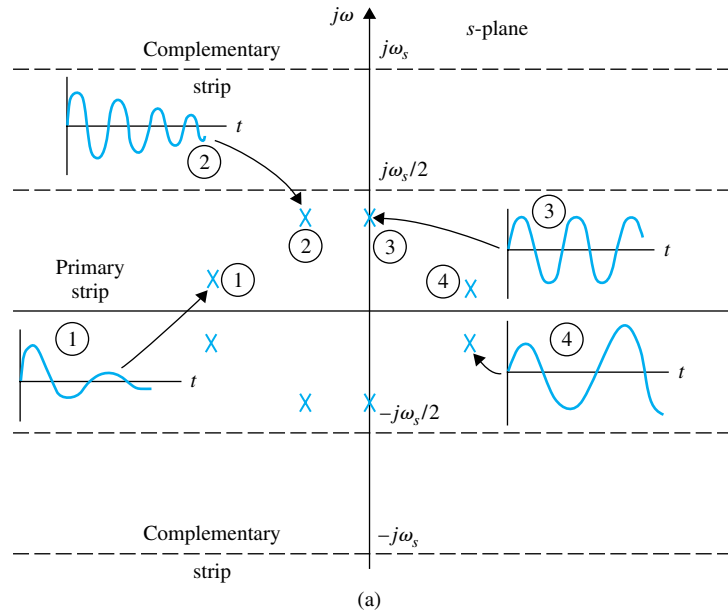
Figure I-27 (a) Transient responses corresponding to various pole locations of $Y^*(s)$ in the s-plane (complex-conjugate poles only). (b) Transient-response sequence corresponding to various pole locations of $Y(z)$ in the z-plane.

keeping in mind that, in general, the zeros of the closed-loop transfer function will also play an important role on the response, but not on the stability, of the system.

Roots on the Positive Real Axis in the z-Plane: Roots on the positive real axis inside the unit circle of the z-plane give rise to responses that decay exponentially with an increase of kT. Typical responses relative to the root locations are shown in Figs. I-27 and I-28. The roots closer to the unit circle will decay slower. When the root is at $z = 1$, the response has a constant amplitude. Roots outside the unit circle correspond to unstable systems, and the responses will increase with kT.

Roots on the Negative Real Axis in the z-Plane: The negative real axis of the z-plane corresponds to the boundaries of the periodic strips in the s-plane. For example, when

(a)

(b)
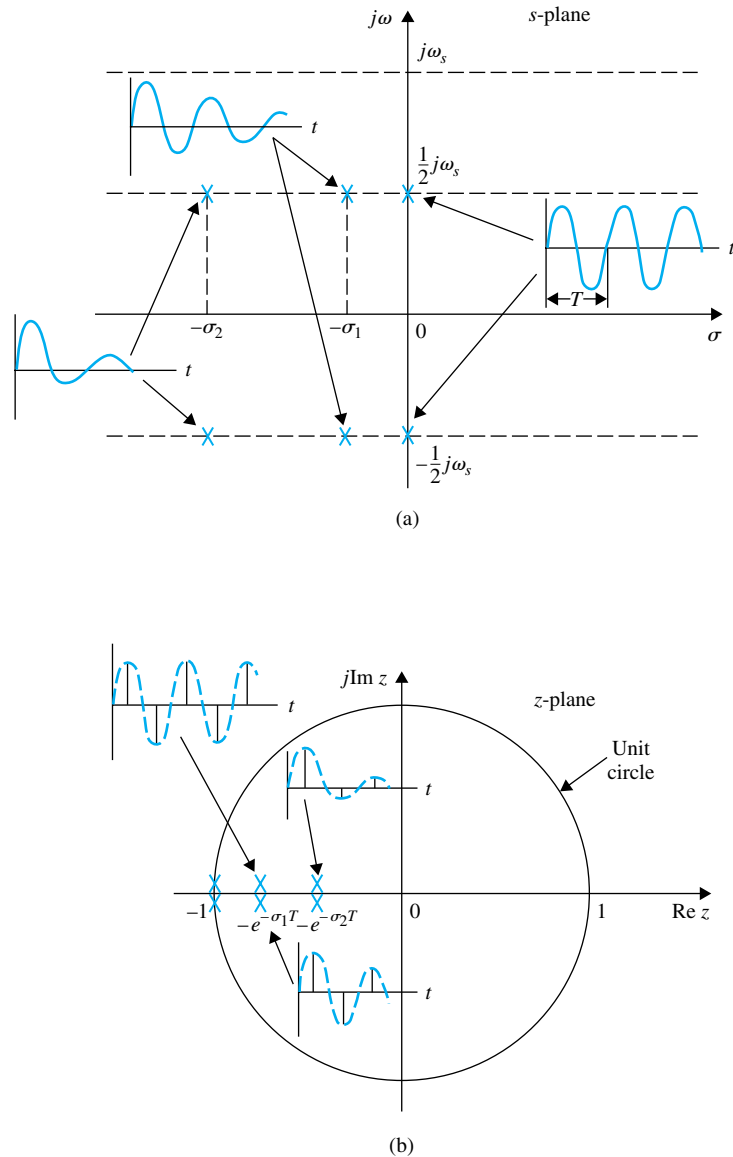
Figure I-28 (a) Transient responses corresponding to various pole locations of $Y^*(s)$ in the s-plane (complex-conjugate poles on the boundaries between periodic strips). (b) Transient-response sequence corresponding to various pole locations of $Y(z)$ in the z-plane.

$s = -\sigma_1 \pm j\omega_s/2$, the complex-conjugate points are on the boundaries of the primary strip in the s-plane. The corresponding z-plane points are

$$z = e^{-\sigma_1 T} e^{\pm j\omega_s T/2} = -e^{-\sigma_1 T} \tag{I-194}$$

which are on the negative real axis of the z-plane. For the frequency of $\omega_s/2$, the output sequence will have exactly one sample in each one-half period of the envelope. Thus, the output sequence will occur in alternating positive and negative pulses, as shown in Fig. I-28(b).

Complex-Conjugate Roots in the z-Plane: Complex-conjugate roots inside the unit circle in the z-plane correspond to oscillatory responses that decay with an increase in kT. Roots that are closer to the unit circle will decay slower. As the roots move toward the second and the third quadrants, the frequency of oscillation of the response increases. Refer to Figs. I-27 and I-28 for typical examples.

▶ I-7 STEADY-STATE ERROR ANALYSIS OF DISCRETE-DATA CONTROL SYSTEMS

Since the input and output signals of a typical discrete-data control system are continuous-time functions, as shown in the block diagram of Fig. I-19, the error signal should still be defined as

$$e(t) = r(t) - y(t) \tag{I-195}$$

where $r(t)$ is the input, $y(t)$ is the output. The error analysis conducted here is only for unity-feedback systems with $H(s) = 1$. Due to the discrete data that appear inside the system, z-transform or difference equations are often used, so that the input and output are represented in sampled form, $r(kT)$ and $y(kT)$, respectively. Thus, the error signal is more appropriately represented by $e^*(t)$ or $e(kT)$. That is,

$$e^*(t) = r^*(t) - y^*(t) \tag{I-196}$$

or

$$e(kT) = r(kT) - y(kT) \tag{I-197}$$

The steady-state error at the sampling instants is defined as

$$e_{ss}^* = \lim_{t \to \infty} e^*(t) = \lim_{k \to \infty} e(kT) \tag{I-198}$$

By using the final-value theorem of the z-transform, the steady-state error is

$$e_{ss}^* = \lim_{k \to \infty} e(kT) = \lim_{z \to 1}(1 - z^{-1})E(z) \tag{I-199}$$

provided that the function $(1 - z^{-1})E(z)$ does not have any pole on or outside the unit circle in the z-plane. It should be pointed out that since the true error of the system is $e(t)$, e_{ss}^* predicts only the steady-state error of the system at the sampling instants.

By expressing $E(z)$ in terms of $R(z)$ and $G_{ho}G_p(z)$, Eq. (I-199) is written

$$e_{ss}^* = \lim_{k \to \infty} e(kT) = \lim_{z \to 1}(1 - z^{-1})\frac{R(z)}{1 + G_{ho}G_p(z)} \tag{I-200}$$

This expression shows that the steady-state error depends on the reference input $R(z)$ as well as the forward-path transfer function $G_{ho}G_p(z)$ Just as in the continuous-data systems, we shall consider only the three basic types of input signals and the associated error constants and relate e_{ss}^* to these and the type of the system.

Let the transfer function of the controlled process in the system of Fig. I-18 be of the form

$$G_p(s) = \frac{K(1 + T_a s)(1 + T_b s)\cdots(1 + T_m s)}{s^j(1 + T_1 s)(1 + T_2 s)\cdots(1 + T_n s)} \tag{I-201}$$

where $j = 0, 1, 2, \ldots$. The transfer function $G_{ho}G_p(z)$ is

$$G_{h0}G_p(z) = (1 - z^{-1})\mathcal{Z}\left[\frac{K(1 + T_a s)(1 + T_b s)\cdots(1 + T_m s)}{s^{j+1}(1 + T_1 s)(1 + T_2 s)\cdots(1 + T_n s)}\right] \tag{I-202}$$

Steady-State Error Due to a Step-Function Input

When the input to the system, $r(t)$, in Fig. I-18 is a step function with magnitude R, the z-transform of $r(t)$ is

$$R(z) = \frac{Rz}{z-1} \tag{I-203}$$

Substituting $R(z)$ into Eq. (I-200), we get

$$e_{ss}^* = \lim_{z\to 1} \frac{R}{1 + G_{ho}G_p(z)} = \frac{R}{1 + \lim_{z\to 1} G_{ho}G_p(z)} \tag{I-204}$$

Let the **step-error constant** be defined as

$$K_p^* = \lim_{z\to 1} G_{ho}G_p(z) \tag{I-205}$$

Equation (I-204) becomes

$$e_{ss}^* = \frac{R}{1 + K_p^*} \tag{I-206}$$

Thus, we see that the steady-state error of the discrete-data control system in Fig. I-18 is related to the step-error constant K_p^* in the same way as in the continuous-data case, except that K_p^* is given by Eq. (I-205).

We can relate K_p^* to the system type as follows.

For a type-0 system, $j = 0$ in Eq. (I-202), and the equation becomes

$$G_{ho}G_p(z) = (1 - z^{-1})\mathcal{Z}\left[\frac{K(1 + T_a s)(1 + T_b s)\cdots(1 + T_m s)}{s(1 + T_1 s)(1 + T_2 s)\cdots(1 + T_n s)}\right] \tag{I-207}$$

Performing partial-fraction expansion to the function inside the square brackets of the last equation, we get

$$G_{ho}G_p(z) = (1 - z^{-1})\mathcal{Z}\left[\frac{K}{s} + \text{terms due to the nonzero poles}\right]$$

$$= (1 - z^{-1})\left[\frac{Kz}{z-1} + \text{terms due to the nonzero poles}\right] \tag{I-208}$$

Since the terms due to the nonzero poles do not contain the term $(z - 1)$ in the denominator, the step-error constant is written

$$K_p^* = \lim_{z\to 1} G_{ho}G_p(z) = \lim_{z\to 1}(1 - z^{-1})\frac{Kz}{z-1} = K \tag{I-209}$$

Similarly, for a type-1 system, $G_{ho}G_p(z)$ will have an s^2 term in the denominator that corresponds to a term $(z - 1)^2$. This causes the step-error constant K_p^* to be infinite. The same is true for any system type greater than 1. The summary of the error constants and the steady-state error due to a step input is as follows:

System Type	K_p^*	e_{ss}^*
0	K	$R/(1 + K)$
1	∞	0
2	∞	0

Steady-State Error Due to a Ramp-Function Input
When the reference input to the system in Fig. I-18 is a ramp function of magnitude R, $r(t) = Rtu_s(t)$. The steady-state error in Eq. (I-200) becomes

$$e_{ss}^* = \lim_{z \to 1} \frac{RT}{(z-1)[1 + G_{ho}G_p(z)]} \tag{I-210}$$

$$= \frac{R}{\lim\limits_{z \to 1} \dfrac{z-1}{T} G_{ho}G_p(z)}$$

Let the **ramp-error constant** be defined as

$$K_v^* = \frac{1}{T} \lim_{z \to 1}[(z-1)G_{ho}G_p(z)] \tag{I-211}$$

Then, Eq. (I-210) becomes

$$e_{ss}^* = \frac{R}{K_v^*} \tag{I-212}$$

The ramp-error constant K_v^* is meaningful only when the input $r(t)$ is a ramp function and if the function $(z-1)G_{ho}G_p(z)$ in Eq. (I-211) does not have any poles on or outside the unit circle $|z| = 1$. The relations between the steady-state error e_{ss}^*, K_v^* and the system type when the input is a ramp function with magnitude R are summarized as follows.

System Type	K_v^*	e_{ss}^*
0	0	∞
1	K	R/K
2	∞	0

Steady-State Error Due to a Parabolic-Function Input
When the input is a parabolic function, $r(t) = Rtu_s(t)/2$; the z-transform of $r(t)$ is

$$R(z) = \frac{RT^2 z(z+1)}{2(z-1)^3} \tag{I-213}$$

From Eq. (I-200), the steady-state error at the sampling instants is

$$e_{ss}^* = \frac{T^2}{2} \lim_{z \to 1} \frac{R(z+1)}{(z-1)^2[1 + G_{ho}G_p(z)]} \tag{I-214}$$

$$= \frac{R}{\dfrac{1}{T^2} \lim\limits_{z \to 1}(z-1)^2 G_{ho}G_p(z)}$$

By defining the **parabolic-error constant** as

$$K_a^* = \frac{1}{T^2} \lim_{z \to 1}[(z-1)^2 G_{ho}G_p(z)] \tag{I-215}$$

the steady-state error due to a parabolic-function input is

$$e_{ss}^* = \frac{R}{K_a^*} \tag{I-216}$$

The relations between the steady-state error e_{ss}^*, K_a^*, and the system type when the input is a parabolic function with its z-transform described by Eq. (I-213) are summarized as follows.

System Type	K_a^*	e_{ss}^*
0	0	∞
1	0	∞
2	K	R/K
3	∞	0

▶ I-8 ROOT LOCI OF DISCRETE-DATA SYSTEMS

The root-locus technique can be can be applied to discrete-data systems without any complications. With the z-transformed transfer function, the root loci for discrete-data systems are plotted in the z-plane, rather than in the s-plane. Let us consider the discrete-data control system shown in Fig. I-29. The characteristic equation roots of the system satisfy the following equation:

$$1 + GH^*(s) = 0 \tag{I-217}$$

in the s-plane, or

$$1 + GH(z) = 0 \tag{I-218}$$

in the z-plane. From Eq (I-64) $GH^*(s)$ is written

$$GH^*(s) = \frac{1}{T} \sum_{n=-\infty}^{\infty} G(s + jn\omega_s)H(s + jn\omega_s) \tag{I-219}$$

which is an infinite series. Thus, the poles and zeros of $GH^*(s)$ in the s-plane will be infinite in number. This evidently makes the construction of the root loci of Eq. (I-217) in the s-plane quite complex. As an illustration, consider that for the system of Fig. I-29,

$$G(s)H(s) = \frac{K}{s(s + 1)} \tag{I-220}$$

Substituting Eq. (I-220) into Eq. (I-219), we get

$$GH^*(s) = \frac{1}{T} \sum_{n=-\infty}^{\infty} \frac{K}{(s + jn\omega_s)(s + jn\omega_s + 1)} \tag{I-221}$$

which has poles at $s = -jn\omega_s$ and $s = -1 -jn\omega_s$, where n takes on all integers between $-\infty$ and ∞. The pole configuration of $GH^*(s)$ is shown in Fig. I-30(a). By using the properties of the RL in the s-plane, RL of $1 + GH^*(s) = 0$ are drawn as shown in Fig. I-30(b) for the sampling period $T = 1$ s. The RL contain an infinite number of branches, and these
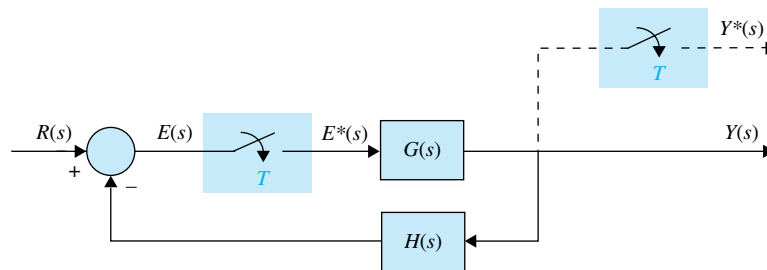
Figure I-29 Discrete-data control system.

(a)

(b)
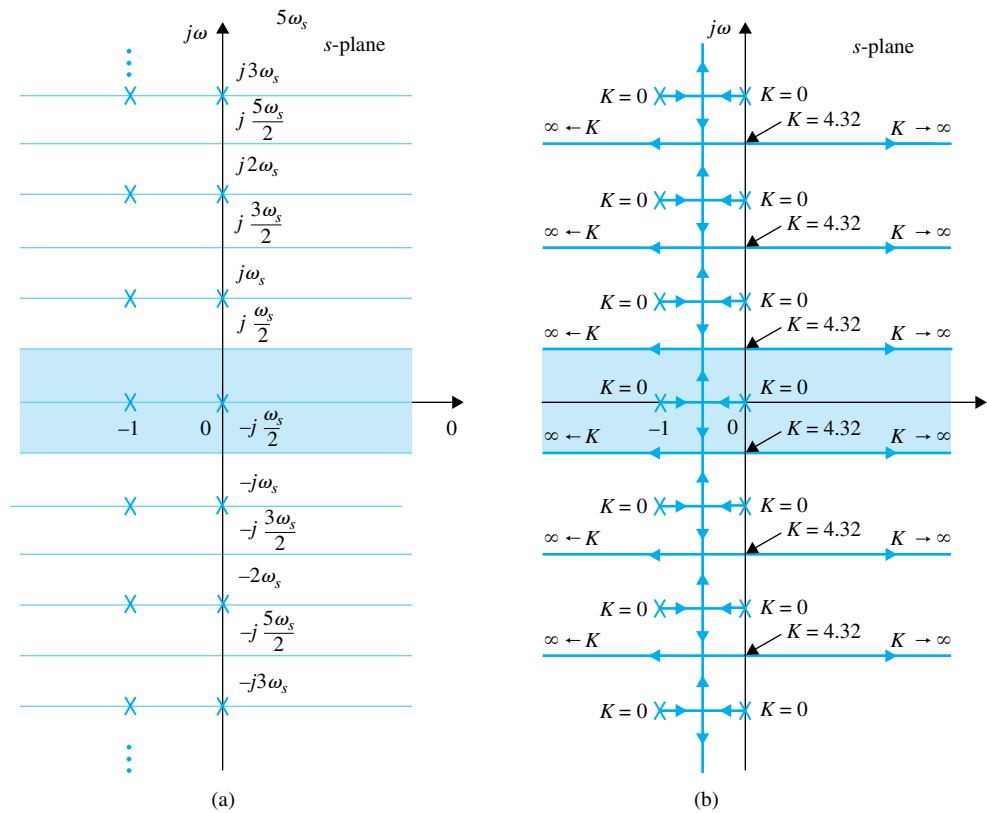
Figure I-30 Pole configuration of $GH^*(s)$ and the root-locus diagram in the s-plane for the discrete-data system in Fig. I-29 with $G(s)H(s) = \dfrac{K}{s(s+1)}$, $T = 1$ sec.

clearly indicate that the closed-loop system is unstable for all values of K greater than 4.32. In contrast, it is well known that the same system without sampling is stable for all positive values of K.

• The same procedures of construction of root loci of continuous-data systems can be applied to root loci of discrete-data systems in the z-plane.

The root-locus problem for discrete-data systems is simplified if the root loci are constructed in the z-plane using Eq. (I-218). Since Eq. (I-218) is, in general, a rational function in z with constant coefficients, its poles and zeros are finite in number, and the number of root loci is finite in the z-plane. The same procedures of construction for continuous-data systems are directly applicable in the z-plane for discrete-data systems. The following examples illustrate the constructions of root loci for discrete-data systems in the z-plane.

▶ **EXAMPLE I-23** Consider that for the discrete-data system shown in Fig. I-29 the loop transfer function in the z domain is

$$GH(z) = \frac{0.632Kz}{(z-1)(z-0.368)} \tag{I-222}$$

The RL of the closed-loop characteristic equation are constructed based on the pole-zero configuration of $GH(z)$, as shown in Fig. I-31. Notice that when the value of K exceeds 4.32, one of the two roots moves outside the unit circle, and the system becomes unstable. The constant-damping-ratio locus may be superimposed on the RL to determine the required value of K for a specified damping ratio. In Fig. I-31, the constant-damping-ratio locus for $\zeta = 0.5$ is drawn, and the intersection with the RL gives the desired value of $K = 1$. For the same system, if the sampling period T is increased
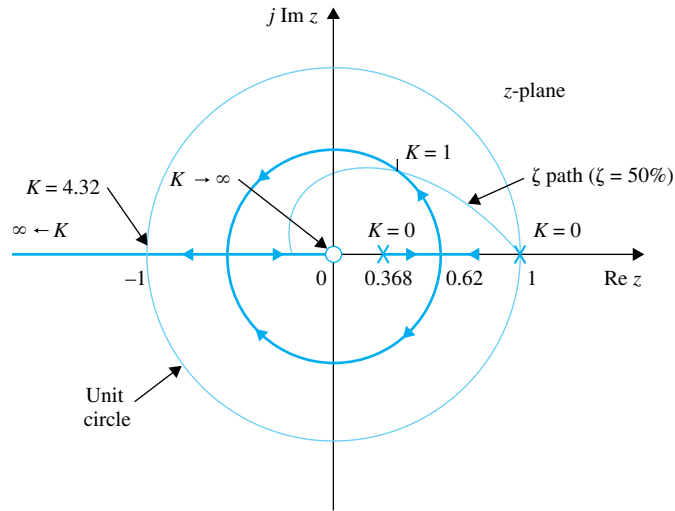
Figure I-31 Root-locus diagram of a discrete-data control system without zero-order-hold.

$$G(s)H(s) = \frac{K}{s(s + 1)},$$

$T = 1$ second.

to 2 seconds, the z-transform loop transfer function becomes

$$GH(z) = \frac{0.865Kz}{(z - 1)(z - 0.135)} \tag{I-223}$$

The RL for this case are shown in Fig. I-32. Note that although the complex part of the RL for $T = 2$ seconds takes the form of a smaller circle than that when $T = 1$ second, the system is actually less stable, since the marginal value of K for stability is 2.624, as compared with the marginal K of 4.32 for $T =$ second.

Next, let us consider that a zero-order-hold is inserted between the sampler and the controlled process $G(s)$ in the system of Fig. I-29. The loop transfer function of the system with the zero-order-hold is

$$G_{ho}GH(z) = \frac{K[(T - 1 + e^{-T})z - Te^{-T} + 1 - e^{-T}]}{(z - 1)(z - e^{-T})} \tag{I-224}$$
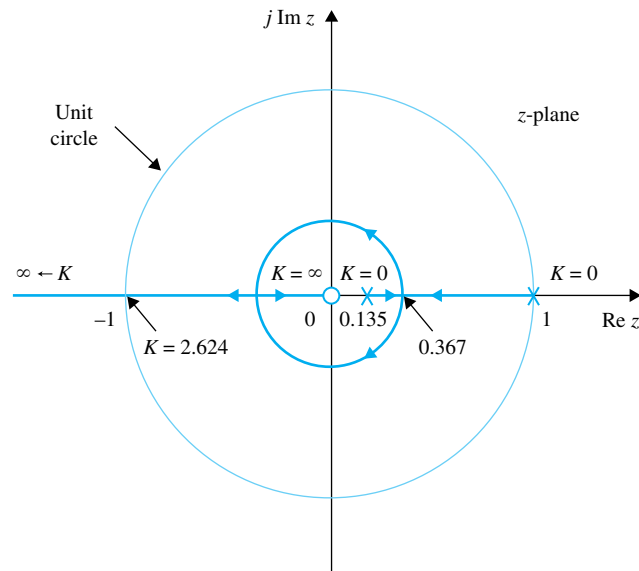
Figure I-32 Root-locus diagram of a discrete-data control system without zero-order-hold.

$$G(s)H(s) = \frac{K}{s(s+1)},$$

$T = 2$ seconds.
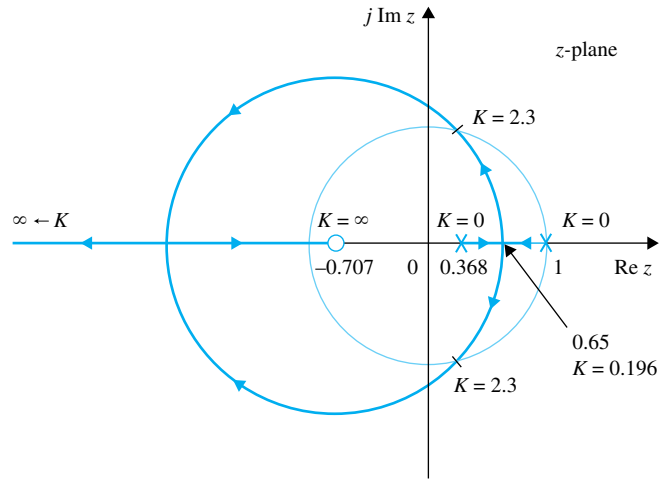
(a) Root loci for $T = 1$ second

Figure I-33 Root-locus diagram of a discrete-data control system with zero-order-hold.
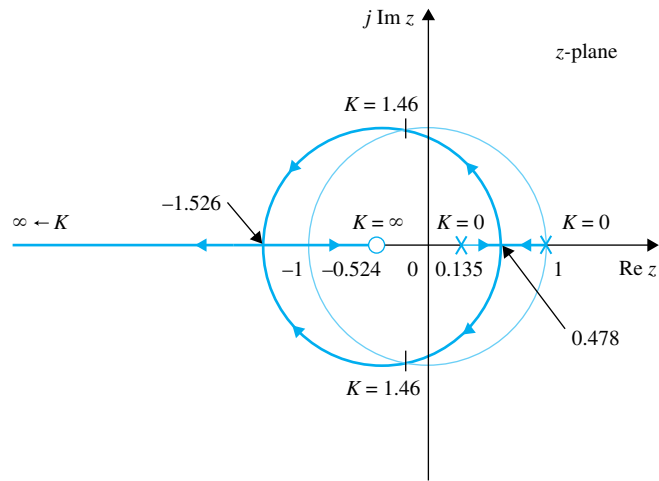
$$G(s)H(s) = \frac{K}{s(s + 1)}.$$

(b) Root loci for $T = 2$ seconds

The RL of the system with ZOH for $T = 1$ and 2 seconds are shown in Fig. I-33(a) and I-33(b), respectively. In this case, the marginal value of stability for K is 2.3 for $T = 1$ second and 1.46 for $T = 2$ seconds. Comparing the root loci of the system with and without the ZOH, we see that the ZOH reduces the stability margin of the discrete-data system.

In conclusion, the root loci of discrete-data systems can be constructed in the z-plane using essentially the same properties as those of the continuous-data systems in the s-plane. However, the absolute and relative stability conditions of the discrete-data system must be investigated with respect to the unit circle and the other interpretation of performance with respect to the regions in the z-plane. ◀

▶ I-9 FREQUENCY-DOMAIN ANALYSIS OF DISCRETE-DATA CONTROL SYSTEMS

All the frequency-domain methods discussed in the preceding sections can be extended to the analysis of discrete-data systems. Consider the discrete-data system shown
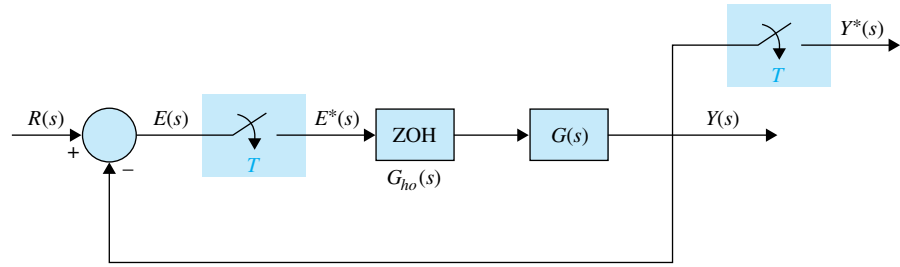
Figure I-34 Closed-loop discrete-data control system.

in Fig. I-34. The closed-loop transfer function of the system is

$$\frac{Y(z)}{R(z)} = \frac{G_{ho}G(z)}{1 + G_{ho}G(z)} \tag{I-225}$$

where $G_{ho}G(z)$ is the z-transform of $G_{ho}(s)G(s)$. Just as in the case of continuous-data systems, the absolute and relative stability conditions of the closed-loop discrete-data system can be investigated by making the frequency-domain plots of $G_{ho}G(z)$. Since the positive $j\omega$-axis of the s-plane corresponds to real frequency, the frequency-domain plots of $G_{ho}G(z)$ are obtained by setting $z = e^{j\omega T}$ and then letting ω vary from 0 to ∞. This is also equivalent to mapping the points on the unit circle, $|z| = 1$, in the z-plane onto the $G_{ho}G(e^{j\omega T})$-plane. Since the unit circle repeats for every sampling frequency $\omega_s(= 2\pi/T)$, as shown in Fig. I-35, when ω is varied along the $j\omega$-axis, the frequency-domain plot of $G(e^{j\omega T})$ repeats for $\omega = n\omega_s$ to $(n + 1)\omega_s$, $n = 0, 1, 2, \ldots$. Thus, it is necessary to plot $G_{ho}G(e^{j\omega T})$ only for the range of $\omega = 0$ to $\omega = \omega_s$. In fact, since the unit circle in the z-plane is symmetrical about the real axis, the plot of $G_{ho}G(e^{j\omega T})$ in the polar coordinates for $\omega = 0$ to $\omega_s/2$ needs to be plotted.

I-9-1 Bode Plot with the *w*-Transformation

The w-transformation introduced in Eq. (I-162) can be used for frequency-domain analysis and design of discrete-data control systems. The transformation is

$$z = \frac{(2/T) + w}{(2/T) - w} \tag{I-226}$$
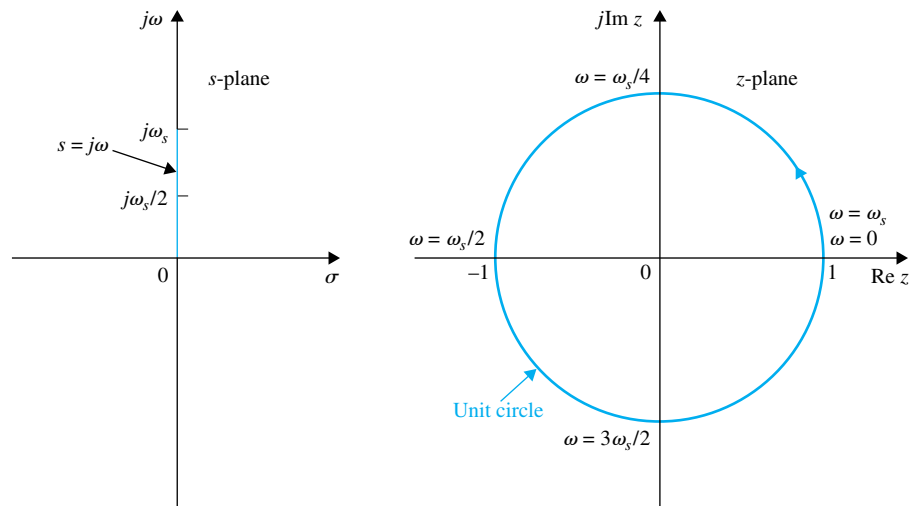
Figure I-35 Relation between the $j\omega$-axis in the s-plane and the unit circle in the z-plane.

In the frequency domain, we set [Eq. (I-166)],

$$w = j\omega_w = j\frac{2}{T}\tan\frac{\omega T}{2} \tag{I-227}$$

For frequency-domain analysis of a discrete-data system, we substitute Eqs. (I-226) and (I-227) in $G(z)$ to get $G(j\omega_w)$; the latter can be used to form the Bode plot or the polar plot of the system.

▶ **EXAMPLE I-24** As an illustrative example on frequency-domain plots of discrete-data control systems, let the transfer function of the process in the system in Fig. I-34 be

$$G(s) = \frac{1.57}{s(s+1)} \tag{I-228}$$

and the sampling frequency is 4 rad/sec. Let us first consider that the system does not have a zero-order-hold, so that

$$G_{ho}G(z) = G(z) = \frac{1.243z}{(z-1)(z-0.208)} \tag{I-229}$$
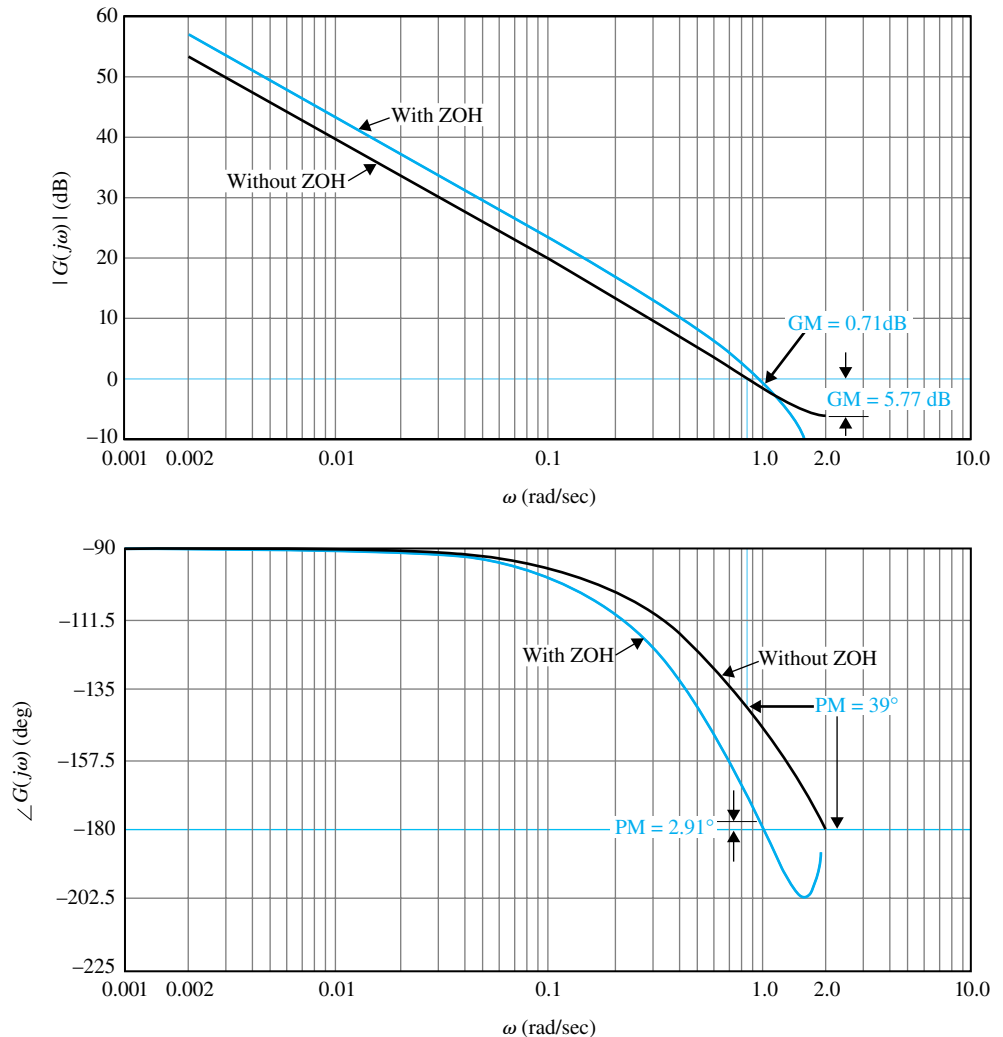
Figure I-36 Bode plot of $G_{ho}G(z)$ of the system in Fig. I-34, with $G(s) = 1.57/[s(s+1)]$. $T = 1.57$ sec, and with and without ZOH.

The frequency response of $G_{ho}G(z)$ is obtained by substituting $z = e^{j\omega T}$ in Eq. (I-228). The polar plot of $G_{ho}G(e^{j\omega T})$ for $\omega = 0$ to $\omega_s/2$ is shown in Fig. I-36. The mirror image of the locus shown, with the mirror placed on the real axis, represents the plot for $\omega = \omega_s/2$ to ω_s.

The Bode plot of $G_{ho}G(e^{j\omega T})$ consists of the graphs of $|G_{ho}G(e^{j\omega T})|$ in dB versus ω, and $\angle G_{ho}G(e^{j\omega T})$ in degrees versus ω, as shown in Fig. I-37 for three decades of frequency with the plots ended at $\omega = \omega_s/2 = 2$ rad/sec.

For the sake of comparison, the forward-path transfer function of the system with a zero-order-hold is obtained:

$$G_{ho}G(z) = \frac{1.2215z + 0.7306}{(z - 1)(z - 0.208)} \tag{I-230}$$

The polar plot and the Bode plot of the last equation are shown in Figs. I-36 and I-37, respectively. Notice that the polar plot of the system with the ZOH intersects the negative real axis at a point that is closer to the $(-1, j0)$ point than that of the system without the ZOH. Thus, the system with the ZOH is less stable. Similarly, the phase of the Bode plot of the system with the ZOH is more negative than that of the system without the ZOH. The gain margin, phase margin, and peak resonance of the two systems are summarized as follows.

	Gain Margin (dB)	Phase Margin (deg)	M_r
Without ZOH	5.77	39.0	1.58
With ZOH	0.71	2.91	22.64

As an alternative, the Bode plot and polar plot of the forward-path transfer function can be done using the w-transformation of Eqs. (I-226). For the system with ZOH, the forward-path transfer
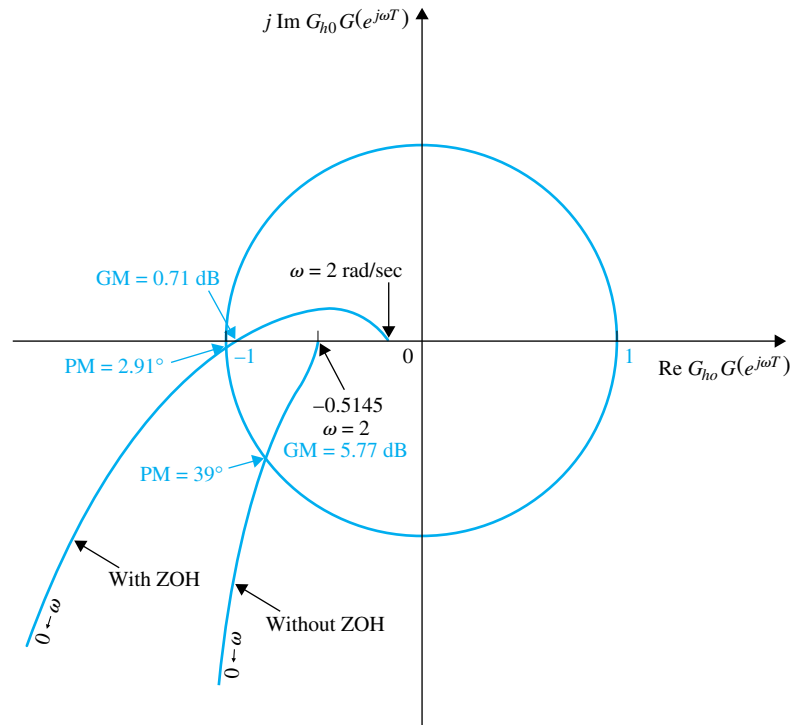
Figure I-37 Frequency-domain plot of $G(s) = \dfrac{1.57}{s(s + 1)}$, $T = 1.57$ seconds, and with and without ZOH.

function in the *w*-domain is

$$G_{ho}G(w) = \frac{1.57(1 + 0.504w)(1 - 1.0913w)}{w(1 + 1.197w)} \tag{I-231}$$
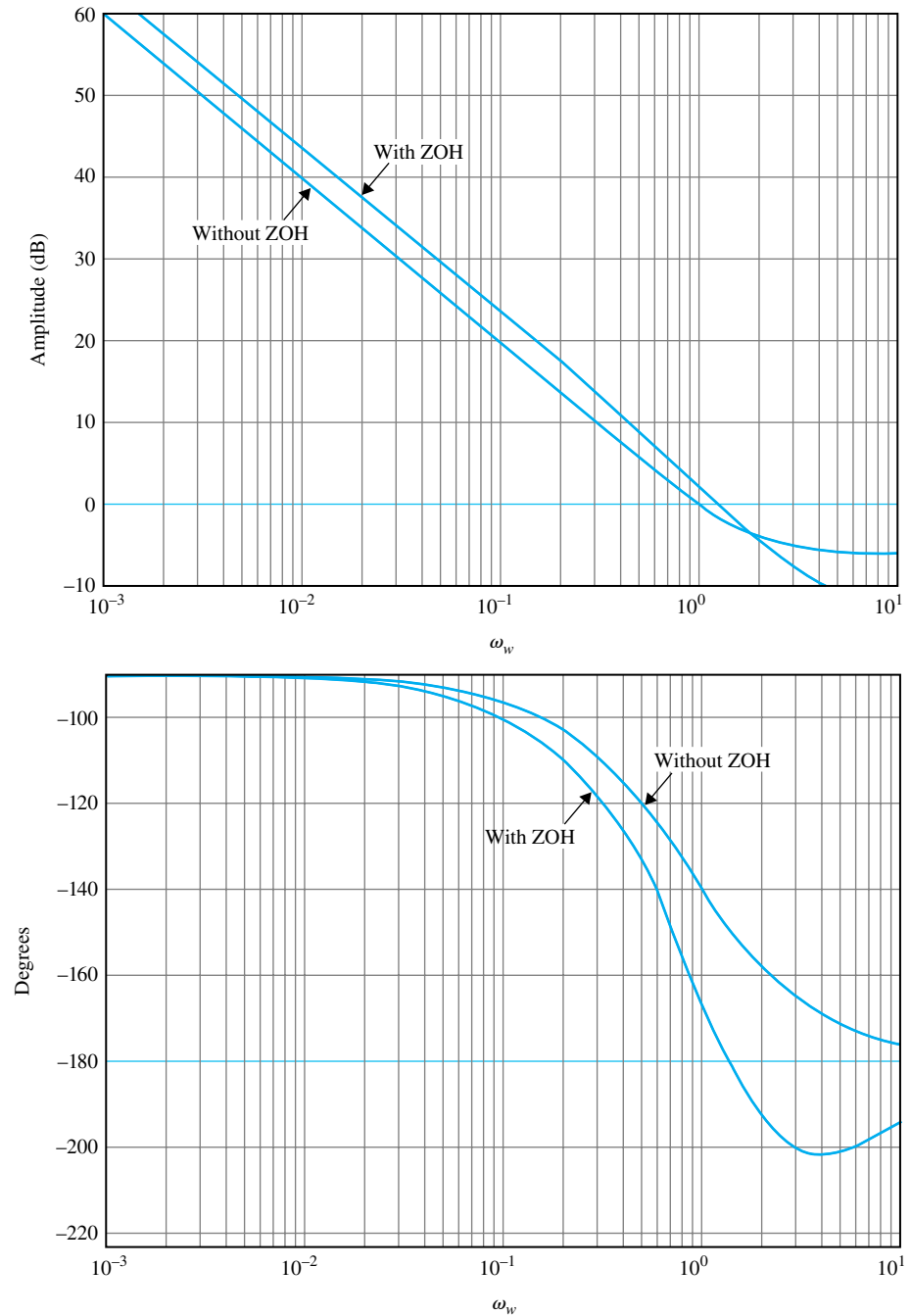
Figure I-38 Bode plot of $G_{ho}G(z)$ of the system in Fig. I-34 with $G(s) = \dfrac{1.57}{s(s + 1)}$, $T = 1.57$ seconds with and without ZOH. The plots are done with the *w*-transformation, $w = j\omega_w$.

For the system without ZOH,

$$G_{ho}G(jw) = \frac{1 - 0.6163w^2}{w(1 + 1.978w)} \tag{I-232}$$

Substituting $w = j\omega_w$ into Eq. (I-232), the Bode plots are made as shown in Fig. (I-38). Notice that the frequency coordinates in Fig. I-38 are ω_w, whereas those in Fig. I-36 are the real frequency ω. The two frequencies are related through Eq. (I-227).

The conclusion from this illustrative example is that once z is replaced by $e^{j\omega T}$ in the z-domain transfer function, or if the w-transform is used, all the frequency-domain analysis techniques available for continuous-data systems can be applied to discrete-data systems. ◄

► I-10 DESIGN OF DISCRETE-DATA CONTROL SYSTEMS

I-10-1 Introduction

The design of discrete-data control systems is similar in principle to the design of continuous-data control systems. The design objective is basically that of determining the controller so that the system will perform in accordance with specifications. In fact, in most situations, the controlled process is the same, except in discrete-data systems the controller is designed to process sampled or digital data.

The design of discrete-data control systems treated in this chapter is intended only for introductory purposes. An in-depth coverage of the subject may be found in books dedicated to digital control. In this chapter we deal only with the design of a control system with a cascade digital controller and a system with digital state feedback. Block diagrams of these systems are shown in Fig. I-39.

Just as with the design of continuous-data control systems, the design of discrete-data control systems can be carried out in either the frequency domain or the time domain. Using computer programs, digital control systems can be designed with a minimum amount of trial and error.
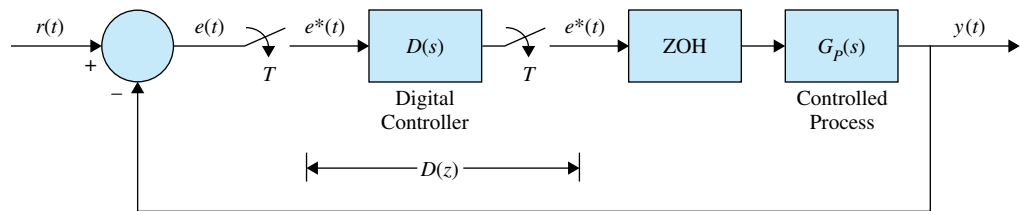
(a)
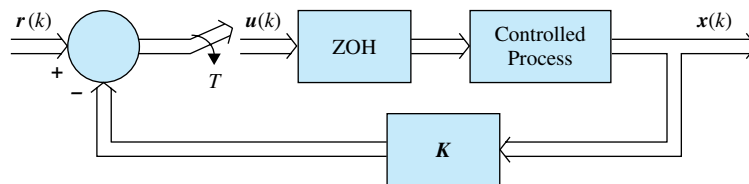
(b)

Figure I-39 (a) Digital control system with cascade digital controller. (b) Digital control system with state feedback.

I-10-2 Digital Implementation of Analog Controllers

It seems that most people learn how to design continuous-data systems before they learn to design digital systems, if at all. Therefore, it is not surprising that most engineers prefer to design continuous-data systems. Ideally, if the designer intends to use digital control, the system should be designed so that the dynamics of the controller can be described by a z-transfer function or difference equations. However, there are situations in which the analog controller is already designed, but the availability and advantages of digital control suggest that the controller be implemented by digital elements. Thus, the problems discussed in this section are twofold: first how continuous-data controllers such as PID, phase-lead or phase-lag controllers, and others can be approximated by digital controllers; and second, the problem of implementing digital controllers by digital processors.

I-10-3 Digital Implementation of the PID Controller

The PID controller in the continuous-data domain is described by

$$G_c(s) = K_P + K_D s + \frac{K_I}{s} \tag{I-233}$$

The proportional component K_P is implemented digitally by a constant gain K_P. Since a digital computer or processor has finite word length, the constant K_P cannot be realized with infinite resolution.

The time derivative of a function $f(t)$ at $t = kT$ can be approximated by the **backward-difference rule**, using the values of $f(t)$ measured at $t = kT$ and $(k - 1)T$, that is,

$$\frac{df(t)}{dt}\bigg|_{t=kT} = \frac{1}{T}(f(kT) - f[(k - 1)T]) \tag{I-234}$$

To find the z-transfer function of the derivative operation described before, we take the z-transform on both sides of Eq. (I-234). We have

$$\mathcal{Z}\left(\frac{df(t)}{dt}\bigg|_{t=kT}\right) = \frac{1}{T}(1 - z^{-1})F(z) = \frac{z - 1}{Tz}F(z) \tag{I-235}$$

Thus, the z-transfer function of the digital differentiator is

$$G_D(z) = K_D \frac{z - 1}{Tz} \tag{I-236}$$

where K_D is the proportional constant of the derivative controller. Replacing z by e^{Ts} in Eq. (I-236), we can show that as the sampling period T approaches zero, $G_D(z)$ approaches $K_D s$, which is the transfer function of the analog derivative controller. In general, the choice of the sampling period is extremely important. The value of T should be sufficiently small so that the digital approximation is adequately accurate.

There are a number of numerical integration rules that can be used to digitally approximate the integral controller K_I/s. The three basic methods of approximating the area of a function numerically are **trapezoidal integration**, **forward-rectangular integration**, and **backward-rectangular integration**. These are described as follows.

Trapezoidal Integration
The trapezoidal-integration rule approximates the area under the function $f(t)$ by a series of trapezoids, as shown in Fig. I-40. Let the integral of $f(t)$ evaluated at $t = kT$ be
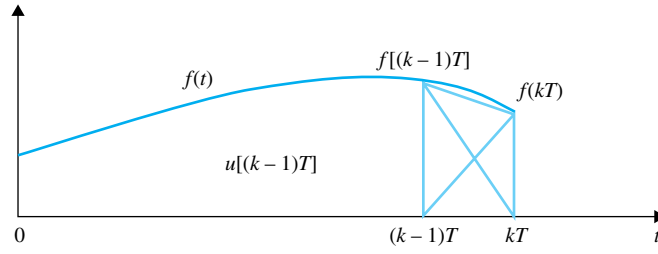
Figure I-40 Trapezoidal-integration rule.

designated as $u(kT)$. Then,

$$u(kT) = u[(k-1)T] + \frac{T}{2}\{f(kT) - f[(k-1)T]\} \tag{I-237}$$

where the area under $f(t)$ for $(k-1)T \le t < kT$ is approximated by the area of the trapezoid in the interval. Taking the z-transform on both sides of Eq. (I-237), we have the transfer function of the digital integrator as

$$G_I(z) = K_I \frac{U(z)}{F(z)} = \frac{K_I T(z+1)}{2(z-1)} \tag{I-238}$$

where K_I is the proportional constant.

Forward-Rectangular Integration

For the forward-rectangular integration, we approximate the area under $f(t)$ by rectangles, as shown in Fig. I-41. the integral of $f(t)$ at $t = kT$ is approximated by

$$u(kT) = u[(k-1)T] + Tf(kT) \tag{I-239}$$

By taking the z-transform on both sides of Eq. (I-141), the transfer function of the digital integrator using the forward-rectangular rule is

$$G_I(z) = K_I \frac{U(z)}{F(z)} = \frac{K_I Tz}{z-1} \tag{I-240}$$

Backward-Rectangular Integration

For the backward-rectangular integration, the digital approximation rule is illustrated in Fig. I-42. The integral of $f(t)$ at $t = kT$ is approximated by

$$u(kT) = u[(k-1)T] + Tf[(k-1)T] \tag{I-241}$$

The z-transfer function of the digital integrator using the backward-rectangular integration rule is

$$G_I(z) = K_I \frac{U(z)}{F(z)} = \frac{K_I T}{z-1} \tag{I-242}$$
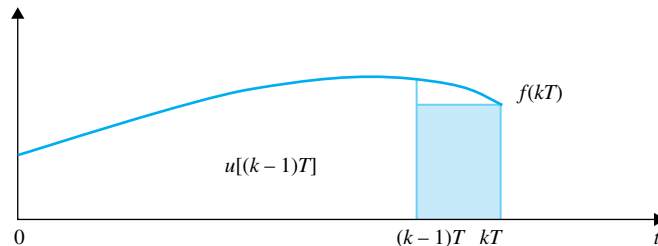
Figure I-41 Forward-rectangular integration rule.
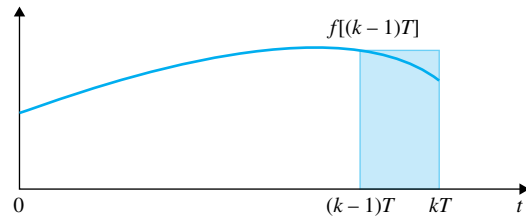
Figure I-42 Backward-rectangular integration rule.

By combining the proportional, derivative, and integration operations described before, the digital PID controller is modeled by the following transfer functions.

Trapezoidal Integration

$$G_c(z) = \frac{\left(K_P + \dfrac{TK_I}{2} + \dfrac{K_D}{T}\right)z^2 + \left(\dfrac{TK_I}{2} - K_P - \dfrac{2K_D}{T}\right)z + \dfrac{K_D}{T}}{z(z - 1)} \qquad \text{(I-243)}$$

Forward-Rectangular Integration

$$G_c(z) = \frac{\left(K_P + \dfrac{K_D}{T} + TK_I\right)z^2 - \left(K_P + \dfrac{2K_D}{T}\right)z + \dfrac{K_D}{T}}{z(z - 1)} \qquad \text{(I-244)}$$

Backward-Rectangular Integration

$$G_c(z) = \frac{\left(K_P + \dfrac{K_D}{T}\right)z^2 + \left(TK_I - K_P - \dfrac{2K_D}{T}\right)z + \dfrac{K_D}{T}}{z(z - 1)} \qquad \text{(I-245)}$$

When $K_I = 0$, the transfer function of the digital PD controller is

$$G_c(z) = \frac{\left(K_P + \dfrac{K_D}{T}\right)z - \dfrac{K_D}{T}}{z} \qquad \text{(I-246)}$$
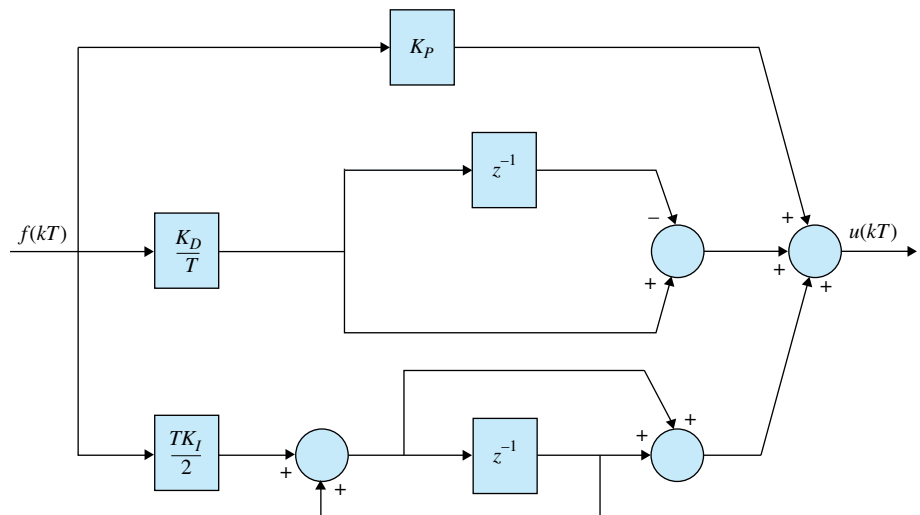
Figure I-43 Block diagram of a digital-program implementation of the PID controller.

Figure I-44 Realization of a digital controller by an analog controller with sample-and-hold units.
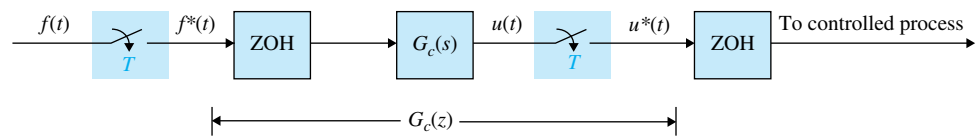
Once the transfer function of a digital controller is determined, the controller can be implemented by a digital processor or computer. The operator z^{-1} is interpreted as a time delay of T seconds. In practice, the time delay is implemented by storing a variable in some storage location in the computer and then taking it out after T seconds have elapsed. Figure I-43 illustrates a block diagram representation of the digital program of the PID controller using the trapezoidal-integration rule.

I-10-4 Digital Implementation of Lead and Lag Controllers

In principle, any continuous-data controller can be made into a digital controller simply by adding sample-and-hold units at the input and the output terminals of the controller and selecting a sampling frequency as small as is practical. Figure I-44 illustrates the basic scheme with $G_c(s)$, the transfer function of the continuous-data controller, and $G_c(z)$, the equivalent digital controller. The sampling period T should be sufficiently small so that the dynamic characteristics of the continuous-data controller are not lost through the digitization. The system configuration in Fig. I-44 actually suggests that given the continuous-data controller $G_c(s)$, the equivalent digital controller $G_c(z)$ can be obtained by the arrangement shown. On the other hand, given the digital controller $G_c(z)$, we can realize it by using an analog controller $G_c(s)$ and sample-and-hold units, as shown in Fig. I-44.

▶ **EXAMPLE I-25** As an illustrative example, consider that the continuous-data controller in Fig. I-44 is represented by the transfer function

$$G_c(s) = \frac{s + 1}{s + 1.61} \tag{I-247}$$

From Fig. I-44, the transfer function of the digital controller is written

$$G_c(z) = \frac{U(z)}{F(z)} = (1 - z^{-1})\mathcal{Z}\left[\frac{s + 1}{s(s + 1.61)}\right] \tag{I-248}$$

$$= \frac{z - (0.62e^{-1.61T} + 0.38)}{z - e^{-1.61T}}$$

The digital-program implementation of Eq. (I-248) is shown in Fig. I-45.
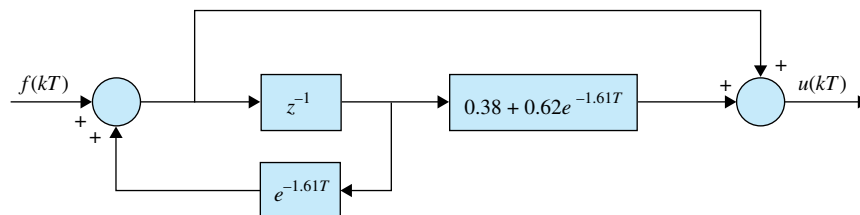
Figure I-45 Digital-program realization of Eq. (I-248). ◀

▶ I-11 DIGITAL CONTROLLERS

• One advantage of the digital controller is that its program can be easily altered.

Digital controllers can be realized by digital networks, digital computers, microprocessors, or digital signal processors (DSPs). A distinct advantage of digital controllers implemented by microprocessors or DSPs is that the control algorithm contained in the controller can be easily altered by changing the program. Changing the components of a continuous-data controller is rather difficult once the controller has been built.

I-11-1   Physical Realizability of Digital Controllers

The transfer function of a digital controller can be expressed as

$$G_c(z) = \frac{E_2(z)}{E_1(z)} = \frac{b_0 + b_1 z^{-1} + \cdots + b_m z^{-m}}{a_0 + a_1 z^{-1} + \cdots + a_n z^{-n}} \tag{I-249}$$

where n and m are positive integers. The transfer function $G_c(z)$ is said to be physically realizable if its output does not precede any input. This means that the series expansion of $G_c(z)$ should not have any positive powers in z. In terms of the $G_c(z)$ given in Eq. (I-249), if $b_0 \neq 0$, then $a_0 \neq 0$. If $G_c(z)$ is expressed as

$$G_c(z) = \frac{b_m z^m + b_{m-1} z^{m-1} + \cdots + b_1 z + b_0}{a_n z^n + a_{n-1} z^{n-1} + \cdots + a_1 z + a_0} \tag{I-250}$$

then the physical realizability requirement is $n \geq m$.

The decomposition techniques presented in Chapter 5 can be applied to realize the digital controller transfer function by a digital program. We consider that a digital program is capable of performing arithmetic operations of addition, subtraction, multiplication by a constant, and shifting. The three basic methods of decomposition for digital programming are discussed in the following sections.

Digital Program by Direct Decomposition

Applying direct decomposition to Eq. (I-249), we have the following equations:

$$E_2(z) = \frac{1}{a_0}(b_0 + b_1 z^{-1} + \cdots + b_m z^{-m})X(z) \tag{I-251}$$

$$X(z) = \frac{1}{a_0}E_1(z) - \frac{1}{a_0}(a_1 z^{-1} + a_2 z^{-2} + \cdots + a_n z^{-n})X(z) \tag{I-252}$$

Figure I-46 shows the signal flow graph of a direct digital program of Eq. (I-249) by direct decomposition for $m = 2$ and $n = 3$. The branches with gains of z^{-1} represent time delays or shifts of one sampling period.
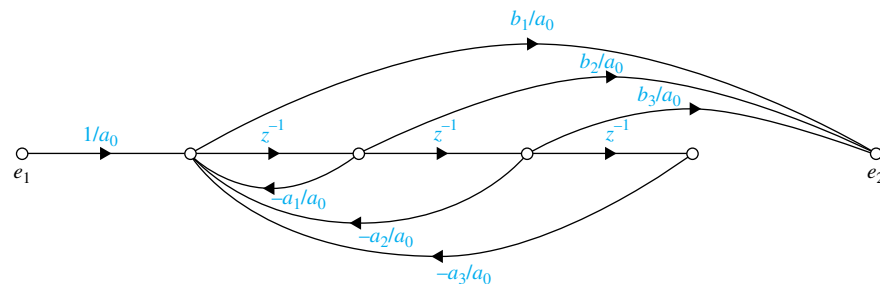
Figure I-46 Signal-flow graph of digital program by direct decomposition of Eq. (I-249) with $n = 3$ and $m = 2$.

Digital Program by Cascade Decomposition

The transfer function $G_c(z)$ can be written as a product of first- or second-order transfer functions, each realizable by a simple digital program. The digital program of the overall transfer function is then represented by these simple digital programs connected in cascade. Equation (I-249) is written in factored form as

$$G_c(z) = G_{c1}(z)G_{c2}(z) \cdots G_{cn}(z) \tag{I-253}$$

where the individual factors can be expressed as

Real Pole and Zero

$$G_{ci}(z) = K_i \frac{1 + c_i z^{-1}}{1 + d_i z^{-1}} \tag{I-254}$$

Complex Conjugate Poles (No Zeros)

$$G_{ci}(z) = \frac{K_i}{1 + d_{i1} z^{-1} + d_{i2} z^{-2}} \tag{I-255}$$

Complex Conjugate Poles with One Zero

$$G_{ci}(z) = K_i \frac{1 + c_i z^{-1}}{1 + d_{i1} z^{-1} + d_{i2} z^{-2}} \tag{I-256}$$

and several other possible forms up to the second order.

Digital Program by Parallel Decomposition

The transfer function in Eq. (I-249) can be expanded into a sum of simple first- or second-order terms by partial-fraction expansion. These terms are then realized by digital programs connected in parallel.

▶ **EXAMPLE I-26** Consider the following transfer function of a digital controller.

$$G_c(z) = \frac{E_2(z)}{E_1(z)} = \frac{10(1 + 0.5z^{-1})}{(1 - z^{-1})(1 - 0.2z^{-1})} \tag{I-257}$$

Since the leading coefficients of the numerator and denominator polynomials in z^{-1} are all constants, the transfer function is physically realizable. The transfer function $G_c(z)$ is realized by the three types of digital programs discussed earlier.

Direct Digital Programming

Equation (I-257) is written

$$G_c(z) = \frac{E_2(z)}{E_1(z)} = \frac{10(1 + 0.5z^{-1})X(z)}{(1 - z^{-1})(1 - 0.2z^{-1})X(z)} \tag{I-258}$$

Expanding the numerator and denominator of the last equation and equating, we have

$$E_2(z) = (10 + 5z^{-1})X(z) \tag{I-259}$$
$$X(z) = E_1(z) + 1.2z^{-1}X(z) - 0.2z^{-2}X(z) \tag{I-260}$$

The last two equations are realized by the digital program shown in Fig. I-47.

Cascade Digital Programming

The right-hand side of Eq. (I-257) is divided into two factors in one of several possible ways.

$$G_c(z) = \frac{E_2(z)}{E_1(z)} = \frac{1 + 0.5z^{-1}}{1 - z^{-1}} \frac{10}{1 - 0.2z^{-1}} \tag{I-261}$$
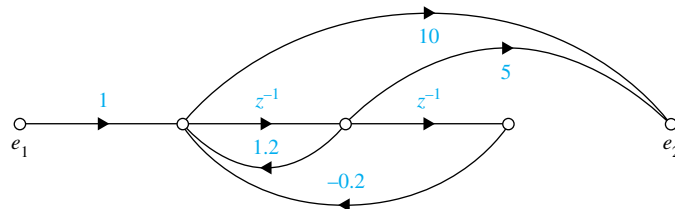
Figure I-47 Direct digital program of Eq. (I-257).

Figure I-48 shows the signal flow graph of the cascade digital program of the controller.
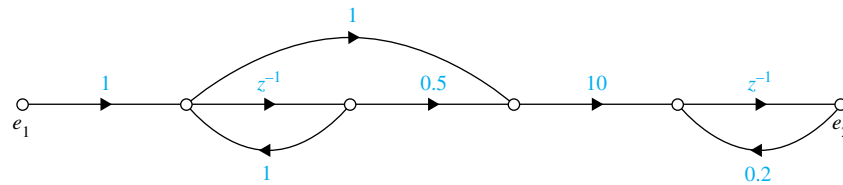
Figure I-48 Cascade digital program of Eq. (I-257).

Parallel Digital Programming

The right-hand side of Eq. (I-257) is expanded by partial fraction into two separate terms.

$$G_c(z) = \frac{E_2(z)}{E_1(z)} = \frac{18.75}{1 - z^{-1}} - \frac{8.75}{1 - 0.2z^{-1}} \tag{I-262}$$

Figure I-49 shows the signal flow graph of the parallel digital program of the controller.
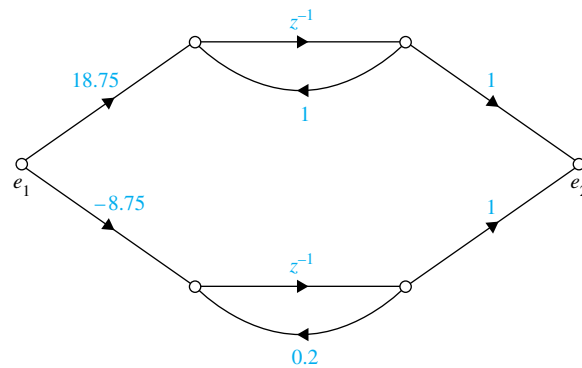
Figure I-49 Parallel digital program of Eq. (I-257). ◄

► I-12 DESIGN OF DISCRETE-DATA CONTROL SYSTEMS IN THE FREQUENCY DOMAIN AND THE z-PLANE

The w-transformation introduced in Section I-5 can be used to carry out the design of discrete-data control systems in the frequency domain. Once the transfer function of the controlled process is transformed into the w-domain, all the design techniques for continuous-data control systems can be applied to the design of discrete-data systems.

I-12-1 Phase-Lead and Phase-Lag Controllers in the *w*-Domain

Just as in the *s*-domain, the single-stage phase-lead and phase-lag controllers in the *w*-domain can be expressed by the transfer function

$$G_c(w) = \frac{1 + a\tau w}{1 + \tau w} \tag{I-263}$$

where $a > 1$ corresponds to phase lead and $a < 1$ corresponds to phase lag. When *w* is replaced by $j\omega_w$, the Bode plots of Eq. (I-263) are identical to those of Figs. 10-28 and 10-45 for $a > 1$ and $a < 1$, respectively. Once the controller is designed in the *w*-domain, the *z*-domain controller is obtained by substituting the *w*-transformation relationship in Eq. (I-163); that is,

$$w = \frac{2}{T}\frac{z - 1}{z + 1} \tag{I-264}$$

The following example illustrates the design of a discrete-data control system using the *w*-transformation in the frequency domain and the *z*-plane.

▶ **EXAMPLE I-27** Consider the sun-seeker control system described in Section 4-9, and shown in Fig. 10-29. Now let us assume that the system has discrete data so that there is a ZOH in the forward path. The sampling period is 0.01 second. The transfer function of the controlled process is

$$G_p(s) = \frac{2500}{s(s + 25)} \tag{I-265}$$

The *z*-transfer function of the forward path, including the sample-and-hold is,

$$G_{h0}G_p(z) = (1 - z^{-1})\mathcal{Z}\left(\frac{2500}{s^2(s + 25)}\right) \tag{I-266}$$

Carrying out the *z*-transform in the last equation with $T = 0.01$ second, we get

$$G_{h0}G_p(z) = \frac{0.1152z + 0.106}{(z - 1)(z - 0.7788)} \tag{I-267}$$

The closed-loop transfer function of the discrete-data system is

$$\frac{\Theta_o(z)}{\Theta_r(z)} = \frac{G_{h0}G_p(z)}{1 + G_{h0}G_p(z)} = \frac{0.1152z + 0.106}{z^2 - 1.6636z + 0.8848} \tag{I-268}$$

The unit-step response of the uncompensated system is shown in Fig. I-50. The maximum overshoot is 66 percent.

Let us carry out the design in the frequency domain using the *w*-transformation of Eq. (I-162),

$$z = \frac{(2/T) + w}{(2/T) - w} \tag{I-269}$$

Substituting Eq. (I-269) into Eq. (I-268), we have

$$G_{h0}G_p(w) = \frac{100(1 - 0.005w)(1 + 0.000208w)}{w(1 + 0.0402w)} \tag{I-270}$$

The Bode plot of the last equation is shown in Fig. I-51. The gain and phase margins of the uncompensated system are 6.39 dB and 14.77°, respectively.

Phase-Lag Controller Design in the Frequency Domain
Let us first design the system using a phase-lag controller with the transfer function given in Eq. (I-263) with $a < 1$. Let us require that the phase margin of the system be at least 50°.
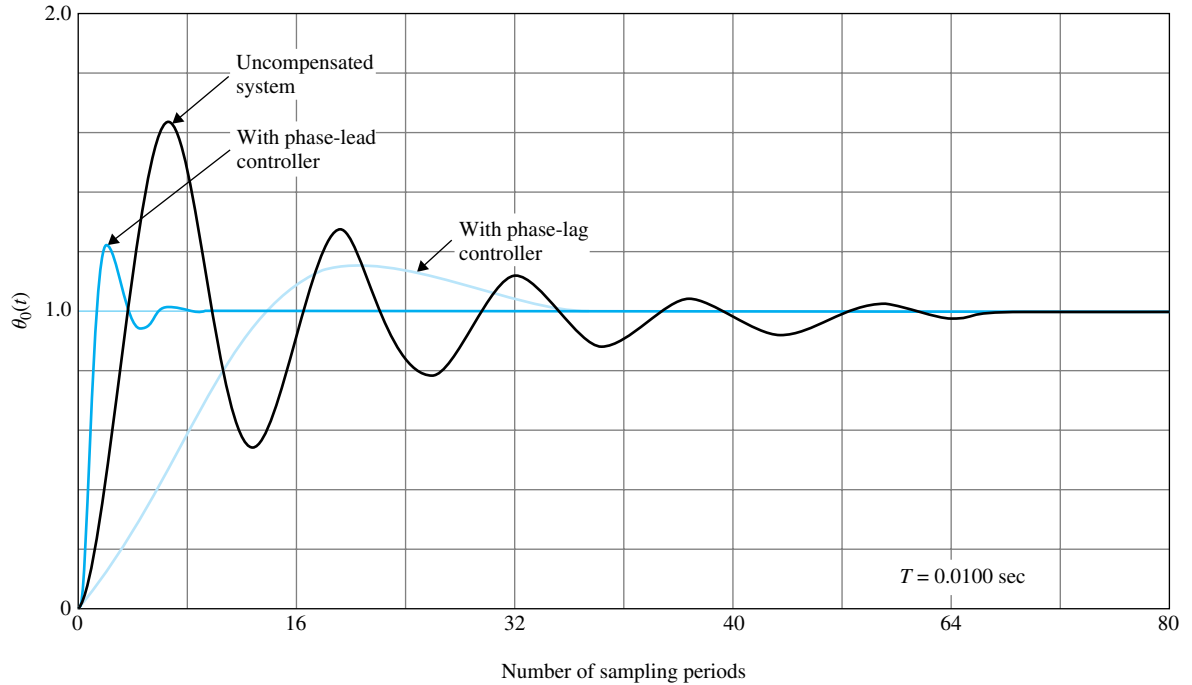
Figure I-50 Step responses of discrete-data sun-seeker system in Example I-27.

From the Bode plot in Fig. I-51, a phase margin of 50° can be realized if the gain crossover point is at $\omega_w = 12.8$ and the gain of the magnitude curve of $G_{ho}G_p(j\omega_w)$ is 16.7 dB.

Thus, we need -16.7 dB of attenuation to bring the magnitude curve down so that it will cross the 0-dB axis at $\omega_w = 12.8$. We set

$$20\log_{10} a = -16.7 \text{ dB} \tag{I-271}$$

from which we get $a = 0.1462$. Next, we set $1/a\tau$ to be at least one decade below the gain crossover point at $\omega_w = 12.8$. We set

$$\frac{1}{a\tau} = 1 \tag{I-272}$$

Thus,

$$\frac{1}{\tau} = a = 0.1462 \tag{I-273}$$

The phase-lag controller in the w-domain is

$$G_c(w) = \frac{1 + a\,\tau w}{1 + \tau w} = \frac{1 + w}{1 + 6.84w} \tag{I-274}$$

Substituting the z-w-transform relation, $w = (2/T)(z - 1)/(z + 1)$, in Eq. (I-274), the phase-lag controller in the z-domain is obtained,

$$G_c(z) = 0.1468\,\frac{z - 0.99}{z - 0.9985} \tag{I-275}$$

The Bode plot of the forward-path transfer function with the phase-lag controller of Eq. (I-274) is shown in Fig. I-51. The phase margin of the compensated system is improved to 55°. The unit-step
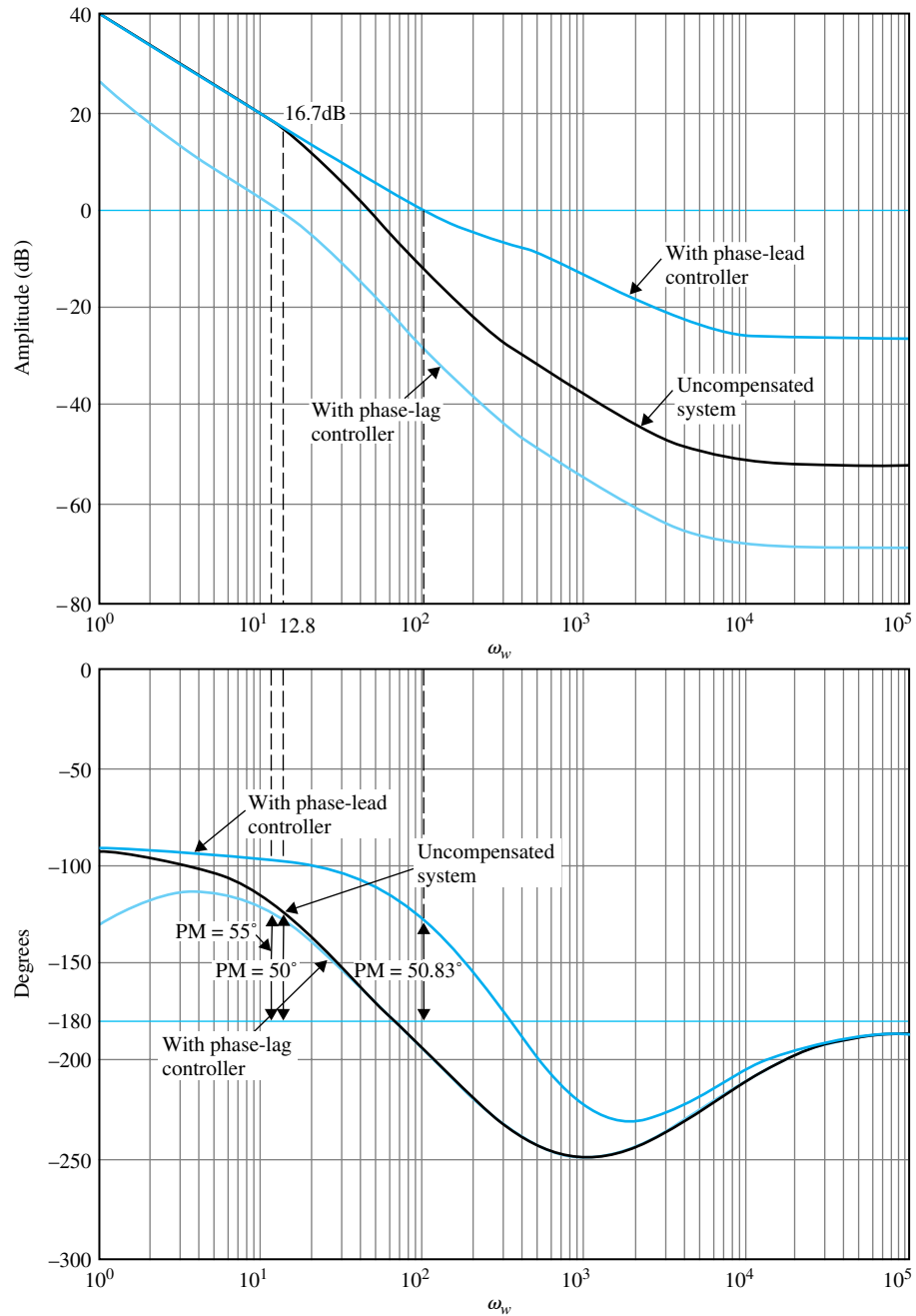
Figure I-51 Bode plots of discrete-data sun-seeker system in Example I-27.

response of the phase-lag compensated system is shown in Fig. I-50. The maximum overshoot is reduced to 16 percent.

Phase-Lead Controller Design in the Frequency Domain

A phase-lead controller is obtained by using $a > 1$ in Eq. (I-263). The same principle for the design of phase-lead controllers of continuous-data systems described in Chapter 10 can be applied here. Since the slope of the phase curve near the gain crossover is rather steep, as shown in Fig. I-51, it is expected that some difficulty may be encountered in designing a phase-lead controller for the

system. Nevertheless, we can assign a relatively large value for a, rather than using the amount of phase lead required as a guideline.

Let us set $a = 20$. The gain of the controller at high values of ω_w is

$$20 \log_{10} a = 20 \log_{10} 20 = 26 \text{ dB} \tag{I-276}$$

From the design technique outlined in Chapter 10, the new gain crossover should be located at the point where the magnitude curve is at $-26/2 = -13$ dB. Thus, the geometric mean of the two corner frequencies of the phase-lead controller should be at the point where the magnitude of $G_{ho}G_p(j\omega)$ is -13 dB. From Fig. I-51 this is found to be at $\omega_w = 115$. Thus,

$$\frac{1}{\tau} = 115\sqrt{a} = 514 \tag{I-277}$$

The w-domain transfer function of the phase-lead controller is

$$G_c(w) = \frac{1 + a\tau w}{1 + \tau w} = \frac{1 + 0.03888w}{1 + 0.001944w} \tag{I-278}$$

The transfer function of the phase-lead controller in the z-domain is

$$G_c(z) = \frac{8.7776z - 6.7776}{1.3888z + 0.6112} \tag{I-279}$$

The Bode plot of the phase-lead compensated system is shown in Fig. I-51. The phase margin of the compensated system is $50.83°$. The unit-step response of the phase-lead compensated system is shown in Fig. I-50. The maximum overshoot is 27 percent, but the rise time is faster.

Digital PD-Controller Design in the z-Plane
The digital PD controller is described by the transfer function in Eq. (I-246), and is repeated as

$$G_c(z) = \frac{\left(K_P + \dfrac{K_D}{T}\right)z - \dfrac{K_D}{T}}{z} \tag{I-280}$$

To satisfy the condition that $G_c(1) = 1$ so that $G_c(z)$ does not affect the steady-state error of the system, we set $K_P = 1$. Applying the digital PD controller as a cascade controller to the sun-seeker system, the forward-path transfer function of the compensated system is

$$G_c(z)G_{ho}G_p(z) = \frac{(1 + 100K_D)z - 100K_D}{z} \frac{0.1152z + 0.106}{(z - 1)(z - 0.7788)} \tag{I-281}$$

We can use the root-contour method to investigate the effects of varying K_D. The characteristic equation of the closed-loop system is

$$z(z^2 - 1.6636z + 0.8848) + 11.52K_D(z - 1)(z + 0.9217) = 0 \tag{I-282}$$

Dividing both sides of the last equation by the terms that do not contain K_D, the equivalent forward-path transfer function with K_D appearing as a multiplying factor is

$$G_{eq}(z) = \frac{11.52K_D(z - 1)(z + 0.9217)}{z(z^2 - 1.6636z + 0.8848)} \tag{I-283}$$

The root contours of the system for $K_D > 0$ are shown in Fig. I-52. These root contours show that the effectiveness of the digital PD controller is limited for this system, since the contours do not dip low enough toward the real axis. In fact, we can show that the best value of K_D from the standpoint of overshoot is 0.022, and the maximum overshoot is 28 percent.

Digital PI-Controller Design in the z-Plane
The digital PI controller introduced in Section I-10-3 can be used to improve the steady-state performance by increasing the system type and, at the same time, improve the relative stability by using
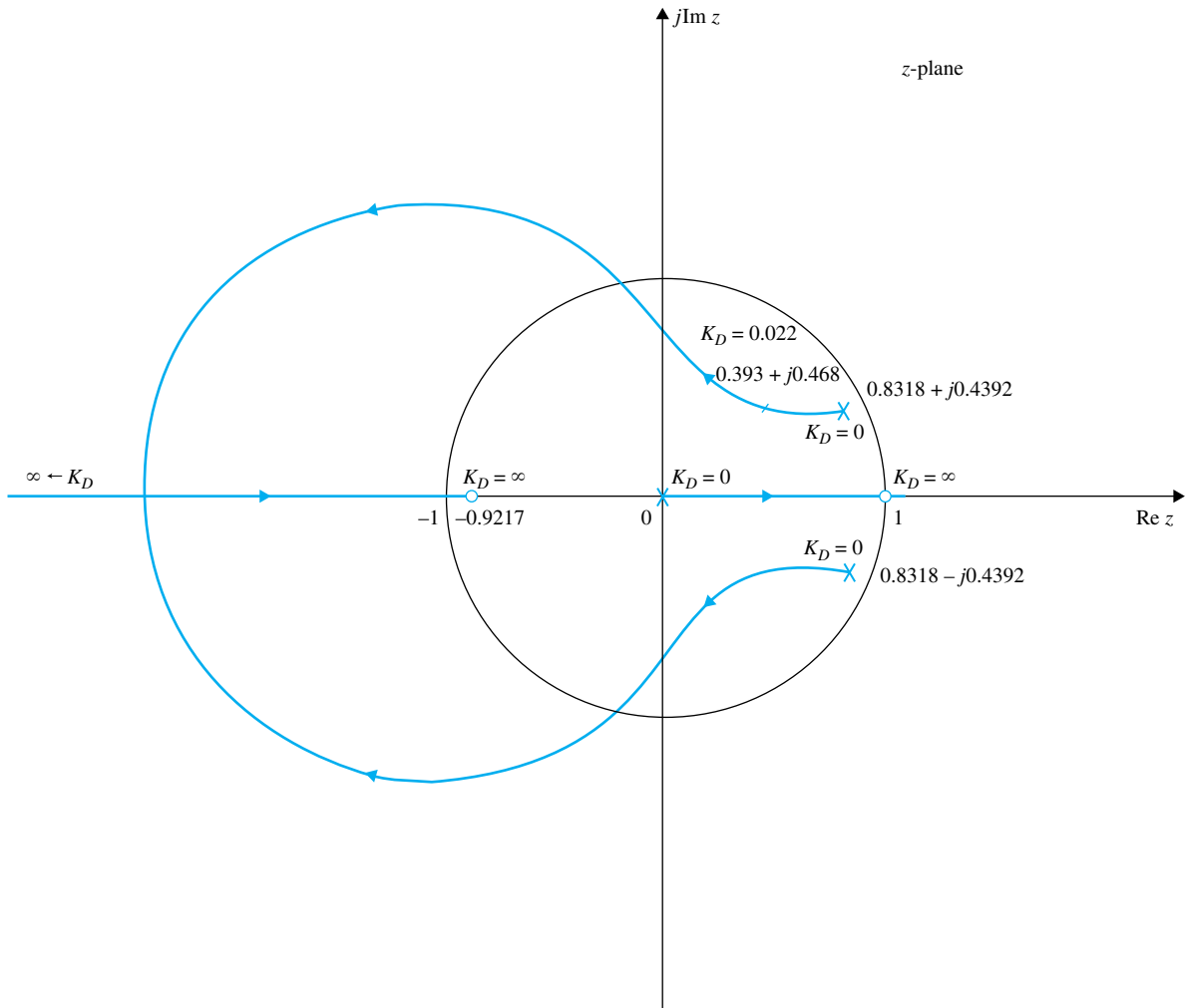
Figure I-52 Root contours of sun-seeker system in Example I-27 with digital PD controller. K_D varies.

the *dipole* principle. Let us select the backward-rectangular integration implementation of the PID controller given by Eq. (I-245). With $K_D = 0$, the transfer function of the digital PI controller becomes

$$G_c(z) = \frac{K_P z - (K_P - K_I T)}{z - 1} = K_P \frac{z - \left(1 - \dfrac{K_I T}{K_P}\right)}{z - 1} \tag{I-284}$$

The principle of the dipole design of the PI controller is to place the zero of $G_c(z)$ very close to the pole at $z = 1$. The effective gain provided by the controller is essentially equal to K_P.

To create a root-locus problem, the transfer function in Eq. (I-267) is written

$$G_{ho}G_p(z) = \frac{K(z + 0.9217)}{(z - 1)(z - 0.7788)} \tag{I-285}$$

where $K = 0.1152$. The root loci of the system are drawn as shown in Fig. I-53. The roots of the characteristic equation when $K = 0.1152$ are $0.8318 + j0.4392$ and $0.8318 - j0.4392$. As shown earlier, the maximum overshoot of the system is 66 percent. If K is reduced to 0.01152, the
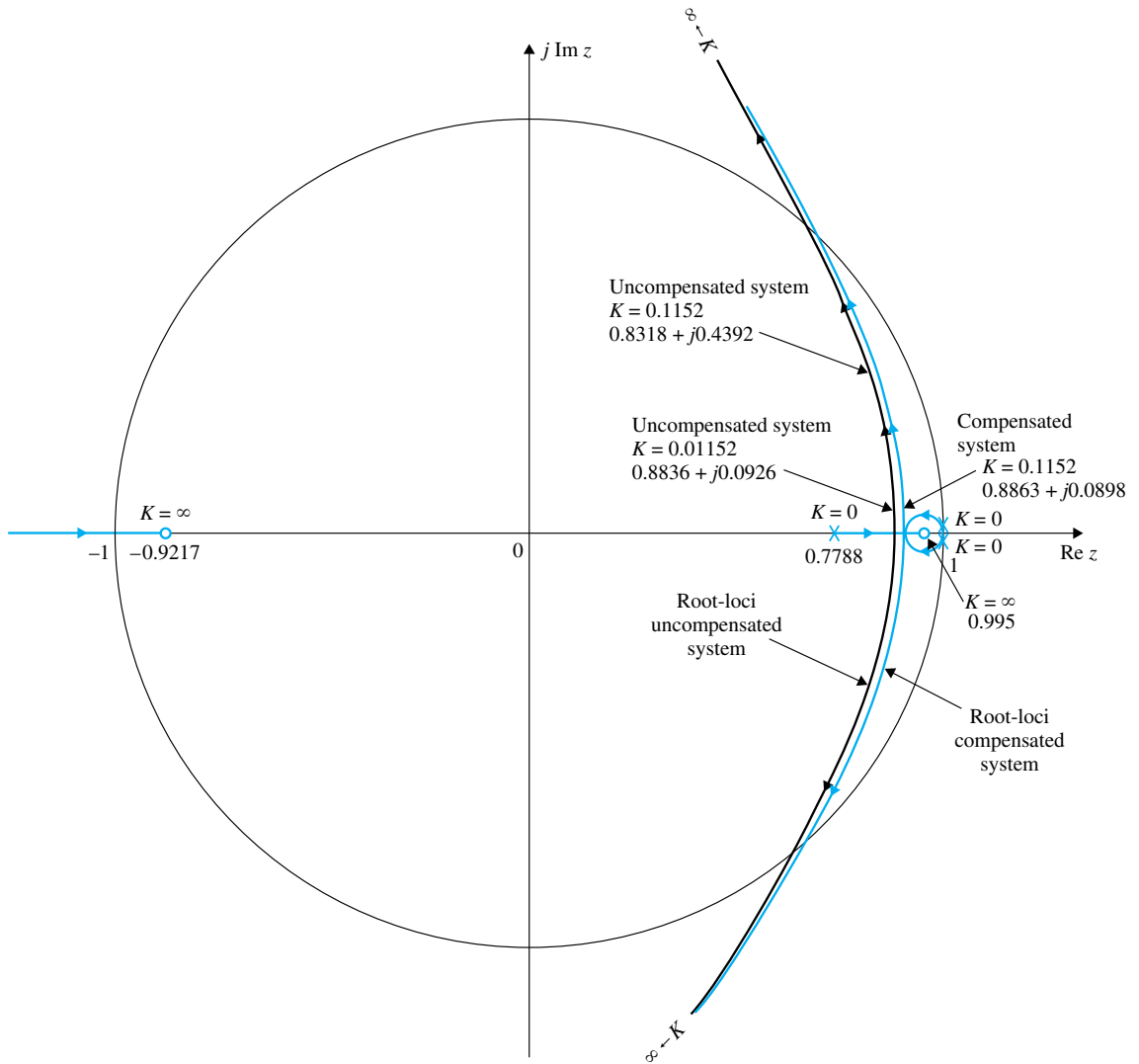
Figure I-53 Root loci of sun-seeker system in Example I-27 with and without digital PI controller.

characteristic equation roots are at $0.8836 + j0.0926$ and $0.8836 - j0.0926$. The maximum overshoot is reduced to only 3 percent.

We can show that if the gain in the numerator of Eq. (I-265) is reduced to 250, the maximum overshoot of the system would be reduced to 3 percent. This means to realize a similar improvement on the maximum overshoot, the value of K_P in Eq. (I-284) should be set to 0.1. At the same time, we let the zero of $G_c(z)$ be at 0.995. Thus,

$$G_c(z) = 0.1\frac{z - 0.995}{z - 1} \tag{I-286}$$

The corresponding value of K_I is 0.05. The forward-path transfer function of the system with the PI controller becomes

$$G_c(z)G_{ho}G_p(z) = \frac{0.1K(z + 0.995)(z + 0.9217)}{(z - 1)^2(z - 0.7788)} \tag{I-287}$$

where $K = 0.1152$. The root loci of the compensated system are shown in Fig. I-53. When $K = 0.1152$, the two dominant roots of the characteristic equation are at $0.8863 + j0.0898$ and $0.8863 - j0.0898$. The third root is at 0.9948, which is very close to the pole of $G_c(z)$ at $z = 1$, and thus the effect on the transient response is negligible. We can show that the actual maximum overshoot of the system with the forward-path transfer function in Eq. (I-287) is approximately 8 percent.

This design problem simply illustrates the mechanics of designing a phase-lead and phase-lag controller using the w-transformation method in the frequency domain and digital PD and PI controllers in the z-plane. No attempt was made in optimizing the system with respect to a set of performance specifications. ◄

► I-13 DESIGN OF DISCRETE-DATA CONTROL SYSTEMS WITH DEADBEAT RESPONSE

One difference between a continuous-data control system and a discrete-data control system is that the latter is capable of exhibiting a **deadbeat response**. A deadbeat response is one that reaches the desired reference trajectory in a minimum amount of time without error. In contrast, a continuous-data system reaches the final steady-state trajectory or value theoretically only when time reaches infinity. The switching operation of sampling allows the discrete-data systems to have a finite transient period. Figure I-54 shows a typical deadbeat response of a discrete-data system subject to a unit-step input. The output response reaches the desired steady state with zero error in a minimum number of sampling periods without intersampling oscillations.

H. R. Sirisena [10] showed that given a discrete-data control system with the controlled process described by

$$G_{h0}G_p(z^{-1}) = \frac{Q(z^{-1})}{P(z^{-1})} \tag{I-288}$$

for the system to have a deadbeat response to a step input, the transfer function of the digital controller is given by

$$G_c(z) = \frac{P(z^{-1})}{Q(1) - Q(z^{-1})} \tag{I-289}$$

where $Q(1)$ is the value of $Q(z^{-1})$ with $z^{-1} = 1$.

The following example illustrates the design of a discrete-data system with deadbeat response using Eq. (I-289).
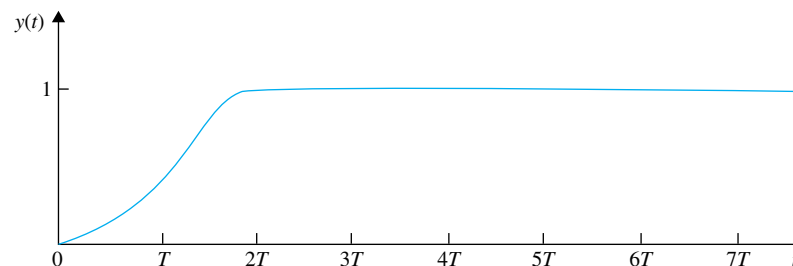
Figure I-54   A typical deadbeat response to a unit-step input.

▶ **EXAMPLE I-28** Consider the discrete-data sun-seeker system discussed in Example I-27. The forward-path transfer function of the uncompensated system is given in Eq. (I-207) and is written as

$$G_{ho}G_p(z^{-1}) = \frac{Q(z^{-1})}{P(z^{-1})} = \frac{0.1152z^{-1}(1 + 0.9217z^{-1})}{(1 - z^{-1})(1 - 0.7788z^{-1})} \tag{I-290}$$

Thus,

$$Q(z^{-1}) = 0.1152z^{-1}(1 + 0.9217z^{-1}) \tag{I-291}$$

$$P(z^{-1}) = (1 - z^{-1})(1 - 0.7788z^{-1}) \tag{I-292}$$

and $Q(1) = 0.22138$.

The digital controller for a deadbeat response is obtained by using Eq. (I-289).

$$G_c(z^{-1}) = \frac{P(z^{-1})}{Q(1) - Q(z^{-1})} = \frac{(1 - z^{-1})(1 - 0.7788z^{-1})}{0.22138 - 0.1152z^{-1} - 0.106z^{-2}} \tag{I-293}$$

Thus,

$$G_c(z) = \frac{(z - 1)(z - 0.7788)}{0.22138z^2 - 0.1152z - 0.106} \tag{I-294}$$

The forward-path transfer function of the compensated system is

$$G_c(z)G_{ho}G_p(z) = \frac{0.1152(z + 0.9217)}{0.22138z^2 - 0.1152z - 0.106} \tag{I-295}$$

The closed-loop transfer function of the compensated system is

$$\frac{\Theta_o(z)}{\Theta_r(z)} = \frac{G_c(z)G_{ho}G_p(z)}{1 + G_c(z)G_{ho}G_p(z)} \tag{I-296}$$

$$= \frac{0.0.5204(z + 0.9217)}{z^2}$$

For a unit-step function input, the output transform is

$$\Theta_o(z) = \frac{0.5204(z + 0.9217)}{z(z - 1)} \tag{I-297}$$

$$= 0.5204z^{-1} + z^{-2} + z^{-3} + \cdots$$

Thus, the output response reaches the unit-step input in two sampling periods.

To show that the output response is without intersampling ripples, we evaluate the output velocity of the system; that is, $\omega_o(t) = d\theta_o(t)/dt$.

The z-transfer function of the output velocity is written

$$\frac{\Omega_o(z)}{\Theta_r(z)} = \frac{G_c(z)(1 - z^{-1})\mathcal{Z}\left[\dfrac{2500}{s(s + 25)}\right]}{G_c(z)G_{ho}G_p(z)} \tag{I-298}$$

$$= \frac{100(z - 1)}{z^2}$$

The output velocity response due to a unit-step input is

$$\Omega_o(z) = \frac{100}{z} = 100z^{-1} \tag{I-299}$$

• The root sensitivity of a system with deadbeat response is poor.

Thus, the output velocity becomes zero after the second sampling period, which proves that the position response is deadbeat without intersampling ripples. The responses of $\theta_o(t)$ and $\omega_o(t)$ are shown in Fig. I-55. The characteristic of a system with deadbeat response is that the poles of the closed-
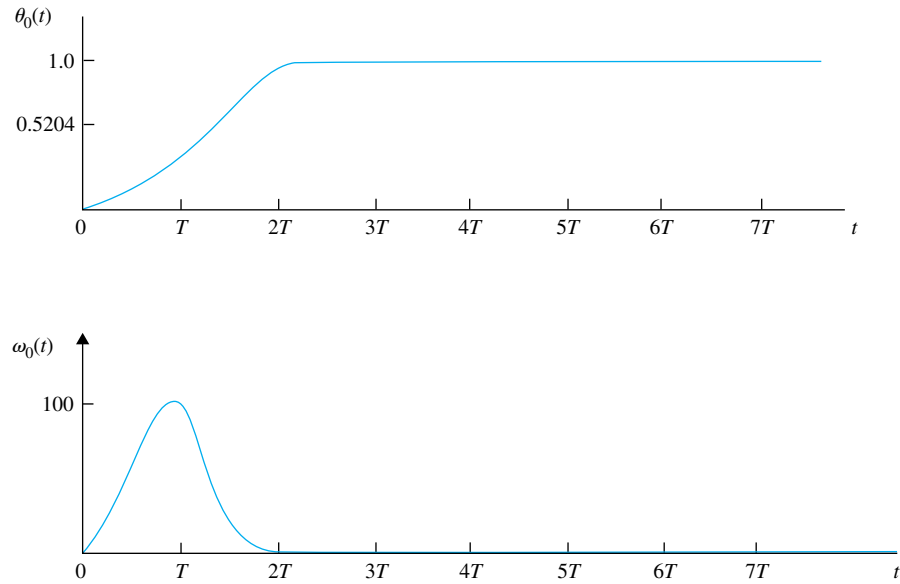
Figure I-55 Output position and velocity responses of discrete-data sun-seeker system in Example I-28.

loop transfer function are all at $z = 0$. Since these are multiple-order poles, from the standpoint of root sensitivity discussed in Chapter 8, the root sensitivity of a system with deadbeat response is very high. ◀

▶ I-14 POLE-PLACEMENT DESIGN WITH STATE FEEDBACK

Just as for continuous-data systems, pole-placement design through state feedback can be applied to discrete-data systems. Let us consider the discrete-data system described by the following state equation:

$$\mathbf{x}[(k + 1)T] = \mathbf{A}\mathbf{x}(kT) + \mathbf{B}u(kT) \tag{I-300}$$

where $\mathbf{x}(kT)$ is an $n \times 1$ state vector, and $u(kT)$ is the scalar control. The state-feedback control is

$$u(kT) = -\mathbf{K}\mathbf{x}(kT) + r(kT) \tag{I-301}$$

where $\mathbf{K}$ is the $1 \times n$ feedback matrix with constant-gain elements. By substituting Eq. (I-301) into Eq. (I-300), the closed-loop system is represented by the state equation

$$\mathbf{x}[(k + 1)T] = (\mathbf{A} - \mathbf{BK})\mathbf{x}(kT) \tag{I-302}$$

Just as in the continuous-data case treated in Section 10-12, we can show that if the pair [$\mathbf{A}$, $\mathbf{B}$] is completely controllable, a matrix $\mathbf{K}$ exists that can give an arbitrary set of eigenvalues of ($\mathbf{A} - \mathbf{BK}$); that is, the n roots of the characteristic equation

$$|z\mathbf{I} - \mathbf{A} + \mathbf{BK}| = 0 \tag{I-303}$$

can be arbitrarily placed. The following example illustrates the design of a discrete-data control system with state feedback and pole placement.

► **EXAMPLE I-29** Consider that the sun-seeker system described in Example 10-9 is subject to sampled data so that the state diagram of the system without feedback is shown in Fig. I-56(a). The sampling period is 0.01 second. The dynamics of the ZOH are represented by the branch with a transfer function of $1/s$. The closed-loop system with state feedback for the time interval $(kT) \le t \le (k + 1)T$ is portrayed by the state diagram shown in Fig. I-56(b), where the feedback gains k_1 and k_2 form the feedback matrix

$$\mathbf{K} = \begin{bmatrix} k_1 & k_2 \end{bmatrix} \tag{I-304}$$

Applying the SFG gain formula to Fig. I-56(b), with $X_1(s)$ and $X_2(s)$ as outputs and $x_1(kT)$ and $x_2(kT)$ as inputs, we have

$$X_1(s) = \left[\frac{1}{s} - \frac{2500k_1}{s^2(s + 25)} \right] x_1(kT) + \left[\frac{1}{s(s + 25)} - \frac{2500k_2}{s^2(s + 25)} \right] x_2(kT) \tag{I-305}$$

$$X_2(s) = \frac{-2500k_1}{s(s + 25)} x_1(kT) - \frac{2500k_2}{s(s + 25)} x_2(kT) + \frac{1}{s + 25} x_2(kT) \tag{I-306}$$

Taking the inverse Laplace transform on both sides of Eqs. (I-305) and (I-306) and letting $t = (k + 1)T$, we have the discrete-data state equations as

$$x_1[(k + 1)T] = (1 - 0.1152k_1)x_1(kT) + (0.2212 - 0.1152k_2)x_2(kT)$$
$$x_2[(k + 1)T] = -22.12k_1x_1(kT) + (0.7788 - 22.12k_2)x_2(kT) \tag{I-307}$$

Thus, the coefficient matrix of the closed-loop system with state feedback is

$$\mathbf{A} - \mathbf{BK} = \begin{bmatrix} 1 - 0.1152k_1 & 0.2212 - 0.1152k_2 \\ -22.12k_1 & 0.7788 - 22.12k_2 \end{bmatrix} \tag{I-308}$$

The characteristic equation of the closed-loop system is

$$|z\mathbf{I} - \mathbf{A} + \mathbf{BK}| = \begin{vmatrix} z - 1 + 0.1152k_1 & -0.2212 + 0.1152k_2 \\ 22.12k_1 & z - 0.7788 + 22.12k_2 \end{vmatrix} \tag{I-309}$$

$$= z^2 + (-1.7788 + 0.1152k_1 + 22.12k_2)z + 0.7788 + 4.8032k_1 - 22.12k_2 = 0$$

Let the desired location of the characteristic equation roots be at $z = 0, 0$. The conditions on k_1 and k_2 are

$$-1.7788 + 0.1152k_1 + 22.12k_2 = 0 \tag{I-310}$$
$$0.7788 + 4.8032k_1 - 22.12k_2 = 0 \tag{I-311}$$

Solving for k_1 and k_2 from the last two equations, we get

$$k_1 = 0.2033 \quad \text{and} \quad k_2 = -0.07936 \tag{I-312}$$

(a)

(b)
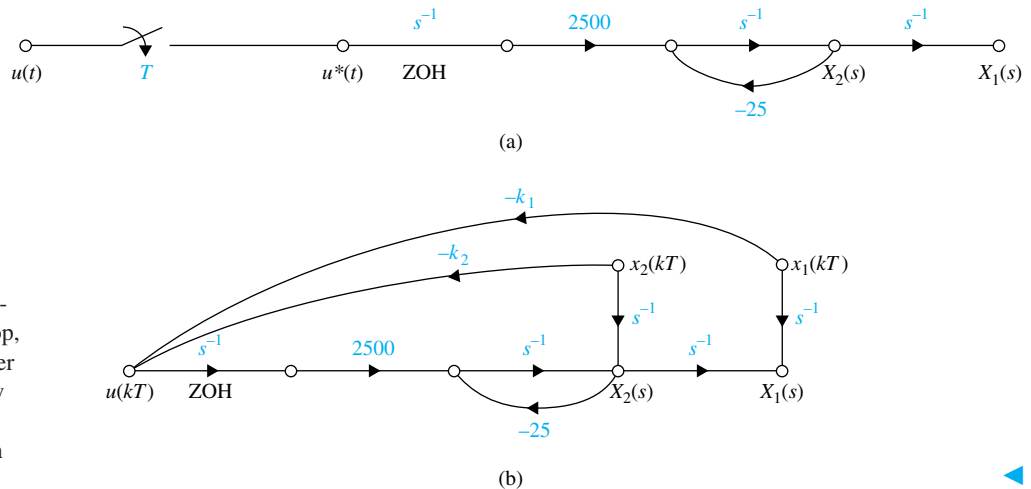
Figure I-56 (a) Signal-flow graph of open-loop, discrete-data, sun-seeker system. (b) Signal-flow graph of discrete-data, sun-seeker system with state feedback.

▶ REFERENCES

1. B. C. Kuo, *Digital Control Systems*, 2nd ed., Oxford University Press, New York, 1992.
2. M. L. Cohen, "A Set of Stability Constraints on the Denominator of a Sampled-Data Filter," *IEEE Trans. Automatic Control*, Vol. AC-11, pp. 327–328, April 1966.
3. E. I. Jury and J. Blanchard, "A Stability Test for Linear Discrete Systems in Table Form," *IRE Proc.*, Vol. 49, No. 12, pp. 1947–1948, December 1961.
4. E. I. Jury and B. D. O. Anderson, "A Simplified Schur-Cohen Test," *IEEE Trans. Automatic Control*, Vol. AC-18, pp. 157–163, April 1973.
5. R. H. Raible, "A Simplification of Jury's Tabular Form," *IEEE Trans. Automatic Control*, Vol. AC-19, pp. 248–250, June 1974.
6. E. I. Jury, *Theory and Application of the z-Transform Method*, John Wiley & Sons, New York, 1964.
7. G. F. Franklin, J. D. Powell, and M. L. Workman, *Digital Control of Dynamic Systems*, 2nd ed., Addison-Wesley, Reading, MA. 1990.
8. K. OGATA, *Discrete-Time Control Systems*, Prentice Hall, Englewood Cliffs, NJ, 1987.
9. C. L. Phillips and H. T. Nagle, Jr., *Digital Control System Analysis and Design*, Prentice Hall, Englewood Cliffs, NJ, 1984
10. H. R. Sirisena, "Ripple-Free Deadbeat Control of SISO Discrete Systems," *IEEE Trans. Automatic Control*, Vol. AC-30, pp. 168–170, February 1985.

▶ PROBLEMS

I-1. Find the z-transforms of the following functions.

(a) $f(k) = ke^{-3k}$ **(b)** $f(k) = k\sin 2k$

(c) $f(k) = e^{-2k}\sin 3k$ **(d)** $f(k) = k^2 e^{-2k}$

• z-transforms

I-2. Determine the z-transforms of the following sequences.

(a) $f(kT) = kT\sin 2kT$

(b) $f(k) = \begin{cases} 1 & k = 0, 2, 4, 6, \ldots, \text{even integers} \\ -1 & k = 1, 3, 5, 7, \ldots, \text{odd integers} \end{cases}$

• Partial-fraction expansion, z-transform

I-3. Perform the partial-fraction of the following functions, if applicable, and then find the z-transforms using the z-transform table.

(a) $F(s) = \dfrac{1}{(s+5)^3}$ **(b)** $F(s) = \dfrac{1}{s^3(s+1)}$

(c) $F(s) = \dfrac{10}{s(s+5)^2}$ **(c)** $F(s) = \dfrac{5}{s(s^2+2)}$

• Inverse z-transform

I-4. Find the inverse z-transforms $f(k)$ of the following functions. Apply partial-fraction expansion to $F(z)$ and then use the z-transform table.

(a) $F(z) = \dfrac{10z}{(z-1)(z-0.2)}$ **(b)** $F(z) = \dfrac{z}{(z-1)(z^2+z+1)}$

(c) $F(z) = \dfrac{z}{(z-1)(z+0.85)}$ **(d)** $F(z) = \dfrac{10}{(z-1)(z-0.5)}$

• z-transform, final-value theorem

I-5. Given that $\mathcal{Z}[f(k)] = F(z)$, find the value of $f(k)$ as k approaches infinity without obtaining the inverse z-transform of $F(z)$. Use the final-value theorem of the z-transform if it is applicable.

(a) $F(z) = \dfrac{0.368z}{(z-1)(z^2-1.364z+0.732)}$ **(b)** $F(z) = \dfrac{10z}{(z-1)(z+1)}$

(c) $F(z) = \dfrac{z^2}{(z-1)(z-0.5)}$ **(d)** $F(z) = \dfrac{z}{(z-1)(z-1.5)}$

Check the answers by carrying out the long division of $F(z)$ and express it in a power series of z^{-1}.

• z-transform solutions

I-6. Solve the following difference equations by means of the z-transform.

(a) $x(k+2) - x(k+1) + 0.1x(k) = u_s(k)$ $x(0) = x(1) = 0$

(b) $x(k+2) - x(k) = 0$ $x(0) = 1, \quad x(1) = 0$

I-7. This problem deals with the application of the difference equations and the z-transform to a loan-amortization problem. Consider that a new car is purchased with a load of P_0 dollars over a period of N months at a monthly interest rate of r percent. The principal and interest are to be paid back in N equal payments of u dollars each.

(a) Show that the difference equation that describes the loan process can be written as

$$P(k + 1) = (1 + r)P(k) - u$$

where $P(k)$ = amount owed after the kth period, $k = 0, 1, 2, \ldots , N$.
$P(O) = P_0$ = initial amount borrowed
$P(N) = 0$ (after N periods, owe nothing)

The last two conditions are also known as the boundary conditions.

(b) Solve the difference equation in part (a) by the recursive method, starting with $k = 0$, then $k = 1, 2, \ldots$, and substituting successively. Show that the solution of the equation is

$$u = \frac{(1 + r)^N P_0 r}{(1 + r)^N - 1}$$

(c) Solve the difference equation in part (a) by using the z-transform method.

(d) Consider that $P_0 = \$15,000$, $r = 0.01$ (1 percent per month), and $N = 48$ months. Find u, the monthly payment.

I-8. Perform the partial-fraction expansion to the following z-transfer functions.

(a) $G(z) = \dfrac{5z}{(z - 1)(z - 0.1)}$ **(b)** $G(z) = \dfrac{10z(z - 0.2)}{(z - 1)(z - 0.5)(z - 0.8)}$

(c) $G(z) = \dfrac{z}{(z - 1)(z - 0.5)^2}$ **(d)** $G(z) = \dfrac{2z}{(z - 1)(z^2 - z + 1)}$

(d) Find $y(t)$ for $t \geq 0$ when the input is a unit-step function. Use $G_4(s)$ as determined in part (b).

I-9. A linear time-invariant discrete-data system has an output that is described by the time sequence

$$y(kT) = 1 - e^{-2kT} \qquad k = 0, 1, 2, \ldots$$

when the system is subject to an input sequence described by $r(kT) = 1$ for all ≥ 0. Find the transfer function $G(z) = Y(z)/R(s)$.

I-10. Find the transfer functions $Y(z)/R(z)$ of the discrete-data systems shown in Fig. IP-10. The sampling period is 0.5 second.

I-11. It is well known that the transfer function of an analog integrator is

$$G(s) = \frac{Y(s)}{X(s)} = \frac{1}{s}$$

where $X(s)$ and $Y(s)$ are the Laplace transforms of the input and the output of the integrator, respectively. There are many ways of implementing integration digitally. In a basic computer course, the rectangular integration is described by the schemes shown in Fig. IP-10. The continuous signal $x(t)$ is approximated by a staircase signal; T is the sampling period. The integral of $x(t)$, which is the area under $x(t)$, is approximated by the area under the rectangular approximation signal.

(a) Let $y(kT)$ denote the digital approximation of the integral of $x(t)$ from $t = 0$ to $t = kT$. Then $y(kT)$ can be written as

$$y(kT) = y[(k - 1)T] + Tx(kT) \qquad (1)$$

where $y[(k - 1)T]$ denotes the area under $x(t)$ from $t = 0$ to $t = (k - 1)T$. Take the z-transform on both sides of Eq. (1) and show that the transfer function of the digital integrator is

$$G(z) = \frac{Y(z)}{X(z)} = \frac{Tz}{z - 1}$$

(a)

(b)

(c)

(d)

(e)

(f)
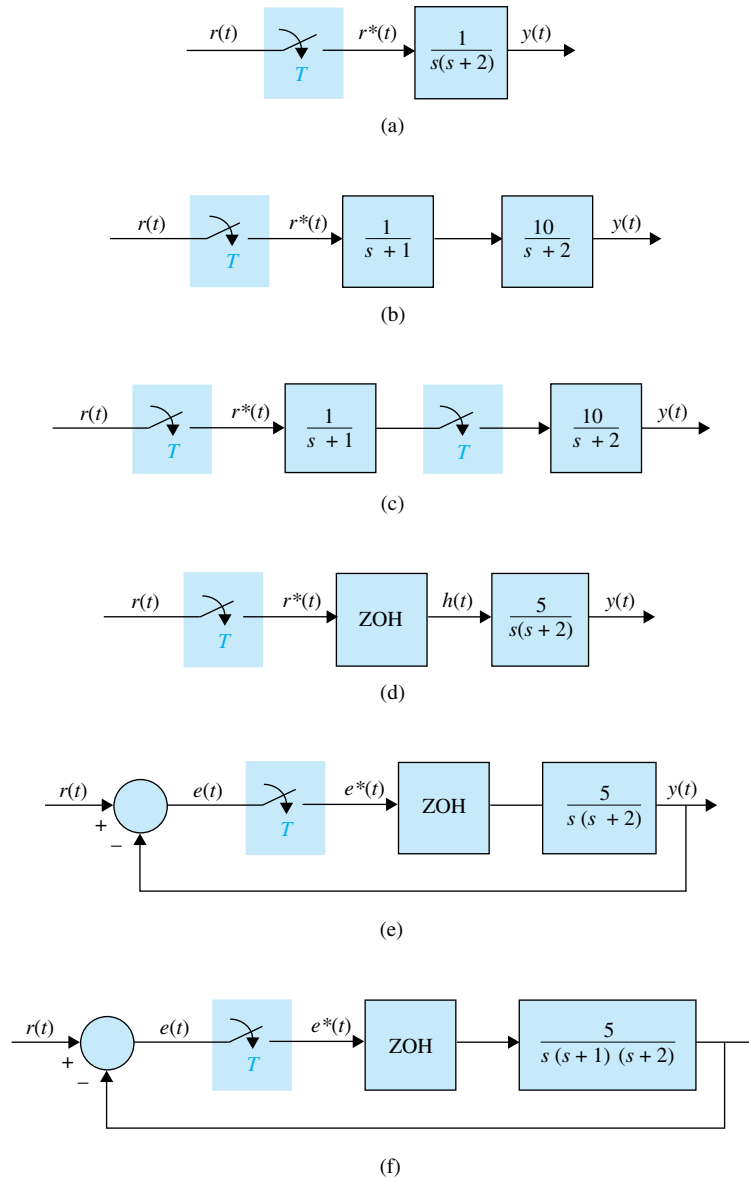
Figure IP-10

(b) The rectangular integration described in Fig. IP-11(a) can be interpreted as a sample-and-hold operation, as shown in Fig. IP-11(b). The signal $x(t)$ is first sent through an ideal sampler with sampling period T. The output of the sampler is the sequence $x(0)$, $x(T)$, ..., $x(kT)$, ... These numbers are then sent through a "backward" hold device to give the rectangle of height $x(kT)$ during the time interval from $(k - 1)T$ to kT. Verify the result obtained in part (a) for $G(z)$ using the "backward" sample-and-hold interpretation.

(c) As an alternative, we can use a "forward" rectangular hold, as shown in Fig. IP-11(c). Find the transfer function $G(z)$ for such a rectangular integrator.

• Vector-matrix discrete state equations

I-12. The block diagram of a sampled-data system is shown in Fig. IP-12. The state equations of the controlled process are

$$\frac{dx_1(t)}{dt} = x_2(t) \qquad \frac{dx_2(t)}{dt} = -2x_1(t) - 3x_2(t) + h(t)$$
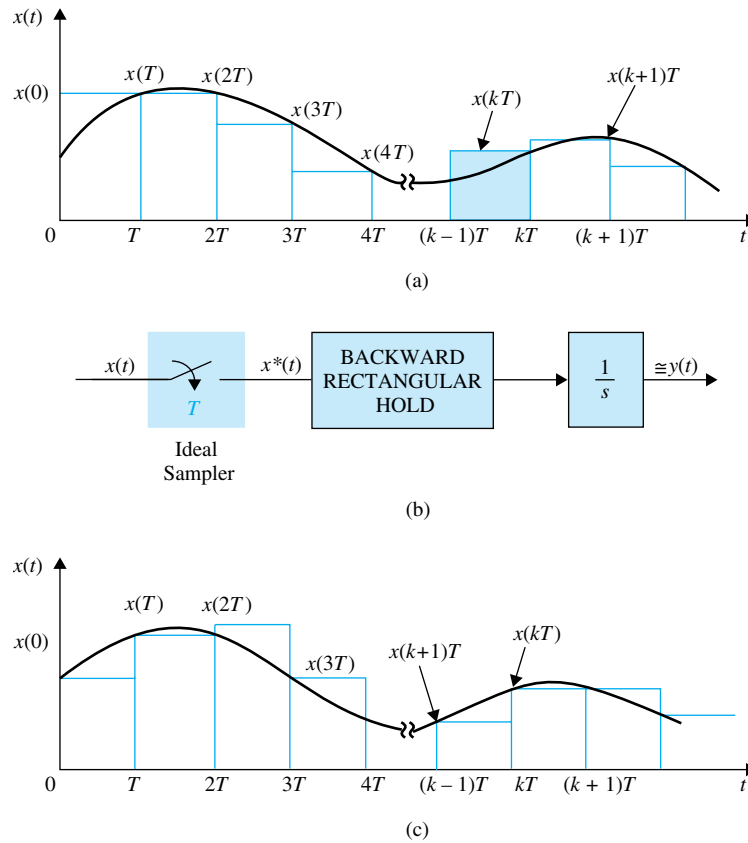
Figure IP-11

where $h(t)$ is the output of the sample-and-hold; that is, $u(t)$ is constant during the sampling period T.

(a) Find the vector-matrix discrete state equations in the form of

$$\mathbf{x}[(k + 1)T] = \phi(T)\mathbf{x}(kT) + \theta(T)u(kT)$$

(b) Find $\mathbf{x}(NT)$ as functions of $\mathbf{x}(0)$ and $u(kT)$ for $k = 0, 1, 2, \ldots N$.
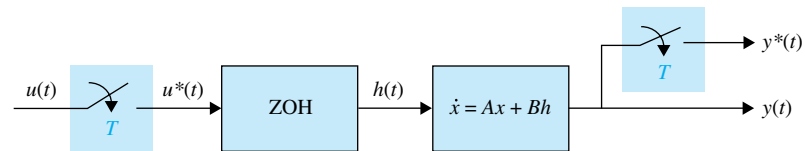
Figure IP-12

• Vector-matrix discrete state equations

I-13. Repeat Problem I-12 for the linear sampled-data system with the following state equations.

$$\frac{dx_1(t)}{dt} = x_1(t) \qquad \frac{dx_2(t)}{dt} = u(t)$$

The sampling period is 0.001 second.

• Discrete-data system, transfer function

I-14. (a) Find the transfer function $\mathbf{X}(z)/U(z)$ for the system described in Problem I-12.

(b) Find the characteristic equation of the system described in Problem I-12.

• Discrete-data system, transfer function

I-15. (a) Find the transfer function $\mathbf{X}(z)/U(z)$ for the system described in Problem I-13.

(b) Find the characteristic equation and its roots of the system described in Problem I-13.

• Digital control, state-diagram characteristic equation

I-16. Draw a state diagram for the digital control system represented by the following dynamic equations:

$$\mathbf{x}(k+1) = \mathbf{A}\mathbf{x}(k) + \mathbf{B}u(k) \qquad y(k) = x_1(k)$$

$$\mathbf{A} = \begin{bmatrix} 0 & 1 & -1 \\ 0 & 1 & 2 \\ 5 & 3 & -1 \end{bmatrix} \qquad \mathbf{B} = \begin{bmatrix} 0 \\ 0 \\ 1 \end{bmatrix}$$

Find the characteristic equation of the system.

• Digital control, state diagram, transfer function

I-17. The state diagram of a digital control system is shown in Fig. IP-17. Write the dynamic equations.

Find the transfer function $Y(z)/R(z)$.
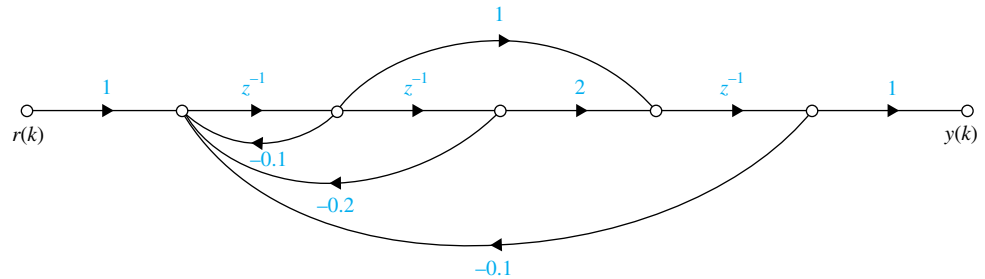
Figure IP-17

• Sampled-data system, state equations, state diagram

I-18. The block diagram of a sampled-data system is shown in Fig. IP-18. Write the discrete state equations of the system. Draw a state diagram for the system.

Figure IP-18

$$G(s) = \frac{1}{s+1} \qquad\qquad T = 1 \text{ sec}$$
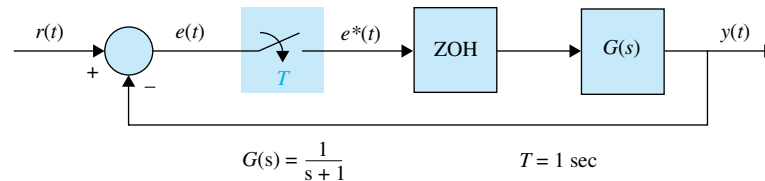
• Stability of discrete-data systems

I-19. Apply the w-transform to the following characteristic equations of discrete-data control systems, and determine the conditions of stability (asymptotically stable, marginally stable, or unstable) using the Routh-Hurwitz criterion.

(a) $z^2 + 1.5z - 1 = 0$ 　　　　(b) $z^3 + z^2 + 3z + 0.2 = 0$

(c) $z^3 - 1.2z^2 - 2z + 3 = 0$ 　(d) $z^3 - z^2 - 2z + 0.5 = 0$

Check the answers by solving for the roots of the equations using a root-finding computer program.

• Stability of digital control system

I-20. A digital control system is described by the state equation

$$x(k+1) = (0.368 - 0.632K)x(k) + Kr(k)$$

where $r(k)$ is the input, and $x(k)$ is the state variable. Determine the values of K for the system to be asymptotically stable.

• Stability of digital control system

I-21. The characteristic equation of a linear digital control system is

$$z^3 + z^2 + 1.5Kz - (K + 0.5) = 0$$

Determine the values of K for the system to be asymptotically stable.

• Stability of discrete-data control system

I-22. The block diagram of a discrete-data control system is shown in Fig. IP-22.

(a) For $T = 0.1$ second, find the values of K so that the system is asymptotically stable at the sampling instants.

(b) Repeat part (a) when the sampling period is 0.5 second.

(c) Repeat part (a) when the sampling period is 1.0 second.
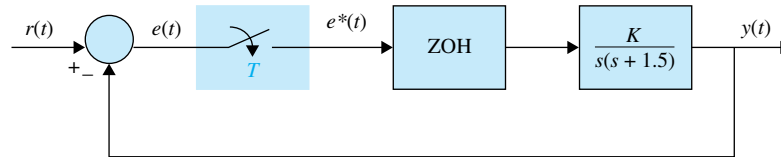
Figure IP-22

I-23. Use a root-finding computer program to find the roots of the following characteristic equations of linear discrete-data control systems, and determine the stability condition of the systems.

(a) $z^3 + 2z^2 + 1.2z + 0.5 = 0$ **(b)** $z^3 + z^2 + z - 0.5 = 0$

(c) $0.5z^3 + z^2 + 1.5z + 0.5 = 0$ **(d)** $z^4 + 0.5z^3 + 0.25z^2 + 0.1z - 0.25 = 0$

• Sampled-data system

I-24. The block diagram of a sampled-data control system is shown in Fig. IP-24.

(a) Derive the forward-path and the closed-loop transfer functions of the system in z-transforms. The sampling period is 0.1 second.

(b) Compute the unit-step response $y(kT)$ for $k = 0$ to 100.

(c) Repeat parts (a) and (b) for $T = 0.05$ second.
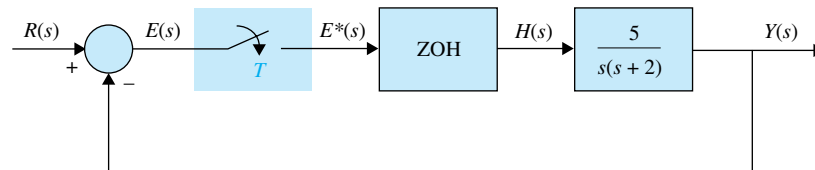
Figure IP-24

• Sampled-data system, error constants

I-25. The block diagram of a sampled-data control system is shown in Fig. IP-25.

(a) Find the error constants K_p^*, K_v^*, and K_a^*.

(b) Derive the transfer functions $Y(z)/E(z)$ and $Y(z)/R(z)$.

(c) For $T = 0.1$ second, find the critical value of K for system stability.

(d) Compute the unit-step response $y(kT)$ for $k = 0$ to 50 for $T = 0.1$ second and $K_t = 5$.

(e) Repeat part (d) for $T = 0.1$ second and $K_t = 1$.
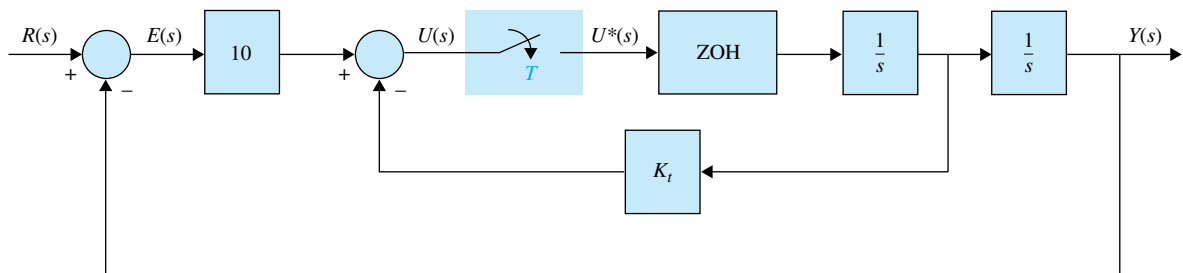
Figure IP-25

I-26. The forward-path dc-motor control system described in Problem 5-33 is now incorporated in a digital control system, as shown in Fig. IP-26(a). The microprocessor takes the information from the encoder and computes the velocity information. This generates the sequence of numbers, $\omega(kT)$ $k = 0, 1, 2, \ldots$. The microprocessor then generates the error signal $e(kT) = r(kT) - \omega(kT)$. The digital control is modeled by the block diagram shown in Fig. IP-26(b). Use the parameter values given in Problem 5-33.

(a) Find the transfer function $\Omega(z)/E(z)$ with the sampling period $T = 0.1$ second.

(b) Find the closed-loop transfer function $\Omega(z)/R(z)$. Find the characteristic equation and its roots. Locate these roots in the z-plane. Show that the closed-loop system is unstable when $T = 0.1$ second.

(c) Repeat parts (a) and (b) for $T = 0.01$ and 0.001 second. Use any computer simulation program.

(d) Find the error constants K_p^*, K_v^*, and K_a^*. Find the steady-state error $e(kT)$ as $k \to \infty$ when the input $r(t)$ is a unit-step function, a unit-ramp function, and a parabolic function $t^2 u_s(t)/2$.

(a)

(b)

Figure IP-26

I-27. The block diagram of a sampled-data control system is shown in Fig. IP-27.

(a) Construct the root loci in the z-plane for the system for $K \geq 0$, without the zero-order hold, when $T = 0.5$ second, and then with $T = 0.1$ second. Find the marginal values of K for stability.

$$G(s) = \frac{K}{s(s + 5)}$$

(b) Repeat part (a) when the system has a zero-order-hold, as shown in Fig. IP-27.
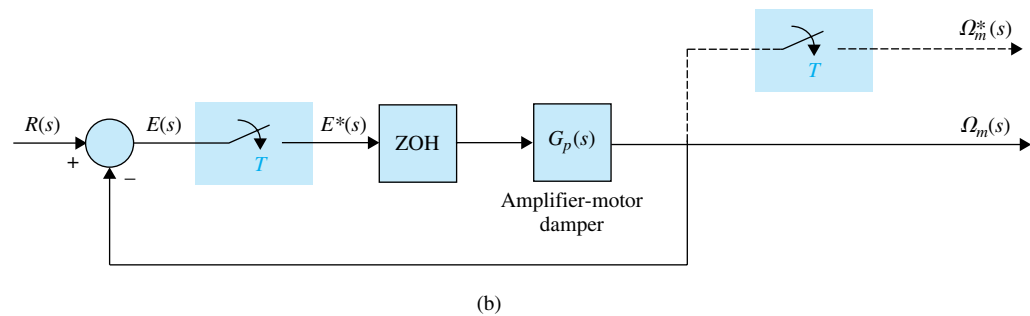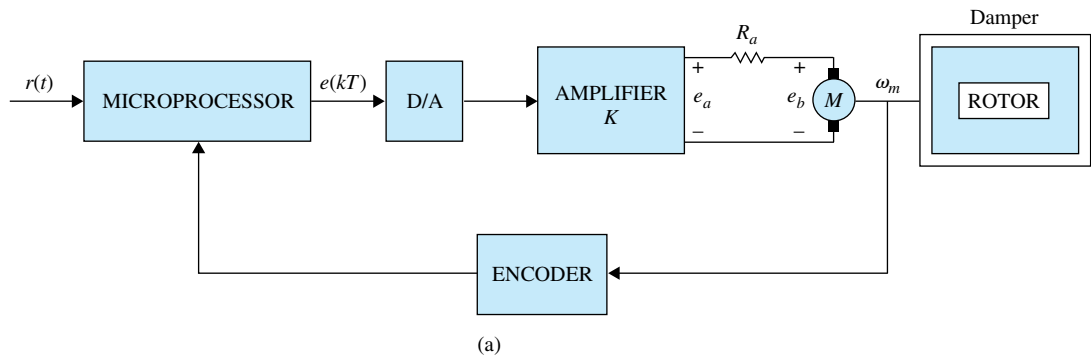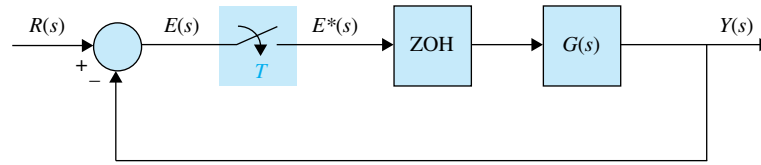
Figure IP-27

• Root loci of sampled-data system

I-28. The system shown in Fig. IP-27 has the following transfer function.

$$G(s) = \frac{Ke^{-0.1s}}{s(s + 1)(s + 2)}$$

Construct the root loci in the z-plane for $K \geq 0$, with $T = 0.1$ second.

• Root loci of discrete-data systems

I-29. The characteristic equations of linear discrete-data control systems are given in the following equations. Construct the root loci for $K \geq 0$. Determine the marginal value of K for stability.

(a) $z^3 + Kz^2 + 1.5Kz - (K + 1) = 0$

(b) $z^2 + (0.15K - 1.5)z + 1 = 0$

(c) $z^2 + (0.1K - 1)z + 0.5 = 0$

(d) $z^2 + (0.4 + 0.14K)z + (0.5 + 0.5K) = 0$

(e) $(z - 1)(z^2 - z + 0.4) + 4 \times 10^{-5}K(z + 1)(z + 0.7) = 0$

• Frequency-domain analysis of discrete-data system

I-30. The forward-path transfer function of a unity-feedback discrete-data control system with sample-and-hold is

$$G_{ho}G(z) = \frac{0.0952z}{(z - 1)(z - 0.905)}$$

The sampling period is $T = 0.1$ second.

(a) Plot the plot of $G_{ho}G(z)$ and determine the stability of the closed-loop system.

(b) Apply the w-transformation of Eq. (I-226) to $G_{ho}G(z)$ and plot the Bode plot of $G_{ho}G(w)$. Find the gain and phase margins of the system.

• Frequency-domain analysis of liquid-level control system with sampled data

I-31. Consider that the liquid-level control system described in Problem 6-13 is now subject to sample-and-hold operation. The forward-path transfer function of the system is

$$G_{ho}G(z) = \frac{1 - e^{-Ts}}{s}\left(\frac{16.67N}{s(s + 1)(s + 12.5)}\right)$$

The sampling period is 0.05 second. The parameter N represents the number of inlet valves. Construct the Bode plot of $G_{ho}G(w)$ using the w-transformation of Eq. (I-226), and determine the limiting value of N (integer) for the closed-loop system to be stable.

• Digital integration

I-32. Find the digital equivalents using the following integration rules for the controllers given. (a) Backward-rectangular integration rule, (b) forward-rectangular integration rule, and (c) trapezoidal-integration rule. Use the backward-difference rule for derivatives.

(i) $G_c(s) = 2 + \dfrac{200}{s}$ **(ii)** $G_c(s) = 10 + 0.1s$ **(iii)** $G_c(s) = 1 + 0.2s + \dfrac{5}{s}$

• Digital program implementation of digital controllers

I-33. A continuous-data controller with sample-and-hold units is shown in Fig. IP-33. The sampling period is 0.1 second. Find the transfer function of the equivalent digital controller. Draw a digital-program implementation diagram for the digital controller. Carry out the analysis for the following continuous-data controllers.

(a) $G_c(s) = \dfrac{10}{s + 12}$ **(b)** $G_c(s) = \dfrac{10(s + 1.5)}{(s + 10)}$

(c) $G_c(s) = \dfrac{s}{s + 1.55}$ **(d)** $G_c(s) = \dfrac{1 + 0.4s}{1 + 0.01s}$
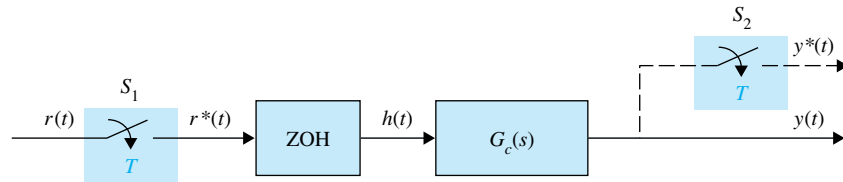
Figure IP-33

• Physical realizability of digital transfer functions

I-34. Determine which of the following digital transfer functions are physically realizable.

(a) $G_c(z) = \dfrac{10(1 + 0.2z^{-1} + 0.5z^{-2})}{z^{-1} + z^{-2} + 1.5z^{-3}}$

(b) $G_c(z) = \dfrac{1.5z^{-1} - z^{-2}}{1 + z^{-1} + 2z^{-2}}$

(c) $G_c(z) = \dfrac{z + 1.5}{z^3 + z^2 + z + 1}$

(d) $G_c(z) = z^{-1} + 0.5z^{-3}$

(e) $G_c(z) = 0.1z + 1 + z^{-1}$

(f) $G_c(z) = \dfrac{z^{-1} + 2z^{-2} + 0.5z^{-3}}{z^{-1} + z^{-2}}$

• Inventory-control system with digital PD controller

I-35. The transfer function of the process of the inventory-control system described in Problem 10-17 is

$$G_p(s) = \frac{4}{s^2}$$

The block diagram of the system with a PD controller and sample-and-hold is shown in Fig. IP-35. Find the transfer function of the digital PD controller using the following equation,

$$G_c(z) = \frac{\left(K_P + \dfrac{K_D}{T}\right)z - \dfrac{K_D}{T}}{z}$$
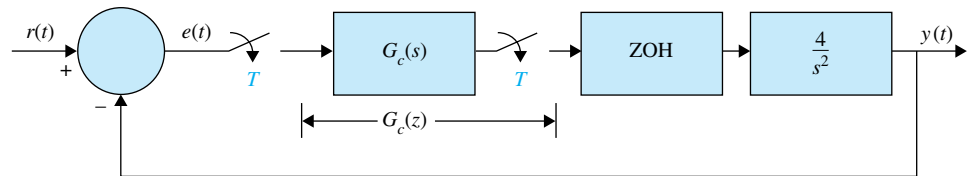
Figure IP-35

Select a sampling period T so that the maximum overshoot of $y(kT)$ will be less than 1 percent.

• Inventory-control system with digital PD controller

I-36. Figure IP-35 shows the block diagram of the inventory-control system described in Problem 10-17 with a digital PD controller. The sampling period is 0.01 second. Consider that the digital PD controller has the transfer function

$$G_c(z) = K_P + \frac{K_P(z - 1)}{T_z}$$

(a) Find the values of K_P and K_D so that two of the three roots of the characteristic equation are at 0.5 and 0.5. Find the third root. Plot the output response $y(kT)$ for $k = 0, 1, 2, \ldots$.

(b) Set $K_P = 1$. Find the value of K_D so that the maximum overshoot of $y(kT)$ is a minimum.

• Inventory-control system with digital phase-lead controller

I-37. For the inventory-control system described in Problem I-36, design a phase-lead controller using the w-transformation so that the phase-margin of the system is at least 60°. Can you design a phase-lag controller in the w-domain? If not, explain why not.

• Aircraft attitude control system with digital controller

I-38. The process transfer function of the second-order aircraft attitude control system described in Problem 10-5 is

$$G_p(s) = \frac{4500K}{s(s + 361.2)}$$

Consider that the system is to be compensated by a series digital controller $G_c(z)$ through a sample-and-hold.

(a) Find the value of K so that the discrete ramp-error constant K_v^* is 100.

(b) With the value of K found in part (a), plot the unit-step response of the output $y^*(t)$ and find maximum overshoot.

(c) Design the digital controller so that the output is a deadbeat response to a step input. Plot the unit-step response.

• Sun-seeker system with digital controller; deadbeat response

I-39. The sun-seeker system described in Example I-5 is considered to be controlled by a series digital controller with the transfer function $G_c(z)$. The sampling period is 0.01 second. Design the controller so that the output of the system is a deadbeat response to a unit-step input. Plot the unit-step response of the designed system.

• Sun-seeker system with state feedback

I-40. Design the state-feedback control for the sun-seeker system in Example I-5 so that the characteristic equation roots are at $z = 0.5, 0.5$.

• State-feedback control

I-41. Consider the digital control system

$$\mathbf{x}[(k + 1)T] = \mathbf{A}\mathbf{x}(kT) + \mathbf{B}u(kT)$$

where

$$\mathbf{A} = \begin{bmatrix} 0 & 1 \\ -1 & -1 \end{bmatrix} \quad \mathbf{B} = \begin{bmatrix} 0 \\ 1 \end{bmatrix}$$

The state-feedback control is described by $u(kT) = -\mathbf{K}\mathbf{x}(kT)$, where $\mathbf{K} = [k_1 \quad k_2]$. Find the values of k_1 and k_2 so that the roots of the characteristic equation of the closed-loop system are at 0.5 and 0.7.

Appendix J
z-Transform Table

z-Transform Table

Laplace Transform	Time Function	z-Transform
1	Unit impulse $\delta(t)$	1
$\dfrac{1}{s}$	Unit step $u_s(t)$	$\dfrac{z}{z-1}$
$\dfrac{1}{1-e^{-Ts}}$	$\delta_T(t) = \displaystyle\sum_{n=0}^{\infty} \delta(t-nT)$	$\dfrac{z}{z-1}$
$\dfrac{1}{s^2}$	t	$\dfrac{Tz}{(z-1)^2}$
$\dfrac{1}{s^3}$	$\dfrac{t^2}{2}$	$\dfrac{T^2 z(z+1)}{2(z-1)^3}$
$\dfrac{1}{s^{n+1}}$	$\dfrac{t^n}{n!}$	$\displaystyle\lim_{\alpha \to 0} \dfrac{(-1)^n}{n!} \dfrac{\partial^n}{\partial \alpha^n} \left[\dfrac{z}{z - e^{-\alpha T}} \right]$
$\dfrac{1}{s+\alpha}$	$e^{-\alpha t}$	$\dfrac{z}{z - e^{-\alpha T}}$
$\dfrac{1}{(s+\alpha)^2}$	$t e^{-\alpha t}$	$\dfrac{Tz e^{-\alpha T}}{(z - e^{-\alpha T})^2}$
$\dfrac{\alpha}{s(s+\alpha)}$	$1 - e^{-\alpha t}$	$\dfrac{(1 - e^{-\alpha T})z}{(z-1)(z - e^{-\alpha T})}$
$\dfrac{\omega}{s^2 + \omega^2}$	$\sin \omega t$	$\dfrac{z \sin \omega T}{z^2 - 2z \cos \omega T + 1}$
$\dfrac{\omega}{(s+\alpha)^2 + \omega^2}$	$e^{-\alpha t} \sin \omega t$	$\dfrac{z e^{-\alpha T} \sin \omega T}{z^2 - 2z e^{-\alpha T} \cos \omega T + e^{-2\alpha T}}$
$\dfrac{s}{s^2 + \omega^2}$	$\cos \omega t$	$\dfrac{z(z - \cos \omega T)}{z^2 - 2z \cos \omega T + 1}$
$\dfrac{s+\alpha}{(s+\alpha)^2 + \omega^2}$	$e^{-\alpha t} \cos \omega t$	$\dfrac{z^2 - z e^{-\alpha T} \cos \omega T}{z^2 - 2z e^{-\alpha T} \cos \omega T + e^{-2\alpha T}}$

Answers to Selected Problems

TO ACCOMPANY

AUTOMATIC CONTROL SYSTEMS
EIGHTH EDITION

BY

BENJAMIN C. KUO

FARID GOLNARAGHI

ISBN 0-471-13476-7

Answers to Selected Problems

The answers given in the following section are for certain selected problems. These answers are given for checking purposes, and thus are often shown for only certain parts of a problem.

CHAPTER 2 Mathematical Foundation

2-1. (a) Poles: $s = 0, 0, -1, -10$;

zeros: $s = -2, \infty, \infty, \infty$.

(c) Poles: $s = 0, -1 + j, -1 -j$;

zero: $s = -2, \infty, \infty$.

2-3. (a) $G(s) = \dfrac{1 - e^{-s}}{s(1 + e^{-s})}$ $\quad G_T(s) = \dfrac{1}{s}(1 - e^{-s})^2$

(b) $G(s) = \dfrac{2(1 - e^{-0.5s})}{s^2(1 + e^{-0.5s})}$

2-6. (a) $g(t) = \dfrac{1}{3} - \dfrac{1}{2}e^{-2t} + \dfrac{1}{3}e^{-3t} \quad t \geq 0$

(e) $g(t) = 0.5t^2 e^{-t} \quad t \geq 0$

CHAPTER 3 Block Diagrams and Signal-Flow Graphs

3-1. (d) Steady-state speed $= 6.66$ ft/sec

3-2. (c) System transfer function: $\dfrac{V(s)}{E_r(s)} = \dfrac{0.002333K(s + 8.5714)e^{-0.5s}}{s^2 + 6s + 0.00035K(s + 8.5714)e^{-0.5s}}$

3-6. $\left.\dfrac{E(s)}{R(s)}\right|_{N=0} = \dfrac{1 + G_3(s)H_1(s) - G_1(s)G_3(s)}{\Delta}$ $\quad \Delta = 1 + G_2(s)G_3(s) + G_3(s)H_1(s)$

$\left.\dfrac{E(s)}{N(s)}\right|_{R=0} = \dfrac{-1}{\Delta}$

3-8. (b) $\dfrac{Y_7}{Y_1} = \dfrac{G_1G_2G_3G_4G_5 + G_6(1 + G_3H_2 + G_4H_3)}{\Delta}$

$\Delta = 1 + G_1G_2H_1 + G_3H_2 + G_4H_3 + G_2G_3G_4G_5H_4 - G_2G_6H_1H_4 + G_1G_2G_4H_1H_3 - G_2G_4G_6H_1H_3H_4$

3-12. (a) $\left.\dfrac{Y_6}{Y_1}\right|_{Y_7=0} = \dfrac{G_1G_2G_3G_4 + G_3G_4G_5}{\Delta}$

$\Delta = 1 + G_2H_1 + G_4H_2 + G_1G_2G_3G_4H_3 + G_3G_4G_5H_3 + G_2G_4H_1H_2$

3-14. (b) $\left.\dfrac{Y(s)}{E(s)}\right|_{N=0} = \dfrac{10(s + 4)}{s^2 + 6s - 20}$

3-16. $G_d(s) = \dfrac{s(s + 10)}{10}$

3-19. (b) $\Delta = 1 - 2[G(s)]^2$

3-20. (b) $y(t) = (20 - 25e^{-t} + 5e^{-5t})u_s(t)$

3-21. (b) Characteristic equation: $\quad s^2 + 7s + 25 = 0$

3-22. (c) Characteristic equation: $\quad s^3 + 5s^2 + 6s + 10 = 0$

(d) Transfer function: $\dfrac{Y(s)}{R(s)} = \dfrac{1}{s^3 + 5s^2 + 6s + 10}$

3-24. (c) Characteristic equation: $\quad s^3 + 21.01s^2 + 30.198s + 10 = 0$

CHAPTER 4 Modeling of Physical Systems

4-1. (b) Force equations: $\dfrac{d^2y_1}{dt^2} = -\dfrac{(B_1 + B_2)}{M}\dfrac{dy_1}{dt} + \dfrac{B_2}{M}\dfrac{dy_2}{dt} + \dfrac{1}{M}f, \quad \dfrac{dy_2}{dt} = \dfrac{dy_1}{dt} - \dfrac{K}{B_2}y_2$

4-3. (b) Torque equations: $\dfrac{d^2\theta_1}{dt^2} = -\dfrac{K}{J}(\theta_1 - \theta_2) + \dfrac{1}{J}T, \quad K(\theta_1 - \theta_2) = B\dfrac{d\theta_2}{dt}$

4-7. (b) Optimal gear ratio: $\quad n^* = \sqrt{J_m/J_L}$

4-8. (b) Transfer function: $\dfrac{Y(s)}{T_m(s)} = \dfrac{r}{s[(J_m + Mr^2)s + B_m]}$

4-12. (a) $\dfrac{H_i(s)}{H_e(s)} = -(R_a + L_a s)$ **(b)** $\left.\dfrac{\Omega_m(s)}{\Omega_r(s)}\right|_{T_L=0} \cong \dfrac{1}{K_b H_e(s)}$

4-14. (d) Forward-path transfer function: $\dfrac{\Theta_o(s)}{\Theta_e(s)} = \dfrac{KK_sK_i n}{s[J_T L_a s^2 + (R_a J_T + B_m L_a)s + R_a B_m + K_i K_b]}$

4-16. (c) Forward-path transfer function: $G(s) = \dfrac{608.7 \times 10^6 K}{s(s^3 + 423.42s^2 + 2.6667 \times 10^6 s + 4.2342 \times 10^8)}$

4-18. (c) Characteristic equation: $Js^2 + (JK_L + B)s + K_2B + K_3K_4e^{-\tau_D s} = 0$

4-21. (b) State equations: $i_a(t)$ as input, $\dfrac{dx(t)}{dt} = v(t)$, $\dfrac{dv(t)}{dt} = -Bv(t) + K_iK_f i_a^2(t)$

4-26. (b) Forward-path transfer function: $\dfrac{Y(s)}{E(s)} = \dfrac{KK_i nG_c(s)e^{-T_D s}}{s\{(R_a + L_a s)[(J_m + J_L)s + B_m] + K_b K_i\}}$

CHAPTER 5 State Variable Analysis

5-3. (a) Eigenvalues: $s = -0.5 + j1.323$, $-0.5 - j1.323$

    (c) State transition matrix: $\phi(t) = \begin{bmatrix} e^{3t} & 0 \\ 0 & e^{-3t} \end{bmatrix}$

    (g) Characteristic equation: $\Delta(s) = s^3 + 15s^2 + 75s + 125 = 0$

5-6. (a) Eigenvalues of $\mathbf{A}$: 2.325, $-0.3376 + j0.5623$, $-0.3376 - j0.5623$

    (b) (3) Output transfer function: $\dfrac{Y(s)}{U(s)} = \dfrac{s + 2}{(s + 1)^2}$

5-8. (c) $\mathbf{S} = \begin{bmatrix} \mathbf{B} & \mathbf{AB} & \mathbf{AB}^2 \end{bmatrix} = \begin{bmatrix} 1 & -1 & 0 \\ 1 & -2 & 4 \\ 1 & -6 & 23 \end{bmatrix}$, $\mathbf{P} = \mathbf{SM} = \begin{bmatrix} 9 & 6 & 1 \\ 6 & 5 & 1 \\ -3 & 1 & 1 \end{bmatrix}$

    (e) $\mathbf{S} = \begin{bmatrix} \mathbf{B} & \mathbf{AB} \end{bmatrix} = \begin{bmatrix} 0 & 1 \\ 1 & -3 \end{bmatrix}$, $\mathbf{P} = \mathbf{SM} = \begin{bmatrix} 1 & 0 \\ -1 & 1 \end{bmatrix}$

5-11. (c) $\mathbf{S} = \begin{bmatrix} 2 & 2 + 2\sqrt{2} \\ \sqrt{2} & 2 + \sqrt{2} \end{bmatrix}$, $\mathbf{S}$ is singular.   **5-13. (a)** $\phi(t) = \begin{bmatrix} \cos t & \sin t \\ -\sin t & \cos t \end{bmatrix}$

5-16. (a) Forward-path transfer function: $G(s) = \dfrac{Y(s)}{E(s)} = \dfrac{5(K_1 + K_2 s)}{s[s(s + 4)(s + 5) + 10]}$

    Closed-loop transfer function: $M(s) = \dfrac{5(K_1 + K_2 s)}{s^4 + 9s^3 + 20s^2 + (10 + 5K_2)s + 5K_1}$

5-19. (b) State transition matrix: $\phi(t) = \begin{bmatrix} e^{-t} & -te^{-t} \\ 0 & e^{-t} \end{bmatrix}$

5-28. (b) State equations: $\begin{bmatrix} \dot{x}_1 \\ \dot{x}_2 \\ \dot{x}_3 \\ \dot{x}_4 \end{bmatrix} = \begin{bmatrix} -2 & 20 & -1 & 0 \\ 0 & -10 & 1 & 0 \\ -0.1 & 0 & -20 & 1 \\ 0 & 0 & 0 & -5 \end{bmatrix} \begin{bmatrix} x_1 \\ x_2 \\ x_3 \\ x_4 \end{bmatrix} + \begin{bmatrix} 0 & -1 \\ 0 & 0 \\ 0 & 0 \\ 30 & 0 \end{bmatrix} \begin{bmatrix} u \\ T_D \end{bmatrix}$

5-32. (b) Characteristic equation: $s^3 + 22s^2 + 170s + 600 = 0$

5-42. The system is controllable.

5-43. (a) Transfer function: $\dfrac{\Theta_v(s)}{R(s)} = \dfrac{K_I H}{J_v s^2(J_G s^2 + K_P s + K_I + K_N)}$

5-45. (b) For controllability, $k_2 \neq -\dfrac{11}{2}$; for observability, $|\mathbf{V}| = -1 + 3k_1 - 3k_2 \neq 0$

CHAPTER 6 Stability of Linear Control Systems

6-1. (b) Poles are at $s = -5, -j\sqrt{2}, j\sqrt{2}$,. Two poles on imaginary axis. Marginally stable.

    (d) Poles are at $s = -5, -1 + j, -1 - j$. All poles in the left-half s-plane. Stable.

6-2. (b) No roots in RHP. **(f)** Two roots in RHP.

6-3. (e) Conditions for stability: $K > 2$ and $K < -2.9055$

6-5. (b) Condition for stability: $K > 4.6667$ **6-9.** Stability requirement: $K_t > 0.081$

6-12. (a) There is one root in the region to the right of $s = -1$ in the s-plane.

CHAPTER 7   Time-Domain Analysis of Control Systems

7-3. (c) $K_p = \infty$, $K_v = K$, $K_a = 0$

7-5. (a) Unit-step input: $e_{ss} = \dfrac{1}{K_H}\left(1 - \dfrac{b_0 K_H}{a_0}\right) = \dfrac{2}{3}$; unit-ramp input: $e_{ss} = \infty$

   (d) Unit-step input: $e_{ss} = 0$; unit-ramp input: $e_{ss} = 0.05$; unit-parabolic input: $e_{ss} = \infty$

7-6. (c) Unit-step input: $e_{ss} = 2.4$; unit-ramp and unit-parabolic inputs: $e_{ss} = \infty$

7-10. (a) Stability requirement: $K_t > 0.02$ and $K > 0$

7-13. Rise time $t_r = 0.2$ sec; $\omega_n = 10.82$ rad/sec; $K = 4.68$; $K_t = 0.0206$

7-15. System transfer function: $\dfrac{Y(s)}{R(s)} = \dfrac{802.59}{s^2 + 25.84s + 802.59}$, $y_{max} = 1.2$ (20% overshoot)

7-24. (b) $k_2^2 = 59 + 10k_1$ **(c)** $k_2 = 13.14$ **7-27. (a)** Stability requirement: $0 < K < 3000.56$

   (c) Stability requirement: $0 < K < 1400$

7-28. (f) $\alpha = 5$ $\left.\dfrac{Y(s)}{D(s)}\right|_{r=0} = \dfrac{100s(s + 2)}{s^3 + 100s^2 + 699s + 1000}$

7-32. (a) $G_L(s) = \dfrac{0.995}{s(s + 0.895)}$ **(e)** $G_L(s) = \dfrac{4.975}{s(s + 0.2225)}$

7-35. (a) $G_L(s) = \dfrac{0.2222}{s(s + 0.7888)}$

CHAPTER 8   Root-Locus Technique

8-2. (a) $K > 0$: $\theta_1 = 135°$ $K < 0$: $\theta_1 = -45°$ **(e)** $\theta_1 = -108.435°$

8-4. (a) Breakaway-point equation: $2s^5 + 20s^4 + 74s^3 + 110s^2 + 48s = 0$

   Breakaway points: -0.7272, -2.3887

8-5. (h) Intersect of asymptotes: $\sigma_1 = -4$; breakaway points: $0, -4, -8$

   (l) Breakaway points: -2.07, 2.07, $-j1.47$, $j1.47$

8-7. (d) $\zeta = 0.707$, $K = 8.4$

8-16. (a) $\sigma_1 = -1.5$; breakaway points: $(K > 0)$ $0, -3.851$

8-21. (a) Breakaway-point equation: $2s^2 + 3(1 + \alpha)s + 6\alpha = 0$

   For no breakaway point other than at $s = 0$, $0.333 < \alpha < 3$.

CHAPTER 9   Frequency-Domain Analysis

9-1. (c) For $K = 100$, $\omega_n = 10$ rad/sec, $\zeta = 0.327$, $M_r = 1.618$, $\omega_r = 9.45$ rad/sec

9-2. (b) $M_r = 15.34$, $\omega_r = 4$ rad/sec, BW $= 6.223$ rad/sec

   (e) $M_r = 1.57$, $\omega_r = 0.82$ rad/sec, BW $= 1.12$ rad/sec

9-5. Maximum $M_r = 1.496$, minimum BW $= 1.4106$ rad/sec

9-9. (a) The Nyquist plot encloses the -1 point. The closed-loop system is unstable. The characteristic equation has two roots in the right-half s-plane.

   (b) Nyquist plot intersects the negative real axis at -0.8333. Thus the closed-loop system is stable.

9-10. (a) The system is stable for $0 < K < 240$.   **9-11. (a)** The system is stable for $-25 < K < \infty$.

9-12. The system is stable for $0 < K < \infty$, except at $K = 1$.

9-14. (a) The system is stable for $|K| < \sqrt{200}$.   **9-15. (a)** For stability, $N < 3$ (N has to be an integer).

9-18. (a) For stability, $T_d = 1.47$ seconds.   **9-21. (b)** Maximum $D = 15.7$ in.

9-25. (e) GM $= 6.82$ dB, PM $= 50.27°$

   (h) GM $=$ infinite, PM $= 13.4°$

9-26. (c) K can be increased by 28.71 dB.   **9-27. (d)** K must be decreased by -2.92 dB.

9-33. (b) PM $= 2.65°$, GM $= 10.51$ dB, $M_r = 17.72$, $\omega_r = 5.75$ rad/sec, BW $= 9.53$ rad/sec

9-35. (a) The gain-crossover frequency is 10 rad/sec.

   (d) $\Phi M = 34.5°$

   (g) BW $= 30$ rad/sec

9-36. (b) $T_d = 0.1244$ second   **9-40. (b)** GM $= 30.72$ dB, PM $=$ infinite

CHAPTER 10   Design of Control Systems

10-3. (a) $K_P = 10$, $K_D = 0.09$ **10-5.** (b) $K_D \cong 0.00175$

10-7. (a) $K_D = 0.09$,   PM $= 93.8°$,   GM $= \infty$, $M_r = 1$, $BW = 1.41$ rad/sec

10-9. (a) $K_P = 1.1$, $K_I = 10$, $K_v = 10$,   PM $= 31.51°$

10-13. (a) $t_s =$ minimum (0.851 sec) when $K_P = 0.6$. $K_P < 4.9718$ for stability.

10-16. (b) $K_D = 399.85$, $K_P = 348.93$ **10-20.** $K_P = 50$, $K_D = 6$, $K_I = 100$

10-22. (a) Set $1/aT = 10$ so that the pole of $G(s)$ at $s = -10$ is cancelled.

    (b) Set the additional phase lead at $67°$. The new gain-crossover frequency $= 70$ rad/sec.

10-25. (a) $R_2 = 2.65 \times 10^5$ gives a relative damping ratio of 0.65.

10-27. (a) $a = 1000$, $T = 0.0004$ (c) $a = 0.074$ **10-30.** (b) $\zeta_p = 1.222$, $\omega_n = 45$ rad/sec

10-34. $K = 5.93$ **10-38.** (c) $G_c(s) = \dfrac{1 + 0.0487s}{1 + 0.00348s}$

10-40. (a) $G_c(s) = \dfrac{1 + 15.63s}{1 + 117.13s}$ **10-43.** (a) $K_1 = 11$

10-45. (a) $k_1 = -64.84$, $k_3 = 20.34$ **10-46.** (b) $K_P = 2$, $K_I = 200$